UNIVERSIDADE DE LISBOA

INSTITUTO SUPERIOR TÉCNICO

DESIGN AND CHARACTERIZATION OF LIPID NANOPARTICLES

FOR AN EFFECTIVE TOPICAL ADMINISTRATION OF ACTIVE COMPOUNDS

Fátima Cristina Romão Vieira Pinto

Supervisor: Doctor Luís Joaquim Pina da Fonseca

Co-supervisor: Doctor Dragana Popovic Correia de Barros

Thesis approved in public session to obtain the PhD Degree in Bioengineering

Jury final classification: Pass

2018

UNIVERSIDADE DE LISBOA

INSTITUTO SUPERIOR TÉCNICO

MASSACHUSETTS INSTITUTE OF TECHNOLOGY

Design and characterization of lipid nanoparticles

for an effective topical administration of active compounds

Fátima Cristina Romão Vieira Pinto

Supervisor: Doctor Luís Joaquim Pina da Fonseca

Co-supervisor: Doctor Dragana Popovic Correia de Barros

Thesis approved in public session to obtain the PhD Degree in Bioengineering

Jury final classification: Pass

Jury

Chairperson: Doctor Duarte Miguel de França Teixeira dos Prazeres, Instituto Superior Técnico, Universidade de Lisboa

Members of the Committee:

Doctor Bruno Filipe Carmelino Cardoso Sarmento, Instituto Universitário de Ciências da Saúde, Gandra

Doctor Ana Catarina Beco Pinto Reis, Faculdade de Farmácia, Universidade de Lisboa

Doctor Pedro Carlos de Barros Fernandes, Instituto Superior Técnico, Universidade de Lisboa

Doctor Abel Martim González Oliva, Instituto de Tecnologia Química e Biológica António Xavier, Universidade Nova de Lisboa

Doctor Dragana Popovic Correia de Barros, individualidade reconhecida na área científica em que se insere a tese

2018

"Como uma âncora, fundemos a nossa esperança nessa humanidade colocada nos Céus à direita do Pai (cf. *Ef* 2, 6). Seja esta esperança a alavanca da vida de todos nós! Uma esperança que nos sustente sempre, até ao último respiro."

Papa Francisco, *Pellegrinaggio del Santo Padre a Fátima – Omelia nella celebrazione eucarística (13 maggio 2017)*

Ao meu pai José,

Porque me inspirou e motivou a querer saber mais e fazer melhor e a vencer as contrariedades que vão surgindo, é com ele e sabendo que estará sempre comigo…

Título: Projecto e caracterização de nanopartículas lipídicas para uma distribuição tópica efectiva de compostos activos

Nome: Fátima Cristina Romão Vieira Pinto

Doutoramento: Bioengenharia - MIT Portugal

Orientador: Doutor Luís Joaquim Pina da Fonseca

Co-orientador: Doutora Dragana Popovic Correia de Barros

Resumo

Novas formulações de nanopartículas lipídicas compostas por ingredientes bioactivos, como os óleos vegetais foram projectadas, optimizadas e produzidas, através da metodologia das miniemulsões, e carregadas com compostos activos hidrofóbicos.

Nanopartículas lipídicas sólidas e transportadores lipídicos nano-estruturados (NLCs) foram formulados com sucesso, considerando o tamanho de partícula e a estabilidade electroestática, usando ácido láurico (C12:0) e óleo de girassol, na sua produção. Ambos os tipos de sistemas de veiculação tópica demonstraram uma elevada eficiência para a encapsulação de β-caroteno e de palmitato de retinol (RP). As formulações de NLCs foram ainda optimizadas usando diferentes tipos de óleos vegetais e tendo em conta o efeito de parâmetros de produção essenciais como a composição e proporção dos lípidos, o tamanho da cadeia de carbonos do lípido sólido e o tipo de agente emulsivo, nas suas propriedades físico-químicas. Estas nanopartículas preparadas com cada tipo de óleo vegetal foram enriquecidas com α-tocoferol (TOC) e demonstraram uma elevada eficiência de encapsulação, uma boa actividade antioxidante, uma libertação controlada do TOC e a capacidade de ser incorporadas em produtos dérmicos estáveis a longo prazo.

A ferramenta estatística, *central composite design*, composta por 5-factores e 3-níveis foi usada para avaliar o efeito das variáveis de formulação seleccionadas, nas características desejadas para a optimização e formulação de NLCs usando RP como modelo de retinóide. A formulação de RP-NLC optimizada foi posteriormente testada para a encapsulação de tretínoina e adapaleno.

Uma cultura de epiderme humana reconstruída (RHE) serviu como modelo para analisar e quantificar os perfis *in vitro* de libertação e irritação da pele, das formulações optimizadas de TOC-NLCs e de RP-NLCs. Estas nanopartículas apresentaram uma boa performance nos modelos de RHE cultivados, provando-se assim estar adequadas para uma fase posterior de aumento de escala e ser incorporadas em veículos secundários para facilitar a sua administração tópica.

Palavras-chave: Nanopartículas lipídicas, metodologia das miniemulsões, óleos vegetais, libertação na pele *in vitro*, modelos de RHE

Title: Design and characterization of lipid nanoparticles for an effective topical administration of active compounds

Abstract

New formulations of lipid nanoparticles composed by bioactive ingredients, as vegetable oils and loaded with lipophilic active compounds, as topical vitamins and retinoids were designed, optimized and produced by the miniemulsions methodology.

Solid lipid nanoparticles and nanostructured lipid carriers (NLCs) were successfully formulated regarding their particle size and electrostatic stability using respectively coconut and sunflower oils. Both nanocarrier types demonstrated high efficiency to encapsulate β-carotene and retinyl palmitate (RP), respectively.

The optimization of NLCs formulations was further developed using sunflower, sweet almond, olive and coconut oils regarding the effect of essential production parameters as the lipids composition and proportion, the solid lipid chain length and the type of surfactant on their physicochemical properties. These formulations with each vegetable oil were enriched with α-tocopherol (TOC), which is recognized as a powerful antioxidant and proved to exhibit high encapsulation efficiencies and drug loading capacities, good antioxidant activities, a well-controlled release of TOC and the ability to be incorporated in long-term stable dermal products.

An effective statistical approach was applied to evaluate the effect of selected formulation variables on NLCs desirable attributes, having RP as model retinoid. A 5-factor, 3-level central composite design was used to optimize a RP-NLCs formulation which was then tested for the encapsulation of tretinoin and adapalene. The developed optimized RP-NLCs, TRT-NLCs and ADP-NLCs dispersions demonstrated appropriate physicochemical characteristics for topical administration and high efficiency with a well-controlled *in vitro* release profile.

Reconstructed human epidermis (RHE) was cultured and served as model to analyse and evaluate the *in vitro* skin delivery and skin irritation profiles of TOC-NLCs and RP-NLCs optimized formulations. These lipid nanoparticles showed a good performance on RHE cultured model, thus proving to be suited for a posteriorly scale up stage and for being incorporated in secondary vehicles to facilitate its topical administration.

Keywords: Lipid nanoparticles, miniemulsions methodology, vegetable oils, *in vitro* skin delivery, RHE models

Título: Projecto e caracterização de nanopartículas lipídicas para uma distribuição tópica efectiva de compostos activos

Resumo alargado

A pele é o maior órgão do corpo humano e representa uma barreira muito eficaz à entrada de substâncias exógenas devido à sua estrutura integrada e complexa. Por esta razão, as patologias dermatológicas, como o cancro da pele e as infecções cutâneas são difíceis de combater, devido à ineficácia das formulações dérmicas existentes que promovem uma baixa concentração de compostos activos em sítios específicos da pele.

O recurso a ferramentas nanotecnológicas revolucionou o conceito de libertação tópica de fármacos. Ao longo dos últimos anos, as indústrias de cosméticos e a farmacêutica realizaram vários estudos para o desenvolvimento de sistemas de veiculação tópica para a administração tópica de substâncias activas. Foram desenvolvidos vários tipos de sistemas de veiculação tópica, apresentando várias vantagens sobre os sistemas de libertação convencionais, tais como o aumento da área superficial, solubilidade e estabilidade do composto activo, possibilidade de uma libertação controlada e direccionada, redução de efeitos secundários associados, protecção do composto activo, aumento da sua permeação e consequente biodisponibilidade na pele.

De entre os vários tipos de nano-transportadores, existe um grupo específico composto por lípidos. Este grupo é diversamente variável considerando a estrutura e composição dos nano-transportadores, incluindo as nanopartículas lipídicas, os lipossomas, niossomas, etossomas, as nanoemulsões, nanocápsulas, entre outros. Os nano-transportadores lipídicos podem ser ajustados na sua arquitectura e características físico-químicas, consoante a sua função terapêutica ou via de administração, servindo assim uma vasta gama de aplicações.

As nanopartículas lipídicas divergem em dois tipos, as nanopartículas lipídicas solidas (SLNs) e os transportadores lipídicos nano-estruturados (NLCs). As SLNs são descritas como a primeira versão das nanopartículas lipídicas e são compostos pela dispersão de um lípido ou lípidos sólidos em meio aquoso, estabilizada por surfactantes. Os NLCs surgem na tentativa de colmatar a fraca capacidade de retenção de fármacos na matriz cristalina dos lípidos sólidos das SLNs, e são compostos pela dispersão de uma mistura de lípidos sólidos com lípidos líquidos, ou óleos, estabilizada por surfactantes.

O principal desafio no desenvolvimento de SLNs e NLCs reside na selecção e optimização de vários factores essenciais que afectam a estrutura, a estabilidade e a capacidade de retenção dos compostos activos que consequentemente irá também influenciar o perfil de libertação dérmica. A composição dos lípidos e o tipo de surfactante são parâmetros fundamentais no controlo das propriedades e estrutura das nanopartículas lipídicas. Para além disso, as características dos lípidos, como a temperatura de fusão, cristalinidade e hidrofobia são também essenciais no controlo da eficiência deste tipo de nano-transportadores. Actualmente, vários trabalhos de investigação têm sido desenvolvidos no âmbito da formulação e caracterização de nanopartículas lipídicas para um determinado tipo específico de composto activo. No entanto, existem ainda poucos estudos que abordam a influência de parâmetros chave na

optimização das propriedades das nanopartículas lipídicas. Existe um enorme potencial no conhecimento sobre as interacções entre os diferentes ingredientes e os compostos activos nas formulações, o qual dependendo também da sua função e aplicação, é fundamental no ajuste da composição das nanopartículas e na escolha da metodologia de produção.

Esta tese teve como finalidade o projecto, a optimização, a produção e a caracterização de novas formulações de nanopartículas lipídicas compostas por ingredientes bioactivos para a administração tópica de compostos activos lipídicos. As nanopartículas lipídicas foram produzidas através da metodologia das miniemulsões, a qual se baseia na aplicação de uma força de cisalhamento por ultra-sons, promovendo uma mistura heterogénea das fases lipídica e aquosa e a formação de nano-gotículas que após arrefecerem permanecem sólidas à temperatura ambiente. Diferentes parâmetros essenciais na produção e formulação das nanopartículas lipídicas foram avaliados em relação ao seu efeito nas principais características físico-químicas destes nano-transportadores lipídicos. Para além disso, a utilização de matérias-primas lipídicas biocompatíveis, biodegradáveis, renováveis, com baixo custo e com propriedades bioactivas, como alguns ácidos gordos saturados e óleos vegetais foi avaliada na formulação das nanopartículas.

Numa primeira fase, a produção dos dois tipos de nanopartículas lipídicas com ácido laurico (C12:0) foi testada e o processo de emulsificação na produção de SLNs através de ultra-sons ou por agitação magnética foi avaliado. Para além disso, o efeito da razão entre lípidos e surfactante, e o tipo de surfactante foram estudados na produção de SLNs e NLCs. A concentração de composto activo encapsulado nos NLCs formulados com óleo de girassol foi também avaliada e ainda, a eficiência de encapsulação dos SLNs e NLCs foi determinada usando β-caroteno (BC) e palmitato de retinol (RP) como modelos de antioxidantes lipídicos. A metodologia das miniemulsões demonstrou ser eficaz na produção dos dois tipos de nanopartículas lipídicas para as formulações em estudo. As SLNs produzidas por ultra-sons apresentaram características físico-químicas mais apropriadas, com tamanhos de partícula entre 105 ± 1 – 146 ± 2 nm e valores de zeta potencial (ZP) ≈ -29 mV, os quais indicaram uma boa estabilidade electroestática em relação às obtidas através de agitação magnética. A análise do efeito da razão entre lípidos e surfactante demonstrou que este parâmetro influenciou significativamente os tamanhos de partícula e índice de polidispersão (PdI) nas formulações de SLNs e NLCs e que o aumento desta razão teve um impacto negativo nas características físico-químicas dos NLCs, com tamanhos de partícula abaixo de 227 ± 14 nm e valores de ZP entre -21 ± 0.7 e -26 ± 0.7 mV. As dispersões de BC-SLN e RP-NLC apresentaram ambas uma elevada eficiência de encapsulação (EE,%) para o BC (≈ 95%) e para o RP (≈ 94%).

Numa fase posterior, foi desenvolvido um trabalho de optimização das formulações de NLCs usando diferentes tipos de óleos vegetais, tais como os óleos de girassol, de coco, de amêndoas doces e o azeite, todos sendo considerados como ingredientes bioactivos com várias propriedades benéficas reconhecidas na literatura. Os efeitos da composição e proporção dos lípidos, do tamanho da cadeia de carbonos do lípido sólido e do tipo de surfactante, foram avaliados nas propriedades físico-químicas destas nanopartículas. E ainda, as formulações de NLCs preparadas com cada tipo de óleo vegetal foram

enriquecidas com α-tocoferol (TOC) e avaliadas, considerando as suas características físico-químicas, a EE,% e capacidade de retenção (DL,%) do TOC variando a concentração deste composto, o grau de cristalinidade da matriz lipídica, morfologia e estrutura interna das nanopartículas, estabilidade da formulação a longo prazo, perfil de libertação *in vitro* do TOC através do método de diálise e actividade antioxidante. Foi demonstrado que os tamanhos e a carga superficial das partículas foram significativamente afectados pela variação destes parâmetros. As formulações com cada óleo vegetal de NLCs apresentaram tamanhos de partícula entre 120 e 350 nm e os TOC-NLCs entre 240 e 315nm, tendo sido obtidos valores elevados de EE, % (≤97,9%) e DL, % os quais provaram ser dependentes da percentagem de TOC encapsulado e também valores elevados de actividade antioxidante, principalmente nas formulações com os óleos de girassol e de amêndoas doces (71.2 ± 4.1% e 70.5 ± 4.0%). Ocorreu uma libertação controlada do TOC em todas as formulações com cada óleo vegetal, com 51,0% de TOC libertado ao fim de 48h pelos NLCs formulados com óleo de amêndoas doces. Todas as formulações de NLCs e TOC-NLCs mantiveram-se estáveis durante um período de 8 meses, mostrando uma pequena variação nos tamanhos de partícula.

O trabalho de optimização das formulações de NLCs prosseguiu com uma abordagem diferente, recorrendo a uma ferramenta estatística, *central composite design* (CCD), para avaliar o efeito de algumas variáveis de formulação seleccionadas, nas características desejadas para os NLCs, usando RP como modelo de retinóide. A formulação de RP-NLC optimizada foi posteriormente testada para a encapsulação de tretinoina (TRT) e adapaleno (ADP), e todas as dispersões resultantes foram caracterizadas relativamente às suas propriedades físico-químicas, morfologia, EE,% e DL,%, cristalinidade da matriz lipídica e perfil de libertação *in vitro*. Foi alcançada uma formulação optimizada de RP-NLCs composta por 2.5% de lípidos totais, com 0.5% de ácido mirístico (C14:0) e 1.5% de óleo de girassol e 1.5% de surfactante. As dispersões de NLCs com os três tipos de retinóides apresentaram tamanhos de partícula abaixo de 134.5 ± 5.4 nm, uma elevada estabilidade electroestática (ZP ≥ –57.9 ± 3.5mV) e EE, % com valores de 84.4 ± 3.0% para o RP, de 84.1 ± 7.8% para a TRT e de 73.7 ± 3.3% para o ADP. Estes valores elevados de EE, % justificam os perfis de libertação bastante controlada que foram obtidos para os três retinóides, com 21.5 ± 1.3% de ADP, 12.2 ± 2.7% de RP e 9.1 ± 2.5 % de TRT após 48h.

Por fim, as formulações optimizadas de TOC-NLCs e de RP-NLCs foram avaliadas relativamente à sua aplicação dérmica através da análise e quantificação dos perfis *in vitro* de libertação e irritação tópica, usando uma cultura de RHE como modelo. As nanopartículas lipídicas optimizadas com TOC e RP apresentaram uma boa performance nos modelos de RHE cultivados, demonstrando ser viáveis para uma posterior fase de aumento de escala e para a sua incorporação em veículos secundários, como geles ou cremes para facilitar e cumprir e a finalidade de uma administração tópica efectiva.

ACKNOWLEDGMENTS/AGRADECIMENTOS

The development of this PhD thesis has been a demanding exercise of perseverance which would have been impossible to complete without the exceptional support of several people to whom I express my sincere gratitude.

I would first like to deeply thank my supervisor, Professor Luis Fonseca for his guidance, encouragement and continuous support in all stages of this thesis and mostly for having accepted me on his amazing team at the Bioengineering Research Group (BERG) of Instituto Superior Técnico (IST) to develop this work, which otherwise would not existed.

Also and foremost, I would like to sincerely thank my co-supervisor, Dr. Dragana Barros, for all her support and strict guidance with detailed suggestions and important advices that kept me on track, all along this difficult journey with very good and very bad times, for being not only an exceptional scientist but more important for the really inspiring, passionate, courageous, truly kind and generous person that she is. Dragana, hvala ti puno što si moj iskren prijatelj I na svoj podršci I snazi koju si mi pružila.

I emphasize a special acknowledgement to Professor Abel Oliva, from ITQB NOVA - Instituto de Tecnologia Química e Biológica António Xavier for his scientific support and for giving me the great opportunity of having me host and warmly integrated in his remarkable team at the lab of Biomolecular Diagnostics to evaluate the efficiency of nanoparticles formulations on reconstructed human epidermis models.

The extend of these acknowledgements and my extreme gratitude to Dr. Sofia Souza, for her friendship in helping me to feel at "my lab" and for her precious unreserved assistance and patience on getting me acquainted with the concepts and methodologies involved in the culture of reconstructed human epidermis and in the histologic analysis of these tissues.

I sincerely express my esteem to Dr. Teresa Cesário, to Dr. Carla Carvalho and to Dr. Pedro Fernandes for their valuable scientific advices and always timely and pleasant coexistence in the laboratory at BERG.

I as well wish to acknowledge the support of different people that have contributed to the completion of this work: Eng. Isabel Nogueira from MicroLab – Electron microscopy laboratory at IST for the kindly support on TEM analysis; Professor Miguel Rodrigues and Dr. Andreia Duarte from Centro de Química Estrutural at IST, for his permission to use the equipment of differential scanning calorimetry and her help and availability in introducing me this technique and teach me how to operate the equipment; Dr. Gaby Martins from UIC: Advanced Imaging Unit at Instituto Gulbenkian de Ciência (IGC) for the availability in producing the outstanding 3D recontructs from confocal laser scanning microscopy analysis that truly enhanced my work; Dr. Joana Rodrigues from Histopathology Unit at IGC for the support in mounting and staining the samples in microscope slides for the histologic analysis; Dr. Patrizia Paradiso from NanoMatLab – Nanostructured Materials and Nanotechnologies Laboratory for making available the atomic

force microscopy equipment and helping in obtaining the respective images; Ricardo Pereira from the Bioengineering Department of IST for all the technical support.

I wish to address special thanks to my dearest colleagues and friends that fortunately were present and have greatly improved my academic path during its different stages. To my colleagues from the Biomolecular Diagnostics lab at ITQB-NOVA, Ana Coelho, Vanja Stojanovic and Patricia Zoio for their support and helpful collaboration during the short but precious time in this group. To my dearest colleagues and friends from MIT Portugal Program with whom I started this demanding but rewarding endeavour, Carlos Teixeira, Andreia Araújo and Duarte Dinis from the EDAM group, Raquel Almeida, Rui Traquete, Henrique Carvalho, Helder Lopes, Raquel Cunha, Maria João Jacinto, Salomé Duarte, Sofia Ferreira, Siddhi Lama, from the Bioengineering group, including the exclusive members of "MITassos", Mauro Luis, Pawel Bujalski, Cátia Salgado, Denis Santos, Diogo Pinto and Maria João Sebastião. To my dearest colleagues and friends at BERG research group, Maria Paris, foste e és uma inspiração de coragem, Ana Pfluck, foste uma grande companhia nesta jornada, "trio maravilha" e "clube da marmita" que à hora de almoço se juntava para dar à língua e para o posterior cafezinho à sombra, Flávio Ferreira, Teresa Esteves, Rui Carvalho, Filipe Carvalho, Vera Esgueira, Alexandra Salvado, Andresa Ribeiro, Luca Lizzi, Ana Rosa and Rita Franca for their enormous support, good team spirit and a friendly and positive environment at work. Finalmente, gostaria de agradecer especialmente à Dona Rosa pela sua incrível generosidade, amabilidade, prontidão e paciência que sempre demonstrou em todas as tarefas que desempenhou.

Finally, I want to deeply thank my family. Ao meu irmão José, por toda a ajuda, apoio e compreensão nas alturas menos boas, por resolveres alguns assuntos complicados em alturas difíceis em que eu estive à distância, pela amizade e forte laço familiar que nos une, por seres um excelente irmão mais velho com o qual sei que poderei sempre contar. Aos meus pais, o meu profundo reconhecimento pela confiança que investiram no esforço de alcançar a meta desta imensurável aprendizagem académica e pessoal, por me apoiarem sempre e incondicionalmente, por me inspirarem e motivarem, como professores que são, a aprender e querer fazer mais e melhor, por me transmitirem os valores que fundamentam a pessoa que sou, muito obrigada por tudo!

LIST OF ABBREVIATIONS AND NOTATIONS

ADP – Adapalene

ADP-NLCs – NLCs loaded with adapaleno

AFM – Atomic force microscopy

BC – β-Carotene

BC-SLN – Solid lipid nanoparticles loaded with β-carotene

CCD – Central composite design

CLSM – Confocal laser scanning microscopy

CO – Coconut oil

DDS – Drug delivery system

DL, % – Drug loading capacity

DLS – Dynamic light scattering

DPPH – 2,2-Diphenyl-1-picrylhydrazyl

DSC – Differential scanning calorimetry

EDS – Energy dispersive spectroscopy

EE, % – Entrapment efficiency

GRAS – Generally Recognized as Safe

GSO – Grape seed oil

HLB – Hydrophilic-lipophilic balance

HPLC – High performance liquid chromatography

HPH – High pressure homogenization

INCI – International nomenclature of cosmetic ingredients

NLC – Nanostructured lipid carrier

OECD – Organization for economic cooperation and development

OV – Olive oil

O/W – Oil in water emulsion

PdI – Polydispersity index

PEG – Polyethylene glycol

RHE – Reconstructed human epidermis

ROS – Reactive oxygen species

RP – Retinyl palmitate

RP-NLCs – NLCs loaded with retinyl palmitate

SA – Sweet almond oil

SC – *Stratum corneum*

SD – Standard deviation

SEM – Scanning electron microscopy

SFE – Supercritical fluid extraction

SF – Sunflower oil

SLN – Solid lipid nanoparticles

SL: S – Solid lipid, wt%: Surfactant, wt%

TEM – Transmission electron microscopy

TOC – α-Tocopherol

TOC-NLCs – NLCs enriched with TOC

TOC-DiO-NLCs – NLCs enriched with TOC and with the fluorescent dye DiO

TL: S – Total lipids, wt%: Surfactant, wt%

TRT – Tretinoin

TRT-NLCs – NLCs loaded with tretinoin

UV – Ultraviolet

W/O – Water in oil emulsion

W/O/W – Water in oil in water emulsion

ZP – Zeta potential

TABLE OF CONTENTS

TABLE OF FIGURES

TABLE OF TABLES

CHAPTER I

MOTIVATION AND THESIS OUTLINE

1.1.   Background

1.2.   Research objectives

1.3.   Research strategy

1.4.   Thesis structure

1. Motivation and Thesis Outline

1.1. Background

In recent years there was a growing interest in nanotechnology that provided extraordinary accomplishments in many fields, including in cosmetic and pharmaceutical industries. Several innovative applications of nanotechnology have transformed the administration of active compounds by generating innovative, safe and effective products (Severino et al., 2012). The topical administration of nanocarriers in dermal formulations have improved the efficacy and the delivery of active substances due to their several advantages over conventional passive delivery systems. Thus, there are currently several types of nanocarriers that are being studied for dermal delivery, as liposomes, lipid nanoparticles, nanoemulsions, polymeric nanoparticles, among others (Attama et al., 2012). Moreover, rapid advances in methodologies and techniques enabled the production of nanocarriers with uniform size, shape and composition which offered the opportunity of developing formulations with specific properties for their use in new therapeutics. Although, the development of suitable nanocarriers presenting interesting properties for a determined dermal application, that effectively enhance the inherent physicochemical properties of incorporated actives compounds and assists a targeted and efficient delivery of these actives, still remains a challenge and is, therefore of the highest academic, industrial and economical relevance.

Lipid nanocarriers refer to a wide group of drug delivery systems that are well-known as effective carriers for lipophilic and hydrophilic active agents and that can be easily integrated into dermal formulations. A variety of lipid nanocarriers can be obtained by adjusting their composition, thus achieving lipid vesicles with high flexibility and deformability for enhanced results in terms of skin absorption. Among these, lipid nanoparticles were introduced in the early nineties as alternative nanoparticles made from solid lipids, also known as solid lipid nanoparticles (SLNs) (Müller et al., 2007). During the last years, due to their biocompatibility and versatility, the interest in lipid nanoparticles increased significantly as evidenced by the high number of published articles regarding this topic (Poland, 2016). Lipid nanoparticles present several advantages of other nanocarriers, such as high biocompatibility, good physical stability, possibility of controlled release of drug and active substances, easy production at large scale and cheap raw materials, minimizing the problems associated with these vehicles. In fact, the first generation of lipid nanoparticles (SLNs) are derived from the replacement of the oil phase of a nanoemulsion by a solid lipid. Although, these lipid nanocarrier systems also present some limitations as drug expulsion during storage, and low drug loading capacity due to the limited solubility of drugs in the solid lipid (Morales et al., 2015). Thus, in order to overcome these drawbacks at the turn of the century, a second generation of lipid nanoparticles was developed, the nanostructured lipid carriers (NLCs). These nanocarriers are

composed by a liquid lipid (oil) mixed with a solid lipid, thus producing several imperfections in the solid lipid lattice, providing more space to locate higher amounts of actives than SLNs and preventing or minimizing the drug expulsion phenomena from their lipid matrix (Müller et al., 2007).

There are several methodologies available for the production of lipid nanoparticles, but in general all require a common step, that is, the formation of a precursor oil-in-water nanoemulsion followed by subsequent solidification of the dispersed lipid phase (Shah et al., 2015). The miniemulsions methodology consist in the production of a heterophase system of stable nanodroplets, narrowly size distributed, dispersed in a continuous phase which is formed by shearing the system with ultrasounds. This methodology offers an appropriate simple and clean alternative for laboratory scale production of lipid nanoparticles due to its non-demanding and fast procedure and to the relatively low cost of the required apparatus (Schwarz et al., 2012). The production method is a very important variable to be considered as it greatly influences the performance and characteristics of lipid nanoparticles, thus demanding an accurate optimization of its parameters for achieving a formulations with certain characteristics appropriated for topical delivery. The physicochemical properties of lipid nanoparticles are also influenced by their composition as the type of used lipids, surfactants and incorporated actives (Zielińska and Nowak, 2016). Vegetable oils are important raw materials as they present several inherent beneficial properties for the skin and are abundant renewable resources (Lacatusu et al., 2014). These type of oils are commonly used in dermal formulations however, their use in the formulation of lipid nanoparticles are still underexplored. Moreover, there are several reports focusing the encapsulation of a certain bioactive compound into lipid nanoparticles, but only few studies addressed the effects of these ingredients on their formulation and resultant properties. Currently, research is still being done to develop new bioactive lipid nanocarriers with wide spectrum health benefits and enhanced delivery properties based in the use of appropriate renewable ingredients. A rational approach for designing and optimizing dermal formulations requires well-defined skin models, able to identify and evaluate the intrinsic properties of the formulation. Once the key formulation features that contribute for the absorption of the active substance are determined, the final optimization of the formulation becomes feasible.

In this work, the use of bioactive ingredients, as vegetable oils and their effects in lipid nanoparticles properties was studied, in order to develop and optimize new formulations for the effective topical administration of active compounds.

1.2. Research Objectives

Although a considerable effort has been put in the formulation of lipid nanoparticles for topical delivery, which is translated by the large number of publications in this subject, there are still enormous challenges to be unravelled.

The finality of this thesis was to develop a new formulation of lipid nanoparticles, through the miniemulsions methodology, by studying and optimizing the effects of their ingredients in their composition and physicochemical properties to achieve more efficacy on skin and an enhanced dermal delivery of lipophilic active compounds. Thus, the two major goals of this thesis were:

(1) to suitably design and optimize the composition of lipid nanoparticles, aiming at understanding the effects of the interaction between their different ingredients for achieving a biocompatible formulation presenting ideal physicochemical properties, high incorporation and protection of lipophilic active substances and an efficient skin absorption profile for topical administration.

(2) to evaluate the intrinsic properties of the developed formulation of lipid nanoparticles, in a well-defined skin model thus avoiding the use of animal models or human explants, in order to identify and adjust some key formulation parameters regarding their skin efficacy and safety.

1.3.   Research Strategy

A research strategy with specific objectives was outlined, in order to fulfil the two proposed major goals. In a first approach, it was essential to conceive an adequate procedure for the production of lipid nanoparticles based in the miniemulsions methodology. Thus, the emulsification step was tested using two techniques, as ultrasounds and magnetic stirring, for the production of SLNs, using lauric acid (C12:0) as solid lipid, which were mainly characterized regarding their particle size, polydispersity index (PdI) and surface charge. Moreover, the effect of formulations composition in the properties of SLNs was assessed in terms of solid lipid, wt%: surfactant, wt% (SL:S) ratio. SLNs produced by ultrasounds achieved better results for all tested formulations, and thus this technique was then selected for the emulsification step. The methodology conditions established in the preparation of SLNs were tested for the production of NLCs using sunflower oil and likewise, the effect of formulations composition in the properties of formulated nanoparticles was assessed in terms of total lipids, wt%: surfactant, wt% (TL:S) ratio. In order to evaluate the entrapment capacity of both types of formulated lipid nanoparticles, β-carotene (BC) and retinyl palmitate (RP) were used as lipophilic antioxidant drug models to be incorporated in SLNs and NLCs, respectively. Moreover, the effect of an increase in RP concentration was analysed regarding the particle size, PdI and surface charge of NLCs.

In a second stage of this work, having set the parameters for the production of lipid nanoparticles, it was then required to focus on the optimization of the formulation composition. Four chemically different vegetable oils, namely sunflower (SF) oil, olive (OV) oil, sweet almond (SA) oil and coconut

(CO) oil, that present a bioactive behaviour were selected to study the influence of oil content and composition on mean particle size, PdI values and zeta potential of NLC formulations prepared with myristic acid (C14:0) as solid lipid and a constant concentration of Tween 80 as surfactant. The results showed that in general, the average size of the vegetable oil NLCs decreased with the increase in the liquid oil percentage, which were consistent to what is described in the literature. Based on the obtained results, a constant solid lipid, wt%: vegetable oil, wt% ratio of 40:60 was defined and was used to evaluate the effect of the solid lipid fatty acids chain length on mean particle size, PdI values and zeta potential of NLCs prepared with a constant concentration of Tween 80 as surfactant. According to the results, it was observed that the NLCs particle size increased with the increase in the solid lipid fatty acid fatty acid chain length from C16:0 and C18:0. Thus, myristic acid (C14:0) was selected as solid lipid to study the influence of the type of surfactant in the NLCs properties, as average particle size, PdI values and zeta potential. It was established that the formulations of NLCs prepared with surfactants presenting a lower hydrophilic lipophilic balance (HLB) value, as Span 60 and Span 80 obtained the highest zeta potential values and consequently higher electrostatic stability when compared with those prepared with Tween 80 and Poloxamer 188, presenting a higher HLB value and consequently a more hydrophilic nature. With the view to have a complementary visual analysis, the morphology and internal structure of NLCs was performed by transmission electron microscopy (TEM) using SF oil and myristic acid in a 40:60, solid lipid, wt%: vegetable oil, wt% ratio and each surfactant, Span 80, Tween 80 and Poloxamer 188.

Since the effects of the ingredients in the NLCs composition and properties of empty NLCs have been characterized, at this point was also crucial to evaluate the encapsulation efficiency (EE, %) and drug loading capacity (DL, %) for a lipophilic active compound using the studied formulations. Thus, α-Tocopherol (TOC) was incorporated into NLCs formulations using three different concentrations. The physicochemical properties of these lipid nanoparticles were evaluated regarding their particle size and surface charge. Moreover, an equilibrium dialysis method was used to study the release behaviour of TOC-NLCs prepared with each vegetable oil and an analysis by differential scanning calorimetry (DSC) was performed to evaluate the changes on the crystalline state of empty NLCs and TOC-NLCs. In order to demonstrate the capacity of empty NLCs and TOC-NLCs being incorporated into stable dermal formulations, the effect of storage time on the stability of these nanoparticles was also investigated at room temperature over 4 and 8 months after their initial preparation. Given the well-recognised antioxidant properties and the protective function in human skin against oxidative stress of TOC and vegetable oils used in the preparation of NLCs formulations, it was imperative to evaluate the *in vitro* antioxidant activity of these ingredients individually and in the nanoparticles.

Aiming at an extensive comprehension of the effects of formulation parameters on NLCs properties, a different approach based on a statistical tool was used for the optimization of these nanoparticles for topical administration. A 5-factor, 3-level central composite design was applied to optimize the selected dependent response variables as the particle size, ZP and EE, %, in function

of the independent variables, as the number of carbons in the solid lipid fatty acid chain and concentration of total lipids, solid lipid, surfactant and incorporated drug. These independent factors were studied at three different levels, in a total of 31 experiments generated by the software STATISTICA 10, and each experiment was performed in triplicate and randomly to minimize the effects of variability from systematic errors. Based on previous results, the nanoparticles were formulated using SF oil as liquid lipid, varying the solid lipid chain length using capric acid (C10:0), myristic acid (C14:0) and stearic acid (C18:0), using Tween 80 as surfactant and RP as a lipophilic model drug. Having achieved an optimized NLCs formulation, it was then interesting to evaluate the capacity of these nanoparticles to incorporate another two retinoids besides RP, as tretinoin (TRT) and adapalene (ADP). Then, the optimized NLCs composition was adjusted by changing the type of surfactant to Span 80, in order to improve the electrostatic stability of the lipid nanoparticles and the solid lipid to myristic acid, with the view to guarantee that the melting point of the nanoparticles was set above 40ºC, which is considered as a pre-requisite for topical delivery. After the incorporation of each retinoid, the resultant RP-NLC, TRT-NLC and ADP-NLC dispersions were characterized in terms of particle size, morphology, surface charge, entrapment efficiency and drug loading capacity, crystallinity of the lipid matrix and *in vitro* release profile through an equilibrium dialysis method.

After the extensive optimization study of the production and formulation parameters of NLCs, the final stage of this work consisted in the evaluation of the efficacy for topical administration of the optimized lipid nanoparticles through an *in vitro* reconstructed human epidermis (RHE) model. The optimized NLCs formulations were produced using sunflower oil and myristic acid as liquid and solid lipids, respectively and RP and TOC as lipophilic model drugs. Also, the fluorescent dye DiO was incorporated along with TOC, resulting in the TOC-DiO-NLCs formulation to enable a qualitative characterization of the *in vitro* absorption studies. The physicochemical characteristics of empty NLCs, RP-NLCs and TOC-DiO-NLCs were characterized, as particle size, zeta potential, entrapment efficiency, drug loading capacity and crystallinity of the lipid matrix. Moreover, their surface morphology and their internal structure were also analyzed by atomic force microscopy and by transmission electron microscopy. *In vitro* absorption studies were performed for RP-NLCs and TOC-DiO-NLCs in customized Franz diffusion cells, through the RHE model and characterized quantitatively by HPLC analysis and qualitatively characterized by fluorescence microscopy and confocal laser scanning microscopy (CLSM). Finally, the *in vitro* skin irritation test on the RHE was also performed for empty-NLCs, RP-NLCs, TOC-NLCs and individually for their ingredients as standards and demonstrated that the produced nanoparticles formulations were non-irritants.

The thesis specific objectives are as follows:

(1) *Production of lipid nanoparticles based in the miniemulsions methodology:*

    1.1. Test two types of emulsification techniques, as ultrasounds or magnetic stirring in the production of SLNs in terms of particle size and surface charge;

1.2. Study the effect of formulations composition in terms of SL:S ratio for SLNs and in terms of TL:S ratio for NLCs, regarding their particle size, PdI values and surface charge;

1.3. Test the entrapment capacity of SLNs and NLCs using BC and RP, respectively as lipophilic antioxidant drug models.

(2) ***Optimization of NLCs composition***

2.1. Study the influence of oil content and composition, using four different vegetable oils in the NLCs physicochemical properties, as average particle size, PdI values and zeta potential;

2.2. Evaluate the effect of the solid lipid fatty acids chain length from C12:0 to C18:0 in the NLCs properties;

2.3. Assess the influence of the type of surfactant in the NLCs properties and complementary in their morphology and internal structure;

2.4. Evaluate the encapsulation efficiency (EE, %) and drug loading capacity (DL, %) of the studied NLCs formulation for TOC;

2.5. Characterize the TOC-NLCs formulations prepared with each vegetable oil regarding their physicochemical properties;

2.6. Study the release behaviour of TOC-NLCs through an equilibrium dialysis method;

2.7. Analyse the changes on the crystalline state of empty NLCs and TOC-NLCs by DSC;

2.8. Assess the effect of storage time on the stability of NLCs at room temperature over 4 and 8 months after their initial preparation;

2.9. Evaluate the *in vitro* antioxidant activity of NLCs formulations and individually, of their ingredients;

(3) ***Maximization of the efficiency of NLCs aiming their topical administration***

3.1. Study the effects of formulation parameters on the properties of NLCs prepared with RP as a lipophilic model drug using a statistical tool;

3.2. Evaluate the capacity of the optimized NLCs formulation with RP to incorporate separately other two retinoids as TRT and ADP;

3.3. Characterize the resultant RP-NLC, TRT-NLC and ADP-NLC dispersions in terms of particle size, morphology, surface charge, entrapment efficiency and drug loading capacity, crystallinity of the lipid matrix and *in vitro* release profile through an equilibrium dialysis method.

(4) ***Assessment of the efficacy for topical administration of the optimized NLCs***

4.1. Characterize the optimized NLCs formulations produced using sunflower oil and myristic acid as liquid and solid lipids, respectively and RP and TOC as lipophilic model drugs

regarding their particle size, zeta potential, entrapment efficiency, drug loading capacity, crystallinity of the lipid matrix, surface morphology and internal structure;

4.2. Incorporate the fluorescent dye DiO along with TOC to enable a qualitative characterization of the *in vitro* absorption studies;

4.3. Study the *in vitro* absorption of RP-NLCs and TOC-DiO-NLCs in Franz diffusion cells through an *in vitro* 3D RHE model, quantitatively by HPLC and qualitatively by fluorescence microscopy and CLSM;

4.4. Assess the *in vitro* skin irritation using the RHE model for empty-NLCs, RP-NLCs and TOC-NLCs and individually for their ingredients as standards.

1.4. Thesis Structure

This thesis is composed of seven chapters, including the current introductory chapter describing the motivation and outline of the developed work (**Chapter 1**). The remaining chapters include: an overview of the state of the art in trends and applications of nanotechnology for topical delivery, more particularly on lipid nanoparticles, with a thorough overview of their composition and structure, production and characterization methods and their effects and performance on skin (Chapter 2); 4 chapters (Chapters 3 to 6) describing the developed work in accordance with the specific objectives outlined above; and a final chapter summarizing the main conclusions achieved from this study (Chapter 7).

The State of the Art (**Chapter 2**) starts by addressing the importance of nanotechnology in topical delivery, thus introducing the main types and characteristics of lipid nanocarriers that are currently used in dermal formulations. It then focuses particularly on lipid nanoparticles, describing the different types and categories of ingredients used in their formulation and that modulate their composition and structure, including the active compounds used in dermal formulations. The second and core section of Chapter 2 also overviews, the production methods that are applied for the preparation of lipid nanoparticles at lab and industrial scale and their characterization methods that enable an accurate analysis of their physicochemical properties. Lastly but not least, important aspects describing skin properties as a natural barrier for the permeation of external compounds, the effects of lipid nanoparticles and their mode of action on skin and the use of *in vitro* reconstructed human epidermis models to study these effects are further addressed.

Chapter 3 describes the first stage of this work that consisted on the evaluation of the miniemulsions methodology potential for the production of both types of lipid nanoparticles, SLNs and NLCs, using lauric acid (C12:0) as solid lipid. Two emulsification techniques, as ultrasounds and magnetic stirring were tested for SLNs production and the effect of formulations composition in the properties of formulated nanoparticles was then assessed in terms of SL:S ratio in the case for SLNs

and in terms of TL:S ratio in the case of NLCs. Also, the influence of an increase in the concentration of loaded active compound on NLCs formulated with sunflower oil was analysed. Finally, the encapsulation efficiency of SLNs and NLCs was determined using BC and RP as lipophilic antioxidant drug models, demonstrating that BC and RP were successfully encapsulated in the lipid nanoparticles matrix, having been reached high entrapment efficiency values for both BC-SLNs and RP-NLCs.

Chapter 4 focuses on work carried out in the optimization of NLCs formulations using different types of vegetable oils, namely sunflower oil, coconut oil, sweet almond oil and olive oil that are commonly used in dermal formulations due to their inherent and recognized beneficial properties for skin. The influence of each vegetable oil composition and proportion in the preparation of NLCs using Tween 80 as a surfactant and myristic acid (C14:0) as a solid lipid were evaluated in terms of particle size and physical stability and likewise, the influence of an increase in the solid lipid fatty acid chain length and the type of used surfactant were analysed. Then, the vegetable oil NLCs were enriched with TOC, to evaluate the incorporation capacity of this lipophilic vitamin into the lipid matrix of the nanoparticles and a differential scanning calorimetry (DSC) analysis was performed to investigate possible changes in the crystalline state of free NLCs and TOC-NLCs formulated using the selected vegetable oils with 2, 3 and 4 wt% of TOC. An equilibrium dialysis method, performed assuring sink conditions was used to study the release behaviour of TOC-NLCs prepared with each vegetable oil and of a pure solution of TOC in water: ethanol (1:1 v/v) that was used as reference. At this point, the effect of storage time on the electrostatic stability was also evaluated by analysing the changes in particle size and surface charge of free NLCs and TOC-NLCs prepared with each vegetable oils and 2 wt% of TOC. Lastly, the *in vitro* antioxidant activity of empty NLCs and TOC-NLCs was assessed, as the scavenging capacity of a pure TOC solution and of each vegetable oil used in the preparation of the lipid nanoparticles that were used as reference.

Chapter 5 describes the systematic optimization of the NLCs composition performed using a statistic tool, namely the "central composite design", aiming at reach a new formulation of lipid nanoparticles for the topical administration of retinoids. The most critical independent variables were selected, as the total concentration of lipids, the concentration of solid lipid, surfactant, drug loaded, and the number of carbons in the solid lipid fatty acid chain. Upper, middle and lower concentration levels of these formulation variables were set in function of particle size, surface charge and entrapment efficiency percentage. An optimal composition of 2.5% of total lipids, comprising 2.0% of myristic acid and 0.5% of sunflower oil and 1.5% of surfactant was effectively formulated and tested for the incorporation of RP, TRT and ADP. The three formulations of RP-NLCs, TRT-NLCs and ADP-NLCs were characterized regarding their particle size, morphology, surface charge, entrapment efficiency and drug loading capacity, crystallinity of the lipid matrix and *in vitro* release profile through an equilibrium dialysis method.

In **Chapter 6**, the performance of optimized RP-NLCs and TOC-NLCs formulations with sunflower oil and myristic acid was evaluated through *in vitro* skin absorption studies developed in Franz diffusion cells and by *in vitro* skin irritation tests, using an *in vitro* RHE model. The fluorescent

dye DiO was incorporated along with TOC in the NLCs optimized formulation to enable a qualitative characterization of the *in vitro* absorption studies trough fluorescence microscopy and confocal laser scanning microscopy. Physicochemical characteristics as particle size, zeta potential, entrapment efficiency, drug loading capacity and crystallinity of the lipid matrix of empty NLCs, RP-NLCs and TOC-DiO-NLCs were characterized, as also their surface morphology, by atomic force microscopy and their internal structure, by transmission electron microscopy.

Chapter 7, summarizes the main achieved conclusions from the developed work. The main achievements, and scientific contributions to the field of lipid nanoparticles formulation and optimization are described. In the perspective of this work continuity, the future perspectives are outlined.

◢ CHAPTER II

STATE OF THE ART

2.1.   Nanotechnology in topical delivery: trends and applications

2.2.   Lipid nanoparticles for the dermal delivery of active compounds

2.3.   Efficacy of lipid nanoparticles for topical administration

2. State of the art

2.1. Nanotechnology in topical delivery: trends and applications

Nanotechnology is a fundamental science that has been consolidated during the twenty-first century in designing, characterizing, and using materials, devices and systems in the nanometre size range, with versatile industrial applications (Guimarães and Ré, 2011, Severino et al., 2016, Yan et al., 2014). There are several innovative applications of nanotechnology in the cosmetic and dermal pharmaceutical industries which have transformed the administration of active compounds and represent outstanding opportunities for both academic and industrial fields (Jain, 2008, Montenegro et al., 2016).

Topical formulations of nanocarriers have been used for an improved delivery of active substances through and inside the skin mostly due to their several advantages over conventional passive delivery systems as skin hydration, increased surface area, smoothness, softness, adhesiveness, occlusion, higher solubility, site-targeted delivery, improved stability, controlled release, reduced skin irritancy, protection from degradation and increased drug loading (Abla et al., 2016, Escobar-Chávez et al., 2012, Mihranyan et al., 2012). Several studies have been conducted by the pharmaceutical industry for the development of nanocarriers for skin delivery. However, the major impact of nanotechnology in this field has perhaps occurred in the cosmetic industry having in consideration the number of patents registered/issued and the growing list of cosmetic products available in the market (Abla et al., 2016, Mishra et al., 2009). The patent records provide a useful source to understand in which area the nanocarriers technology is being used and what types of nanocarrier are mainly employed **Figure 2.1** (Poland, 2016). In a study published by the Danish Environmental Protection Agency (Poland, 2016), a total of 181 patents are reported concerning the use of nano-enabled technologies of which 165 patents (91%) had direct application in cosmetics.
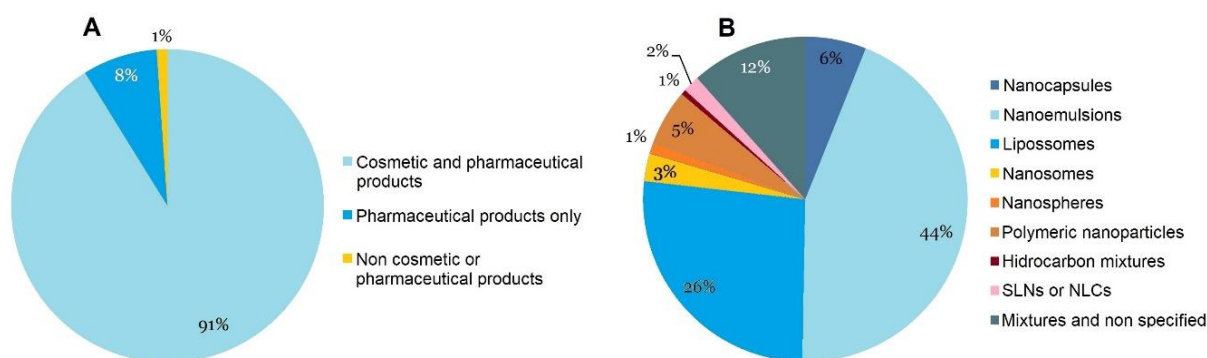
Figure 2.1 – Results regarding the field of application (A) and the type (B) of nanocarriers reported in patents. Adapted from (Poland, 2016).

Several approaches addressing nano-enabled technologies have been developed in order to increase drug bioavailability and to enhance its absorption or permeation in the skin (Severino et al., 2016). The size of these nanocarriers is the characteristic that confers them more efficiency than currently available formulations (e.g. O/W and WO emulsions) and also determines their effectiveness and targeted delivery (Montenegro et al., 2016). The application of nanocarriers into cosmetic and pharmaceutical products offers several advantages as the possibility to protect active substances from degradation, to encapsulate poorly water-soluble compounds and to confer a controlled release which avoids repeated administrations and promotes patient compliance (Garcês et al., 2017, Souto et al., 2007).

Nanotechnology has revolutionized the design of topical formulations by generating innovative, safe and effective products and patent applications that are currently increasing and represent an extraordinary alternative to existing market formulations.

The types of nanocarriers that are currently being study for topical administration are the liposomes (Jose et al., 2018), lipid nanoparticles (Alvarez-Trabado et al., 2017, Pathan et al., 2018, Puglia et al., 2017, Teeranachaideekul et al., 2017), nanoemulsions (Tamayo et al., 2017), polymeric nanoparticles (Sahle et al., 2017), hydrogels (Paolicelli et al., 2017) and microneedles (Arya et al., 2017). The physicochemical and biological properties of these nanocarrier structures and systems substantially varies in terms of their ingredients and production methods, thus providing numberless and unique functional applications. **Table 2.1** summarizes important characteristics of the most used lipid nanocarrier systems in dermal formulations, as liposomes, micro and nanoemulsions and lipid nanoparticles, which will be further discussed in more detail.

2.1.1. Types and characteristics of lipid nanocarriers for topical administration

Lipid nanocarriers as drug delivery systems (DDS) are designated as a formulation or a device that assists the introduction of an active compound in the body and improves its efficacy and safety by protecting it from biological degradation and controlling their delivery (Jain, 2008a, Poland, 2016). This group of DDS is diversely variable regarding the composition of each lipid nanocarrier which can differ distinctly and may include polymers and surfactants in addition to lipids (Poland, 2016).

Lipid nanocarriers can be tailored based on their architecture and particle size to meet a wide range of product requirements that are dictated by disease condition, route of administration and considerations of cost, product stability, toxicity and efficacy. These nanocarriers can be applied in a wide spectrum of administration routes and are good candidates for the formulation of cosmetics, pharmaceuticals, food supplements and vaccines (Shrestha et al., 2014).

Different types of lipid based nanocarriers include liposomes, niosomes, lipid nanoparticles as SLNs and NLCs, nanoemulsions, nanospheres/nanocapsules, among others, which are classified based on its structure and within these different types, they differs in terms of their specific

composition (Attama et al., 2012). **Figure 2.2** shows some examples of the different types of lipid based nanocarriers and their main advantages.
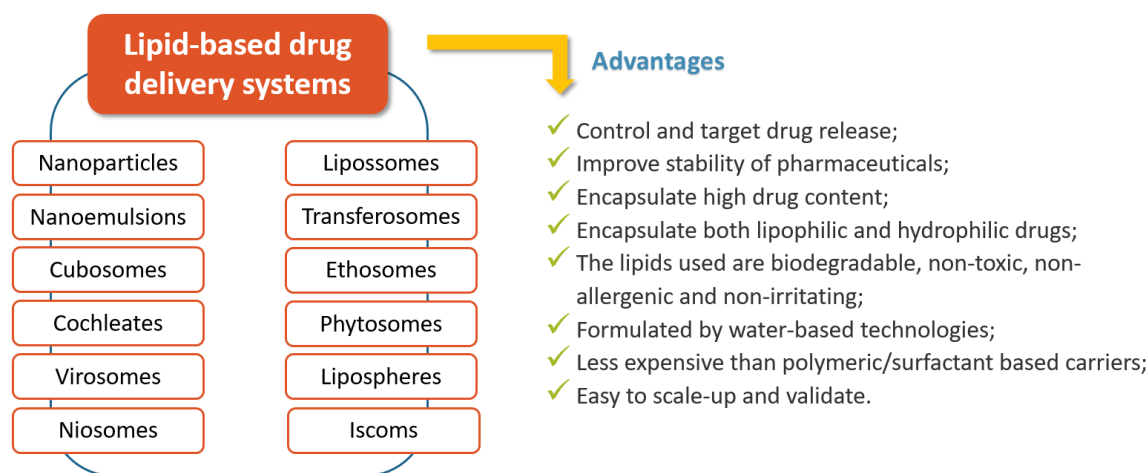
Figure 2.2 – Types of lipid based nanocarriers and their main vantages. Adapted from (Attama et al., 2012).

2.1.1.1. Liposomes

Lipossomes are defined as amphiphilic vesicular structures formed by bilayers of hydrated phospholipids (**Figure 2.3, A**). The bilayers are separated from one another by aqueous domains and under the critical micelle concentration are able to organize themselves spontaneously into closed spherical shell-type structures enclosing an aqueous core (Attama et al., 2012, Severino et al., 2016). The resultant vesicular structure is a liposome when phosphatidylcholine, phosphatidylserine, or phosphatidylethanolamine are used as phospholipids (Severino et al., 2016). Liposomes are the first class of lipid nanocarriers developed by Bangham (Bangham and Horne, 1964) as drug delivery systems (Abla et al., 2016) and consequently, the most popular methodology for the production of liposomes was the thin-film hydration or Bangham method in which a mixture of phospholipids and cholesterol were dispersed in organic solvent and then, the organic solvent was removed by means of evaporation using a rotary evaporator (Laouini et al., 2012b).

Due to their amphiphilic character, liposomes are able to transport hydrophilic and lipophilic active compounds and its basic structure of hydrated phospholipid bilayers is versatile to extensive modifications allowing their use in various applications such as cosmetology, radiology and vaccinology (Attama et al., 2012). It is possible to obtain small unilamellar vesicles (SUV) with dimensions of 20 up to 100 nm, large unilamellar vesicles (LUV) which are larger than 100 nm, and multilamellar vesicles (MLV) with dimensions exceeding 500 nm to a few microns, depending on the method of preparation, process and excipients selected for the manufacture (Abla et al., 2016, Korting and Schäfer-Korting, 2010).

Lipossomes have been used to improve the incorporation of active substances through the skin and to provide a controlled release for topical applications (Mezei, 2017). Current research are being developed regarding the application of liposomes as carriers for topical administration. Dorrani et al. 2016, reported the topical delivery of siRNA which presents several therapeutic applications in various dermatological diseases such as psoriasis, atopic dermatitis, and cancer (Dorrani et al., 2016). Jøraholmen et al., 2015 studied the release and permeation of resveratrol for topical vaginal formulations due to its biological activities against the pathogens of sexually transmitted diseases (Jøraholmen et al., 2015). Also, the prevention of skin aging and pigmentation by the topical delivery of hyaluronic acid and naringenin (Tsai et al., 2015, Vázquez-González et al., 2015) and the treatment of cutaneous fungal infections and leishmaniasis by the topical delivery of amphotericin B (Perez et al., 2016) were reported.
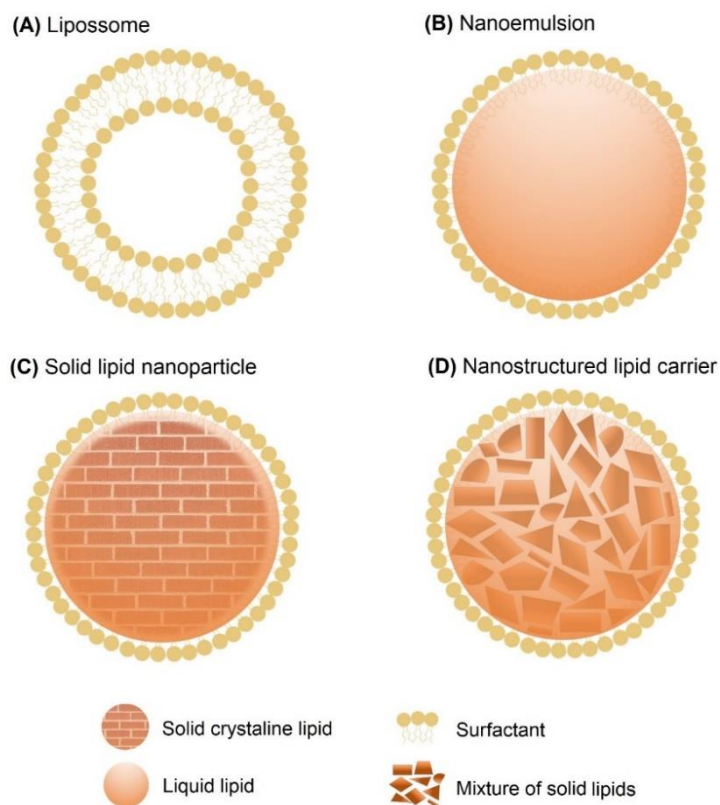
Figure 2.3 – Lipid nanocarriers that have been described in the literature for topical administration. Adapted from (Morales et al., 2015)

2.1.1.2. Micro- and Nanoemulsions

In 1959, Schulman et al. (Schulman et al., 1959) has first described the term microemulsion to define a transparent, optically isotropic and thermodynamically stable Newtonian non-viscous liquid

system composed of colloidal oil droplets dispersed in an immiscible aqueous medium, stabilized by surfactants (Montenegro et al., 2016, Morales et al., 2015). However, these systems were later designated as nanoemulsions (**Figure 2.3, B**) as the droplet sizes were in the nanometre range (Azeem et al., 2009). Both micro- and nanoemulsions have droplet sizes from 10 to 100 nm, differing mainly in their physicochemical characteristics (Poland, 2016).

Microemulsions are thermodynamically stable and can be formed spontaneously, without the use of high shear equipment, or with a very low energy input but they require a higher concentration of surfactant (Korting and Schäfer-Korting, 2010). On the contrary, nanoemulsions are metastable systems being kinetically but not thermodynamically stables and their characteristics mainly depends on the preparation methods, which usually require high-energy inputs and lower concentrations of surfactants (Korting and Schäfer-Korting, 2010, Montenegro et al., 2016). High energy methods result from the use of equipments such as high-shear stirrers, high pressure homogenizers, ultrasonic homogenizers and others to generate intense shearing forces that mix both aqueous and oil phases and break the droplets into smaller structures (Morales et al., 2015, Qian and McClements, 2011). Micro- or nanoemulsions can be formed by low energy methods by the rapid diffusion of the surfactant from the dispersed phase to the continuous phase and depends on the spontaneous formation of nanodroplets under specific compositions or environmental conditions resultant from changes on its interfacial properties (Ostertag et al., 2012).

The lipid phase of micro- or nanoemulsions is generally composed by natural or synthetic oils (e.g., Witepsol® [Cremer Oleo Divisions], Myritol® [BASF, Ludwigshafen, Germany], isopropyl myristate and Miglyol, among others) while the aqueous phase consists of water, surfactants (e.g., polysorbate, Gelucire® [Gattefosse]) and optionally co-surfactants (e.g. PEG, glycerin and ethylene glycol) which may act as as penetration and occlusive enhancers (Korting and Schäfer-Korting, 2010, Poland, 2016, Sharma and Sarangdevot, 2012).

Due to their sensorial and biophysical properties, nanoemulsions can be stable for 15 years as indicated by Li et al. 2011 (Li et al., 2011a), conferring them a great potential to be used as carriers of active cosmetic ingredients (Poland, 2016). Several research works were currently developed using nanoemulsions for topical applications. Argenta et al. 2018 developed a formulation with coumestrol which is an isoflavonoid-like compound and inhibit Herpes Simplex Virus types 1 (HSV-1) and 2 (HSV-2) replication, to tissues (Argenta et al., 2018). Choi et al. 2017, suggested a strategy for promoting the healing process and skin regeneration in wound management by developing a topical a DDS consisting of a nanoemulsion-dispersed polyvinylpyrrolidone hydrogel loaded with three growth factors (Choi et al., 2017). The topical delivery of the powerful antioxidant coenzyme Q10, which is crucial for cellular energy production and is low regenerated by skin after a certain age was investigated by Kaci et al. 2018 (Kaci et al., 2018). Also, the prevention of premature of skin aging characterized by dry and rough skin, wrinkles and black spots was studied by Pratiwi et al. 2017 through the development of a self-nanoemulsifying drug delivery system (SNEDDS) of mangosteen peels for topical administration (Pratiwi et al., 2017).

2.1.1.3. Solid lipid nanoparticles (SLN)

The history of lipid nanoparticles started around the 90´s, and at the beginning, different names were used as lipid nanospheres (Müller, 1991) and even lipid microparticles or microspheres (Gasco, 1993, Gasco, 2002) to designate solid lipid nanoparticles (SLNs) (**Figure 2.3, C**) which was then the name assigned by the inventors to describe a type of nanocarriers structurally similar to nanoemulsions but containing a solid matrix composed by a solid lipid (Muller et al., 2011). These nanocarrier systems were first developed as an efficient alternative to traditional carriers as emulsions, liposomes, and polymeric nanoparticles and explored to avoid some of its issues in biological media (Severino et al., 2016).

SLNs are described in literature as the first generation of lipid nanoparticles and are defined as colloidal spherical particles with sizes ranging from 40-1000 nm, composed by solid lipids, dispersed in an aqueous phase and stabilized by surfactants (Abla et al., 2016, Keck et al., 2014, Muller et al., 2011, Zielińska and Nowak, 2016). SLNs are produced using one crystalline solid lipid or a mixture of solid lipids, as glycerides or waxes in concentrations typically varying from 0.1 to 30% w/w and surfactants in contents ranging from 0.5 to 5% w/w (Abla et al., 2016, Zielińska and Nowak, 2016). An important prerequisite of the lipids is that they should be solid at 37ºC that is considered as the body temperature (Müller et al., 2016) and more than one surfactant can be used to prevent aggregation of particles in the dispersions (Zielińska and Nowak, 2016). Similarly to nanoemulsions, SLNs are obtained by replacing the oil phase of the emulsion (O/W) by the solid lipid or a mixture of solid lipids. The incorporation of active substances occurs by melting the solid lipid and dissolving or suspending the drug in the melted lipid. Then, the droplets of melted lipid recrystallize and self-assemble typically yielding a mixture of high-energy crystallized form (α and β′), and low-energy form (β′) lipid modifications. However, during storage the lipid molecules incline to increase their order and convert from α/β′ to β modification which can lead to a subsequent decrease in imperfections of the lipid matrix lattice and consequently occurs the loss or leakage of active substance from the nanocarrier (Abla et al., 2016, Müller et al., 2016). The main advantages of SLNs are their physicochemical stability, providing higher protection for incorporated active substances from chemical and physical degradation and the controlled release and transport of drugs to target sites, consequently increasing its bioavailability and efficacy (Souto et al., 2013). Also, the use of biocompatible solid lipids is a great benefit which allows to encapsulate generally lipophilic drugs on SLNs crystalline matrix lattice, on its lipid layers and or between the chains of fatty acids (Severino et al., 2016). The most commonly well described method used to produce SLNs is the high-pressure homogenization which permits the manipulation of particle size according to the desired application or route of administration (Morales et al., 2015). Moreover, the release profile of the encapsulated drugs can be adjusted for a specific application through the selection of a specific combination of lipids and fatty acids (Müller et al., 2002a, Severino et al., 2016).

According to the chemical structure of the encapsulated active and the production method, SLNs can be divided into three basic types. The SLN type I (**Figure 2.4**) is characterized by a homogeneous matrix model since there is a uniform molecular distribution of the active ingredient in the whole volume of the lipid core (Korting and Schäfer-Korting, 2010, Zielińska and Nowak, 2016). This type is usually obtained by high pressure homogenization using optimized ratios of active compound and lipid above its melting point, or even by cold homogenization and its structure enables controlled release properties (Souto and Müller, 2007).

The SLN type II (**Figure 2.4**) is obtained when a low concentration of the active substance is melted in the lipid and remains in the outer part of the nanoparticles. During the cooling step after homogenization of the nanoemulsion, occurs the precipitation of the lipid phase forming a solidified lipid core which pushes the active substance in the remaining melted lipid to an outer shell. Thereby, this nanoparticles model is more appropriate to obtain a burst release of the drug and also good occlusive properties of the lipid matrix (Korting and Schäfer-Korting, 2010).

In the SLN type III (**Figure 2.4**), there is a high concentration of active compound within the core of the nanoparticles which is formed when the drug concentration is almost at the saturation solubility level in the melted lipid. At the cooling step of the nanoemulsion, after the saturation solubility level of the active substance being exceeded it occurs its precipitation which is enclosed by a shell of lipid. This SLN model is more advantageous in applications that requires a very well-controlled release of the active compound, once it is well encapsulated within the lipid core (Zielińska and Nowak, 2016).
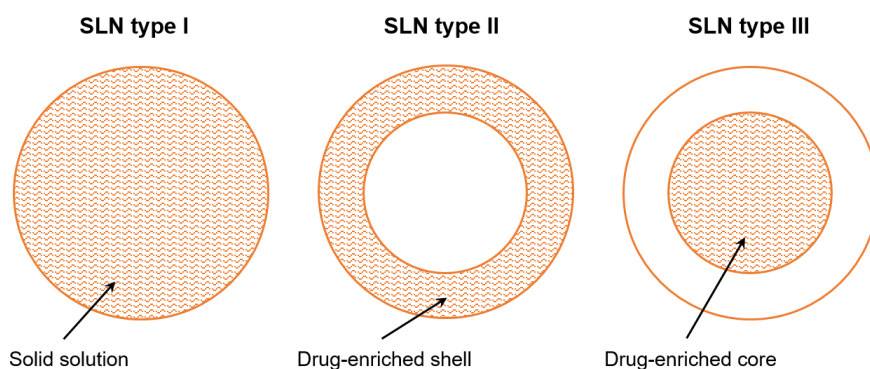
Figure 2.4 – Types of solid lipid nanoparticles (SLNs). Adapted from (Zielińska and Nowak, 2016).

The research work on topical applications of SLNs that is currently being developed are focused on the encapsulation of anti-inflammatory drugs (Daneshmand et al., 2018, Peng et al., 2017), sunscreens (Netto MPharm and Jose, 2017, Souza and Campos, 2017), antibiotics (Severino et al., 2017, Valdes et al., 2018), anti-aging cosmetic actives (Chen et al., 2017, Rocha et al., 2017), elasticity and hydration enhancers (Marto et al., 2017) and on the increase of skin permeability (Montenegro et al., 2017).

2.1.1.3. Nanostructured lipid carriers (NLC)

A new generation of lipid nanoparticles was introduced in late 90´s by Muller et al. (Muller et al., 1999), derived from SLNs, to overcome their main limitations related to low drug capacity and its loss or leakage from the nanocarrier during storage (Abla et al., 2016, Montenegro et al., 2016, Müller et al., 2002a). The 2.0 version or 2nd generation of lipid nanoparticles, named as nanostructured lipid carriers (NLCs) (**Figure 2.3, D**) are composed by an unstructured solid lipid matrix consisting on a mixture of liquid and solid lipids dispersed in an aqueous phase containing a surfactant of a mixture of surfactants (Beloqui et al., 2016). Generally, the solid lipids are blended with the liquid lipids in ratios from 70:30 up to 99.9:0.1, while the surfactant concentration usually varies from 1.5% to 5% (w/v) (Pardeike et al., 2009). The incorporation of liquid lipids in the solid matrix results in a melting point depression compared to the pure solid lipid. Also, the addition of oils leads to a substantial crystal order disturbance producing a high number of imperfections in the crystalline lattice, which provides more space to accommodate active compounds, increase the drug loading capacity and avoids or reduces the drug expulsion during storage due to a higher drug incorporation capacity, in comparison with previous developed SLNs (Montenegro et al., 2016, Morales et al., 2015, Müller et al., 2016). However, despite the limited drug loading capacity of SLNs that often constrains the amount of active substance in relation to the amount of solid lipid, obtained encapsulation efficiencies for this type of lipid nanoparticles can reach very high values and usually exceeds 90% particularly with lipophilic actives (Korting and Schäfer-Korting, 2010).

In order to achieve a high degree of imperfections on the lipid crystal lattice, the lipid blends should comprise structurally different molecules as e.g. solid lipids with longer chain fatty acids and oils with shorter chain fatty acids. Nevertheless, when choosing the composition of the lipid blends it is necessary to have in consideration that the melting point of the blends still need to be above the body or skin temperature at 37ºC (Müller et al., 2016).

NLCs can be produced as SLNs by several methods described in the literature, through high-pressure homogenization (Moradi et al., 2017, Pang et al., 2017), microemulsion technique (Mojahedian et al., 2013, Qidwai et al., 2016), solvent emulsification evaporation method (Abdolahpour et al., 2017, Khan et al., 2016), membrane emulsification (Laouini et al., 2012a, Li et al., 2011b), supercritical fluid-based method (Hu et al., 2011, Santo et al., 2013a), ultrasonication (Lason et al., 2013, Rosli et al., 2015), among others.

Similarly to the 1st generation of lipid nanoparticles, NLCs can also be categorized in three incorporation types, mainly differing in the lipid blends used in their preparation. The NLC type I (**Figure 2.5**) is characterized by a highly disordered structure consisting in a lipid matrix presenting several crystal imperfections that is formed by mixing solid lipids with a low amount of oils (Souto and Muller, 2010, Zielińska and Nowak, 2016). The structurally different solid lipids used to prepare this nanoparticles model, varying on its fatty acids chain length, once blended with mono-, di- and

triacylglycerols, form structural imperfections that are able to very well-accommodate active substances (Müller et al., 2002a).

NLC type I   **NLC type II**   **NLC type III**

Solid lipids   Encapsulated drug   Solid lipid

Amorphous lipid   Oil nanocompartments
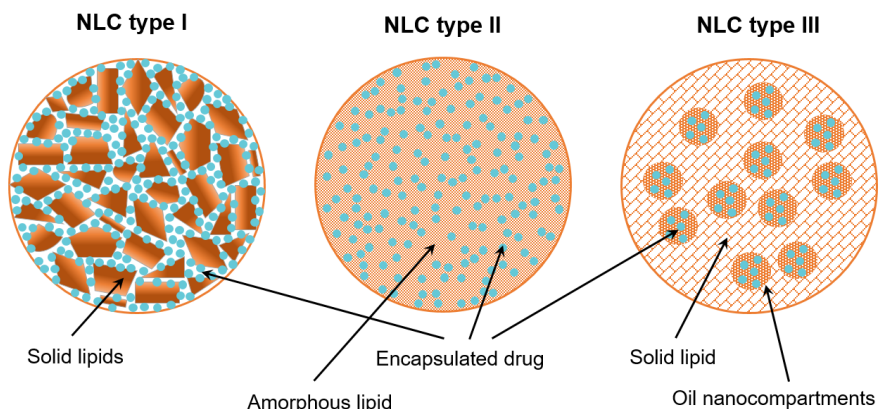
Figure 2.5 – Types of nanostructured lipid carriers (NLCs). Adapted from (Zielińska and Nowak, 2016).

The NLC type II (**Figure 2.5**) is composed by a structure less solid amorphous matrix which is obtained through the mixture of specific lipids (e.g. hydroxy octacosanyl hydroxyl stearate, isopropyl myristate and dibutyl adipate) that do not recrystallize after the nanoemulsion homogenization and cooling steps (Ganesan and Narayanasamy, 2017). The structure of this amorphous NLC matrix that avoid or delays the recrystallization of lipids, allows a reduction of active substance loss during the storage (Souto and Muller, 2010).

The NLC type III (**Figure 2.5**) is derived from the multiple water in oil in water emulsion (W/O/W) production method and results by the mixture of solid lipids with oils and long-chain triacylglycerols in such a ratio that the solubility of the oil molecules in the solid lipid is exceeded (Guimarães and Ré, 2011, Souto and Muller, 2010, Zielińska and Nowak, 2016). The lipid matrix of this NLC multiple model is composed of very small oily nanocompartments that are surrounded by the solid lipid core, which enables the advantage of an increase in the capacity to incorporate active ingredients (Ganesan and Narayanasamy, 2017, Souto and Muller, 2010).

Recent research works published in literature describe the use of NLCs form the topical delivery of active compounds as anti-allergenic substances (Surassmo et al., 2017), photosensitizers (Calixto et al., 2016, Md et al., 2017), antioxidants (Lasoń et al., 2017, Puglia et al., 2017), anti-inflammatory compounds (Abdel-Salam et al., 2017, Moghddam et al., 2017, Pivetta et al., 2018), anti-cancer drugs (Bhise et al., 2017, Carbone et al., 2018, Estanqueiro et al., 2017), analgesics and anaesthetics (Bakonyi et al., 2018, da Silva et al., 2017, You et al., 2017), compounds to treat or prevent alopecia (Kaur et al., 2017, Noor et al., 2017, Yazdani-Arazi et al., 2017), among others that serve a very wide range of applications.

The physicochemical and biological properties of these nanocarriers structure substantially vary in terms of their ingredients and production methods, thus providing numberless and unique functional applications. **Table 2.1** describes some important characteristics of the lipid nanocarrier systems that were previously addressed.

2.1.2. Lipid nanocarriers in dermal pharmaceutical products and cosmetics

There is a very thin line separating the application of lipid nanocarriers for dermal delivery in pharmaceutical products and cosmetics and despite the high resemblance there are a few differences mainly concerned with technical aspects (Poland, 2016). For instance, the time between production and market introduction of a dermal pharmaceutical product is much longer compared with a cosmetic due to very complex regulatory requirements (Puglia and Bonina, 2012). This is justified by the need of imperatively have a good understanding about the interaction of dermal formulations containing drug nanocarriers with the skin and their potential toxicological effects. It is obtained a higher degree of reliability for dermal pharmaceutical products which are validated and approved through rigorous clinical trials according specific application criteria (dose, area and duration of exposure, etc) (Poland, 2016, Weissig et al., 2014). In **Table 2.2** are listed some examples of marketed pharmaceutical products for dermal applications based on lipid nanocarriers.

In the past few years, there have been efforts to introduce in the market advanced cosmetics through the incorporation of active compounds, thus surpassing their main role as products for beauty care that serve the preservation, restoration or improvement of beauty in human body. For example, cosmetic products can offer protection against pathological lesions, or can be employed to prevent, treat, or alleviate diseases (Draelos, 2012). As such products are more than simply cosmetics, the term "cosmeceuticals" that combines the English terms "cosmetics" and "pharmaceuticals" was introduced to describe these hybrid products that have a positive effect on the skin, but not a medical-therapeutic effect (Lohani et al., 2014). However, the U.S. Food and Drug Administration does not recognize the "cosmeceuticals" category and labels them simply as cosmetics (Draelos, 2012, Lohani et al., 2014, Reszko et al., 2009). The cosmetic and pharmaceutical industries have devoted much attention to the development of "pharmacologically" active cosmetics and to cosmetically oriented medications, thus increasing the medical importance of cosmeceuticals (Kerscher and Buntrock, 2016).

Table 2.1 – Overview of some important lipid nanocarriers used in topical delivery. Adapted from (Poland, 2016).

Type of lipid nanocarrier	Size (nm)	Description	Advantages	Limitations
Lipossomes	20 – few hundred microns	Spherical, closed vesicular structures formed by bilayers of hydrated phospholipids enclosing an aqueous core	✓ Capacity to incorporate both hydrophilic and lipophilic active compounds ✓ Non-toxic, biocompatible, biodegradable, and non-immunogenic for systemic and non-systemic administrations ✓ Highly versatile for a wide range of applications ✓ Enhanced efficacy and therapeutic index of drugs ✓ Increased stability of encapsulated active compounds ✓ Able to reduce the toxicity of the encapsulated agent ✓ Flexibility to cope with site-specific ligands to achieve active targeting	✗ Low Solubility ✗ Short half-life ✗ Phospholipids can undergo oxidation and hydrolysis-like reaction ✗ Leakage and fusion of encapsulated molecules ✗ High production costs
Nanoemulsions	10 - 100	Colloidal oil droplets dispersed in an immiscible liquid	✓ Good substitute for liposomes and vesicles which are much less stable ✓ Small-sized droplets with enhanced surface area providing higher absorption, improving the bioavailability of encapsulated active compounds and increasing their stability ✓ Easy to be produced by non-toxic, biocompatible and biodegradable ingredients ✓ Possibility to be formulated as foams, creams, liquids, or aerosols ✓ High drug payloads ✓ Efficient delivery of active ingredients through the skin ✓ Enhanced stability of chemically unstable compounds ✓ Possibility of controlled drug release and drug targeting	✗ High energy inputs to reduce the droplets size ✗ Large concentration of surfactant and co-surfactant for stabilizing the nanodroplets ✗ Limited solubility capacity for high melting substances ✗ Nanoemulsions stability is influenced by environmental parameters such as temperature and pH

(Continued next page)

Table 2.1 (Continued)

Type of lipid nanocarrier	Size (nm)	Description	Advantages	Limitations
SLNs	80 - 1000	1st generation of lipid nanoparticles characterized by colloidal carriers with a lipid matrix composed by crystalline solid lipids dispersed in an aqueous media and stabilized by surfactants	✓ Molecular dispersion of the active substance in the lipid matrix, providing higher protection and resulting in a controlled release and high drug loading ✓ Particles in the nanometer size range, increasing the surface area ✓ Produced using generally recognized as safe (GRAS), with good biocompatibility and lower cytotoxicity ✓ Easy to scale up and sterilize with avoidance of organic solvents in the preparation process ✓ Wide potential of application spectrum due to the long term stability of nanoparticles	✗ Insufficient capacity for the active substance ✗ Leakage of encapsulated drug molecules resulting from the ordered crystalline structure of the solid lipid ✗ Tendency for particle growth during storage
NLCs	10 - 1000	2nd generation of lipid nanoparticles consisting in colloidal carriers composed by blends of liquid and solid lipids forming a less ordered lipid matrix	✓ Produced using GRAS ingredients, biocompatible and biodegradable ✓ Easy to scale-up and produce, with low costs and equipment requirements ✓ High loading capacity ✓ Excelent protenction of the active substance, preventing its expulsion from the lipid matrix ✓ Well-controlled drug release ✓ Long term-stability	✗ Relatively high content of dispersions ✗ Nanotoxicity associated to the use and concentration of some surfactants ✗ Low capacity to incorporate hydrophilic active compounds due to partitioning effects during preparation

Lipid nanoparticles are very effective carriers of active compounds used in cosmetics in order to moisturize the skin due to their occlusive properties, to improve skin elasticity due to their ability to increase skin hydration, to reduce wrinkles and to be used antioxidant agents in antiaging formulations (Mitrea et al., 2014, Müller et al., 2016, Pardeike et al., 2009, Souto and Müller, 2007, Zielińska and Nowak, 2016).These nanoparticles are also excellent carriers of perfumes and insect repellent thanks to their adhesive properties and the possibilities of sustained release (Guimarães and Ré, 2011, Mitri et al., 2011, Puglia and Bonina, 2012) and are commonly used in physical and chemical sunscreens since they can reflect radiation and produce a synergistic effect of protection, thus reducing the amount of incorporated UV filter which limits the possibility of irritation and also reduces the associated production costs (Zielińska and Nowak, 2016).

Table 2.2 – Examples of commercially available pharmaceutical products for dermal applications based on lipid nanocarriers. Modified from (Korting and Schäfer-Korting, 2010, Mansour et al., 2016, Patravale et al., 2012, Weissig et al., 2014).

Type of lipid nanocarrier	Commercial product name	Company	Active compound	Indication
Liposomes	Pevaryl® Lipogel	Janssen-Cilag, Switzerland	Ecosanole	Dermatomicoses
	Diclac® Lipogel	Hexal, Germany	Diclofenac sodium	Osteoarthritis or rheumatoid arthritis
	Visudyne®	Valeant Pharmaceuticals, Inc, Canada	Verteporfin	Pathological myopia, ocular histoplasmosis syndrome
	LMX®-4	Ferndale Laboratories	Lidocaine	Topical anesthesia
Nanoemulsion	Estrasorb®	Novavax, United States	Estradiol	Topical emulsion for the reduction of vasomotor symptoms
	Flexogan®	AlphaRx, Canada	Methyl salicylate, menthol, camphor	External Analgesic
	BF-200 ALA-gel	Biofrontera	5-Aminolevulinic acid	Actinic keratosis for photodynamic therapy
	Restasis®	Allergan	Cyclosporine	Chronic dry eye disease
Lipocomplex	Amphocil®	Sequus Pharmaceutical, United States	Amphotericin B	Severe fungal infections

The incorporation of lipid nanoparticles in cosmetics holds several advantages over traditional personal care products including improving the stability of cosmetic actives, enhancing the product aesthetics, targeting active ingredients to the desired sites, controlling active ingredient release to

achieve prolonged effects and conferring skin protection due to their occlusion property (Mu and Sprando, 2010, Padamwar and Pokharkar, 2006). This type of nanocarriers is mainly proposed in cosmetics used in anti-aging products, moisturisers to maintain skin hydration, sunscreens, as well as hair, skin, lip and nail care products to maintain personal hygiene and appearance but also other novel uses such as fragrance release (Hosseinkhani et al., 2015, Poland, 2016).

The antiaging gel Capture™ launched by Christian Dior, France, in 1986 was the first cosmetic formulation containing nanocarriers, namely liposomes (Abla et al., 2016). NLCs were first introduced in the market in 2005 by Dr. Rimpler GmbH and Prof. R.H. Müller at the "BEAUTY FORUM" in Munich/Germany presenting the first two NLC products, Cutanova Cream Nanorepair Q10 and the respective serum (**Figure 2.6**).

Figure 2.6 – The first two NLCs cosmetic products marketed in the world, Cutanova Cream Nanorepair Q10 (right) and the respective serum (series NanoCare) (left), presented by Dr. Rimpler GmbH and Prof. R.H. Müller at the "BEAUTY FORUM" Munich in 2005. Adapted from (Müller et al., 2016)

Meanwhile, many more cosmetic products using lipid-based nanocarriers have been marketed worldwide (Abla et al., 2016). **Table 2.3** provides an insight to examples of products which are currently on the market containing lipid nanocarriers.

Table 2.3 – Examples of cosmetic products containing lipid nanocarriers that are currently on the market. Modified from (Müller et al., 2016, Puthli et al., 2012, Zielińska and Nowak, 2016).

Type of lipid nanocarrier	Company	Commercial product name	Main active ingredients	Indication
Nanoemulsion	Dr. Theiss – Medipharma Cosmetics	Olivenöl Intensivcreme	Olive oil, retinol and vitamin E	Skin care
Liposomes	Keenwell	Biologics – Revital Triple Action Reaffirming Serum	DMAE (Dimethylamino ethanol), silanol-mannuronate, GP4G: Diguanosine tetraphosphate, obtained from Artemia salina	Skins with flaccidity or lacking tone and elasticity
Nanosomes	L´Oreal	Revitalfift	Pro-retinol A and fibrelastyl	Anti-aging
SLN	Astellas	Nanobase Repair	Paraffin nanoparticles	Moisturizer
NLCs	Dr. Rimpler	Cutanova Nanorepair Q10	Coenzyme Q10, polypeptide, hibiscus extract and extracts, ketosugar	Anti-aging
		Intensive Serum Nano-Repair Q10	Coenzyme Q10, polypeptide, Acmella oleracea extract	Anti-aging
		Cutanova Nano-Vital Q10	Coenzyme Q10, TiO 2 , polypeptide, ursolic acid, oleanolic acid, sunfl ower seed extract	Anti-aging day care with UV protection
		Cutanova Nano Sensitive Cream	Hemp oil, Squalane, Defensil®, Ximenia Americana, seed oil, microsilver, ferment extract	Anti-inflamatory, moisturizer
	Amore Pacific – IOPE	Super Vital - Collection	Coconut oil, niacinamid, Myrica cerifera leaf extract, selaginella extract, safflower extract, tocopherol, caffeine, theanine, green tea extract	Moisturizer, anti-aging, firming cream
	Isabelle Lancray	Surmer – Soft ostorizing protecting cream	Coconut oil, Noni tree extract, magnolia, green tea, coconut milk essence, cell-renewing peptides, and extract from wild Indigo	moisturizer
		Surmer – Rich restouring cream	Coconut oil, magnolia, green tea, coconut milk essence, cell-renewing peptides, extract from wild Indigo, tamanu oil.	Anti-aging

Table 2.3 (Continued)

Type of lipid nanocarrier	Company	Commercial product name	Main active ingredients	Indication
NLCs	Isabelle Lancray	Surmer – Remodeling eye contour cream	Coconut oil, magnolia, green tea, coconut milk essence, cell-renewing peptides	Anti-aging, moisturizer, regenerator
		Surmer – Firming neck care	Coconut oil, Mangosteen tree, quince, tamanu oil, wheat germ oil	Anti-aging, moisturizer, regenerator
	Dr. Theiss – Medipharma Cosmetics	Olivenöl Augenpflegebalsam	Extra virgin olive oil, rose root and caffeine	Anti-aging
	Bellamora	Collagen cellular repair cream and advanced exfoliant	Laminaria digitata extract, Shea butter, Green tea extract, Palmitoyl oligopeptides, Multivitamin (vitamin A, C, E, F) nanolipids, Elastine, Collagen	Anti-aging, regenerator
	Bellamora	Collagen cellular repair cream and advanced exfoliant	Laminaria digitata extract, Shea butter, Green tea extract, Palmitoyl oligopeptides, Multivitamin (vitamin A, C, E, F) nanolipids, Elastine, Collagen	Anti-aging, regenerator
	Naturalia Sintesi	Regenatur NG11 ProgressiveE	Undeciylenoyl Phenylalanine & Hydroxyphenoxy Propionic Acid - Propionic Acid, Vitamin C	Anti-aging, regenerator

It is estimated that more than 500 products containing NLCs can be found worldwide (Müller et al., 2016). However, in some cases NLCs are not designated and listed on INCI nomenclature of cosmetic products, but instead they present the INCI names of their excipients and actives ingredients, as e.g., coenzyme Q10, carnauba wax, and black current seed oil, but on contrary, some companies advertise the use of NLCs in markets where it is known that nano-cosmetics are popular (Müller et al., 2016). NLCs are also often used to optimize the skin feeling of products, they are added in small amounts to a product granting them unique sensation properties which can be experienced by the consumer (Müller et al., 2016).

2.2. Lipid nanoparticles for the dermal delivery of active compounds

Lipid nanoparticles, including SLNs and NLCs are colloidal carriers composed of a lipid matrix that is solid at body temperature. These lipid nanocarriers have attracted great interest and have been intensively studied for their use in dermal applications.

The composition and structure of lipid nanoparticles intrinsically influences their performance. In general, the lipid nanoparticles are formulated as aqueous dispersions using lipids that are usually solid at room temperature and surface-tailored by surfactants and optionally by co-surfactants to improve the dispersion stability. These excipients are generally recognized as safe (GRAS), being well-tolerated in physiological conditions and even some lipids could present bioactive properties granting to lipid nanoparticles a biocompatible and multifunctional character.

The encapsulation and preservation of active compounds are other aspects to be considered regarding the structure of lipid nanoparticles since these parameters will influence their release properties, protection and stability during storage until the final dermal application. However, it is only possible to quantify the amount of active compound that is incorporated into the lipid core, while the interactions between the encapsulated compound and the lipids are not yet possible to characterize in terms of state and location in the nanoparticle lipid matrix.

The selection of the production method is also determinant and is mainly dependent of the final product application, considering its physical and chemical stability, concentration, required particle size, release mechanism and manufacturing costs.

2.2.1. Formulation, composition and structure

In general, lipid nanoparticles are composed by solid lipid(s), surfactant(s), co-surfactant (optional) and active ingredients (Shah et al., 2015).The lipids are usually physiological lipids (biocompatible and biodegradable) with low acute and chronic toxicity (Das and Chaudhury, 2011) and are structurally diverse being categorized mainly into fatty acids, fatty esters, fatty alcohols, triglycerides or partial glycerides (Ganesan and Narayanasamy, 2017). There are also, few reports of the use of waxes in the preparation of lipid nanoparticles (Jenning et al., 2000b). The physiochemical diversity and biocompatibility of lipids and their ability to enhance the bioavailability of active compounds have granted lipid nanoparticles as very attractive carriers for several administration routes but primarily for dermal delivery (Das and Chaudhury, 2011, Ganesan and Narayanasamy, 2017).

2.2.1.1. Lipids

As their designation stands for, lipid nanoparticles are mainly composed by solid lipids which molecular structure and blends may influence their drug loading capacity, their stability and the sustained release behaviour of nanoparticles formulations. Liquid lipids, or oils, are specifically introduced in the production of NLCs to decrease the crystallinity order of the lipid matrix and improve the drug loading capacity.

One important pre-requisite of lipids is their physiological tolerance, thus the majority of lipids used in lipid nanoparticles formulations are GRAS, including natural, semi-synthetic or synthetic lipids varying in structure as fatty acids, waxes, mono-, di- and trigliceraldeides and phospholipids (Blasi et al., 2013, Doktorovova et al., 2014a, Durán-Lobato et al., 2013, Montenegro et al., 2016, Shah et al., 2015). Examples of lipids which have been used in the preparation of lipid nanoparticles, both SLNs and NLCs, are sumarized in **Table 2.4.** For the preparation of lipid nanoparticles, it can be used only one type of lipid or a mixture of different types of lipids, which according to their melting points, crystallinity and polymorphic characteristics will present different functional properties. It is essential that the lipids have solubilization properties for the specific lipophilic active compound to be encapsulated because it invariably influences the drug encapsulation efficiency and loading capacities, and subsequently the usefulness of the lipid nanoparticles as effective nanocarriers (Attama et al., 2012a). Thus, the selection of appropriate lipids is crutial prior to their use in the preparation of lipid nanoparticles (Shah et al., 2015). In the case of NLCs, the solid and liquid lipids blend screening in very important and It should be ensured that the mixture of both lipids is uniform, presenting only one phase, in the molten state but also, and mainly in the solid state (Müller et al., 2016). The lipids screening may be performed by testing different ratios of solid and liquid lipids, by melting and mixing them, and by analyzing then by macroscopic evaluation (Müller et al., 2016).

The lipids polymorphism or the occurrence of multiple crystaline forms in solid lipids is another important aspect that influences the structure and properties of lipid nanoparticles and is particularly useful as it provides structural defects in which drug molecules can be accommodated. A perfect crystalline lattice is thermodynamically more stable and thus, thermodynamically less stable forms eventually tend to transform into stable forms which constitutes a significant challenge in the development of SLNs since the crystal imperfections tend to disappear with time and the active molecules that were there accommodated will be released, promoting consequently drug expulsion during storage or burst release after administration. Thus, tendency of lipids to form perfect crystalline lattice structures is a factor that influences the selection an appropriate lipid for the preparation of lipid nanoparticles, however, there are currently no definitive guidelines for the choice of lipids based on these properties (Müller et al., 2016, Shah et al., 2015).

Table 2.4 – Example of lipids used in the formulation of lipid nanoparticles. Adapted from (Montenegro et al., 2016, Shah et al., 2015).

Fatty acids	Waxes
Lauric acid (C12:0)	Beeswax
Myristic acid (C14:0)	Carnauba wax
Palmitic acid (C16:0)	Cetyl palmitate (Precifac® ATO 5, Cutina® CP)
Stearic acid (C18:0)	Hard fat (Witepsol® E 85, Suppocire® NA 150)
Monoglycerides	Hydrogenated Coco-Glycerides (Softisan® 142)
Glyceryl monostearate (Imwitor® 900, Geleol®)	Hydrogenated Palm Oil (Softisan® 154)
Glyceryl hydroxystearate	**Liquid lipids**
Glyceryl behenate (Compritol® 888 ATO)	Soya bean oil
Diglycerides	Oleic acid (C18:1)
Glyceryl palmitostearate (Precirol® ATO 5)	Medium chain triglycerides (MCT)
Glyceryl dibehenate	α-tocopherol/Vitamin E
Triglycerides	Squalene
Caprylate triglyceride	Castor oil
Caprate triglyceride	Hydroxyoctacosanylhydroxystearate
Glyceryl trilaurate (Dynasan® 112)	**Cationic lipids**
Glyceryl trimyristate (Dynasan® 114)	Stearylamine
Glyceryl tripalmitate (Dynasan® 116)	Cetrimide (tetradecyl trimethyl ammonium bromide)
Glyceryl tristearate (Dynasan® 118)	Cetyl pyridinium chloride (hexadecyl pyridinium chloride)
Glyceryl tribehenate/Tribehenin	Dimethyl dioctadecyl ammonium bromide

2.2.1.2. Surfactants

Along with lipids, surfactants constitute a key ingredient in the formulation of lipid nanoparticles. They are also known as emulsifiers or surface-active agents molecularly they are amphiphilic (**Figure 2.7**) possessing a hydrophilic group (polar) and a lipophilic group (non-polar), which grant them a water-insoluble (or oil-soluble, head) component and a water-soluble component (tail) (Shah et al., 2015). At low concentrations, surfactants will difuse in water and adsorb onto the surface of a system or interface between air and water or at the interface between oil and water, in the case where water is mixed with oil. They are essential to stabilize lipid nanoparticle dispersions and prevent particle agglomeration, since they reduce the surface or interfacial free energy and consequently reduce the surface or interfacial tension between the two phases (Shah et al., 2015, Tewes et al., 2013).
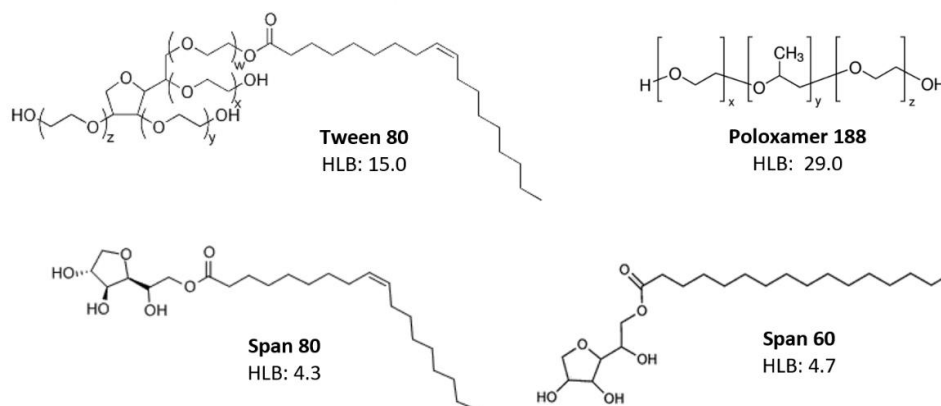
Figure 2.7 – Molecular structure of some non-ionic surfactants with their respective hydrophilic-lipophilic balance (HLB).

The surfactant properties such as charge, molecular weight, chemical structure, their effect on lipid modification and particle size, their role in *in vivo* degradation of the lipid and the respective hydrophile-lipophile balance (HLB), which concern their effective proportions of both hydrophilic and lipophilic groups, will determine the selection conditions for the formulation of a particular type of lipid nanoparticles (Attama et al., 2012). To be more precisely, the HLB of a surfactant is given by the balance between the size and strength of the hydrophilic and the lipophilic groups and is a major characteristic to be considered in the selection process. Also, the choice of surfactants for the preparation of lipid nanoparticles is dependent of the route of administration, as for instance, in topical administration the issue of skin sensitization has to be considered, while for the oral route, the surfactant should not produce any physiological effect at its concentration in formulation (Severino et al., 2012).

In the preparation of lipid nanoparticles, surfactants act in two distinct and important roles, they disperse the lipid melt in the aqueous phase during the production process and stabilize the lipid nanoparticles in dispersions after cooling. Moreover, they can be used in combination to produce synergistic effect and better stabilize the formulation (Lovelyn and Attama, 2011). It has been suggested that the composition and concentration of surfactant essentially contribute to the properties of lipid nanoparticles such as their toxicity (Scholer et al., 2001), physical stability (Han et al., 2008) and crystallinity (Bunjes et al., 2003, Karn-Orachai et al., 2014).

Surfactants are grouped into three classes based on their charge, as ionic, non-ionic and zwitterionic or amphoteric (Shah et al., 2015). **Table 2.5** shows examples from each class of surfactants used in the preparation and stabilization of lipid nanoparticles.

Table 2.5 – Examples of surfactants and co-surfactants commonly used in the preparation of lipid nanoparticles. Adapted from (Montenegro et al., 2016, Shah et al., 2015).

Non-ionic surfactants	*Ionic surfactants*
Sorbitan monododecanoate (Span® 20)	Sodium cholate
Sorbitan monostearate (Span® 60)	Sodium glycocholate
Sorbitan monooleate (Span® 80)	Sodium taurocholate
Sorbitane trioleate (Span® 85)	Sodium taurodeoxycholate
Tyloxapol	Sodium oleate
Poloxamer 188 (Lutrol® F68, Pluronic® F68)	Sodium dodecyl sulphate
Poloxamer 407 (Pluronic® F127)	*Amphoteric surfactants*
Poloxamine 908	
Polysorbate 80 (Tween® 80)	Egg phosphatidylcholine (Lipoid E PC S)
Polysorbate 65 (Tween® 65)	Soy phosphatidylcholine (Lipoid S 100, Lipoid S PC)
Polysorbate 20 (Tween® 20)	Hydrogenated egg phosphatidylcholine (Lipoid E PC-3)
Brij78	Hydrogenated soy phosphatidylcholine (Lipoid S PC-3,
Polyglyceryl-3 Methylglucose Distearate (Tego® Care 450)	Phosphatidylcholine (Epikuron® 200, Phospholipon® 80/H)
Solutol HS15	Egg phospholipid (Lipoid E 80, Lipoid E 80 S)
Cremophor EL	Soybean lecithin (Lipoid® S75)
	Co-surfactants
	Butanol
	Butyric acid

Ionic surfactants are referenced to infer electrostatic stability, while non-ionic surfactants are pointed to infer steric repulsion stability (Shah et al., 2015). Some non-ionic surfactants show great potential for improving the stability of nanoparticles (Tan et al., 2010, Zadeh et al., 2010), especially those with large sized hydrophilic portions, for example, members from Tween® family containing hydrophilic polyoxyethylene groups (Karn-Orachai et al., 2014, Zadeh et al., 2010). Amphoteric surfactants, as phospholipids and phosphatidylcholines are also commonly employed in lipid nanoparticle formulation, presenting properties of both cationic and anionic surfactants at low and high pH conditions, respectively (Shah et al., 2015).

2.2.1.3. Other ingredients for the formulation of lipid nanoparticles

In addition to lipids and surfactants, other agents are also used in the formulation of lipid nanoparticles, including counter-ions and surface modifiers (**Table 2.6**) (Aditya P. Nayak, 2011, Shah et al., 2015). Lipid nanoparticles have the intrinsic disadvantage of low encapsulation of hydrophilic compounds associated with the lipophilicity of their solid lipid matrix (Cavalli et al., 2003, Shah et al., 2015). Thus, in order to overcome this limitation, counter ions such as polymers and esters (organic salts) are used to neutralise the charge of the hydrophilic active compounds to be encapsulated (Aditya P. Nayak, 2011). For instance, modifying the surface of lipid nanoparticles formulated for "stealth" or long-circulating carriers that stay longer in the systemic circulation and increase the residence of drug in

blood, with surface-modifiers such as hydrophilic polymers (poloxamers, poloxamines or polyethylene glycol) may reduce their uptake by the reticuloendothelial system (RES) (Shah et al., 2015).This technique is also valuable to minimise the clearance of these nanoparticles by phagocytosis (Bocca et al., 1998) due to their high surface hydrophobicity (Aditya P. Nayak, 2011).

Table 2.6 - Commonly used counter-ions and surface modifiers in the formulation of lipid nanoparticles. Adapted from (Aditya P. Nayak, 2011, Shah et al., 2015)

Counter-ions	
Organic salts	*Ionic polymers*
Mono-octyl phosphate Mono-hexadecyl phosphate Mono-decyl phosphate Sodium hexadecyl phosphate	Dextran sulphate sodium salt Hydrolyzed and polymerized epoxidised soybean oil
Surface modifiers	
Dipalmitoyl-phosphatidyl-ethanolamine conjugated with polyethylene glycol 2000 (DPPE-PEG2000) Distearoyl-phosphatidyl-ethanolamine-N-poly(ethyleneglycol) 2000 (DSPE-PEG2000) Stearic acid-PEG 2000 (SA-PEG2000) α-methoxy-PEG 2000-carboxylic acid-α-lipoamino acids (mPEG2000-C-LAA18) α-methoxy-PEG 5000-carboxylic acid-α-lipoamino acids (mPEG5000-C-LAA18)	

2.2.2. *Active compounds used in dermal formulations*

Essential properties of galenic and cosmetic formulations as efficacy and tolerability are determined not only by the nature of the active compound but also by the vehicle. Thus, a well-formulated base of empty lipid nanoparticles may have numerous positive effects on skin, as occlusion and stabilization of the epidermal barrier. Moreover, the effects of many active compounds are dependent from the overall formulation and preparation as it may confer them more stability and protection, increasing their bioavailability. The interactions between the carrier, active ingredient and the skin greatly influences their effects in the formulation as well the release profile of the active substance (Kerscher and Buntrock, 2016).

Research studies on the encapsulation of some examples of different active compounds in lipid nanoparticles are shown in **Table 2.7** and the categories in which these active substances belong will be presented and further discussed.

Table 2.7 – Studies on the encapsulation of different active compounds in lipid nanoparticles reported by different researchers. Adapted from (Casanova and Santos, 2016, Ganesan and Narayanasamy, 2017)

Lipid nanoparticle	Active compound	Class/ Function	Excipients	Encapsulation method	Principal results	Reference
SLNs	Retinol (Vitamin A)	Retinoid	Glyceryl behenate	Melt solidification	Particle size: 224 nm Release after 6 h: 3400 ng out of 500 mg Retinol SLN incorporated in o/w cream showed better localizing action results	(Jenning et al., 2000a)
SLNs	Benzophenone-3	Benzophenone/ Sunscreen	Cetyl palmitate Poly(-caprolactone)	Hot high pressure homogenization; Precipitation	Particle size: 133.0 to 147 nm The sun protection factor increased when benzophenone-3 was encapsulated in both nanostructures	(Marcato et al., 2011)
NLCs	Benzophenone-3	Benzophenone/ Sunscreen	Carnauba wax Isodecyl oleate	Hot high pressure homogenization	Particle size: 0.3 to 8 mm Encapsulation efficiency: 90% (max)	(Lacerda et al., 2011)
NLCs	Acitretin	Retinoid	Precirol ATO 5 Labrasol	Solvent diffusion technique	Particle size: 223 ± 8.92 nm Greater efficacy in the treatment of Psoriasis with a reduction in side effects	(Agrawal et al., 2010)
NLCs	Ascorbyl palmitate	Vitamin derivative/ Antioxidant	Imwitor 900 Labrafil M1944	High pressure homogenization	Particle size: 170–240 nm Viscoelastic measurements is appropriate for topical/dermal application	(Teeranachaideekul et al., 2008b)
NLCs	Benzocain	Ester/ Local anesthetic	Comprotol©888 ATO Miglyol©812 Lutrol©F68	Ultrasonication	Particle size: 386.1 ± 65.6 nm Targeting and prolonged release effects in dermal delivery	(Puglia et al., 2011)
NLCs	Calcipotriol Methtrexate	Vitamin derivative/ Immune system suppressant	Myverol™ 18-04K, Precirol® ATO 5 Pluronic® F68 Squalene	Solvent evaporation method	Particle size: 267.3 ± 12.3 nm Enhanced skin permeation, negligible skin irritation, and the compatibility of the two drugs	(Lin et al., 2010)
NLCs	Coenzyme-Q10	Benzoquinona/ Antioxidant	Miglyol®812, Precifac® ATO Tegocare 450 Labrasol	High pressure homogenization	Particle size: 195.9 ± 3.6 nm Good physical stability and showed biphasic release pattern i.e. a fast release initially for skin saturation then slow and prolong release profile to maintain the skin concentration of Q10	(Obeidat et al., 2010)

Table 2.7 (Continued)

Lipid nanoparticle	Active compound	Class/ Function	Excipients	Encapsulation method	Principal results	Reference
SLNs	Dexamethasone	Corticosteroid/ Anti-inflammatory and Immunosuppressant	Compritol 888 ATO	Ultrasonication	Particle size: 106.8 nm Efficient drug delivery for topical use	(Chen et al., 2008)
NLCs	Flurbiprofen	Phenylalkanoic acid/ Nonsteroidal anti-inflammatory drugs	Compritol 888 ATO Miglyol1 812 Castor Oil	High pressure homogenization	Particle size: 179.7 ± 3.1 nm Highly effective, non-irritant carrier for topical administration of flurbiprofen and improved drug permeation	(Gonzalez-Mira et al., 2010)
NLCs	Flurbiprofen	Phenylalkanoic acid/ Nonsteroidal anti-inflammatory drugs	Compritol ATO 888 Miglyol 812 Gelucire 44/14 Solutol HS Tween 80 Glycerol	Ultrasonication	Particle size: 55.4 nm Longer retention time due to mucous-adhesive nature and improved penetration rate	(Liu and Wu, 2010)
NLCs	Ketoprofen	Propionic acid/ Nonsteroidal anti-inflammatory drugs	Compritol®888 ATO Labrafac lipophile Lutrol® F68 Xanthum gum	Ultrasonication	Particle size: 494 ± 47 nm Improvement in the dissolution and skin permeation properties	(Cirri et al., 2012)
SLNs	Ketoprofen	Propionic acid/ Nonsteroidal anti-inflammatory drugs	Mixture of beeswax and carnauba wax	Microemulsion technique	Particle size: 75 ± 4 nm to 250 ± 9.38 nm Faster drug release	(Kheradmandnia et al., 2010)
NLCs	Ketoprofen	Propionic acid/ Nonsteroidal anti-inflammatory drugs	Compritol 888 ATO/ Labrafac lipophile	Nanoemulsification and ultrasonication	Particle size: 300–500 nm Improvement in both the dissolution and the skin permeation properties of drug	(Cirri et al., 2012)
NLCs	Lidocain	Amide/ Local Anesthetic and Antiarrhythmic	Compritol®888ATO, Precirol®ATO5, Miglyol®812,T80	Ultrasonication	Particle size: 72.1 nm Long duration of deep local anesthesia in guinea pig	(Pathak and Nagarsenker, 2009)
NLCs	Lidocain	Amide/ Local Anesthetic and Antiarrhythmic	Compritol 888 ATO Miglyol 810	Ultrasonication	Particle size: 78.1 nm Long duration of local anesthesia in guinea pigs	(Pathak and Nagarsenker, 2009)

Table 2.7 (Continued)

Lipid nanoparticle	Active compound	Class/ Function	Excipients	Encapsulation method	Principal results	Reference
NLCs	Oxybenzone	Benzophenones/ Sunscreen	GMS, Miglyol 812, Oleic acid, Carbopol® 934P PVA	Solvent evaporation	Particle size: 327 ± 30 to 797 ± 100 nm Enhanced the sunscreen efficacy to about six fold while reducing its side effects Increased the *in vitro* sun protection factor and UVA erythema protection factor of oxybenzone more than 6- and 8-folds, with fewer side effects	(Sanad et al., 2010)
NLCs	Psoralens	Furocoumarins/ Treatment for psoriasis, eczema, vitiligo, and cutaneous T-cell lymphoma	Precirol/Squalene	High pressure homogenization	Particle size: $\sim$ 300 and 200 nm Enhanced permeation and controlled release of the drug	(Fang et al., 2008)
SLNs	Quercetin	Flavonol/ Antioxidant	Glyceryl monostearate Soya lecithin Tween-80 PEG 400	Emulsification-solidification	Particle size: 155.3 ± 22.1 nm Improved bioavailability	(Li et al., 2009)
NLCs	Quercetin	Flavonol/ Antioxidant	GMS/MCT	Emulsion evaporation solidification	Particle size: 215.2 nm Increased drug retention in epidermis and enhanced the therapeutic effect	(Chen-yu et al., 2012)
NLCs	Resveratrol	Polifenol/ Antioxidant	Compritol 888 ATO/Miglyol	Ultrasonication	Particle size: 287.2 ± 5.1 and 110.5 ± 1.3 nm The drug loaded NLCs with smaller particle size and high drug loading showed greater antioxidant activity as compared to SLNs	(Gokce et al., 2012)
NLCs	Triamcinolone acetonide	Synthetic corticosteroid	Precirol ATO 5/Squalene	High pressure homogenization	Particle size: 173.3 ± 0.32 nm Improved stability	(Araújo et al., 2011)

2.2.2.1. Vegetable oils and fatty acids

Current research on dermal formulation has been steered towards the use of vegetable ingredients by both consumer's preferences and by excelent results of scientific research on the properties of natural origin raw materials (Rigano I., 2006). Vegetable oils are abundant renewable and readily available sources exhibiting great interest as raw materials in the development of natural and eco-friendly dermal products (Badea et al., 2015, Balboa et al., 2014). These lipids are liquid vegetable fats that remain in the liquid form at room temperature which are most commonly extracted from various parts of plants such as seeds, fruits, or plant seedlings. Oils are composed by a combination of triglycerides of higher saturated and unsaturated fatty acids (Zielińska and Nowak, 2014). These compounds are esters of glycerol and higher fatty acids, containing in their structure long aliphatic carbon chains and in small amounts they may contain phospholipids, free sterols, tocols (tocopherols and tocotrienols), triterpene alcohols, hydrocarbon sand fat soluble vitamins (Badea et al., 2015, Karak, 2012, Zielińska and Nowak, 2014).

Depending upon the individual percentages of fat acids in their molecules, vegetable oils exhibit multiple skin benefits and a therapeutic activities as antioxidant properties, providing skin protection against reactive oxygens species (ROS) (Dhavamani et al., 2014, Tehranifar et al., 2011), and also anti-carcinogenic and anti-inflammatory activities (Badea et al., 2015, Cicerale et al., 2012). In dermal formulations, vegetable oils are used as moisturizers and emollients by increasing the hydration and preventing water loss through the skin, mainly by means of making a protective layer on the epidermis (Saraf et al., 2010, Zielińska and Nowak, 2014). Moreover, the beneficial effects of vegetable oils are well-recognized in the biological synthesis of components of cell membranes and in the transport and oxidation of cholesterol, thus playing a very important role in the proper functioning of the human body (Zielińska and Nowak, 2014).

There are a few research works reporting the use of vegetable oils in the formulation of lipid nanoparticles. Badea et al. (Badea et al., 2015) described a study involving the selection of seven vegetable oils, namely pomegranate seed oil, blackcurrant seed oil, sesame seed oil, raspberry seed oil, carrot root oil, wheat germ oil and rice bran oil to design and produce NLCs as nanocarriers for the encapsulation of diethylamino hydroxybenzoyl hexyl benzoate (DHHB) which is a synthetic sunscreen by hot high pressure homogenization. They obtained appropriate sized NLCs, having mean particle sizes ranging between 100 nm and 145 nm and showed that vegetable oils and especially their combinations have a great potential to be used in the development of antioxidant nanostructured lipid carriers loaded with a UV-A filter in order to boost their photo-protective action. Lacatusu et al. (Lacatusu et al., 2012) explored the potential of squalene (Sq) and grape seed oil (GSO) to prepare biocompatible antioxidant NLCs as a safety and protective formulation for BC by a melt high-shear homogenization process and obtained nanoparticles with average diameters of about 85 nm for GSO and 89 nm for Sq with excellent antioxidant properties mainly attributed to the presence of Sq and

GSO. Also, Lacatusu et al. (Lacatusu et al., 2014) successfully synthesized by a combination of high shear and high pressure homogenization techniques, soft and functional nanocarriers based on pumpkin and amaranth oils able to co-encapsulate and co-deliver avobenzone and octocrylen, two UV-A and UV-B filters with mean diameters of 100 and 160 nm, good antioxidant activity and strong anti-UV properties.

2.2.2.2. Retinoids

Retinoids are poorly water-soluble compounds, chemically related natural and synthetic vitamin A derivatives that in part present different biological activities (Morales et al., 2015, Sorg et al., 2006). This group includes various substances or derivatives of retinol, as retinaldehyde, retinoic acid (tretinoin) or retinyl esters as retinyl palmitate (**Figure 2.8**) (Sorg et al., 2006). In this context, it is possible to differentiate two major retinoids families of acids, including isotretinoin and tretinoin, and non-acids. As lipophilic molecules, they can diffuse through cellular and other phospholipid membranes (de Nóvoa et al., 2015).
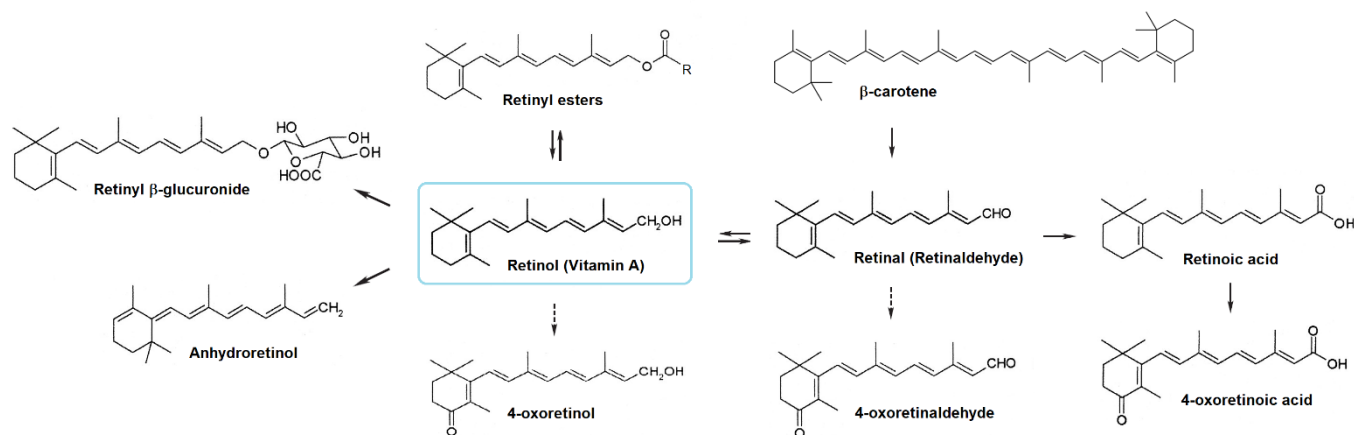
Figure 2.8 – Molecular structure of natural retinoids. The black bolded arrows shows enzyme-catalysed conversions and the dotted-lined arrows represent probable conversions, although they have not been confirmed. Adapted from (Sorg et al., 2006).

In the skin, retinoids play a crucial regulatory role in epidermal growth and differentiation, they increase skin elasticity, decrease skin roughness and prevent the peroxidation of skin lipids (Morales et al., 2015, Pople and Singh, 2006). Research studies have demonstrated that retinoids present several therapeutic benefits and can be helpful in (*i*) renewing epidermal cells, (*ii*) acting as UV filters, (*iii*) preventing oxidative stress, (*iv*) controlling cutaneous bacterial flora, and (*v*) improving skin aging and photo-aging (Sorg et al., 2006). Some biological effects of retinoids include improvement of fine wrinkles and acne vulgaris, decrease in roughness, improvement in reducing actinic keratoses, and hyperpigmentation (Morales et al., 2015). Moreover, topical retinoids act as antioxidants, preventing

tissue atrophy and the loss of collagen that is generally a result of aging (Thomas et al., 2013) and show antimicrobial activity against the bacteria that are typically involved in acne (Raza et al., 2013c, Ridolfi et al., 2012).

Some retinoids as retinol (vitamin A), retinyl palmitate, beta carotene, tretinoin, isotretinoin, adapalene, and tazarotene have a great impact in topical administration (de Nóvoa et al., 2015). Retinol is the most commonly used substance in modern anti-aging preparations, which in comparison with tretinoin present less irritant effects to the skin and is generally well-tolerated in topical administrations (Kerscher and Buntrock, 2016). Retinol and their derivative retinyl esters are currently considered as the "gold standard" of antiaging agents and can be applied at a maximal concentration of up to 0.3% as the clinical efficacy of these compounds has been scientifically well studied and proven (de Nóvoa et al., 2015, Kerscher and Buntrock, 2016). Tretinoin has been commonly used in dermatology since the early 1960s, but it was only in the 1980s that its importance in the treatment of aging skin was discovered (de Nóvoa et al., 2015). Isotretinoin is a neo-collagenous substance that inhibits the functioning of metalloproteinases and is more tolerable than tretinoin which although being typically recommended for the treatment of acne, it is also viewed as an alternative approach to photo-aging (Kligman et al., 1986, Mukherjee et al., 2006).

Despite the numerous beneficial effects of retinoids in the skin that were previously mentioned, the development of topical systems containing these compounds also present some drawbacks as poor water solubility, high chemical instability and photo-instability and potential irritation upon administration (Brisaert and Plaizier-Vercammen, 2000, Morales et al., 2015). Thus, retinoid-loaded lipid nanoparticles have been pointed to help in decreasing the adverse effects of these molecules and protect them against degradation (Morales et al., 2015, Prasad et al., 2012, Raza et al., 2013b, Raza et al., 2013c).

2.2.2.3. Antioxidants

Antioxidants are a heterogeneous group of substances that prevent oxidative stress from tissues of the body and offer protection to cell membranes by reducing or neutralizing the concentration of toxic oxygen molecules and free radicals (Kerscher and Buntrock, 2016, Salavkar et al., 2011). During the aging process, antioxidants are significantly reduced by extrinsic and intrinsic factors of human body. Between the various factors contributing to skin aging are photo-damage, free radicals and oxidation, smoking, hormones, heredity and life style (Kerscher and Buntrock, 2016).

Topical administration of antioxidants is considered as powerful strategy to reduce skin damage produced by reactive oxygen species (ROS) and restore or improve its antioxidant defence mechanisms (Montenegro, 2014). This has driven the design of several pharmaceutical and cosmetic formulations to prevent or correct the injuries related to skin aging, thus improving skin healthiness and appearance (Kerscher and Buntrock, 2016, Vinardell and Mitjans, 2015). Some of the most commonly employed antioxidants in skin care formulations, claiming anti-aging effects are based on

exogenous antioxidants such as vitamins, enzymes, plant-derived active ingredients as polyphenols, and synthetic compounds that cannot be synthesized by human body (**Figure 2.9**) (Kerscher and Buntrock, 2016, Montenegro, 2014).
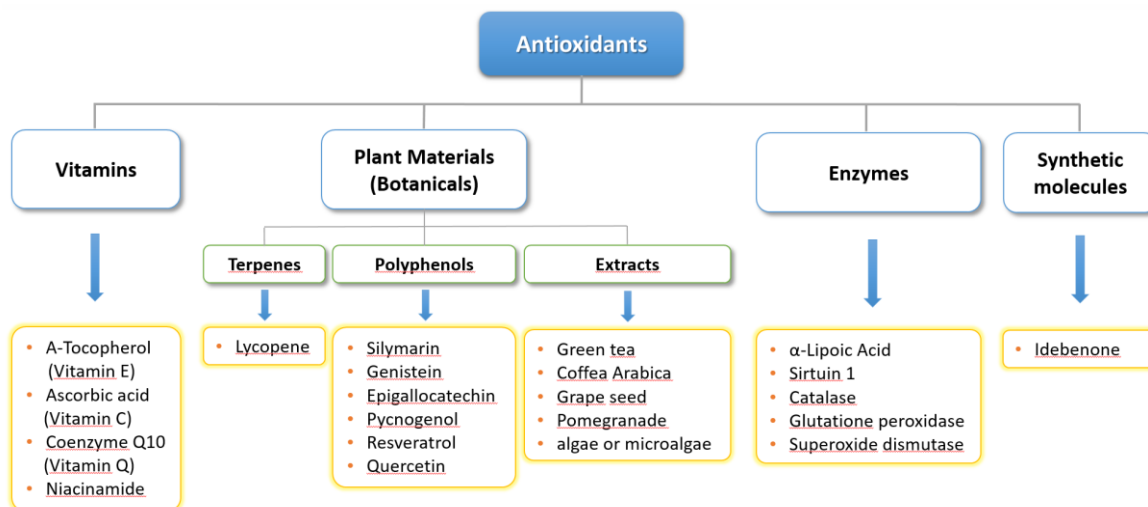
Figure 2.9 – Diagram of some antioxidants most commonly used in dermal formulations. Adapted from (Montenegro, 2014)

There are many skin care products based on botanical active ingredients and extracts due to its potent antioxidant activity that are produced by plants to counteract the effect of UV radiation to which they are regularly exposed (Salavkar et al., 2011). Besides the antioxidant important characteristic, many topical products based on plant-derived active ingredients show other biologic properties such as anti-inflammatory and anti-carcinogenic activities (Montenegro, 2014). As an example of such cases is resveratrol which belongs to the polyphenolic phytoalexins family and is found in grapes, nuts, fruits (coloured berries), and many red wines. Resveratrol has pronounced antioxidant activity with strong anti-inflammatory, anti-proliferative, and sirtuin-activating properties (Kerscher and Buntrock, 2016, Montenegro, 2014).

Vitamins as vitamin E (α-tocopherol), vitamin C (l-ascorbic acid) and vitamin B3 (niacinamide) are at present the most common active ingredients in cosmetic formulations to treat premature skin aging (Bissett et al., 2005, Friedland and Buchel, 2000). TOC is a lipid-soluble antioxidant that is found in concentrations of 2%–20% in countless skin care products, in various foods such as vegetables, seeds, in meat and in the skin (Kerscher and Buntrock, 2016). It has demonstrated good tolerability on the skin with very positive effects and it can also be used as a protective agent against oxidation in dermal and food formulations. Besides its physiologic anti-inflammatory, immunostimulatory, and antiproliferative effects, α-tocopherol helps skin repair itself, protects it from harmful bacteria, and also creates a moisture barrier so that the epidermis is less likely to dry (de Nóvoa et al., 2015, Kullavanijaya and Lim, 2005) . Moreover, this vitamin also showed anti-aging effects, it accelerates

the epithelialization of the skin, increase enzyme effects, and have photoprotective effects (Kerscher and Buntrock, 2016b).

The main drawback of most compounds with proven antioxidant activity is that they do not show suitable properties to achieve adequate concentrations in the skin layers where they should exert their action. Thus, rationale design of skin delivery systems based on lipid nanocarriers could promote the delivery of these compounds more efficiently and could represent an undeniable benefit for many anti-aging skin care products (Montenegro, 2014).

2.2.2.4. Moisturizers

Moisturizing creams aims at maintaining skin integrity and the well-being by providing a healthy appearance of the individual. The products can be regarded as cosmetics, but may also be regulated as medicinal products if they are marketed against dry skin diseases, such as atopic dermatitis and ichthyosis (Lodén, 2005). Moisturizers smooth a rough skin surface and protect it from dryness, containing emollients, occlusive agents and moisture-retaining substances (Kerscher and Buntrock, 2016). Thus, they are classified according to mechanism of action of their compounds as occlusive, emollients, and humectants (**Figure 2.10**) (de Nóvoa et al., 2015).
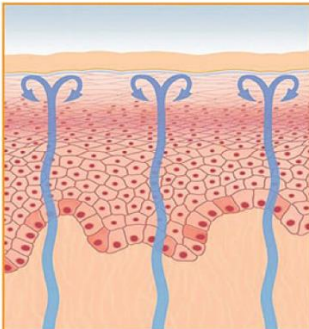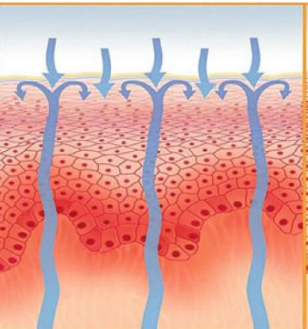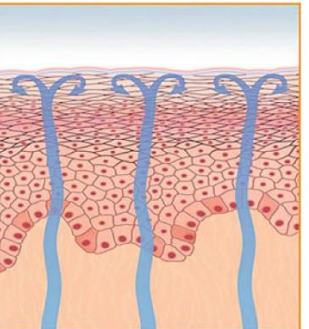
Occlusive	Humectants	Emollients
Hydrocarbon oils/ waxes	Glycerin	Protective emollients
Petrolatum	Honey	Diisopropyl dimer dilinoleate
Mineral oil	Ammonium lactate	Isopropyl isostearate
Paraffin	Urea	Castor beans
Scalene	Propylene	Fat liquors
Silicone derivatives	Sodium pyrrolidone carboxylate (sodium PCA)	Propylene
Dimethicone	Hyaluronic acid	Jojoba oil
Cyclomethicone	Sorbitol (glucitol)	Ceramides
Phospholipids	Panthenol	Octyl octanoate
Fatty alcohols	Polyglycerylmethacrylate	Isopropyl palmitate
Sterile alcohol	Gelatin	Glycol stearate
Lanolin alcohol	Sodium lactate	Lanolin
Lecithin		Cetyl stearate

Figure 2.10 – Classes of moisturizers according to their mechanism of action and some examples of each type used in dermal formulations. Adapted from (de Nóvoa et al., 2015).

Most frequently, commercially available products use compounds of each of these classes in their formulations. Moisturizers not only serve as lipid-replenishing and rehydrating skin care of dry skin, but also help maintain the health of aging skin (Lodén, 2005).

2.2.2.5. Polypeptides

At the molecular and functional level, polypeptides are capable of increasing collagen regeneration and preventing their degradation. Polypeptides with improved anti-aging activity are divided into signalers, neurotransmitter inhibitors, and enzyme carriers and inhibitors and are classified according to their main functional effects (**Table 2.8**) (de Nóvoa et al., 2015).

Table 2.8 – Examples of polypeptides used in dermal formulations. Adapted from (de Nóvoa et al., 2015)

Main signaling peptides	Main neurotransmitter inhibitory peptides	Main enzyme peptides	Peptides with "Cinderella effect"
Glycyl-histidyl-lysine tripeptide	Argireline	Derivatives of soy protein	Tensine
Palmitoyl pentapeptide	Vialox pentapeptide-3	Rice-derived peptides	Raffermine
Tripeptide 10	Leuphasyl	(Colhibin)	Easylift
Citrulline	Syn-Coll peptide	Silk protein	PephaTight
Pentamid-6			Sesaflash
Aquaporin			

There is evidence that amino acids and peptides may enhance the texture and consistency of skin surface with impressive anti-aging results without undesirable effects (de Nóvoa et al., 2015). Currently, it became possible to produce peptide sequences that imitate body's own molecules, such as collagen or elastin and thus influencing metabolic processes such as collagen synthesis (Kerscher and Buntrock, 2016).

2.2.2.6. Topical volumizers and fillers

There are some compounds that may act as fillers on rhytids, increasing the skin volume. These substances, in addition to settling on the skin surface, interact, penetrate, and modify the treated skin (de Nóvoa et al., 2015, Kerscher and Buntrock, 2016). Some examples of topical volumizers are listed in **Table 2.9**.

Table 2.9 – Examples of topical volumizers and fillers used in dermal formulations. Adapted from (de Nóvoa et al., 2015)

Topical volumizers and fillers	
Hyaluronic acid	Growth factors
Coenzyme Q10 (Ubiquinone)	Hibiscus and chestnut extracts
Asiaticoside	Commiphora mukul extract
Dimethylaminoethanol	Tetrahydroxypropyl ethylenediamine
Anthraquinone	

2.2.3. Production methods of lipid nanoparticles

The production method of lipid nanoparticles is a very important variable to be considered as it greatly influences the performance and characteristics of lipid nanoparticles (Shah et al., 2015). A number of production techniques have been introduced and developed for the production of lipid nanoparticles since the origin of these nanocarriers. One major constraints associated with the selection of the production method is the energy consumption. The production methods of SLNs and NLCs were categorized into two groups: (i) high energy methods for the dispersion of the lipid phase, as high pressure homogenization, high sheer homogenization and ultrasonication and (ii) methods that involve the precipitation of nanoparticles from homogeneous systems, as microemulsions, solvent-based techniques, membrane contactors and coacervation. Besides its energy consumption, the selection of the production method relies in the physicochemical properties and stability of the active compound to be incorporated, in the desired nanoparticle characteristics of the colloidal system and on the availability of the production equipment, its ease of applicability and feasibility and high yield potential (Ganesan and Narayanasamy, 2017, Shah et al., 2015).

A brief outline and description of the currently existent production methods of lipid nanoparticles, is given in **Table 2.10**, pointing some of their major advantages and disadvantages and the most common used techniques will be further discussed.

Table 2.10 – Mechanism, advantages and disadvantages of methods used in the preparation of lipid nanoparticles. Adapted from (Shah et al., 2015)

Production method	Mechanism of particles preparation	Advantages	Disadvantages
High pressure homogenization (HPH)	High mechanical shear due to strong turbulent eddies Lowering of pressure across the valves of homogenizers Strong cavitation forces	**Hot homogenization** ✓ Well established technology ✓ Effective dispersion of particles ✓ Reproducible ✓ High lipid content ✓ Simple to scale-up **Cold homogenization** ✓ Effective dispersion of particles ✓ Suitable for thermo-sensitive drugs ✓ No complex lipid modifications ✓ Increased drug-loading due to rapid cooling ✓ Suitable for hydrophilic drugs; reduced lipid melting reduces drug loss ✓ Simple to scale-up	**Hot homogenization** ✗ Extremely high energy inputs (heat and shear forces) ✗ High polydispersity ✗ Temperature-induced degradation of drugs ✗ Complex crystallization; leads to several lipid modifications and occurrence of super-cooled melts ✗ Inappropriate for hydrophilic drugs; readily distribute in the aqueous phase ✗ Reduction in homogenization efficiency at elevated Temperatures **Cold homogenization** ✗ Extremely high energy inputs ✗ Large particles with high polydispersity ✗ Drug expulsion on storage
Ultrasonication and/or high shear homogenization	Shear between adjacent particles Formation, growth and implosive collapse of bubbles due to cavitation forces	✓ Use of organic solvents can be avoided ✓ Use of large amounts of surfactants can be avoided ✓ Simple technique with lower production cost ✓ Higher energy inputs	✗ Unsuitable for higher lipid contents ✗ High polydispersity ✗ Physical instability due to high shearing ✗ Metal contamination due to ultrasonication
Microemulsion technique	Lipid crystallization due to rapid solidification of microemulsion	✓ Sophisticated equipment not required ✓ Low energy inputs ✓ Higher temperature gradients; faster lipid crystallization, avoids particle aggregation ✓ Simple to scale-up	✗ Low lipid content

(Continued next page)

Table 2.10 (Continued)

Production method	Mechanism of particles preparation	Advantages	Disadvantages
Membrane contactor method	Lipid/oil phase infuses through membrane pores into the tangentially flowing aqueous phase to form droplets Oil droplets crystallize to form lipid nanoparticles	✓ Controlled particle size with selection of membrane with correct pore size ✓ Simple to scale-up	✗ Clogging of membrane pores; ✗ frequent replacement or cleaning ✗ procedures
Supercritical fluid extraction of emulsions	Parallel processes of supercritical fluid extraction (diffusion) of organic solvent from emulsions and lipid dissolution Expansion of organic phase; leads to lipid crystallization	✓ Rapid and efficient solvent removal ✓ Monodispersity ✓ Removal of low molecular weight impurities is easy ✓ with supercritical fluids ✓ Supercritical fluid carbon dioxide causes plasticization of lipid structures; thermodynamically stable lipid nanoparticle dispersions ✓ Supercritical fluid lower melting point of lipids; suitable for thermo-sensitive drugs	✗ Use of organic solvents ✗ Sophisticated equipment ✗ required
Solvent evaporation	Lipid crystallization due to solvent evaporation in an anti-solvent	✓ Sophisticated equipment not required ✓ Highly suitable for thermo-sensitive drugs ✓ Small particle diameters ✓ Simple to scale-up	✗ Toxicological issues due to use of organic solvents ✗ Particle aggregation in absence of rapid solvent evaporation ✗ Low lipid content
Solvent diffusion	Lipid crystallization due to diffusion of solvent from internal organic phase to external aqueous phase	✓ Sophisticated equipment not required ✓ Pharmaceutically accepted organic solvents used; solvent recycling feasible ✓ Small particle diameters and low polydispersity ✓ Simple to scale-up	✗ Although rare, risk of toxicological risks due to incomplete evaporation of organic solvents ✗ Low lipid content
Solvent injection (or displacement)	Lipid crystallization due to rapid diffusion of solvent from internal organic phase to external aqueous phase	✓ Sophisticated equipment not required ✓ Pharmaceutically accepted organic solvents used; ✓ solvent recycling feasible ✓ Highly efficient and versatile technique ✓ Higher performance ✓ Simple to scale up	✗ Solvent removal difficult; use of freeze-drying or evaporation under- reduced-pressure ✗ Low lipid content

Table 2.10 (Continued)

Production method	Mechanism of particles preparation	Advantages	Disadvantages
Double emulsion	Lipid crystallization due to solidification of emulsion	✓ Sophisticated equipment not required ✓ Low energy inputs	✖ Low lipid content
Coacervation technique	Decrease in pH of micellar solution of an alkaline salts of fatty acids by acidification (coacervating solution) in presence of a polymeric stabilizer causes proton exchange an lipid precipitation (coacervation)	✓ Suitable for lipophilic drugs (by solubilising in the micellar solution after coacervation) ✓ Suitable for hydrophobic ion pairs of hydrophilic drugs ✓ Solvent-free technique ✓ Use of sophisticated technique not required ✓ Monodispersity ✓ Simple to scale-up	✖ Suitable for lipids that an form alkaline salts ✖ Not suitable for pH-sensitive drugs
Phase inversion temperature technique	Spontaneous inversion of o/w emulsion to w/o emulsion due to thermal treatment (subsequent heatingcooling cycles) Lipid crystallization as a result of emulsion breakage due to irreversible shock induced by rapid cooling	✓ Solvent-free technique ✓ Use of large amounts of surfactants can be avoided ✓ Combines structural advantages of polymeric nanocapsules and liposomes; imparts stability to the system ✓ Suitable for thermo-sensitive drugs ✓ Shorter heating periods avoids drug degradation	✖ Particle aggregation ✖ Excipients influence the phase inversion behavior ✖ Emulsion instability
Microwave-assisted microemulsion technique	Direct coupling of microwaves with molecules Lipid crystallization due to rapid solidification of microemulsion	✓ Controlled microwave heating ✓ Rapid and efficient heating ✓ Low energy inputs ✓ Shorter duration of preparation ✓ Higher temperature gradients; faster lipid crystallization	✖ Scalability issues

2.2.3.1. High pressure homogenization

Being the most reliable and influential production method at industrial scale, high pressure homogenization (HPH) was the first choice for the preparation of lipid nanoparticle dispersions (Zielińska and Nowak, 2016). HPH satisfies key industrial requirements, as regulatory aspects and the large-scale production is of relatively low cost (Yadav et al., 2013). HPH can be performed at high temperatures (hot homogenization) or below room temperature (cold homogenization) (**Figure 2.11**). In both cases, this method involves a preparatory step in which the active compound is incorporated into the bulk lipid by dissolving or dispersing it in the lipid melt (Zielińska and Nowak, 2016).
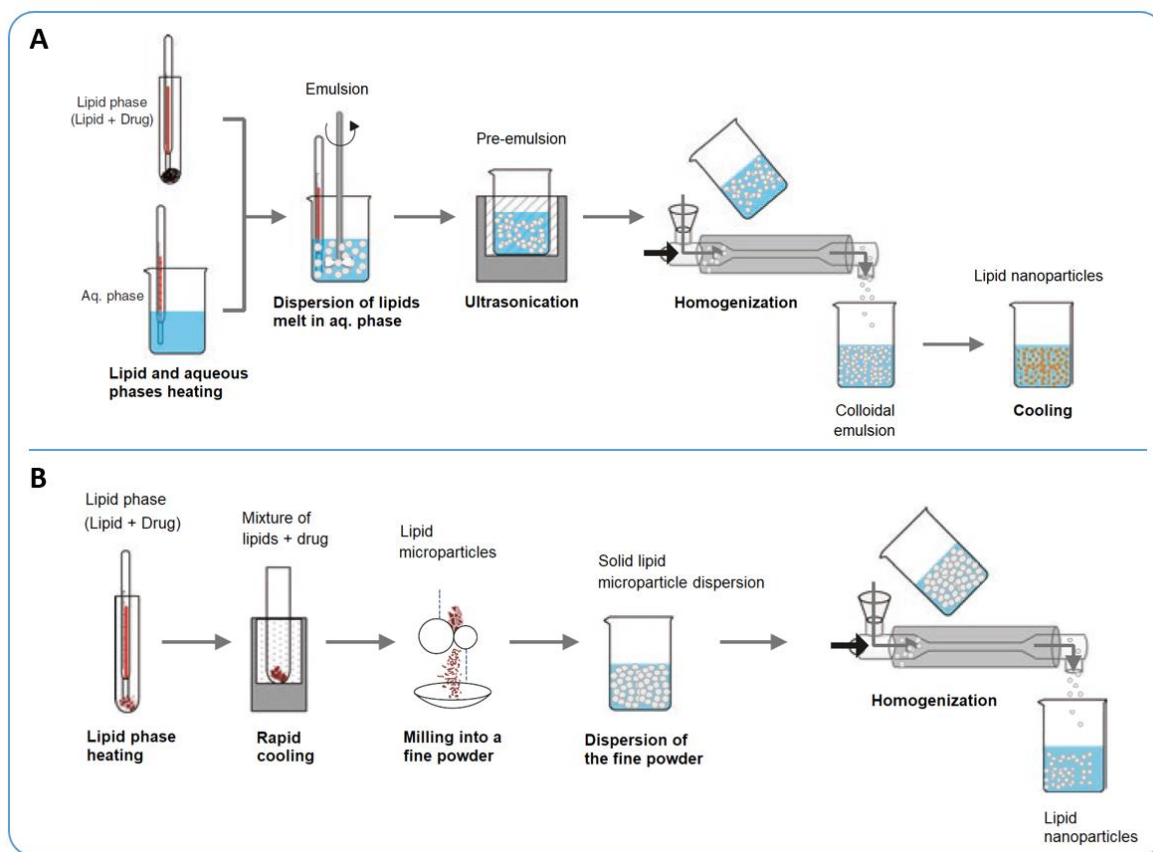
Figure 2.11 – Schematic illustration of the steps involved in the hot homogenization technique. (A) Hot homogenization; (B) Cold homogenization. Adapted from (Shah et al., 2015).

2.2.3.1.1. Hot homogenization

The high-pressure hot homogenization (**Figure 2.11, A**) is performed at temperatures above the melting point of the used lipids of the pre-emulsion. In a first step, the solid lipids are melted and the active substance is solubilized in the melted lipids, then this mixture is dispersed in a hot aqueous

surfactant solution, maintained at the same temperature, under high speed stirring and after an ultrasonication step the pre-emulsion is formed. After these steps, the pre-emulsion is pushed through a micron size gap of the homogenizer, and then by the high rotational speed of the rotor the liquid accelerates to high speed, and the resulting shear stress and cavitation lead to an optimum dispersion of the suspension. Finally, the hot colloidal dispersion is cooled to room temperature in order to recrystallize the emulsion droplets and generate the lipid nanoparticles (Ganesan and Narayanasamy, 2017, Mishra et al., 2010, Shah et al., 2015, Zielińska and Nowak, 2016).

2.2.3.1.2. Cold homogenization

The high-pressure cold homogenization (**Figure 2.11, B**) was mainly developed to overcome some drawbacks of the hot homogenization technique (Jaiswal et al., 2016), as the temperature-induced drug degradation, the distribution of the active compound into the aqueous phase during homogenization and the undefined crystallization of the lipid nanoparticles (Mehnert and Mäder, 2001). Similar to the hot homogenization method, the first step involves the incorporation and dissolution of the active compound in the melted solid lipids and then the resultant hot mixture is rapidly cooled with dry ice or liquid nitrogen. This favours a homogenous distribution of the active compounds in the lipids blend. The solid is then milled into a fine microparticles powder which is subsequently dispersed in a cold aqueous surfactant solution. Then, the resultant dispersion is subjected to high pressure homogenization to produce de lipid nanoparticles (Ganesan and Narayanasamy, 2017, Shah et al., 2015, Zielińska and Nowak, 2016).

2.2.3.2. Ultrasonication and/ or high shear homogenization

Ultrasonication and/ or high shear homogenization (**Figure 2.12**) and are mechanical dispersing techniques trough which lipid nanoparticles can be obtained. This method primarily involves the heating of both aqueous and lipid phases to approximately 5–10 °C above the solid lipids melting point. The lipid phase is dispersed in the aqueous phase containing a surfactant and both phases are mixed under high speed stirring to form a pre-emulsion. The resultant dispersion is then subjected to ultrasounds thus reducing the droplets size of the emulsion. Finally, the warm emulsion is cooled to room temperature, which should be below the crystallization temperature of the lipid, and the lipid nanoparticles are formed (Ganesan and Narayanasamy, 2017, Shah et al., 2015).

Ultrasonication is a very effective method for the size reduction of both liquid and solid particles and allows an improvement in the uniformity and stability of the emulsion. Also, the exact control over the operational parameters permits controllable and repeatable results, which is essential for the quality of the nanoparticles obtained (Pardeike et al., 2009, Zielińska and Nowak, 2016).
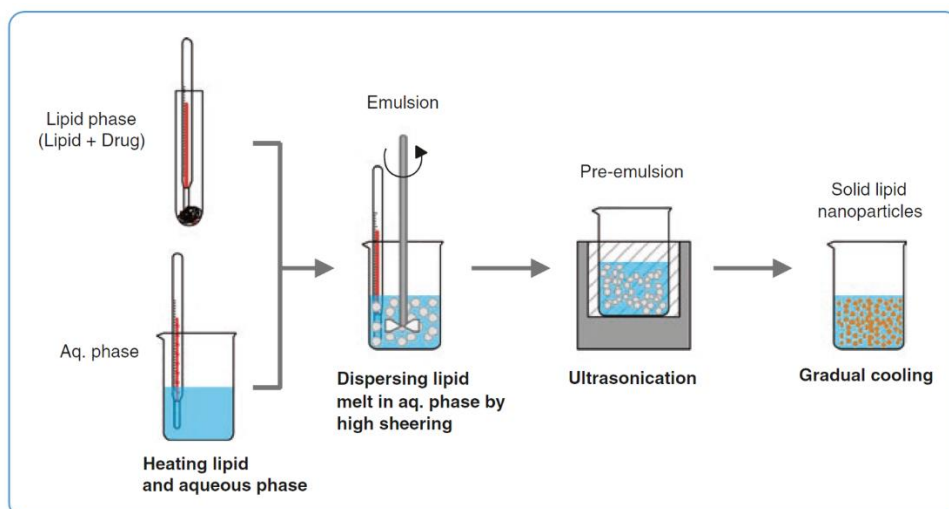
Figure 2.12 – Schematic illustration of the steps involved in the ultrasonication and/ or high shear homogenization. Adapted from (Shah et al., 2015).

2.2.3.3. Microemulsion method

The microemulsion method (**Figure 2.13**) is an extremely effective technique for the preparation of lipid nanoparticles. A microemulsion consists in optically transparent lipid mixtures and thermodynamically stable systems composed by water and oil and stabilized by a surfactant or if required a co-surfactant.

They are prepared by separately heating the lipid phase containing the active substance and the aqueous phase with the surfactant, to a temperature above the melting point of the solid lipid. Both phases are then mixed under continuous stirring to yield a hot microemulsion, which is then dispersed in cold water (typically 2–4 °C), under mechanical stirring, to yield the lipid nanoparticles. The right proportions of excipients are essential in this method, being recurrent the use of phase diagrams to analyze the areas of microemulsion formation (Priano et al., 2007, Shah et al., 2015, Zielińska and Nowak, 2016).
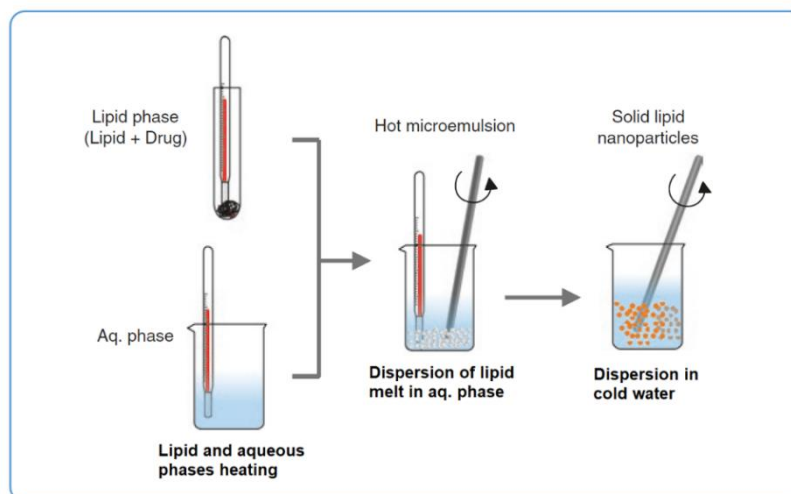
Figure 2.13 – Schematic illustration of the steps involved in the microemulsion method. Adapted from (Shah et al., 2015).

2.2.3.4. *Membrane contactor method*

The membrane contactor method (**Figure 2.14**), is considered the most advanced for the production of lipid nanoparticles at industrial scale. In the first step, the lipid melt is pressed through the pores of a membrane contactor at a temperature above the melting point of the solid lipid to produce lipid droplets. These are then separated from the membrane pores by the water phase which flows in a tangential direction with respect to the membrane surface. The aqueous flow carries the droplets formed at the pore outlets as a result of gradual cooling of the mixture, at first to a temperature below the lipid melting point and then to room temperature (Charcosset and Fessi, 2005, Shah et al., 2015, Zielińska and Nowak, 2016).
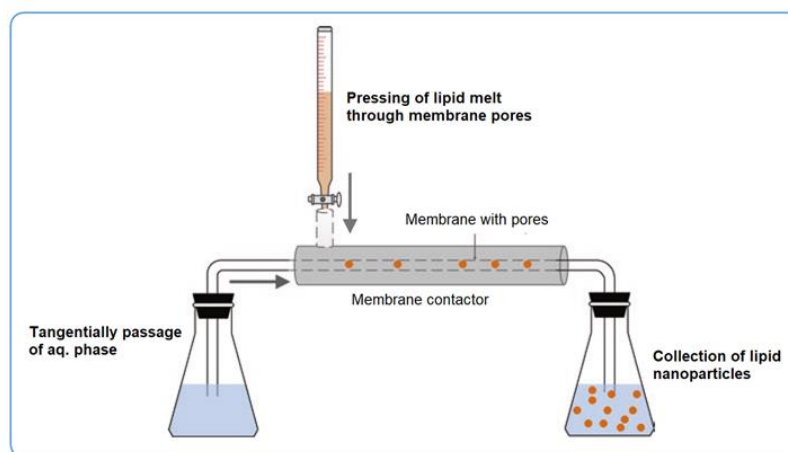
Figure 2.14 – Schematic illustration of the steps involved in the membrane contactor method. Adapted from (Shah et al., 2015).

2.2.3.5. Supercritical fluid extraction of emulsions

Another alternative method of preparation of lipid nanoparticles is supercritical fluid extraction (SFE) of emulsions (**Figure 2.15**). SFE technology is based on the precipitation of a compound using a compressed anti-solvent such as supercritical carbon dioxide. The lipids and the active compound are solubilized in an organic solvent such as chloroform with the addition of a suitable surfactant. The organic solution is then dispersed into an aqueous solution and this mixture is passed through a high pressure homogenizer to form an o/w emulsion which is posteriorly introduced from one end of the extraction column and at the same time the supercritical fluid is introduced counter-currently. The lipid nanoparticles are formed by a continuous extraction of solvent from the O/W emulsion. It is important that the obtained particles are a dry powder instead of a suspension (Chattopadhyay et al., 2007, Santo et al., 2013b, Shah et al., 2015, Zielińska and Nowak, 2016).
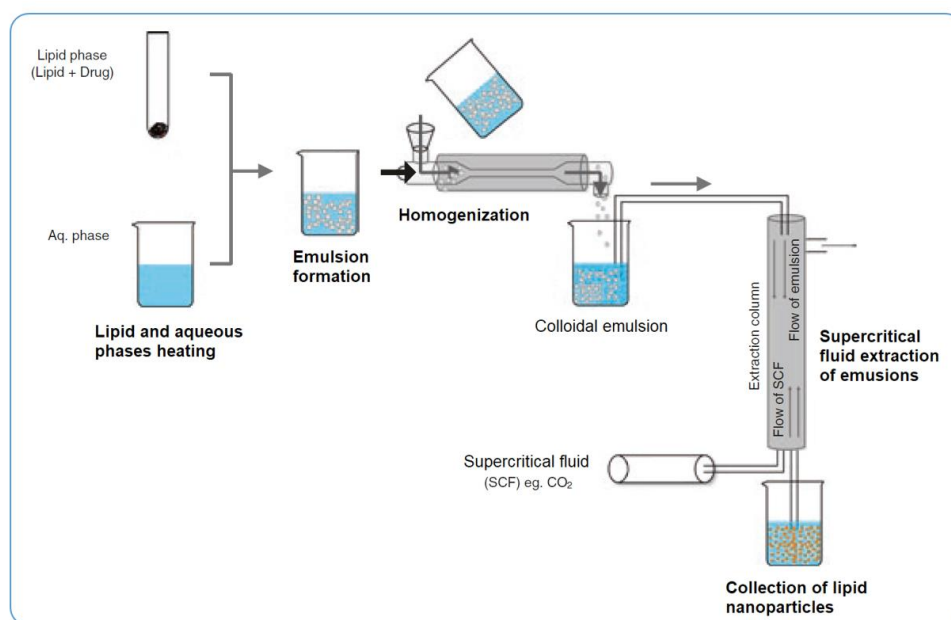
Figure 2.15 – Schematic illustration of the steps involved in the supercritical fluid extraction of emulsions. Adapted from (Shah et al., 2015).

2.2.3.6. Solvent evaporation method

The process of emulsification and evaporation of the solvent (**Figure 2.16**) is another well-established method for obtaining lipid nanoparticles. Initially, the lipid phase with the active compound is dissolved in an organic solvent such as cyclohexane, chloroform or ethyl acetate (Cortesi et al., 2002). This organic phase is then emulsified in an aqueous solution containing a surfactant to form an organic solvent-in-water emulsion. As a result of this process, a lipid nanoparticulate suspension is formed in the aqueous phase (Ganesan and Narayanasamy, 2017, Shah et al., 2015).
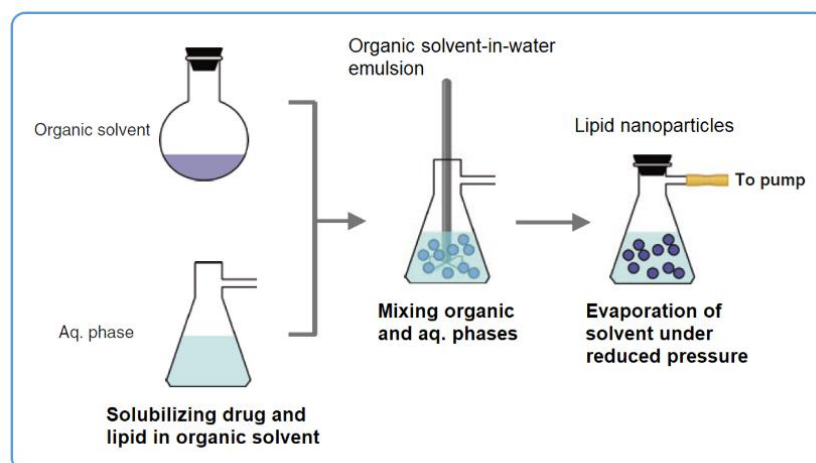
Figure 2.16 – Schematic illustration of the steps involved in the solvent evaporation method. Adapted from (Shah et al., 2015).

2.2.4. Analytical characterization of lipid nanoparticles

It is necessary an adequate and proper characterization of lipid nanoparticle formulations for product design and development with desired properties suitable for their intended application, and also for quality control related to large-scale industrial production. It is required a detailed characterization plan to investigate the structure and behavior of these complex colloidal carriers. However, its complex structure, dynamic nature and colloidal size makes their physicochemical characterization a real challenge. The most important parameters to be evaluated are: (i) particle size, (ii) physical stability, given by the zeta potential (iii) degree of crystallinity and polymorphism and (iv) morphological and ultrastructural aspects (Guimarães and Ré, 2011).

2.2.4.1. Particle size

The particle size is a key parameter that influences the material properties of the lipid nanoparticles and determines its function and efficiency in the biological environment. Formulation and process parameters affects the size and crystallization of lipid particles (Shah et al., 2015). It is thus essential to perform its evaluation for determining the necessary optimum conditions to obtain a product with desired properties and also for evaluating its expected stability kinetics during storage or identifying any possible aggregation tendency (Guimarães and Ré, 2011). Particle sizing can be used as an indicator of formulation instability as the occurrence of an increase on particle size before macroscopic changes observed is an evidence for an unstable systems (Heurtault et al., 2003).

Photon correlation spectroscopy (PCS), also referred to as dynamic light scattering (DLS), because of the ability to measure fluctuations in the intensity of scattered light caused by molecular motion, is the most widely used method to determine the particle size of lipid nanoparticles in a dispersion (Obeidat et al., 2010, Shah et al., 2015).This technique is rapid, non-invasive and non-destructive and requires a very small amount of sample without extensive preparation. DLS is effective for detect particles over the size range of approximately 3–3,000 nm (Zielińska and Nowak, 2016).

DLS measurement is based on the analysis of the random thermal, or Brownian motion, of the particles suspended in the dispersion medium when they are exposed to laser radiation. The particles scatter the laser radiation and the particle movement is related to the particle size, as larger particles move slower, and smaller particles move faster (Guimarães and Ré, 2011). Thus, DLS measures the statistical intensity fluctuations in scattered light from multiple collisions of particles as a function of time. The scattering intensity-time curve is analysed by an autocorrelation function that is used to derive parameters that relate to particle size its distribution (Shah et al., 2015). The "method of cumulants" can be used to derive the particle size, determined as z-average diameter and polydispersity index (PdI), indicative of the width of the particle size distribution, from the autocorrelation function (Zielińska and Nowak, 2016).

Lipid nanoparticles are well-characterized in terms of particle size using effective diameter and PI values in very fast measurements (results are generated in 1–2 min). High PdI values exclude accurate interpretations of the results based on the method of cumulants while low PdI values indicates the existence of a more monodisperse the suspension (Gaumet et al., 2008, Zielińska and Nowak, 2016). Most researchers recognize PI values below 0.3 as optimum and values below 0.5 are considered as acceptable (Kaur et al., 2008).

DLS is commonly referred as a simple, robust and reliable technique for characterizing particles size with a narrow and monomodal size distribution pattern in nanometer range. It is although less useful for dispersions with broad or multimodal size distributions as the presence of large particles or aggregates may have a significant impact on particle size measurements (Guimarães and Ré, 2011, Shah et al., 2015).

2.2.4.2. Zeta potential

Each particle surface is surrounded by an electrical double layer formed by ions in the interfacial area and ions that have the opposite charge to the particles at the surface which distribution is influenced by their electrical charge (Zielińska and Nowak, 2016). There is thus, a hypothetical boundary within which the particle and surrounding ions form a stable entity layer. This is called the surface of hydrodynamic shear which potential is the zeta potential. Zeta potential defines the potential difference between the dispersion medium and the stationary layer of fluid attached to the dispersed particle and is the concept used to describe the electro-kinetic potential in colloidal dispersions (Shah et al., 2015).

The measurement of zeta potential values indicates the degree of electrostatic repulsion between adjacent, similarly charged particles in a dispersion which allow predictions about the storage stability of colloidal dispersion (Guimarães and Ré, 2011, Zielińska and Nowak, 2016). For instance, particles that are small enough and demonstrate a high zeta potential will confer stability, meaning that the solution or dispersion will resist aggregation. While with low zeta potential values, attractive forces may exceed this repulsion and the dispersion may break and aggregate. It is generally established that particles of absolute zeta potential value higher than |30| mV are considered stable (Estanqueiro et al., 2014, Gaumet et al., 2008, Guimarães and Ré, 2011, Shah et al., 2015, Zielińska and Nowak, 2016).

2.2.4.3. Crystallinity and Polymorphism

In most of the production methods used to prepare lipid nanoparticles there is a heating step of the lipids phase above its melting point which solidifies after being dispersed in the aqueous phase and cooled to room temperature. However, in a colloidal dispersed state many lipid materials may crystallize at temperatures much lower than their melting points or even not crystallize (Shah et al., 2015). The incorporation of active substances or the inclusion of a liquid lipid, in the case of NLCs, greatly influences the crystallization tendency of lipid nanoparticles, leading to a suppression of crystallization temperature, and to a decrease in the melting point which is usually lower than the crystallization temperature (Ali et al., 2010, Müller et al., 2008).

Considering these arguments, it seems essential to assess the information regarding the crystalline structure of lipid nanoparticles for the evaluation of its lipid matrix order/disorder degree after the solidification/recrystallization step upon cooling and to investigate the possible occurrence of polymorphic phenomena. The analysis of these parameters may be performed by differential scanning calorimetry (DSC) (Guimarães and Ré, 2011).

DSC is a thermo-analytical technique that has been commonly used to evaluate used to investigate the energetic states of materials. DSC explores the fact that different materials have different melting temperatures and enthalpies. The basic principle underlying this technique consists in monitoring the heat flow to and from the sample, during a controlled temperature scan, and compared to an inert reference (Shah et al., 2015). The result of a DSC experiment is a curve which displays the heat flow per gram of sample as a function of time or temperature and can be further used to determine crystallization and polymorphic transitions from transition temperatures (melting point) and the correspondent enthalpy by directly integrating the peak corresponding to a given transition. DSC is mainly used to confirm the solid nature of lipid nanoparticles through the detection of a melting transition during heating (Estanqueiro et al., 2014, Guimarães and Ré, 2011, Shah et al., 2015, Zielińska and Nowak, 2016).

2.2.4.4. Particle Morphology and Ultrastructure

The morphology of a particle is mainly referred to its exterior surface and may be characterized by shape and surface structure while the ultrastructure generally relates to the internal structure of the particle and is related to the formulation itself, indicating the presence and orientation of the various components of the formulation (Shah et al., 2015).

Both parameters, including particle size, shape, structure and presence of other colloidal structures within the dispersion, are usually evaluated by Transmission electron microscopy (TEM) (Friedrich et al., 2010). TEM micrographs are of low resolution which interferes with results interpretation and are just a two dimensional projection of a three dimensional anisometric particle that stays attach to the copper grid, in which the sample is prepared, in a preferred orientation (Harris, 2007, Zielińska and Nowak, 2016).

Scanning electron microscopy (SEM) is the next more widely used technique for characterizing the morphology, size and distribution of particles. Prior to the analysis is necessary to perform the sample preparation in which the particles are dried by freeze drying, and their surface is coated by sputtering with a conducting material such as gold. The main limitation of SEM is the application of vacuum during the analysis and the sample preparation which may affect the particles integrity, leading to uncertain experimental observations (Guimarães and Ré, 2011, Shah et al., 2015).

Another commonly used technique for the evaluation of lipid nanoparticles morphology is Atomic force microscopy (AFM) (Estella-Hermoso de Mendoza et al., 2008, Shah et al., 2015, Sitterberg et al., 2010). This technique allows imaging under hydrated conditions, providing a high-resolution image of the particle surface, being thus established as an important characterization tool for particulate or biological samples. AFM is based on acting forces between a particle surface and a tip of a cantilever. This technique does not require a sophisticated sample preparation which represents a major advantage. However, probe-sample interactions can result in image distortion. The particle size parameters obtained by AFM are often close to one obtained by DLS, which validates the results given by both techniques (Guimarães and Ré, 2011, Shah et al., 2015, Zielińska and Nowak, 2016).

56

2.3. Efficacy of lipid nanoparticles for topical administration

At present, NLCs have been gaining distinction through their multiple advantages for the management of skin diseases and have been pointed as a promising cutting-edge technology enable to target the therapeutic payload to deep skin layers.

Skin may represent a readily accessible surface area for potential drug absorption, but still skin-targeted drug delivery remains challenging. After a rational approach for designing and optimizing skin formulations destined for either topical administration, it seems strictly necessary the use of well-defined skin models to identify and evaluate the intrinsic properties of this formulation.

The main approach used in preclinical development of new dermal formulations destined for topical administration currently relies on the use of suitable *ex vivo* animal/human models. However, due to recent regulatory changes regarding the use and handling of animals and human skin testing in the field of cosmetics stimulated the search for suitable artificial *in vitro* skin models as an important tool in the permeation, penetration and skin irritancy studies.

2.3.1. *Skin morphology and barrier function*

The skin is the largest organ of the human body and in an adult represents a surface area of about 2 m², which corresponds to 15% of the total body weight (Alexander et al., 2012, Sala et al., 2018). The skin has an integrated complex structure, and it serves as a very effective barrier to the entry of exogenous substances (Abla et al., 2016, Jain et al., 2014). The full thickness of human skin is composed of three types of three layers: the epidermis, dermis, and hypodermis (**Figure 2.17**).

The most inner layer is the hypodermis which is rich in triglycerides and acts as an insulator. Sweat and pilosebaceous glands arise from the hypodermis and open at the surface of the epidermis (Abla et al., 2016). Hair follicles in humans are low in number compared to furry animals (Jacobi et al., 2005, Korting and Schafer-Korting, 2010).

The vascularised dermis lies below the epidermis is 1–3 µm thick and is rich in fibres (collagen, elastin), embedded in a ground substance surrounding fibroblasts which are the most numerous cell in the dermis. It is mostly made up of connective tissue and is more hydrophilic in nature and provides nutrients and oxygen to the skin (El Maghraby et al., 2008, Sala et al., 2018).

The epidermis is the outermost layer of the skin which is composed of five different layers detectable by cellular differentiation: *the stratum lucidum*, *stratum granulosum*, *stratum spinosum*, *stratum germinativum* (which together form the viable epidermis), and the non-viable but chemically active *stratum corneum* (SC) which is the outermost layer exposed to the environment consisting in about 15 layers of flat apoptotic keratinocytes, the so-called corneocytes (Abla et al., 2016, Flaten et

al., 2015, Korting and Schafer-Korting, 2010, Sala et al., 2018). The thickness of the horny layer amounts to about 10–15 µm, the thickness of the viable epidermis to 50–100 µm (Korting and Schafer-Korting, 2010, Sala et al., 2018). Keratinocytes migrate toward the skin surface and undergo maturation to differentiate in corneocytes. These are flat dead cells containing high amounts of keratin filaments and water. The common concept used to illustrate the SC is the "bricks and mortar" model, where the bricks are the corneocytes embedded in a mortar which is the surrounded by a hydrophobic matrix composed of keratin, ceramides, cholesterol, cholesterol esters, and fatty acids (Abla et al., 2016, Riviere and Papich, 2001, Sala et al., 2018). Considering the great complexity of the SC, it is easy to conceive that this layer represent the main barrier for the passage of active compounds through skin. The deeper layers of the dermis are not significantly influencing the possible percutaneous absorption. However, a very lipophilic active compound which can overcome the SC barrier will face serious obstacles to absorption through the subsequent aqueous interface (Flaten et al., 2015).
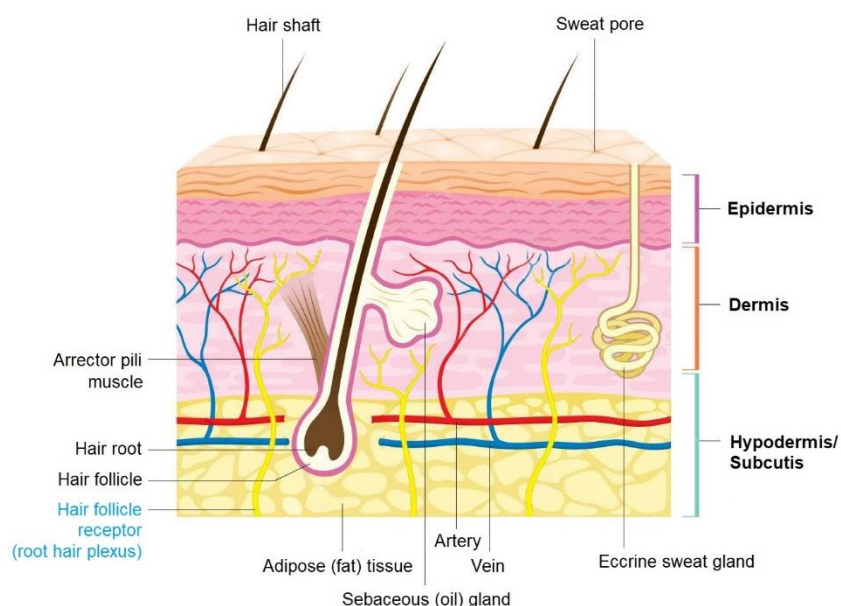
Figure 2.17 – Morphology of human skin. From (https://www.123rf.com).

The strong skin barrier slows the drug absorption rates, limits the drug uptake and contributes to lack of the dosing precision (Lam and Gambari, 2014). The final absorption potential of an active can be increased or limited by the choice of a suitable carrier/vehicle for transdermal or dermal delivery, respectively. The interactions between the carrier/vehicle and the active substance are of a great interest in formulation development (Flaten et al., 2015). Therefore, the characteristics of an active such as its partitioning into skin and exposure at the skin surface are identified as major properties contributing to absorption. The carrier can directly affect the mentioned characteristics and improve their limitations (Chittenden et al., 2014, Flaten et al., 2015).

2.3.2. *In vitro reconstructed human epidermis models*

The progress in tissue engineering resulted in the development of several culture-based human epidermis models and in their commercial availability (Van Gele et al., 2011). There are several commercially available types of reconstructed human epidermis (RHE) models which are usually classified as epidermal, with SC and viable epidermis (e.g. EpiSkin®, SkinEthic®, EpiDerm®) or full thickness skin model with SC, viable epidermis and dermal equivalent (GraftSkin®, EpiDermFT®, Pheninon®) (Auxenfans et al., 2009, Flaten et al., 2015, Kuchler et al., 2013, Van Gele et al., 2011). Nevertheless, in-house generated skin equivalents also undergo substantial progress (Bellas et al., 2012, Kuchler et al., 2013). These models are composed of human cells consisting on keratinocytes and/or fibroblasts grown in tissue cultures and matrix equivalents normally present in the skin (Godin and Touitou, 2007). The use of RHE models has become a widely accepted approach for the pharmacology and toxicology evaluation of both finished dermal products and formulations with active ingredients (Flaten et al., 2015).

The *in vitro* RHE models mimic the physiology of human skin and are globally used in both industrial and academic research laboratories, and regulatory bodies endorse their use as valid alternatives to animal testing requirements (Spielmann et al., 2007). The Organization for Economic Cooperation and Development (OECD) approved the use of RHE models for skin corrosion (Bellas et al., 2012), acute skin irritation (OECD, 2015) and phototoxicity testing (Kuchler et al., 2013).

Besides their proven efficacy and advantages compared to the use of human cadaver and/or animal skin in terms of reproducibility, availability in large numbers, metabolism, and typical "tissue response," RHE models are not exact copies of human skin *in vivo* (De Wever et al., 2015). The reconstructed epidermis equivalents are significantly more permeable, but are more consistent in the permeability than the human skin, which is highly variable (Netzlaff et al., 2006). For example, the permeation of highly hydrophobic compounds was found to be even 800-folds higher than in the split-thickness human skin (Flaten et al., 2015). Thus, their major limitation is still the relatively weak barrier function, which limits their applicability for dermal absorption studies (De Wever et al., 2015, Netzlaff et al., 2005) For this reason, RHE models are not yet approved by OECD for drug absorption testing, although the guidance document no. 428 (OECD, 2004) declares that these models are a suitable option given the comparability of their percutaneous drug absorption data and *ex vivo* skin (Flaten et al., 2015). Labouta et al. (2013) (Labouta et al., 2013) have reported that in vitro skin equivalents could serve as a fast screening in testing the behaviour of nanoparticles and extrapolation of their penetration behaviour into human skin.

Currently, there are more research efforts in the field of reconstructed skin disease models. Despite some skin diseases as atopic dermatitis and psoriasis being major public health problems, almost nothing is known about skin absorption in diseased skin. However, most likely skin diseases

alter the dermal drug absorption, especially diseases that are associated with damages of the outermost barrier by scratching, wounding or inflammation, or those linked to a disturbed keratinocyte differentiation (Gattu and Maibach, 2011, Kuchler et al., 2013).

2.3.3. *Skin absorption pathways*

There are many factors which affect the absorption through the skin as differences between species, skin age and environment, skin temperature, state of the skin (normal, abraded, or diseased), area of application, contact time, degree of hydration of the skin, pre-treatment of the skin, and physical characteristics of the penetrant. The mechanism of skin absorption is diffusion which is concentration dependent (Alexander et al., 2012, Bhoyar et al., 2012). The dermal delivery can be classified into topical and transdermal; a topically active compound is meant to act locally, whereas transdermal route aims at systemic delivery. The advantages offered by skin delivery include by passing hepatic metabolism, avoiding side effects associated with oral delivery of drugs which act on skin, easy removal of medication in case of overdose, sustained release of drug, and patient compliance (Abla et al., 2016, Banga, 2011).

The most external layer of skin, SC is generally considered to be the main barrier to absorption of externally applied substances and as the primary protection of the body from external contaminants, limiting the potential therapeutic effectiveness of topically applied compounds. It is well acknowledged that a molecule will permeate across the SC via one of the three established pathways into/through the skin (**Figure 2.18**), i.e., transcellular (intracellular), intercellular and the appendageal (follicular) (Abla et al., 2016, Lane, 2013, Sala et al., 2018).
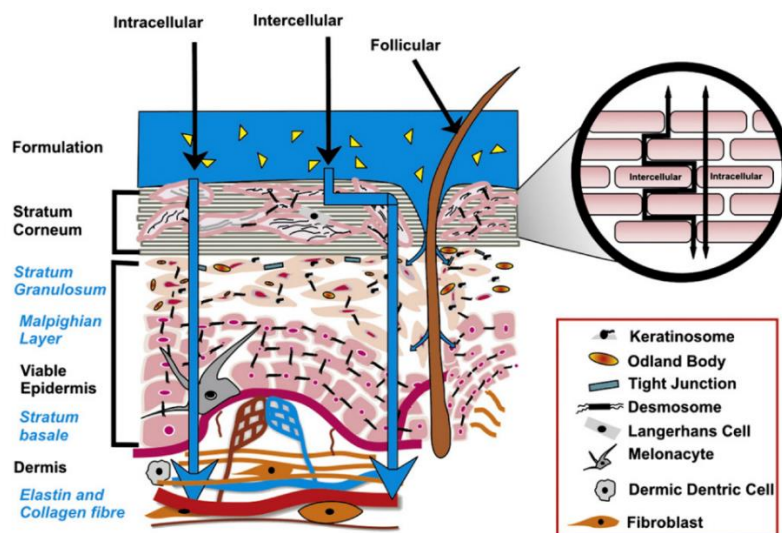
Figure 2.18 – Schematic representation of different skin absorption pathways. From (Alexander et al., 2012)

The passage of active compounds through keratinocytes is called the transcellular route, whereas passage via the lipid matrix is called the intercellular route. The appendageal route is across hair follicles, sweat glands, and sebaceous glands (Abla et al., 2016, Banga, 2011). These pathways are not mutually exclusive, with most compounds possibly permeating the skin by a combination of pathways and the relative contribution of each being related to the physicochemical properties of the permeating molecule (Benson, 2012).

The permeation process involves a series of processes starting with release of the permeant from the formulation, followed by diffusion into and through the SC, then partitioning to the more aqueous epidermal environment and diffusion to deeper tissues or uptake into the cutaneous circulation. These processes are highly dependent on the solubility and diffusivity of the permeant within each environment. The diffusion coefficient of an active substance is dependent on the permeant properties including the molecular size, solubility and melting point, ionization and potential for binding within the environment, and also factors related to the environment such as its viscosity and tortuosity or diffusional path length (Abla et al., 2016, Benson, 2012).

The transcellular route has been considered as a polar route through the SC. This is mainly due to the intracellular keratin matrix of corneocytes, that is relatively hydrated and thus polar in nature, which conditions the permeation requiring a repeated partitioning between this polar environment and the lipophilic domains surrounding the corneocytes (Benson, 2012). Nevertheless, it is commonly admitted that the transport through the SC is predominantly by the intercellular route. Within the intercellular lipid domains, transport can take place via both lipid (diffusion via the lipid core) and polar (diffusion via the polar head groups) pathways. The diffusional rate - limiting region of very polar permeants is the polar pathway of the SC, which is fairly independent of their partition coefficient, while less polar permeants probably diffuse via the lipid pathway, and their permeation increases with increase in lipophilicity (Benson, 2012). The appendageal route is considered to be more appropriate for molecules with a high molecular weight which diffuse slowly through the skin and also for nanoparticles (Lademann et al., 2015). Hair follicles represent around 0.1% of the skin surface which makes them a potential pathway for drug permeation. Indeed, the SC layer in the deeper parts of hair follicles is thinner than other regions in the epidermis. Moreover, the profound invagination facilitates access to the capillary network, making hair follicles the pathway of choice for transdermal delivery (Knorr et al., 2009).

The lipids used in the formulation of lipid-based colloidal carriers have structural similarities with those composing the epidermis and in particular the SC. Zhai and Zhai, 2014 (Zhai and Zhai, 2014) proposed different mechanisms of interaction between lipid-based colloidal carriers and corneocytes to promote skin absorption (**Figure 2.19**).
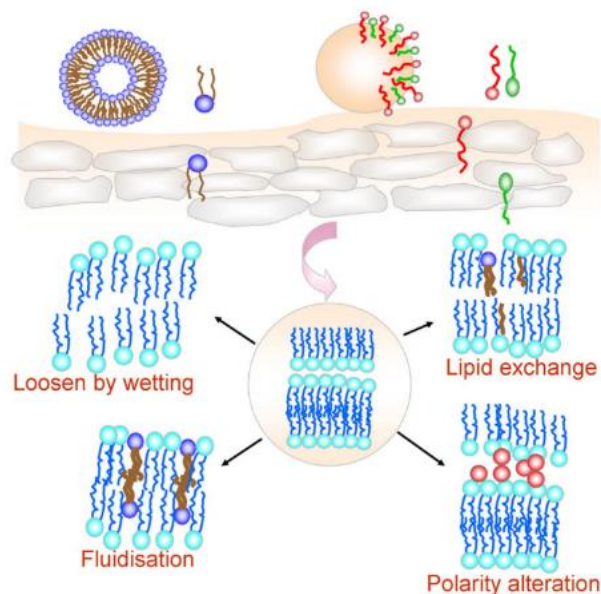
Figure 2.19 – Interaction mechanisms of lipid-based carriers with corneocytes. Lipid-based carriers could attach themselves onto the skin surface, promote adhesiveness and increase skin hydration, gradually lead to loose structure, polarity alteration, fluidization and even lipid exchange within the intercellular lipid domain. From (Zhai and Zhai, 2014).

After adhesion to the skin surface, lipid-based carriers may disrupt into the SC through different mechanisms such as lipid exchanges or looseness of the structure, polarity alteration or SC fluidization following an increased hydration (Sala et al., 2018, Zhai and Zhai, 2014).

2.3.4. Properties of lipid nanoparticles and their effects on skin

Lipid nanoparticles, both SLNs and NLCs are relatively easy-to-make, providing an increased absorption of active substances on skin and are highly effective carriers based on physical and chemical principles. Their effects on skin relies on these principles: *(1)* Physical adhesion to the skin, due to their small size and consequently increased surface area and interaction; *(2)* Physical film formation creating occlusion *(3)* Physical occlusion promoting the absorption of active substances and *(4)* Chemical interaction between the lipids from the particles with the skin lipids (Abla et al., 2016).

2.3.4.1. Mechanisms of skin absorption from lipid nanoparticles

The topical administration of lipid nanoparticles (SLNs and NLCs) on the skin results in a monolayer film due to their adhesiveness property. This film formation is even more pronounced when

the amount of nanoparticles in the formulation is higher and is able to sufficiently cover the skin surface. NLCs were therefore also called the "invisible dermal patch" (Müller et al., 2016, Müller et al., 2013). This film is hydrophobic and its resistance and effects are dependent on the size of the particles that constitutes it. Moreover, due to its hydrophobicity, it has an occlusive effect. In addition, the lipids of the particles may also interact with the skin lipids, thus affecting the distribution of the active compound between the lipid structures of the skin and affecting its absorption depth. However, this is little understood by now and the ideal lipid matrix composition to reach this interaction with the skin lipids has to be found empirically (Müller et al., 2016, Souto and Muller, 2008). **Figure 2.20** shows a proposed mechanism for this interaction between lipids. It demonstrates that the lipid nanoparticles primarily remain on skin without interaction with the skin lipids if their lipids matrix are not miscible with SC lipids, or if the particle matrix possesses a very high melting point. The particles might only be slightly flattened by the application pressure. On the other hand, the interaction between lipids in case of good miscibility and especially when the onset of the melting peak of the particles' lipids is below the skin temperature may occur. This leads to partial softening of the particle matrix promoting inter-diffusion of lipids between particles and SC lipids, potentially integrating the lipid nanoparticle in the lipid film on the SC (Müller et al., 2016).

Zhai and Zhai, 2014 (Zhai and Zhai, 2014) demonstrated that NLCs could disrupt the intercellular packing that embeds the keratinocytes and corneocytes especially by acting on its lipids composition. The tight anomalies junctions in SC would lead to the barrier function defectiveness and would promote the skin permeation of drugs (Sala et al., 2018).
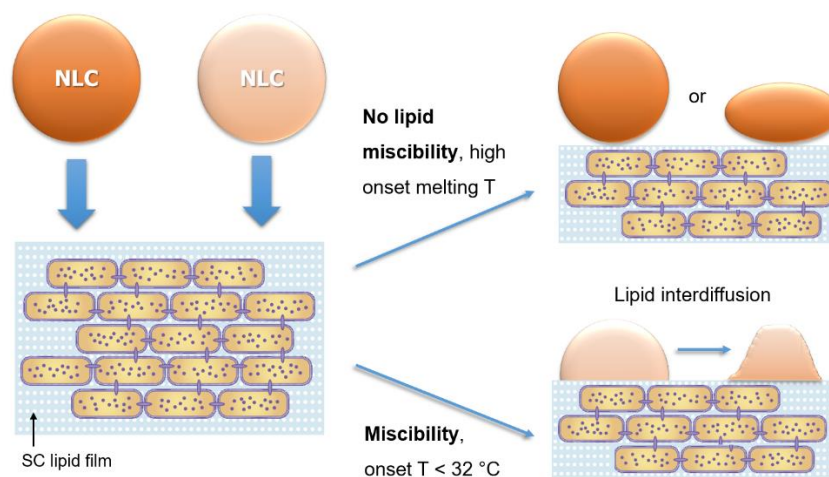
Figure 2.20 – Proposed mechanism for the interaction of lipid nanoparticles with lipids of the SC lipid film. Upper right: No interaction for particles with no lipid miscibility/high melting temperature; Lower right: Interdiffusion of lipids in case of miscibility, particle integration into skin lipid film by fusion, and "interdiffusion". Modified from (Müller et al., 2016).

For SLNs, Jensen et al. 2011 (Jensen et al., 2011) proposed a skin absorption mechanism in which they remain on the skin surface and in the SC forming a drug reservoir in the upper layers of the skin from where they release the encapsulated active molecules with a degree depending on the lipophilicity of the active ingredient to reach the target cells in the lower epidermis and dermis. In this mechanism, the SLNs would release the active substance in a biphasic way, with an initial burst release from the surface of the particles and the aqueous phase followed by a reservoir effect from the surface skin and SC (Jensen et al., 2011, Sala et al., 2018). The interaction of the SLNs with the skin lipids and sebum is observed to be influenced by the drug lipophilicity and the drug partitioning in the lipid particle, the nature of the lipid matrix and the type of interacting skin lipid. Both SLNs and NLCs systems could take the appendageal pathway because their high lipophilicity promotes follicular deposition (Sala et al., 2018).

2.3.4.2. Occlusion

The SC is compactly embedded in a continuous lipid layer known as the "brick mortar" model which represent a barrier for water-soluble and lipid-soluble materials (Müller et al., 2016, Schäfer-Korting et al., 2007). The lipid nanoparticles adhere to the skin leading to a film formation and subsequently to an occlusion effect (**Figure 2.21**) with an increased hydration effect (Guimarães and Ré, 2011, Müller et al., 2007, Souto and Muller, 2008).
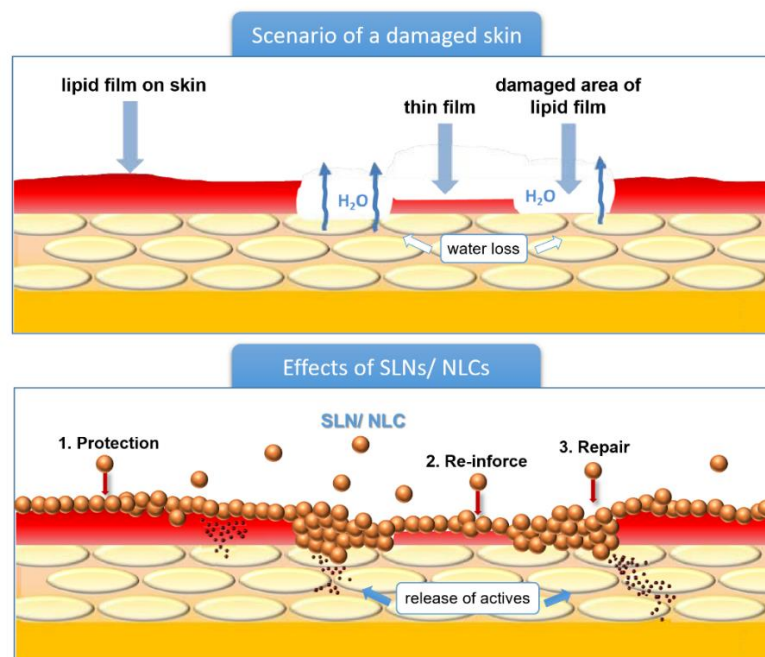
Figure 2.21 – Properties of lipid nanoparticles on the skin. Upper: Situation on damaged skin with reduced protection, increased moisture loss and distorted cell function. Lower: Action of SLNs/NLCs with less water loss, increased skin adhesiveness and hydration, increased retention time and increased bioactivity. Modified from (Muller et al., 2011).

This hydration effect contributes to a healthy appearance of the skin, and also directly influences the percutaneous absorption of active substances. For topical administrations it is important that the active is not systemically absorbed, but instead is crucial that a certain absorption occurs in the skin in order to the desired effect take place (Cevc and Vierl, 2010, Guimarães and Ré, 2011).

The occlusion resultant from a mono-layered hydrophobic film formation, reduces water evaporation from the skin and increases the hydration of the SC which normally has only 10–15 % water content. Consequently, the corneocytes become less compact and the inter-corneocyte gaps become wider. These changes increase the permeability of the SC and can promote drug penetration (Müller et al., 2016, Schäfer-Korting et al., 2007). It was reported that approximately 4% of lipid nanoparticles with a diameter of about 200 nm should theoretically form a monolayer film when c. 4 mg of formulation is applied per cm^2 (Souto and Muller, 2008, Wissing et al., 2001). This occlusion factor is directly dependent on several factors: (i) lipid content, (ii) degree of crystallinity of the re-crystallized lipid and also (iii) particle size (Guimarães and Ré, 2011). By manipulating the particle size of lipid nanoparticles, different effects can be obtained (Souto and Muller, 2008). The occlusion can be increased by decreasing the particle size (at a given lipid concentration) or alternatively at a given particle size by increasing the number of particles (concentration of lipid) and therefore, a "controlled occlusion effect" can be achieved (**Figure 2.22**) (Escobar-Chávez et al., 2012, Müller et al., 2007).
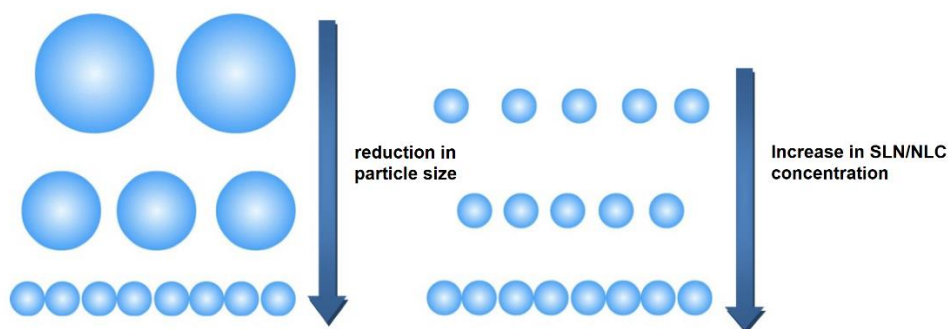
Figure 2.22 – The controlled occlusion effect of lipid nanoparticles in function of the particle size. Left: At a given identical lipid content, reducing the particle size leads to an increase in particles number which results in a denser film. Right: At a given particle size, increasing the lipid concentration leads to an increase in particle number and density of the film which also result in a higher occlusion effect. Adapted from (Escobar-Chávez et al., 2012, Müller et al., 2007)

It was reported that the particle size has to be less than 260 nm (Mardhiah Adib et al., 2016) to accomplish a higher occlusion and a greater interaction with the skin surface. Moreover, it was also reported that an increase in liquid content may reduce the occlusive effect, being this higher for lipid

nanoparticles possessing highest crystallinity which indicates that SLNs had a higher occlusive effect than NLCs (Müller et al., 2016, Souto et al., 2004, Teeranachaideekul et al., 2008a). Lombardi Borgia et al. 2005 (Lombardi Borgia et al., 2005) reported that after SLNs application on the skin, its water content evaporates which results in a recrystallization phenomenon inducing the partial release of the active and its skin penetration (Sala et al., 2018).

The occlusion effect induced by typical ointment formulations does not ensure rapid hydration. It is then desirable to use a preparation capable of supplying water which lipid nanoparticle suspensions are suitable to offer. Moreover, due to their hydration properties, it can be assumed that lipid nanoparticles may enhance skin elasticity (Wissing and Müller, 2003), and that these particles can be further used to formulate anti-ageing products (Souto and Muller, 2008).

2.3.4.3. Enhanced stabilization of actives and skin bioavailability

The solid matrix of both SLNs and NLCs represent one of their most important features as it enables the advantage of stabilize active ingredients that are chemically labile against degradation by light, oxidation and hydrolysis (Guimarães and Ré, 2011, Souto and Muller, 2008). The selection of an appropriate lipid is a major factor to be considered as the active compound must be totally solubilized/ retained within the lipid matrix during the storage time (Müller et al., 2007, Souto and Muller, 2008).

The effect of chemical stability of actives after their incorporation into lipid nanocarriers was already proven for, e.g. coenzyme Q10 (Teeranachaideekul et al., 2007a, Wissing et al., 2004), ascorbyl palmitate (Teeranachaideekul et al., 2007a, Üner et al., 2005) and retinoids (Guimarães and Ré, 2011, Jee et al., 2006, Liu et al., 2007b, Pople and Singh, 2006, Souto and Muller, 2008).

The lipids composition of lipid nanoparticles will also determine their skin bioavailability and targeting in two possible ways: *(1)* the differences in lipid composition might lead to different interactions with the lipids of the SC and consequently to a different localization of the active compound; *(2)* the lipid composition will determine the localization of the active compound inside the particle, modulating its bioavailability and release (Müller et al., 2007, Sivaramakrishnan et al., 2004).

2.3.4.4. Lightening effects in creams

The appearance of a cosmetic or pharmaceutical product is an important factor for it to be sold as for instance, not only the packaging should be attractive but also the appearance of the product itself (Müller et al., 2016). White products are preferred by the consumers and the whitening effects of lipid dispersions are one of the most elegant properties of such formulations (Souto and Muller, 2008). Compounds like coenzyme Q10 are coloured (yellow) leading to a yellowish appearance of the cream. This coloration can be weakened by addition of a white lipid nanoparticles dispersion (Muller R. H., 2005).

Other examples are those actives that can turn into coloured intermediate products during the shelf life (vitamins) (Radomska et al., 1999). In case such coloration occurs, even if it is weak, it will be associated by the consumer to a spoiled product−despite the percentage of such degradation products might be not relevant and not impair the product quality (Muller R. H., 2005). Thus, the incorporation of those actives into SLNs or NLCs leads to a whitening effect which is considered more appealing to the customer from the marketing point of view (Souto and Muller, 2008).

2.3.4.5. *Modulation of actives release and supersaturation effects*

Before the incorporated active ingredient on SLNs and NLCs may exercise their function into the skin, it is prime necessary its release (Castro et al., 2007, Souto and Muller, 2008). The release profile of lipid nanoparticles is a multifactorial event, where many factors interplay (Muller R. H., 2005). Thus, it is dependent the method of preparation, the composition of the formulation (i.e. composition and concentration of surfactant), the solubilizing properties of the surfactant for the incorporated active, and in addition to the solubility (and concentration) of the active in the lipid matrix (oil/ water partition coefficient) (Muller R. H., 2005, Souto and Muller, 2008). These factors influence the inner structure of the lipid nanoparticles and therefore the rate of release of incorporated ingredient (Bunjes et al., 2007, Pople and Singh, 2006, Souto et al., 2004). Depending on the matrix structure, the release profiles can vary from very fast release, medium release or extremely prolonged release (Müller et al., 2002b, Souto and Muller, 2008). Moreover, the release of actives can also be promoted by enzymatic lipid degradation due to the microbial flora existing on skin or electrolyte changes in the SC (Schäfer-Korting et al., 2007). The electrolytes might cause changes in the lipid structure of the particles, promoting transform to more ordered polymorphic form and drug expulsion (Muller R. H., 2005, Müller et al., 2016).

A majority of active dermal substances are not intended for deeper skin penetration and absorption and having only a local effect and superficial action, it is thus undesired to have an absorption into the blood (Souto and Muller, 2008). Moreover, it seems perfectly clear that a release profile over weeks is not interesting for in vivo topical delivery. Although, lipid nanoparticle dispersions show the ability to control the rate of actives penetration into the skin and to modulate the drug release, i.e., to adapt it accordingly the therapeutic needs (Muller R. H., 2005). Modulation of drug release into certain layers of the skin and, therefore, drug absorption across skin membranes can also be achieved as a consequence of the creation of a supersaturated system (De Vringer, 1997). These systems can be created by incorporation of lipid nanoparticles into topical formulations (creams, ointments, emulsions, and gels). The increase in saturation solubility will lead to an increased diffusion pressure of drug into the skin (Muller R. H., 2005, Souto and Muller, 2008). During storage, the active remains entrapped into the lipid matrix of the lipid nanoparticles since it preserves its polymorphic form. After the application of a supersaturated cream into the skin and due to an increase in temperature and water evaporation, the lipid matrix of the lipid nanoparticles transforms from a more unstable

polymorph to a more ordered polymorph leading to drug expulsion. Consequently, the active is expelled from the lipid matrix into the emulsion already saturated with the same active, and thus creating a supersaturation effect. This phenomenon increases the thermoactivity and leads to active absorption into the skin (Muller R. H., 2005, Souto and Muller, 2008).

◢ CHAPTER III

MINIEMULSIONS FOR THE FORMULATION OF LIPID NANOPARTICLES LOADED WITH B-CAROTENE AND RETINYL PALMITATE

Fátima Pinto, Clara Lopes, Dragana P.C. de Barros, Luis P. Fonseca
European Journal of Lipid Science and Technology – Prepared for submission

3. Miniemulsions for the formulation of lipid nanoparticles loaded with β-carotene and retinyl palmitate

This work aims to assist the selection of proper lipid nanocarriers for the delivery of bioactive compounds in cosmetic, pharmaceutical or food products. Two types of lipid nanocarriers, namely SLNs and NLCs were produced by the miniemulsions methodology and characterized regarding their particle size and physical stability. SLN and NLC dispersions produced by ultrasounds presented particle sizes in the nanometre range (≈105 to ≈146nm and ≈131 to ≈227nm, respectively) and an appropriate physical stability (ZP≥ -25mV). The ratio of total lipids: surfactant influenced significantly the physicochemical properties of both lipid nanocarriers. BC-SLN and RP-NLC showed good entrapment efficiencies of ≈95% and ≈94%, respectively and demonstrated their potential to enhance the bioaccessibility of the incorporated bioactive substances.

3.1.   Introduction

Advances in nanotechnology have introduced numerous applications in the pharmaceutical, cosmetic and food industries, by transforming the administration of bioactive compounds (Hejri et al., 2013, Montenegro et al., 2016). The development of nanoencapsulated compounds was intended to create new delivery systems to improve drug therapeutic effectiveness and to overcome biological barriers, as mainly the skin (Gutiérrez et al., 2013, Oliveira et al., 2014). Colloidal systems have been widely explored to improve skin permeation and in particular, those consisting in biocompatible and biodegradable components such as lipids (Montenegro et al., 2016). As a consequence, different types of lipid based delivery systems were developed such as liposomes, nanoemulsions, nanocapsules, SLNs and NLCs among others (Morales et al., 2015).

At the beginning of 90´s, SLNs were introduced as new colloidal delivery systems by replacing the liquid lipid of O/W emulsions by a solid lipid (Hejri et al., 2013, Lucks and Muller, 1993). In general, SLN consist in crystalized nanoemulsions composed of a solid lipid core (0.1–30%, w/w) dispersed in an aqueous medium and stabilized by surfactants and co-surfactants (optional), presenting normally mean particle sizes from 40 to 1000nm (Lucks and Muller, 1993, Mehnert and Mäder, 2001, Morales et al., 2015, Shah et al., 2015). These nanocarriers have attracted much attention since they overcome several disadvantages, as the use of organic solvents, low encapsulation capacity and large scale production problems of other traditional delivery systems such as polymeric nanoparticles, liposomes and emulsions (Hejri et al., 2013, Mehnert and Mäder, 2001, Muller et al., 2000). Evolved from SLNs, NLCs are the so-called second generation of these lipid based colloidal carriers. NLCs are composed of biocompatible blends of solid and liquid lipids that remain in the solid state and are solid at body

temperature (Lacatusu et al., 2012, Morales et al., 2015). The result of such binary lipid mixture is a strong crystal order disturbance on the nanoparticles lattice, giving rise to great imperfections in the solid matrix which increases its potential to accommodate active compounds, improve the drug loading capacity and prevent leakage, modulating the release profile (Liu and Wu, 2010, Shah et al., 2015). NLCs present some advantages by comparison with SLNs as the possibility to incorporate more active compounds by solubilizing them in the liquid lipid and to improve the chemical and physical stability of the bioactive compound by preventing its microphase separation from the solid lipid matrix (Lacatusu et al., 2012, Zhuang et al., 2010).

SLNs and NLCs have been widely investigated as delivery systems for different routes of administration such as oral, parenteral and topical, due to their great versatility and significant advantages (Doktorovova et al., 2014b, Montenegro, 2014). These lipid nanocarriers demonstrates some advantages such as the use of biocompatible lipids in their composition avoiding the use organic solvents and the availability of established processes for their scale-up. Moreover, they present an increased surface area, and provide to the bioactive compound a controlled release, higher solubility, stability and protection from degradation (Vinardell and Mitjans, 2015). Additionally, SLNs and NLCs have been tested to improve the safety and effectiveness of antioxidants which are commonly used in cosmetic products (Montenegro, 2014). Such bioactive compounds are chemically unstable and sensitive to pH, temperature light and oxidation (Casanova and Santos, 2016). BC and RP are examples of antioxidants that are widely used in anti-aging cosmetic products (Montenegro, 2014, Salavkar et al., 2011, Vinardell and Mitjans, 2015). BC is the most representative of all carotenoids, being the main source of vitamin A in the human body. This powerful antioxidant, also known as provitamin A, can scavenge reactive oxygen radicals showing great benefits on skin, also presenting colorant properties and have been involved in the prevention of some human diseases as cataracts, heart disease and cancer (Che Man and Tan, 2012, Lacatusu et al., 2012). However, BC is a highly hydrophobic compound which limits its dispersion and is very sensitive to heat, light and oxygen (Hejri et al., 2013, Lacatusu et al., 2012). Therefore, there are several reports on the incorporation of BC in lipid nanoparticles for its delivery in food (Gomes et al., 2013, Hejri et al., 2013, Lacatusu et al., 2012, Oliveira et al., 2016) or cosmetic products (Gasperlin and Gosenca, 2011, Trombino et al., 2009). Likewise, RP is an ester of retinol and the most stable form of this vitamin found in epidermis taking part in cellular differentiation and carcinogenesis, it have been widely used in pharmaceutical and cosmetic formulations (Oliveira et al., 2014, Sorg et al., 2005). To overcome its chemical instability and the incidence of unpleasant side effects as skin irritation, the incorporation of RP into lipid nanoparticles was also widely reported (Clares et al., 2014, Lee et al., 2015, Oliveira et al., 2014).

Both types of lipid nanoparticles, SLNs and NLCs can be produced by several methods reported in literature, including high-pressure homogenization (Shi et al., 2012), microemulsification (Fadda et al., 2013), emulsification-solvent evaporation (Kushwaha et al., 2013), emulsification-solvent diffusion (Noriega-Pelaez et al., 2011), solvent injection (Schubert and Müller-Goymann, 2003), phase

inversion (Montenegro et al., 2011), multiple emulsification (Li et al., 2010), ultrasonic dispersion (Siddiqui et al., 2014) and membrane contactors (Charcosset et al., 2005, Gutiérrez et al., 2013, Morales et al., 2015).

In this work, the miniemulsion methodology (Landfester, 2003) was selected as production method, which is based on high shear mixing by ultrasounds. A miniemulsion is a heterophase system consisting of stable nanodroplets, narrowly size distributed of 50 to 500 nm, dispersed in a continuous phase which is formed by shearing the system with ultrasounds (Landfester, 2001, Landfester, 2003, Landfester, 2006). Due to the relatively low cost of the required apparatus and its non-demanding and fast procedure, ultrasonic dispersion offers an appropriate alternative for laboratory scale production of lipid nanoparticles (Schwarz et al., 2012).

Up to date, the search for a closer to ideal nanocarrier for the controlled delivery of lipophilic bioactive compounds, is still on scope of many researchers (Akhoond Zardini et al., 2018, Daneshmand et al., 2018, Tian et al., 2018). The properties and structure of lipid nanocarriers are mostly affected by the composition and characteristics of their components, namely the lipids composition which will determine the entrapment efficiency for the selected bioactive compound and the type and amount of emulsifying agent which affects the particle size and surface charge (Gutiérrez et al., 2013). In this context, this work aims to deliver new formulations for SLNs and NLCs, using the miniemulsion methodology and assess the incorporation of two important antioxidant compounds used in cosmetic products, as BC and RP, providing their enhanced efficacy and safety. Moreover, critical production parameters of lipid nanoparticles, as the emulsification process, the ratio of total lipids: surfactant, the type of surfactant and the concentration of encapsulated antioxidant were evaluated in terms of their effect on particle size, surface charge and morphology.

3.2. Material and Methods

3.2.1. *Materials*

Solid lipid: lauric acid, C12:0 (≥98%) was purchased from Sigma-Aldrich (St. Louis, MO, USA). **Liquid lipid:** Sunflower oil, food grade product (Fula, Portugal). **Surfactants:** two nonionic surfactant were used, Lutensol AT 50, a poly(ethylene oxide)-hexadecyl ether with an EO block length of about 50 units, was a donation from BASF (HLB = 18) and Tween 80, (polyoxyethylene sorbitan monooleate, HLB = 15.0) was obtained from PanReacAppliChem (Darmstadt, Germany). n-Hexadecane (99%) was purchased from Sigma-Aldrich (St. Louis, MO, USA), and it was used in the formulations with Lutensol AT 50, as a hydrophobic agent for osmotic stabilization of the lipid nanoparticles. The aqueous phase of miniemulsions was prepared with Milli-Q water. **Bioactive substances:** *β*-Carotene (BC) (≥97.0%) was obtained from Sigma-Aldrich (St. Louis, MO, USA) and Retinyl pamitate (RP) was a cosmetic grade product purchased from MakingCosmetics® (Snoqualmie, Washington, USA); Acetonitrile RS, diclorometane RS and methanol RS were

purchased from CARLO ERBA Reagents S.A.S. (Z.I. de Valdonne, France) for special use in analytic techniques, HPLC/[1]NMR. All other reagents were of analytical grade.

3.2.2. Production of lipid nanoparticles

Both types of lipid nanoparticles, SLNs and NLCs, were produced by the miniemulsions methodology (Landfester, 2003). The aqueous and lipid phases of these systems were separately prepared before mixing. Lauric acid (C12:0) was selected as solid lipid in all formulations but two different types of surfactants were used for each lipid nanocarrier. The components of produced SLN and NLCs formulations and their percentage composition are listed in **Table 3.1.**

Table 3.1 - Percentage composition of each component in the formulations of SLN and NLCs.

Formulations	Total Lipids, wt%	Solid lipid, wt%	Liquid lipid, wt%	Surfactant, wt%	Co-surfactant, wt%	Bioactive substance, wt%
SLN 1	2.9	2.9	-	Lutensol AT 50, 7.5	Hexadecane, 3.2	-
SLN 2	4.3	4.3	-	Lutensol AT 50, 7.5	Hexadecane, 3.2	-
SLN 3	5.6	5.6	-	Lutensol AT 50, 7.5	Hexadecane, 3.2	-
SLN 4	6.9	6.9	-	Lutensol AT 50, 7.5	Hexadecane, 3.2	-
SLN 5	8.2	8.2	-	Lutensol AT 50, 7.5	Hexadecane, 3.2	-
SLN 6	10	10	-	Lutensol AT 50, 7.5	Hexadecane, 3.2	-
BC-SLN	6.9	6.9	-	Lutensol AT 50, 7.5	Hexadecane, 3.2	0.3
NLC 1	3	1.8	1.2	Tween 80, 2.5	-	-
NLC 2	3.5	2.1	1.4	Tween 80, 2.5	-	-
NLC 3	4	2.4	1.6	Tween 80, 2.5	-	-
NLC 4	4.5	2.7	1.8	Tween 80, 2.5	-	-
NLC 5	5	3	2	Tween 80, 2.5	-	-
NLC 6	6	3.6	2.4	Tween 80, 2.5	-	-
NLC 7	8	4.8	3.2	Tween 80, 2.5	-	-
NLC 8	10	6	4	Tween 80, 2.5	-	-
RP-NLC 1	4.5	2.7	1.8	Tween 80, 2.5	-	0.05
RP-NLC 2	4.5	2.7	1.8	Tween 80, 2.5	-	0.1
RP-NLC 3	4.5	2.7	1.8	Tween 80, 2.5	-	0.25
RP-NLC 4	4.5	2.7	1.8	Tween 80, 2.5	-	0.5
RP-NLC 5	4.5	2.7	1.8	Tween 80, 2.5	-	1
RP-NLC 6	4.5	2.7	1.8	Tween 80, 2.5	-	2

In SLN formulations, the aqueous phase consisted in Lutensol AT 50 and n-Hexadecane as co-surfactant dissolved in Milli-Q water and the lipid phase consisted in lauric acid as solid lipid or a mixture of this saturated fatty acid with BC. SLNs were synthesized by testing two emulsification

methods, as simple magnetic stirring and ultrasounds dispersion. The temperature for melting and blending the lipid phase was 70°C.

In NLC formulations, the aqueous phase consisted in Tween 80 without the addition of a co-surfactant dissolved in Milli-Q water and the lipid phase consisted in a blend of lauric acid as solid lipid with sunflower oil as liquid lipid and additionally, RP. NLCs were synthesized using an ultrasounds probe and the temperature for melting and mixing the lipids blend was also 70°C.

In both cases of SLN and NLC production, the lipid phase was added to the aqueous phase after being heated to form a uniform and clear oil phase and the two phases were mixed with magnetic stirring at 300rpm during 45 min at the same temperature of melting. The pre-miniemulsions were then fully homogenized with a probe-type sonicator (Sonopuls - Ultrasonic homogenizer, Bandelin, Germany) for 10 min (Amplitude: 48°; probe on: 10s, probe off: 5s). The resultant nanoparticles dispersions were subsequently cooled to room temperature and stored.

3.2.3. Characterization of SLN and NLCs prepared by miniemulsion methodology

3.2.3.1. Particle size, PdI and surface charge analysis

The hydrodynamic mean particle size (Z-Average) and particle size distribution expressed as the PdI were determined by DLS, using a Malvern Zetasizer Nano ZS (Malvern Instruments, UK). Particle size measurements were made by transferring 1 mL of sample without dilution in disposable cells at 25°C, by non-invasive back scatter with dynamic light scattering detected at an angle of 173°. PdI is calculated from a cumulants analysis of the DLS-measured intensity autocorrelation function (Luykx et al., 2008). The processing was run by the software of the equipment and the particle size data were evaluated using intensity distribution. Each measurement was performed in triplicate and the data was given as average of three individual measurements. The reported values are the mean ± standard deviation (SD) of at least three different batches of each formulation. The ZP reflects the electric charge on the particle surface and indicates the physical stability of colloidal systems. ZP was determined (Malvern Zetasizer Nano ZS) by measuring the electrophoretic mobility of the nanoparticles in an electric field, using the Helmholtz–Smoluchowsky equation. Before measurements the samples were diluted with Milli-Q water (1:10, v/v) and placed at a folded capillary cell (DTS1060) where an alternating voltage of ±150mV was applied. Likewise, all measurements were performed at 25°C, in triplicate and the mean ± SD value was reported.

3.2.3.2. Determination of entrapment efficiency (EE)

The EE, % of both SLN and NLCs loaded with BC and with RP, respectively was calculated by measuring the concentration of bioactive compound in the dispersion medium of the lipid nanoparticles using **Equation 3.1**:

$$EE, \% = \frac{W_{total} - W_{free}}{W_{total}} \times 100 \qquad (3.1)$$

where W_{total} is the total amount of bioactive substance added in the whole system, W_{free} is the amount of free bioactive substance determined in the dispersion medium, i.e., non-encapsulated in SLN or NLCs and assayed after extraction. The reported results are the mean ± SD of at least three different batches of each NLC formulation.

Two different procedures were used to determine the encapsulated content of each bioactive substance.

3.2.3.3. Determination of BC in SLN dispersions

The concentration of free BC in the dispersion medium of SLN formulations was measured by a colorimetric analysis in a UV–VIS spectrophotometer.

SLNs were diluted and washed in Milli-Q water, then the dispersion was vortexed and centrifuged at 12000 rpm for 30 min at 4ºC using centrifuge (Centrifuge 5810 R, Eppendorf). The supernatant was collected and the pellet was re-suspended in fresh Milli-Q water. This procedure was repeated three times. After the washing process, the amount of BC dissolved in the supernatant was quantified by measuring the absorbance at 548 nm (selected wavelength to avoid interference of other formulation compounds present in solution), in 1cm quartz cells, using a double beam UV–VIS spectrophotometer (Model U-2000, Hitachi). The calibration curve of BC was obtained with concentrations varying from 10 to 50 μg/mL of the bioactive substance dissolved in Milli-Q water.

3.2.3.4. Determination of RP in NLC dispersions

The concentration of free RP in the dispersion medium of NLC formulations was measured using a reverse-phase high-performance liquid chromatography (RP-HPLC) method. The non-encapsulated active substance was separated by an extraction procedure adapted from Yakushina and Taranova (1995) (Yakushina and Taranova, 1995) as it follows, 2.0 mL of each NLC dispersions were transferred into a centrifuge tube and 2.0 ml of n-hexane (1:1, v/v) were added for the separation of RP. Then, the tube was sealed and the mixture was uniformly mixed with gentle magnetic stirring for 15 min 150 rpm. The mixture was then centrifuged at 3000 rpm for 10 min and the supernatant consisting on n-hexane extract was collected and evaporated under nitrogen to remove the solvent. The residue of RP was dissolved on the mobile phase for analysis. The HPLC analytic system was composed by a Lachrom, Merk-Hitachi L-7400 apparatus equipped with a

quaternary pump, an auto-sampler unit and UV detector and by a Purospher® RP-18 endcapped column (Merk Millipore, EUA). The operating conditions were set based on the methodology described by Yakushina and Taranova, (1995) (Yakushina and Taranova, 1995), as it follows. An isocratic elution was performed using a mixture of acetonitrile, methanol and dichloromethane (60:20:20) as mobile phase, at a constant flow rate of 1.0 mL/min. The UV detector was set at 325 nm for the detection of RP. The method was linear in concentrations varying from 0.2 to 100 µg/mL. All standards and samples were filtered using a PTFE membrane 0.22µm (Merk Millipore, EUA) prior to injection and an injection volume of 10 µL was used in both methods.

3.2.3.5. Morphologic and structural analysis

The morphology and matrix structure of BC-SLN and RP-NLC were observed by transmission electron microscopy (TEM). Imaging was performed on TEM (Hitachi H-8100 II, Tokyo, Japan) with thermionic emission (LaB6) and 200kV acceleration voltage, resolution of 2.7 Å point to point, equipped with an energy dispersive spectroscopy (EDS) light elements detector. The sample was prepared by placing a drop of the dispersion into a copper grid with 200-mesh coated with carbon membranes and dried at air for 5 min. The grids were then observed with a CCD MegaView II bottom-mounted camera

3.3. Results

3.3.1. Production of lipid nanoparticles by the miniemulsion methodology

3.3.1.1. Influence of emulsification process and solid lipid: surfactant ratio on SLN particle size and physical stability

SLNs formulations were prepared through the miniemulsions methodology by testing the effect of two production parameters as the emulsification process and the ratio of solid lipid, wt%: surfactant, wt% (SL: S) on particle size and surface charge of the lipid nanocarriers. The surfactant concentration (7.5%) was kept constant and the solid lipid concentration varied between 2.9 and 10%, thus the SL: S ratio ranged between 0.4 and 1.3. The composition of SLNs formulations (SLN 1 to SLN 6) that were characterized in terms of these parameters is showed in **Table 3.1**. All formulations were prepared using lauric acid as a solid lipid, Lutensol AT 50 as a surfactant and hexadecane which is a polymeric co-surfactant used to inhibit coalescence and diffusional instability caused by a phenomenon known as Ostwald ripening (Wang and Schork, 1994). The average particle sizes and respective PdI of SLNs prepared using magnetic stirring and ultrasounds are presented in **Figure 3.1**.
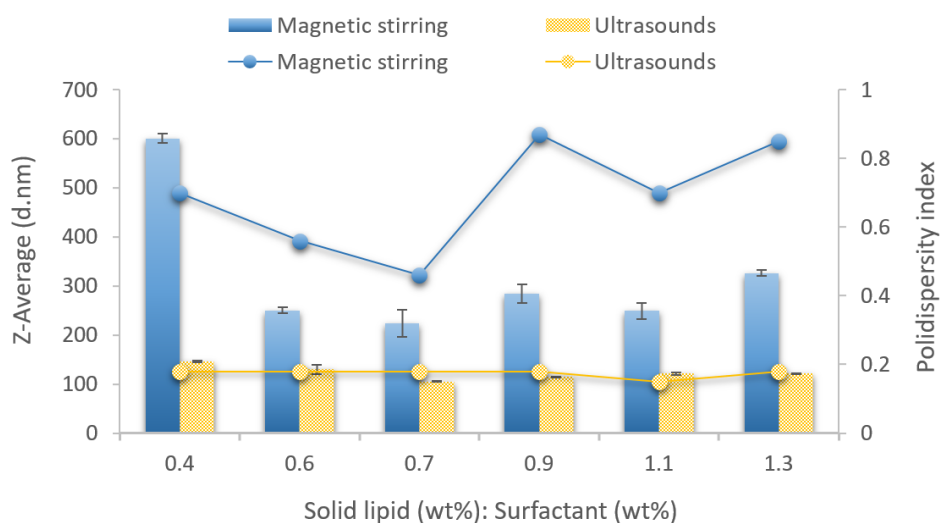
Figure 3.1 - Effect of solid lipid: surfactant ratio on particle size and polydispersity index (PdI) of SLN formulations prepared using magnetic stirring and ultrasounds.

There is a significant difference in Z-Average and in PdI resulting from the type of emulsification method used to produce SLNs. Smaller particle sizes were obtained for SLN prepared using ultrasounds, ranging between 105 ± 1 nm and 146 ± 2 nm, while with magnetic stirring the obtained particles sizes ranged between 224 ± 28 nm and 601 ± 10 nm. Moreover, resultant PdI values of nanoparticles produced with ultrasounds were all close to 0.18 which indicates a very narrow size distribution and the presence of monodisperse particles (Lacatusu et al., 2012). On contrary, SLNs prepared with magnetic stirring demonstrated a more relative size distribution with PdI values ranging from 0.46 to 0.87. Additionally, in these conditions, this parameter seems to be considerably affected by the variation of the SL: S ratio. In **Figure 3.1** it is possible to observe that SLN dispersions produced with a SL: S ratio of 0.9 and magnetic stirring presented the highest PdI value of 0.87, which indicates a very broad distribution of particle sizes (Shaw, 2013), and that with a lower SL: S ratio of 0.7 it was obtained the lowest PdI value of 0.46 indicating a more uniform size distribution. The effect of the SL: S ratio on particle size is also more evident in SLN formulations prepared with magnetic stirring. Thus, there is a high discrepancy between the highest particle size (601 ± 10 nm), which was obtained with a SL: S ratio of 0.4 and the lowest particle size (224 ± 28 nm) that was observed with a SL: S ratio of 0.7.

Another important parameter to be considered is ZP which allows to predict the physical stability of SLN dispersions (**Figure 3.2**). The ZP values obtained for nanoparticles dispersions prepared with magnetic stirring were slightly more negative, ranging between -27.5 ± 0.2 mV and 32.4 ± 0.3 mV, than those obtained for SLNs formulations prepared with ultrasounds (-28.8 ± 0.7 to -29.4 ± 0.7mV). Moreover, the variation of the SL: S ratio seems to have no influence on the physical stability

of SLNs dispersions (**Figure 3.2**), since the ZP values were all within a short range of values between -25 mV and -32 mV.
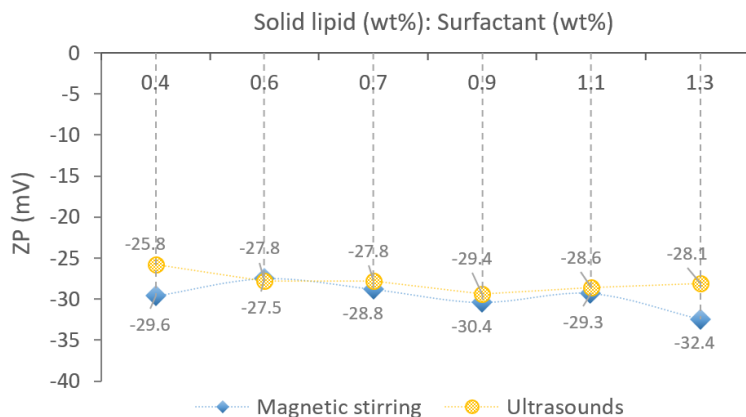
Figure 3.2 - Influence of solid lipid: surfactant ratio on zeta potential of SLN formulations prepared using magnetic stirring and ultrasounds.

The macroscopic observation of SLNs dispersions prepared using the two selected mixer types during the emulsification process was also performed (**Figure 3.3**). It was possible to observe that the type of emulsification method used during the SLN production have a significant influence on the macroscopic appearance and on the consistency of the dispersions. The nanoparticles dispersions obtained from magnetic stirring (**A**) presented a milky aspect while those obtained using ultrasounds (**B**) showed a transparent bluish brightness appearance which is in accordance with their smaller particle size.
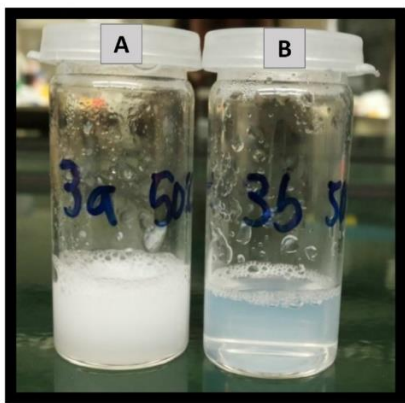
Figure 3.3 - Macroscopic appearance of SLN dispersions (SLN 3) obtained using magnetic stirring (A) and ultrasounds (B) during the production process.

3.3.1.2. Influence of total lipids: surfactant ratio on NLCs size and physical stability

Similarly to SLN, NLC dispersions were produced through the miniemulsion methodology by using ultrasounds, which was pointed in the previous section as the type of emulsification process that provided better results regarding to particle size and PdI. Likewise, the effect of total lipids, wt%: surfactant, wt% (TL: S) ratio was assessed for NLCs dispersions. The obtained results for SLNs dispersions showed that there was no correlation between the particle size and surface charge of the lipid nanoparticles and the variation of the SL: S ratio in a lower range of values (0.4 to 1.3). Thus, the effect of the TL: S ratio on NLCs particle size and surface charge was evaluated by varying this parameter in a higher interval of values ranging from 1.2 to 4. **Table 3.1** shows the composition of NLCs formulations (NLC 1 to NLC 8) that were characterized in terms of their physicochemical properties. The surfactant concentration (2.5%) was kept constant and the total lipids concentration varied between 3 and 10%. All formulations were prepared using lauric acid as solid lipid, sunflower oil as liquid lipid and Tween 80 as surfactant. In general, the Z-Average of developed NLCs was found to be lower than 227 ± 14 nm. NLCs formulated with a TL: S ratio of 1.8 presented the lowest particle size (131 ± 18 nm). **Figure 3.4** shows that the particle size of these nanoparticles indicated no significant difference between the values of the TL: S ratio of 1.2 and 2 (131 ± 18 nm and 144 ± 16 nm). Although, it was observed that the particle size of NLCs dispersions increased 37.1%, between the values of the TL: S ratio of 2 and 4.
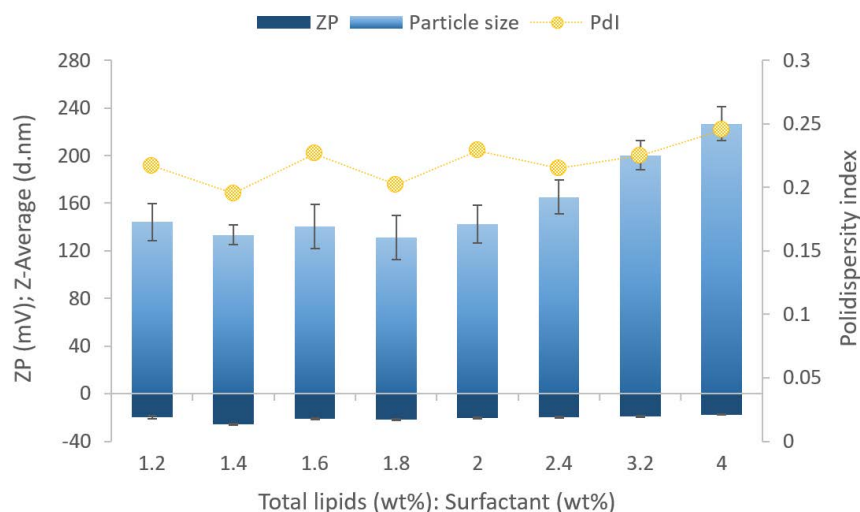
Figure 3.4 - Effect of total lipids: surfactant ratio on particle size, polydispersity index (PdI) and zeta potential of NLC formulations.

PdI values showed no significant variation (ranging between 0.20 and 0.25) by increasing the TL: S ratio and ranged between 0.20 and 0.25 (**Figure 3.4**), indicating that the all NLC dispersions presented a homogeneous size distribution.

The analysis of obtained ZP values demonstrated that an increase of the TL: S ratio have no influence on the surface charge of the nanoparticles and consequently on their physical stability (**Figure 3.4**). Although, more negative ZP values were observed between the values of the TL: S ratio of 2 and 1.4, ranging from -21 ± 0.7 to -26 ± 0.7 mV, respectively.

3.3.1. Incorporation of β-carotene in SLNs and retinyl palmitate on NLCs

3.3.1.1. Size distribution and physical stability of BC-SLNs and RP-NLCs

From the study on the influence of the SL: S ratio on SLNs main physicochemical properties, the more adequate formulation conditions to incorporate BC in these lipid nanoparticles were established. **Table 3.2** summarises the results of parameters that characterize the lipid nanoparticles in terms of their physicochemical properties and lists the composition of their lipid phase without the incorporation of BC (SLN 4) and with BC (BC-SLNs). It was found that the formulation BC-SLNs, presented a good Z-Average of 281 ± 19 nm and that comparatively the formulation SLN 4, showed an increase of 30.2% on particle size (196 ± 2 nm). PdI values of both SLNs dispersions with and without BC were similar and demonstrated that the lipid nanoparticles were uniformly size distributed. Similarly, ZP values presented no significant variation for particles with and without the incorporation of BC (**Table 3.2**).

Table 3.2 - Lipid phase composition and physicochemical characterization of SLN formulations without and with the incorporation of β-carotene.

Formulation	Lauric acid, wt%	β-carotene, wt%	Z-Average (d.nm)	PdI	ZP (mV)	EE, %
SLN 4	6.9	-	196 ± 2	0.30	- 31 ± 0.2	-
SLN 7	6.9	0.3	281 ± 19	0.34	- 29 ± 5	95 ± 5

The size distribution and physical stability of RP-NLCs particles were investigated by varying the TL: S ratio. From the above optimization study, the concentration of total lipids that was used in NLCs formulations with RP was established and kept constant. The composition of these formulations (RP-NLC 1 to RP-NLC 6) is presented in **Table 3.1**. The concentration of RP was analysed in order to determine the effect of this parameter on RP-NLCs size and surface charge. **Figure 3.5** shows the Z-Average with respective PdI values and the ZP of increasing concentrations of RP incorporated in NLCs.
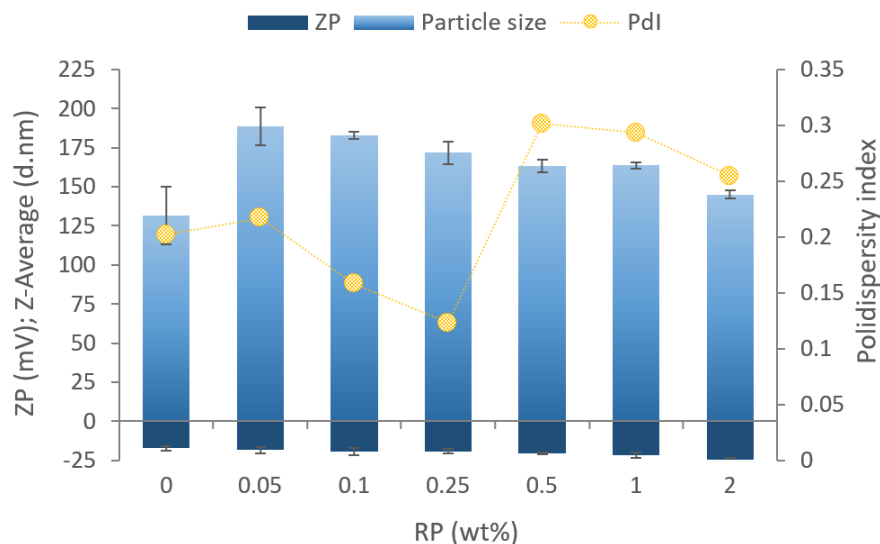
Figure 3.5 - Influence of retinyl palmitate concentration on particle size, polydispersity index and zeta potential of NLC formulations.

In general, all RP-NLCs dispersions presented higher particle sizes than those obtained with NLCs dispersions without RP (131 ± 18 nm) and the same concentration of total lipids, ranging from 145 ± 3 nm and 189 ± 12 nm for RP concentrations of 2 and 0.05%, respectively. It was also observed a slight decrease on particle size with the increase on RP concentration (**Figure 3.5**). It was detected a slight decrease in PdI values until being reached the RP concentration of 0.25% (PdI of 0.12) indicating the occurrence of monodisperse particles. Then the PdI values considerably increased, ranging between 0.30 and 0.25, with RP concentrations from 0.5 to 2%, indicating a uniform size distribution.

ZP values were slightly more negative with RP concentrations from 0.25 to 2%, ranging between -19 ± 1.6 mV to -25 ± 0.9 mV (**Figure 3.5**). Moreover, in general ZP results of RP-NLC were also more negative when compared with NLC dispersions without RP and the same concentration of total lipids (-17 ± 1.6 mV).

3.3.1.2. *Morphology of BC-SLNs and RP-NLCs*

TEM analysis was performed to observe the morphology and internal structure of both types of lipid nanoparticles, BC-SLNs and RP-NLCs. Representative TEM images with different amplification factors of dried suspensions of BC-SLNs and RP-NLC 1 (**Table 3.1**) are shown in **Figure 3.6**. Both type of lipid nanoparticles present a well-defined spherical shape with diameter sizes ≤ 200nm. However, it is possible to observe some differences on the lipid matrix of each nanocarrier. In the case of BC-SLN, the lipid core of the nanoparticles is characterized by an ordered crystalline dark structure which are aligned in a relatively disperse way. On the other hand, the lipid matrix of RP-NLCs

presented a less ordered structure characterized by an irregular crystal lattice with many imperfections. These nanoparticles appear to be moderately dispersed, thus showing some aggregates.
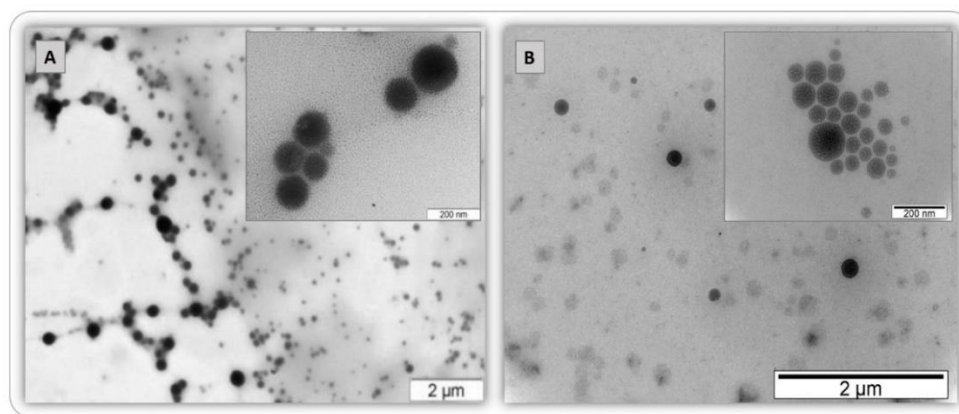
Figure 3.6 - Transmission electron microscopy images of BC-SLNs (A) and RP-NLC 1 (B).

3.3.1.3. Determination of entrapment efficiency of BC-SLNs and RP-NLCs

The EE, % of BC and RP was determined to analyse the solubilisation capacity of these two cosmetic antioxidants in each type of lipid nanoparticles, SLNs and NLCs respectively. The developed BC-SLN **(Table 2),** showed a high ability to incorporate BC by presenting a high EE, % value of 95 ± 5%.

Also a high encapsulation capacity for RP-NLCs formulations was obtained (**Figure 3.7**). In this case, the solubilisation capacity of increasing concentrations of RP was analysed by the determination of the EE, % of each correspondent RP-NLCs dispersion. As showed in **Figure 3.7** it was observed an increase in the EE, % values with the increase on the concentration of RP that was incorporated on NLCs. The highest EE, % value was 94 ± 0.9% and it was obtained with 2% of RP, while the lowest value was 64 ± 1.5% and it was obtained with 0.05% of RP.
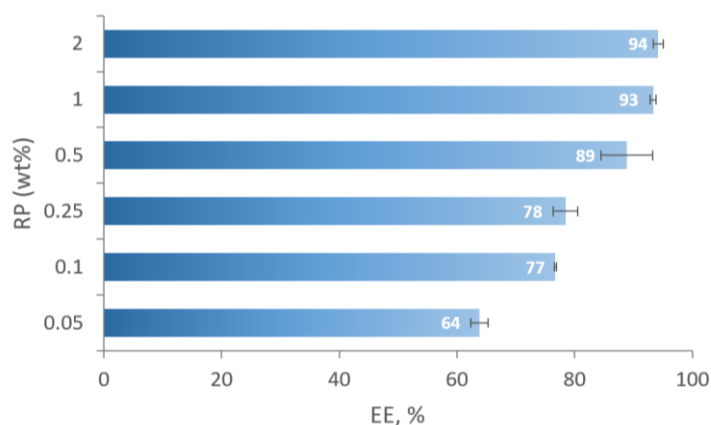
Figure 3.7 - Entrapment efficiency (EE, %) of increasing concentrations of retinyl palmitate on NLCs.

3.4. Discussion

Currently, the development of advanced eco-friendly cosmetic products is based on nanotechnology (Lacatusu et al., 2014). There is an urgent need to deliver new effective nanocarriers of bioactive compounds using biocompatible and renewable materials, thus improving their potential pharmaco-cosmetic performance (Cortesi et al., 2017). The main objective of this work was to deliver two different types of lipid nanocarriers, namely SLNs and NLCs, produced using renewable ingredients with inherent bioactive properties to enhance the safety and stability of the incorporated compounds.

The effect of the emulsification process and the influence of the SL: S ratio on particle size and physical stability of developed SLNs were analysed (**Figure 3.1**). It was verified that the physicochemical characteristics of SLNs are significantly influenced by these two parameters. Smaller particles were obtained for this type of lipid nanoparticles using ultrasounds during the emulsification process. Moreover, the PdI values indicated very homogenous dispersions with monodisperse particles when using this method for the preparation of the miniemulsion systems. This can be related to the fact that the emulsification process is not spontaneous, thus it requires an input of energy which is usually provided by mechanical shear generated by several types of mixers and this determines that the final droplet size of the emulsion is not only dependent on the chemistry but also on the amount of applied energy (Sciences, 2009). Ultrasonic devices are effectively used to produce emulsions with nanosized droplets, however they are not practical do scale-up (Sciences, 2009). Having this in mind, is important to test and compare alternative emulsification methods for the same nanoparticles formulation that will allow its posterior scale-up. Although, the miniemulsion methodology based on ultrasonic dispersion offers an appropriate alternative to run rapid proof of concept studies at the laboratory scale due to its simple and fast procedure and to the relative low cost of the equipment (Lason et al., 2013, Schwarz et al., 2012). Analysing the results from the study on the influence of the SL: S ratio on particle size and respective PdI values, it was observed that these two properties of nanoparticles varied significantly and that SLNs dispersions produced using magnetic stirring presented higher particle sizes with a more relative size distribution. The ZP values of developed SLNs, indicated that the physical stability of the nanoparticles prepared with magnetic stirring were slightly more negative than those obtained with ultrasounds dispersion. This may be due to fact that when using a more gentle type of mixing during the emulsification process, with a lower input if energy, the droplet size is more affected by the formulation chemistry and composition (Sciences, 2009). Thus, the increase of the SL: S ratio produced a more evident effect on particle size and PdI of SLNs produced using magnetic stirring, resulting in general to a decrease of their Z-Average. The decrease in the nanoparticles size with the increase of the SL: S ratio may be attributed to the existence of an optimum level of surfactant concentration that can be reached and that results in a reduction of the surface tension between the lipid and aqueous phases, thus enhancing the separation of particles with

lower sizes (Mandpe and Pokharkar, 2015, Thakkar et al., 2014). Lutensol AT 50 was used as surfactant in the formulation of these lipid nanoparticles which in combination with n-hexadecane that was used as co-surfactant can increase the dispersion entropy and reduce the interfacial tension, thus providing a steric hindrance, avoiding emulsion droplets from coming close to each other and thus preventing flocculation and coalescence (Clares et al., 2014, Lerch et al., 2013). Despite its recognized low toxicity (Landfester and Musyanovych, 2010, Lerch et al., 2013), there is no report of using Lutensol AT 50 in lipid nanoparticles formulations. The variation of the SL: S ratio demonstrated to have no apparent influence on the physical stability of SLN dispersions, since the obtained ZP values were all within a small interval between -25 and -32mV (**Figure 3.2**). Typically, higher ZP values (>|30|) are considered to stabilize nanoparticles dispersions due to an adequate electrostatic repulsion between particles with the same electrical charge (Aditya et al., 2014, Clares et al., 2014). Even though the developed SLN suspensions have sufficiently negative ZP values that guarantee their physical stability without forming aggregates.

The effect of the TL: S ratio on particle size and physical stability of NLCs dispersions was also analysed (**Figure 3.4**). The observed results show that all NLCs formulations presented good particle sizes in the nanometre range and that PdI values showed no significant variation, indicating that the developed NLC dispersions presented a homogeneous size distribution. Moreover, it was demonstrated that the increase of the TL: S ratio have no influence in the surface charge of these lipid nanoparticles. The obtained ZP values were all above -26 ± 0.7 mV, indicating a relative physical stability to the particles. Although, it was noticed a slight increase on particle size with the increase of the TL: S ratio from 2 to 4. This can be explained by the formation of a more viscous dispersed phase when the total lipids concentration increases, thus promoting the increase in surface tension and consequently the formation of larger particles (Niculae et al., 2014, Sanad et al., 2010).

The incorporation of BC on SLNs and RP on NLCs was investigated and the developed lipid nanocarriers were analysed in terms of their main physicochemical characteristics. Both types of nanocarriers revealed good particles sizes in the nanometre range and in both cases was observed an increase on particle size with the encapsulation of the bioactive compounds, which was of 30.2% for BC-SLN. The ZP value of the BC-SLNs system indicated that there was no significant change in the surface charge of these lipid nanoparticles with the incorporation of BC and that this system is physically stable (**Table 3.2**).

In the case of RP-NLCs, all dispersions demonstrated a slight increase in particle size in comparison with the NLC formulations without RP. Additionally, it was observed a decrease in the Z-Average with the increase in RP concentration (**Figure 3.5**). The ZP values of RP-NLCs systems were slightly more negatives for increasing concentrations of RP, indicating a higher physical stability with the incorporation of this bioactive compound. There are possible explanations for the occurrence of variations on the physicochemical properties of the lipid nanocarriers after the incorporation of both bioactive substances. The differences in size and ZP could be due to the interaction between the surfactant and the bioactive substances during the formation of the loaded nanodroplets or the

occurrence of competitive adsorption on the lipid interface (Lacatusu et al., 2012). Moreover, the incorporation of RP in increasing concentrations results in a decrease on the viscosity of the dispersed phase, thus decreasing the surface tension and consequently providing the formation of smaller particles, which reflects a good compatibility among the solid and liquid lipids and the incorporated drug (Badea et al., 2015, Niculae et al., 2014).

TEM analysis of both BC-SLNs and RP-NLCs systems was performed to observe their morphology and internal structure (**Figure 3.6**). TEM micrographs showed that the particles presented a well-defined spherical shape in the nanometre range and revealed a good dispersion, which is in agreement with the results obtained by DLS. Although, there was some evident differences on the lipid matrix of each lipid nanocarrier. BC-SLNs presented an ordered crystalline dark structure in its lipids core, while RP-NLCs showed a less ordered structure characterized by an irregular crystal lattice with many imperfections (**Figure 3.6**). This is mainly attributed to the type of lipid constituents of each lipid nanocarrier which after crystallization will determine their polymorphic transitions (Lacatusu et al., 2012). The use of different lipids in NLCs composition results in the formation of a more disordered lattice with more space for guest molecules (Aditya et al., 2014, Niculae et al., 2014). The beneficial physicochemical properties of these type of lipid nanoparticles relies on their solid state. For instance, their encapsulation efficiency and drug release are intrinsically related with the transition of the nanoparticles lipids core from a less ordered to a more ordered solid state (Lacatusu et al., 2012, Triplett and Rathman, 2009).

The solubility capacity of BC and RP on SLNs and NLCs was determined by the analysis of their entrapment efficiencies. Both developed lipid nanocarriers shown high EE, % regardless the differences in their lipids composition (**Table 3.2, Figure 3.7**). The incorporation of BC in SLN present some advantages as enhanced solubility in aqueous products, increased bioavailability and protection against oxidation (Gomes et al., 2013). Thus, giving the high EE, % result for BC-SLN it seems important to perform the evaluation of BC protection by its incorporation on SLN during a relative long period of time and testing some storage conditions. Regarding the results for RP-NLC, it was observed that the EE, % was influenced by the amount of RP encapsulated into the lipid nanocarriers and that it was obtained a better entrapment efficiency with the increase of this bioactive substance concentration (**Figure 3.7**). As mentioned before, the presence of higher amounts of liquid lipids in the nanocarrier structure prevents the formation of perfect crystals, thus enhancing the encapsulation of the bioactive substances and preventing its expulsion during storage (Chen et al., 2010, Oliveira et al., 2016).

3.5. Conclusions

Two types of lipid nanoparticles, namely SLNs and NLCs were successfully produced by the miniemulsion methodology. The emulsification process demonstrated to have a significant impact on

the physicochemical properties of these nanocarriers. It was verified that SLNs developed using an ultrasounds probe showed more suitable physicochemical properties in relation to magnetic stirring. Thus, SLN dispersions with an appropriate size in the nanometer range (105 ± 1 to 146 ± 2 nm) and good physical stability (≈ -29 mV) were obtained by ultrasounds. The analysis of the influence of the SL: S ratio showed a higher impact on physicochemical properties of SLNs prepared using magnetic stirring, especially on their particle size and PdI. In general, all NLCs formulations prepared by ultrasounds dispersion and different values of the TL:S ratio showed good particle sizes, below 227 ± 14 nm with an homogeneous size distribution (PdI values ranged between 0.20 and 0.25) and an appropriate physical stability (-21 ± 0.7 to -26 ± 0.7 mV). It was observed that higher values of the TL: S ratio demonstrated to have an impact in the physicochemical properties of NLCs with an increase in their particle size and respective PdI values.

BC and RP were used as antioxidant models to evaluate the potential of SLNs and NLCs, respectively as efficient nanocarriers of bioactive compounds by enhancing their bioavailability and safety. The developed BC-SLNs dispersions showed a well-defined spherical shape with an ordered crystalline dark structure that allowed a high encapsulation efficiency for BC of ≈ 95%. The morphology results were in agreement with those obtained with DLS analysis which showed a good particle size of 281 ± 19 nm with a uniform size distribution without the occurrence of aggregates.

All formulations of RP-NLCs presented appropriate particle sizes in the nanometer range (145 ± 3 nm to 189 ± 12 nm) with the occurrence of monodispersed particles (PdI values of ≈ 0.12) and with a more relative physical stability, showing ZP of ≈ -25 mV. The morphology analysis of these lipid nanocarriers showed a less ordered structure presenting many imperfections in its lipid matrix which allowed a high encapsulation efficacy for RP of ≈ 94%.

This work represents the first stage of the characterization process that is necessary to properly assist the selection of suitable lipid nanocarriers with specific desirable properties to be used in the delivery of bioactive compounds by enhancing their safety and efficacy. Although, further studies are needed to investigate the efficiency and safety of these lipid nanocarriers regarding their storage stability, the crystallinity of their lipid matrix, their release profile and antioxidant activity.

◢ CHAPTER IV

DESIGN OF MULTIFUNCTIONAL NANOSTRUCTURED LIPID CARRIERS ENRICHED WITH α-TOCOPHEROL USING VEGETABLE OILS

Fátima Pinto, Dragana P.C. de Barros, Luis P. Fonseca

4.1.   Introduction

4.2.   Materials and Methods

4.3.   Results and Discussion

4.4.   Conclusions

4. Design of multifunctional nanostructured lipid carriers enriched with α-tocopherol using vegetable oils

Vegetable oils are commonly used as components in many cosmetic products intended for daily care due to their high beneficial and multifunctional effect on skin. The general objective of this study was to develop new nanostructured lipid carrier (NLC) formulations containing vegetable oils and enrich them with α-tocopherol (TOC) in order to explore their potential as effective and safe advanced biocosmetic prototypes. The influence of lipids composition and physical state on the production and physicochemical properties of vegetable oil NLCs and enriched nanoparticles with TOC (TOC-NLCs), as a model bioactive antioxidant compound, was studied. Sunflower, sweet almond, olive and coconut oils were successfully used in the development of free and loaded NLCs. The formulations of free lipid nanoparticles with each vegetable oil presented an appropriate nanoscale size from approximately 120 to 350 nm and good physical stability with zeta potential values ranging between −45.6 to −65.9 mV. Likewise, the TOC-NLCs demonstrated suitable particle sizes from approximately 240 to 315 nm and zeta potential values raging between –45.6 to –55.1 mV, being then verified that these parameters were affected by differences on the lipids core composition. TOC-NLCs presented a high entrapment efficiency with values above 79.4% and also assured a controlled release of TOC, independently of the percentage of incorporated active compound. Differential scanning calorimetry results showed that the incorporation of TOC and the increase of its concentration on NLCs lipids matrix caused a decrease on the onset and melting temperatures, indicating a reduced crystallinity of the obtained vegetable oil TOC-NLCs. These lipid nanoparticles and free NLCs presented good antioxidant activity with scavenging activity values above 56.7%, which was improved by the encapsulation of TOC (scavenging activity values above 64.3%) and demonstrated the ability to be incorporated in long-term stable cosmetic products based on stability studies performed during 8 months.

4.1. Introduction

There is a growing demand for innovative natural products to address consumers' needs of healthy appearance and well-being. Cosmetic manufacturers are focusing their efforts in the development of eco-friendly cosmetics based on vegetable oils as raw materials, since they are abundant renewable resources most commonly extracted from various parts of plants (Badea et al., 2015, Balboa et al., 2014). Vegetable oils are a combination of triglycerides of higher saturated and unsaturated fatty acids. Due to their beneficial influence on skin these type of oils are becoming most commonly used as components of cosmetic products (Zielińska and Nowak, 2014). Antioxidant properties have been attributed to vegetable oils which can provide skin protection against reactive oxygen species (ROS) (Dhavamani et al., 2014, Tehranifar et al., 2011) synergistically improving the

photoprotective properties of sunscreens (Dario et al., 2018). Moreover, oils can prevent water loss through the skin and also present anti-carcinogenic and anti-inflammatory biological actions (Cicerale et al., 2012a).

Topical supplementation with antioxidants is considered as one of the most promising strategies to prevent or treat skin aging. Most skin care formulations claiming anti-aging effects are based on exogenous antioxidants such as vitamins, polyphenols, and flavonoids that cannot be synthesized by our body (Montenegro, 2014). α-Tocopherol (TOC) is one of the most active lipophilic antioxidant in biological membranes demonstrating a very important role in protecting skin and other organs. This fat-soluble antioxidant can effectively scavenge lipid peroxyl radicals, act as a synergist with other antioxidants and presents a moisturizing effect by limiting trans-epidermal water loss (Byun et al., 2011, Yenilmez and Yazan, 2010). However, TOC is present in limited quantities, humans cannot synthesize it and it is readily depleted by UV radiation and other oxidative stresses such as ozone (de Carvalho et al., 2013, Nada et al., 2014). Given its importance, TOC is widely used in the formulation of several cosmetic and daily care products and there is a commercially available nanoemulsion, TOCOSOL™, composed of TOC as oil phase, TPGS and Poloxamer 407 as surfactants for paclitaxel intra-venous delivery (Feng and Mumper, 2013, Nada et al., 2014, Constantinides et al., 2000). The great majority of antioxidants, including TOC, that are presently used in skin care formulations show unfavorable physicochemical properties such as excessive lipophilicity or hydrophilicity, chemical instability and poor skin penetration that actively limit their effectiveness after topical application (Montenegro, 2014). One good strategy to reduce these effects is the design of nanomaterials with an intrinsic multifunctional character based on its excipients to encapsulate these antioxidant substances. Therefore, different lipid nanocarriers such as liposomes, niosomes, microemulsions and nanoparticles have been widely investigated as delivery systems for antioxidants to improve their beneficial effects in the treatment of skin aging (Nada et al., 2014). The main advantages of lipid nanocarriers over conventional passive delivery are good biocompatibility, increased surface area, higher solubility, improved stability, good production scalability, controlled release, avoidance of organic solvents in the preparation process and wide potential application spectrum (Vinardell and Mitjans, 2015). Solid lipid nanoparticles (SLNs) are often referred in literature as the first generation of lipid nanocarriers (Attama et al., 2012, Müller et al., 2002b). In order to overcome some difficulties with SLNs regarding its inherent low incorporation rate due to the crystalline structure of the solid lipid, nanostructured lipid carriers (NLCs) were introduced as the second generation of solid lipid nanoparticles (Aditya et al., 2014, Weber et al., 2014). NLCs are submicron particles, usually with spherical shape and mean diameters ranging between 50 and 500 nm, composed of a mixture of solid and liquid lipids (oils) dispersed in an aqueous medium and stabilized by an outer shell of surfactants (Niculae et al., 2014, Puri, 2010). The oil incorporation in the solid matrix allows the formation of an overall amorphous nanostructure with many imperfections within its matrix, providing NLCs with higher drug capacity and a lesser degree of drug expulsion during storage then SLNs (Fang et al., 2013, Pinto et al., 2014). These lipid nanocarriers are one of the most effective

encapsulation technologies developed in the field of nanotechnology with a wide range of applications in the cosmetics, food and pharmaceutical industries (Zheng et al., 2013a). Moreover, they are safe for human use and biodegradable carriers due to their generally recognized as safe (GRAS) ingredients (Müller et al., 2000). The physicochemical properties of NLCs are influenced by a number of factors, including the type of used oil and surfactant (Badea et al., 2015). There are several reports focusing a certain bioactive-loaded NLC but only few studies addressed the influence of different lipids and surfactants on the formulation of NLC and their properties (Badea et al., 2015, Lacatusu et al., 2014, Niculae et al., 2014). The novelty of the present work consist on the production of new formulations of NLC based on the use of bioactive ingredients such as the selected four vegetable oils, and α-tocopherol as model lipophilic drug to be encapsulated.

The present study aimed to investigate the effects of different vegetable oils and surfactants on the design of multifunctional NLCs formulations enriched with TOC as a model antioxidant excipient. SF, SA, OV and CO oils were chosen as liquid lipids not only for their physicochemical properties but also for their intrinsic multifunctional character as moisturizers, antioxidant agents and anti-carcinogenic and anti-inflammatory biological actions. Also, vegetable oil NLCs were formulated using four non-ionic surfactants (Tween 80, Poloxamer 188, Span 60 and Span 80), to further improve the particles size and stability. The miniemulsions methodology (Landfester, 2003), a simple solvent free and low energy method, was used for preparing the NLCs. Additionally, vegetable oil NLCs were characterized in terms of particle size and zeta potential, crystallinity and melting behavior, and morphology. Additionally, entrapment efficiency, loading capacity, release profile, stability studies and *in vitro* antioxidant activity were also evaluated.

4.2. Material and Methods

4.2.1. Materials

Solid lipids: lauric acid (≥98%); myristic acid (Sigma Grade, ≥99%); palmitic acid (≥99%) and stearic acid (≥95%) were purchased from Sigma-Aldrich (St. Louis, MO, USA). **Liquid oils:** Sunflower (SF) oil, (Fula, Portugal) and Olive (OV) oil, (Gallo, Portugal) were food grade commercial products; Sweed almond (SA) oil, (Well's, Portugal) was a cosmetic grade product and Coconut (CO) oil, with analytical grade (Supelco, USA). **Surfactants:** Tween 80, (polyoxyethylene sorbitan monooleate, HLB 15.0) was obtained from PanReacAppliChem (Darmstadt, Germany); Poloxamer 188, (Pluronic F-68, HLB 29.0) was purchased from AppliChem (Darmstadt, Germany); Span 60 (Sorbitan monostearate, HLB 4.7) from Tokio Chemial Industries (Tokyo, Japan); and Span 80 (Sorbitan monooleate, HLB 4.7) from Alfa Aesar, ThermoFisher (Karlsruhe, Germany). The aqueous phase of miniemulsions was prepared with Milli-Q water. α-Tocopherol (TOC) was obtained from Glicerinas e Parafinas de Portugal (Lisboa, Portugal); Acetonitrile RS, diclorometane RS and methanol RS were purchased from CARLO

ERBA Reagents S.A.S. (Z.I. de Valdonne, France) special for HPLC/NMR 1 and 2,2-diphenyl-1-picrylhydrazyl (DPPH) was obtained from Sigma-Aldrich (St. Louis, MO, USA). All other reagents were of analytical grade.

4.2.2. Preparation of vegetable oil NLCs

Four chemically different vegetable oils (SF, OV, SA and CO) that could better incorporate TOC in NLCs and present a bioactive behavior suitable for topical use were selected as liquid oils in the formulation. Both free and TOC-NLCs were prepared by the miniemulsions methodology (Landfester, 2003) with an ultrasonication step. Four different surfactants were selected for this study based on its chemical structure and on its hydrophilic-lipophilic balance (HLB). The aqueous phase in the miniemulsion system consisted in one of each surfactant dissolved in Milli-Q water. The lipid phase consisted in a blend of a saturated fatty acid as solid lipid (from lauric acid, C12:0 to stearic acid, C18:0) with each selected vegetable oil and additionally TOC. The percentage composition of the components in the formulation of NLCs is presented in **Table 4.1.** The lipid phase was heated to 10ºC above the melting point of the used solid lipid to prevent lipid memory effect (How et al., 2013, Jores et al., 2004), until forming a uniform and clear oil phase, and added to the aqueous phase at the same temperature using magnetic stirring at 300 rpm during 45 min. The pre-miniemulsion was then fully homogenized with a probe-type sonicator (Sonopuls - Ultrasonic homogenizer, Bandelin, Germany) for 10 min. The resultant nanoemulsion was subsequently cooled to room temperature and stored.

Table 4.1 – Percentage composition of each component in the formulations of NLCs.

	TOC, wt%	*Total Lipids, wt%*	*Tween 80, wt%*	*Milli-Q H$_2$O, wt%*
Free NLCs	-	4.0	2.5	93.5
TOC-NLC 1	2.0	4.0	2.5	91.5
TOC-NLC 2	3.0	4.0	2.5	90.5
TOC-NLC 3	4.0	4.0	2.5	89.5

4.2.3. Physicochemical characterization of the vegetable oil NLCs

4.2.3.1. Particle size, PdI and surface charge analysis

The hydrodynamic mean particle size (z-Average) and particle size distribution expressed as the polydispersity index (PdI) were determined by dynamic light scattering (DLS), using a Malvern Zetasizer Nano ZS (Malvern Instruments, UK). PdI is calculated from a cumulants analysis of the DLS-measured intensity autocorrelation function (Luykx et al., 2008). All measurements were performed at

25°C and using a 173⁰ scattering angle. The processing was run by the software of the equipment and the particle size data were evaluated using intensity distribution. 1 mL of sample without dilution was transferred to disposable cells and each measurement was performed in triplicate. The data was given as average of three individual measurements. The reported values are the mean ± standard deviation (SD) of at least three different batches of each NLC formulation. Statistical analysis of variance for particle size was performed in Microsoft Excel® 2013 software by Normal Distribution using a significance level of α=0.05, the average of particle size (μ) of all measurements from formulations with each vegetable oil and its standard deviation (σ). The zeta potential (ZP) reflects the electric charge on the particle surface and indicates the physical stability of colloidal systems. ZP was measured (Malvern Zetasizer Nano ZS) by measuring the electrophoretic mobility of the nanoparticles in an electric field, using the Helmholtz–Smoluchowsky equation. Before measurements the samples were diluted with Milli-Q water (1:10, v/v) and placed at a folded capillary cell (DTS1060) where an alternating voltage of ±150mV was applied, using a dispersant (water) dielectric constant of 78.5. Likewise, all measurements were performed at 25⁰C, in triplicate and the mean ± SD value was reported.

4.2.3.2. Determination of entrapment efficiency (EE) and drug loading capacity (DL)

The EE and DL of TOC-NLCs was determined by measuring the concentration of free vitamin in the dispersion medium of the nanoparticles using a reverse-phase high-performance liquid chromatography (RP-HPLC) method. The non-encapsulated TOC was separated by an extraction procedure adapted from (Yakushina and Taranova, 1995) as it follows, 2.0 mL of T-loaded NLC dispersion was transferred into a centrifuge tube and 2.0 ml of n-hexane (1:1, v/v) was added. Then, the tube was sealed and the mixture was uniformly mixed with gentle magnetic stirring for 15 min 150 rpm. The mixture was then centrifuged at 3000 rpm for 10 min and the supernatant consisting on hexane extract was collected and evaporated under nitrogen to remove the solvent. The TOC residue was dissolved on the mobile phase that consisted of acetonitrile: methanol: dichloromethane (60:20:20) and quantified by HPLC. The analytic system was composed by a Lachrom, Merk-Hitachi L-7400 apparatus equipped with a quaternary pump, an auto-sampler unit and a UV detector set for detection at 290 nm and by a Purospher® RP-18 endcapped column (Merk Millipore, EUA). An isocratic elution was performed at a constant flow rate of 1.0 mL/min. For these conditions, TOC was eluted at 5.93 min and a run time of 8 min was established for the separation of the compounds. The method was linear in concentrations varying from 0.2 to 100 μg/mL. All standards and samples were filtered using a PTFE membrane 0.22 μm (Merk Millipore, EUA) prior to injection and an injection volume of 10 μL was used. The EE% and DL% were calculated using **Equation 3.1** (presented in chapter 3, section 3.2.3.2.) and **Equation 4.1**, respectively:

$$DL, \% = \frac{W_{total} - W_{free}}{W_{lipid}} \times 100 \qquad (4.1)$$

where W_{total} is the total amount of α-tocopherol added in the whole system, W_{free} is the amount of free TOC determined in the dispersion medium, i.e., non-encapsulated in NLCs and assayed after extraction, and W_{lipid} is the weight of the lipid phase in the nanoparticles formulation. DL_{max} was determined considering $W_{free} = 0$.

4.2.3.3. Assessment of the lipid matrix crystallinity

Differential scanning calorimetry (DSC) analysis was performed to investigate the degree of crystallinity of the lipid nanoparticles formulated using the four selected vegetable oils. The thermograms were recorded using a DSC 200 F3 Maia (Netzsch, Germany). Approximately 5-6 mg of pure excipients or equivalent dried NLCs were weighted into standard aluminum pans and hermetically sealed. An empty pan was used as a reference. Each sample was submitted to a heating cycle from 20 to 110ºC, at the rate of 5ºC/min. A nitrogen purge was used to provide an inert gas atmosphere within the DCS cell at a flow rate of 60 mL/min. The melting points (Mp), and enthalpies (ΔH) were evaluated using the software Proteus Analysis (Netzsch, Germany).The determination of crystallinity index (*CI*,%) was calculated from the enthalpy of fusion using **Equation 4.2** (How et al., 2013, Schubert and Muller-Goymann, 2005):

$$CI, \% = \frac{\Delta H_{NLC}}{\Delta H_{solid\ lipid}} \times 100 \qquad (4.2)$$

where ΔH_{NLC} and $\Delta H_{solid\ lipid}$ are the enthalpies of fusion of the nanoparticles and solid lipids used as excipients, respectively.

4.2.3.4. Morphologic and structural analysis

The morphology and matrix structure of the vegetable oil-NLCs were observed by transmission electron microscopy (TEM). Imaging was performed on TEM (Hitachi H-8100 II, Tokyo, Japan) with thermionic emission (LaB6) and 200kV acceleration voltage, resolution of 2.7 Å point to point, equipped with an energy dispersive spectroscopy (EDS) light elements detector. The sample was prepared by placing a drop of the dispersion into a copper grid with 200-mesh coated with carbon membranes and dried at air for 5 min. The grids were then observed with a CCD MegaView II bottom-mounted camera.

4.2.3.5. Long-term stability

A stability study was performed to investigate the effect of storage on the average size, PdI and physical appearance. Samples of free vegetable oil-NLC dispersions and NLCs loaded with 2 wt% of TOC were kept in the dark at room temperature (25ºC) for 4 and 8 months. Stability of the samples was estimated in triplicates.

4.2.3.6. In vitro drug release

In vitro release studies were performed to investigate the potential of vegetable oil NLCs as delivery systems. The lipid nanoparticles formulated using the four vegetable oils were enriched with 2, 3 and 4 wt% of TOC (**Table 4.1**). The procedure was accomplished according to Zheng et al. 2013 (Zheng et al., 2013b) as it follows. The studies were conducted for 48 h, using a dialysis regenerated cellulose membrane (OrDial D14-MWCO 12,000-14,000flat width 25 mm, Orange Scientific, Belgium). Each membrane bag containing 5 mL of NLC suspension were immersed on 200 mL of receptor medium (composed of water/ethanol 1:1 v/v), maintained at 37 Cº with magnetic stirring at 300 rpm in a closed container to prevent evaporation, and to assure that sink conditions were obtained during the experiments. The receptor medium was collected in 1mL aliquots at pre-determined time points and replaced with the same volume of fresh medium. Samples were stored at 4 Cº until analysis. The released TOC was quantified by HPLC using the same conditions described in section 4.2.4. Also, the diffusion profile of a non-encapsulated TOC solution (1mg/mL in water/ethanol 1:1 v/v) was observed as a control, using the same dialysis process as for NLC suspensions.

4.2.3.7. Antioxidant activity assay

The free radical scavenging (antioxidant) capacity of free TOC, vegetable oils standards and both types of formulations of free and TOC-NLCs were measured by 1,1-diphenyl-2-picrylhydrazyl (DPPH) assay, a method previously reported by Kumari et al. 2010 and Souza et al. 2014 (Kumari et al., 2010, Souza et al., 2014). This method was carried out with slight modifications as it follows, 200 μL of sample solution was added to 100 μL of DPPH solution (0.2mM) prepared in absolute ethanol. The reaction mixture was incubated in the dark at room temperature for 30 min and the absorbance was measured at 517 nm using a microplate UV–Vis spectrophotometer (Spectra max Plus 384, China) against the DPPH control solution. The radical scavenging activity was calculated using **Equation 4.3**:

$$Scavenging\ activity\ (\%) = \left(1 - \frac{A_{sample,\ 517nm}}{A_{control,\ 517nm}}\right) \times 100 \qquad (4.3)$$

All determinations were performed in triplicate and the results are given as the mean ± SD.

4.3. Results and Discussion

4.3.1. Characterization of particle size and physical stability of NLCs

4.3.1.1. Influence of vegetable oil type and proportion

The effects of the vegetable oil composition and proportion in the preparation of NLCs using Tween 80 as a surfactant and myristic acid (C14:0) as a solid lipid on the particle size and physical stability were evaluated. The percentage of lipid phase (blend of solid lipid and liquid oil) on the miniemulsions was kept constant (**Figure 4.1**), while the solid lipid, wt%: vegetable oil, wt% ratio in the lipid phase varied. The mean particle size, the PdI and zeta potential of the lipid nanocarriers are illustrated in **Figure 4.1**.
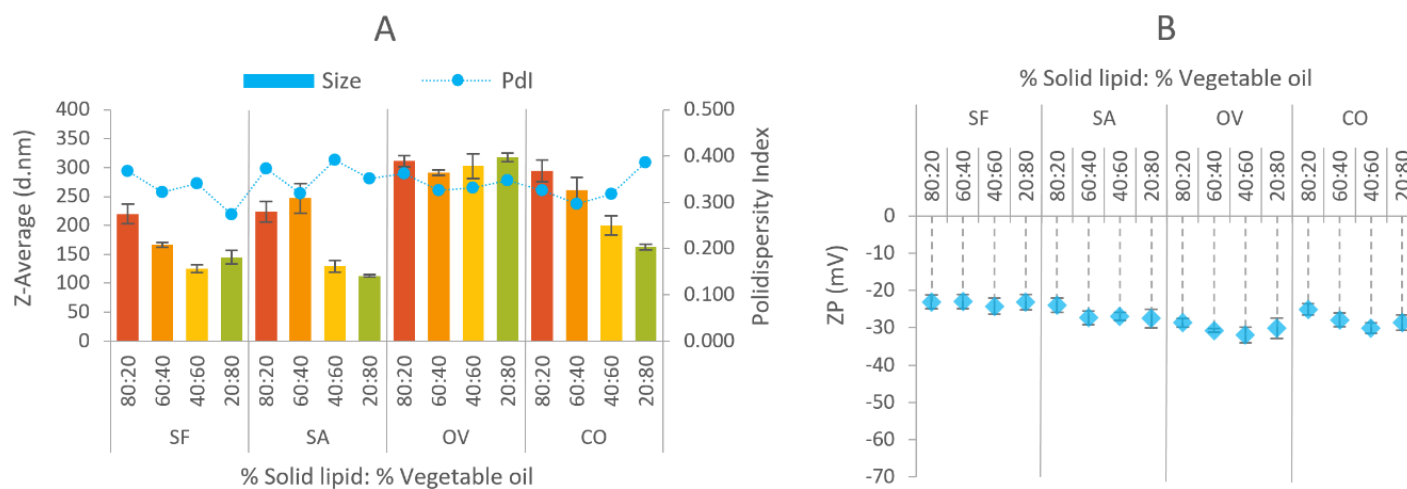
Figure 4.1 - Influence of oil content and composition on mean particle size and PdI values (A, on the left) and zeta potential (B, on the right) of NLC formulations prepared with myristic acid (C14:0) as solid lipid and with Tween 80 as surfactant.

The particles size are statistically significant and ranged between 125 ± 7.2 and 220 ± 16.7 nm for NLCs prepared with SF (*p*-values of 0.131 and 0.370, respectively with α=0.05), 113 ± 2.1 and 247 ± 25.7 nm) for NLCs prepared with SA (*p*-values of 0.204 and 0.061, respectively with α=0.05), 291 ± 4.6 nm and 318 ± 7.7 nm for NLCs prepared with OV (*p*-values of 0.379 and 0.241, respectively with α=0.05) and 162 ± 4.8 nm and 295 ± 18.8 nm for NLCs prepared with CO (*p*-values of 0.073 and 0.078, respectively with α=0.05).

The obtained polydispersity indexes (from 0.274 to 0.392 for all formulations) revealed a relatively uniform size distribution of the lipid nanoparticles (**Figure 4.1, A**). According to these results the average size of the vegetable oil NLCs decreased in general with the increase in the liquid oil percentage for SF (with an exception for the 20:80 ratio, % solid lipid:% SF oil), for SA (with an exception for the 60:40 ratio, % solid lipid:% SA oil) and for CO. These results are in agreement with those reported by Zheng et al. 2013 (Zheng et al., 2013a), which states that this was due to the liquid oil being easily dispersed into the aqueous phase which contributed to smaller particles. However, regarding the particles size obtained for the OV oil NLCs it was observed that these do not change significantly when varying the solid lipid, wt%: vegetable oil, wt% ratio. This may be due to the specific OV oil composition regarding the unsaturated/ saturated fatty acids ratio and in particular a higher percentage of palmitic acid (C16:0) when compared with the other used oils (**Table 4.2**). Without considering the formulations prepared with OV oil in which the particles size did not change considerably, it was observed that in the other formulations and independently of the type of used oil, the lowest average particles size were obtained with 40:60 and 20:80 solid lipid, wt%: vegetable oil, wt% ratios.

Table 4.2 - Fatty acid composition of the vegetable oils used in the preparation of NLCs. Adapted from (Giwa and Ogunbona, 2014, YCW, 2014).

	SF oil	*SA oil*	*OV oil*	*CO oil*
Unsaturated/Saturated ratio	7.3	8.0	4.6	0.1
Capric acid (C10:0)	-	-	-	6
Lauric acid (C12:0)	-	-	-	47
Myristic acid (C14:0)	-	-	-	18
Palmitic acid (C16:0)	7	9	13	9
Stearic acid (C18:0)	5	2	3	3
Oleic acid (C18:1)	19	70	71	6
Linoleic acid, ω6 (C18:2)	68	18	10	2
α-Linolenic acid, ω3 (C18:3)	1	1	1	-

Note: Percentages may not add to 100% due to rounding and other constituents not listed in this table

The physical stability of colloidal systems was determined in function of zeta potential, which quantifies the charge on particle surface. High values of zeta potential, either positive or negative, contribute to stabilize the suspension and minimize aggregation due to the electrostatic repulsion between particles with the same electrical charge, especially for charged particles with pronounced zeta potential| (>|30|) (Pinto et al., 2014). The obtained zeta potential values did not varied considerably in all the formulations with the four different vegetable oils and ranged between − 23.0 and −32.0 mV, which predicts a relatively short-term stability to the particles. Once again, the results

obtained for NLCs prepared with OV presented some discrepancies when compared with others. It also showed higher negative zeta potential and consequently higher stability (**Figure 4.1, B**).

4.3.1.2. *Influence of solid fatty acids chain length*

The effect of the solid fatty acid chain length on particle size and physical stability was evaluated. The NLCs were prepared using Tween 80 as a surfactant, saturated solid fatty acids ranging from C12:0 to C18:0 as solid lipid and the four vegetable oils in a constant solid lipid, wt%: vegetable oil, wt% ratio of 40:60. The particle sizes and PdI of the NLCs are presented in **Figure 4.2, A**. According to these results, when increasing the chain length of the solid fatty acid from C12:0 to C14:0 a slight influence on NLCs size was observed. Moreover, an increase in particle size of NLCs formulated with solid lipids from C16:0 and C18:0 and each vegetable oil was noted, with an exception for OV oil. The obtained results for particle size of NLC are statistically significant for all vegetable oil formulations prepared using solid lipids from C12:0 to C16:0, presenting *p*-values ≥ 0.05.
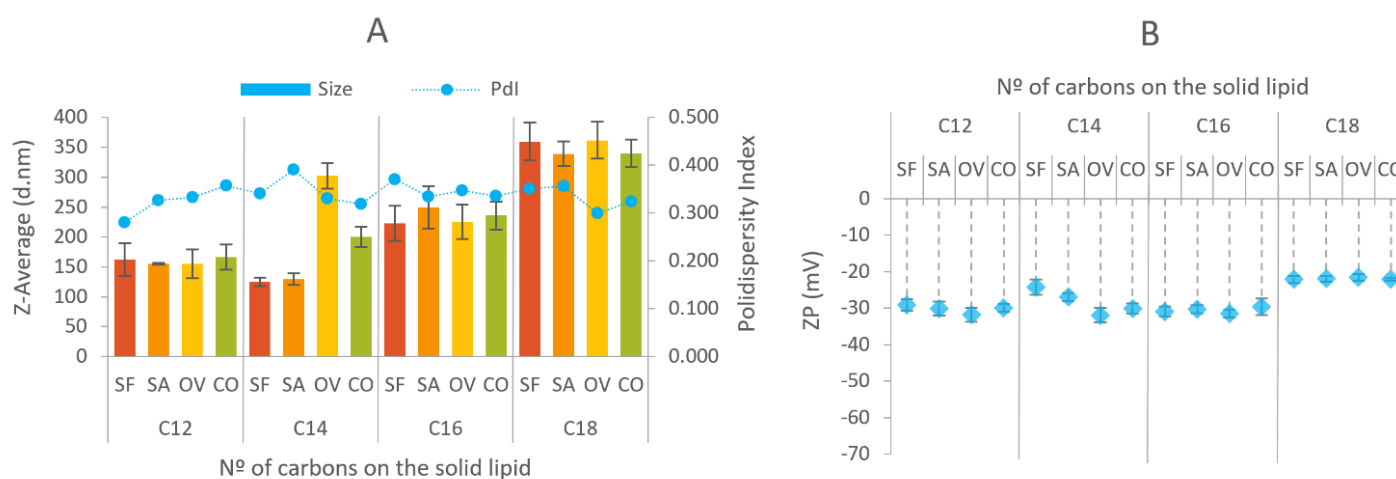
Figure 4.2 - Influence of the solid fatty acids chain length on NLCs prepared with Tween 80 as surfactant on mean particle size and PdI values (A, on the left) and zeta potential (B, on the right).

The particle size of NLCs prepared with C18:0 almost doubled in comparison with those formulated with C12:0 (from 162 ± 26.9 nm to 360 ± 31.7 nm for NLCs prepared with SF oil; from 155 ± 1.5 nm to 339 ± 20.5 nm for NLCs prepared with SA oil; from 155 ± 23.7 nm to 362 ± 31.1 nm for NLCs prepared with OV oil and from 167 ± 20.9 nm to 340 ± 23.4 nm for NLCs prepared with CO oil) and the results obtained with C18:0 presents *p*-values ≤ 0.05 (*p*-values of 0.0067, 0.0241, 0.0079 and 0.0438 for formulations with SF oil, SA oil, OV oil and CO oil, respectively) which demonstrated that are not statistically significant. This fact can be attributed to the formation of a more viscous lipid phase which leads to the increase on surface tension and consequently to the formation of larger particles

(Ekambaram et al., 2012, Niculae et al., 2014, Sanad et al., 2010). Although, the results showed a decrease on particle size with the increase of the solid fat chain length from C12:0 to C14:0 for NLCs formulated with SF and SA oils. This could be due to a higher ratio of unsaturated to saturated lipids (**Table 4.1**) in these oils composition when compared with the other two oils. But then again, it was observed an increase on particle size for NLCs prepared with SF and SA oils and solid lipids from C16:0 to C18:0. On the other hand, NLCs formulated with OV and CO oils demonstrated a tendency to increase the particle size when using solid lipids with fatty acids of longer chain length.

The polydispersity parameter gives an important information on size homogeneity (Pinto et al., 2014). The obtained polydispersity indices are close to those obtained in the previous study (0.281 to 0.392 for all formulations) and once more they reflect a relatively homogeneous size of lipid nanoparticles.

Regarding the physical stability of the obtained lipid nanocarriers, it was found that no significant variation on the results with zeta potential values above -32.0 mV when increasing the fatty acid chain length of the solid lipid in the NLCs formulations prepared with the different vegetable oils (**Figure 4.2, B**). Lower zeta potential values of -22 mV were observed for the particles prepared with stearic acid (C18:0) for each tested vegetable oils.

4.3.1.3. Effect of the surfactant

The physicochemical properties of lipid nanoparticles are mainly affected by some factors, including the type and concentration of solid and liquid lipids, the viscosity of the lipid phase and the type of surfactant (How et al., 2013). The choice of the proper surfactant is a crucial variable since it can alter the solubility, diffusion, dissociation rate, and thermodynamic activity of an encapsulated active compound (Balakrishnan et al., 2004, How et al., 2013). Three additional non-ionic surfactants, one with a more hydrophilic character based on its HLB value, Poloxamer 188, and two with more lipophilic characteristics, Span 60 and Span 80, were examined for their effects on particle size and surface charge on NLCs. The formulations of NLCs were prepared based on the results discussed on the previous sections 1.1 and 1.2, with a constant percentage of each vegetable oil on the lipid phase, (40:60, solid lipid, wt%: vegetable oil, wt% ratio) and myristic acid (C14:0) as solid lipid. The results were compared with those obtained from the NLCs formulations prepared with the surfactant Tween 80 which presents an HLB value of 15.0. These results demonstrated that the major increase on particle size was observed with Span 60 in comparison with the others surfactants (**Figure 4.3, A**). Likewise, the PdI values obtained with this hydrophobic surfactant were significantly higher for all vegetable oil NLCs indicating a more heterogeneous size distribution. These results could be mainly attributed to the differences on the chemical structure of the used surfactants and their compatibility and conformational rearrange with the lipid matrix (Teeranachaideekul et al., 2007a, Saberi et al., 2012). In general, the nanoparticles prepared with SF and SA oils presented smaller sizes, specially using the surfactants Tween 80 which NLCs presented sizes of 125 ± 7.2 nm and 129 ± 9.8 nm

respectively and Span 80 with which were obtained sizes of 140 ± 21.1 nm and 172 ± 26.5 nm respectively **(Figure 4.3, A)**. This could be due to the resemblance on the molecular structure of these two surfactants (Twee 80 and Span 80) which in both cases present the same lipophilic tail composed of a mono unsaturated fatty acid (C17:1) that is then most probably located on the inside of the NLCs lipid matrix. However, it was observed a significant difference on particle size in NLC formulations using OV oil and the surfactants Tween 80 and Span 80 (302 ± 21.4 nm and 134 ± 17.5 nm, respectively).
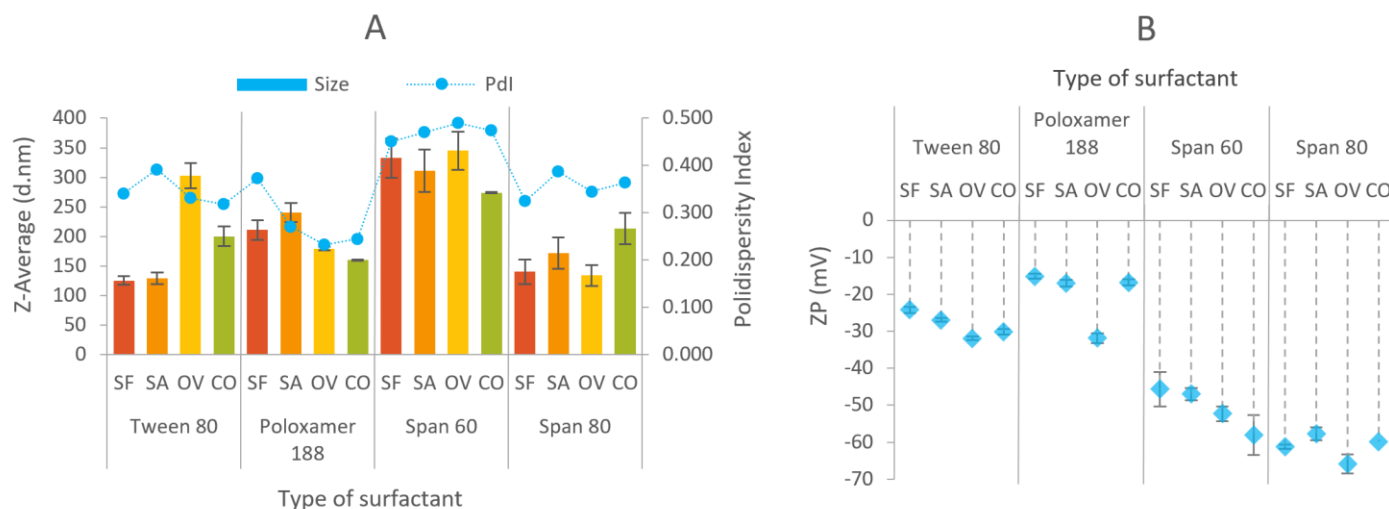
Figure 4.3 - Influence of used type of surfactant on NLCs formulations with myristic acid (C14) on mean particle size and PdI values (A, on the left) and zeta potential (B, on the right).

It was noticed, in **section 4.3.1.1.,** that NLCs formulated with this vegetable oil and Tween 80 presented a higher particle size compared with the other vegetable oils in study, independently of the solid lipid, wt%: vegetable oil, wt% ratio. This may be attributed to the specific composition of OV oil in terms of its unsaturated/ saturated fatty acids ratio and in particular, its higher proportion of palmitic acid (C16:0) (**Table 4.2**). Moreover, there is a different geometrical packing of the surfactants Tween 80 and Span 80 at the oil-water interface in dispersed oil droplets (Bjorkegren et al., 2015), which combined with the various long chain fatty acid esters present in OV oil composition may justify the difference on particle size of NLCs formulated with this vegetable oils and these two surfactants. It was verified that the obtained particle size results for NLC formulations prepared with each selected vegetable are all statistically significant with p-values ≥ 0.05 with one exception for the formulation with SF oil and the surfactant Span 60 (333 ± 34 nm, *p*-value = 0.020, α= 0.05).

Among the selected vegetable oils, the higher negative zeta potential value was achieved with OV with each surfactant (**Figure 4.3, B**). The formulations of NLCs prepared with surfactants presenting a lower HLB value (Span 60 and Span 80) obtained the highest zeta potential values

ranging between −45.6 and −65.9 mV and consequently higher physical stability when compared with those previously prepared with Tween 80 and Poloxamer 188.

The morphology of NLCs prepared using SF oil with myristic acid (C14:0) as solid lipid (40:60, solid lipid, wt%: vegetable oil, wt% ratio) and three surfactants (Span 80, Tween 80 and Poloxamer 188) was evaluated by TEM analysis. The micrographs of the dried suspension of vegetable oil-NLCs were presented in **Figure 4.4**. These images represent views collected from different regions of the dried sample and with different amplification factors. The NLC particles present spherical shape and particle sizes in the nanometer range.
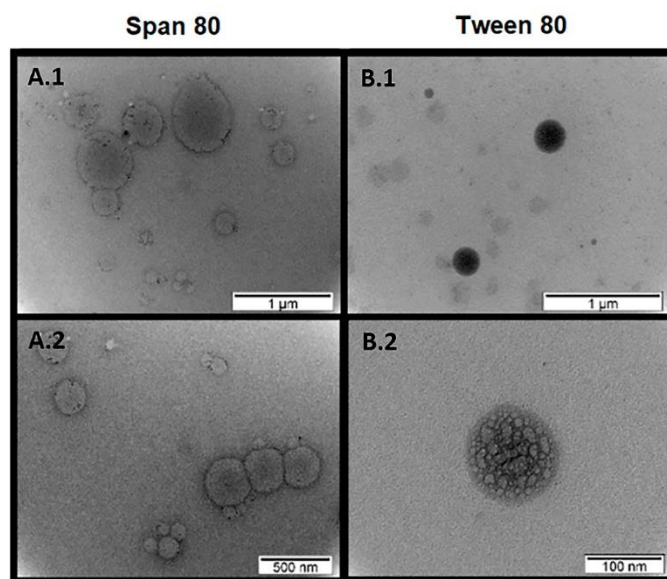
Figure 4.4 - TEM micrographs of NLCs formulated with Span 80 and Tween 80 as surfactants and sunflower oil: myristic acid (C14:0) in a 40:60 solid lipid, wt%: vegetable oil, wt% ratio presented in views from different positions and amplification factors.
A.1-2: NLCs formulated with Span 80;
B.1-2: NLCs formulated with Tween 80;

The micrographs from the formulation prepared with Span 80 are displayed in **Figure 4.4, A** which depicts evident differences on the crystallization form of the lipid matrix compared with the particles obtained with the other two surfactants with a hydrophilic character. Moreover, it was noticed an agglomeration tendency from these particles (**Figure 4.4, A 1-2**) and for this reason there was a slight discrepancy regarding the particle size obtained by DLS which was about 150 nm. However, the values of zeta potential from the NLC particles prepared with Span 80 were in the range of − 61.2 ± 0.5 mV which indicate an appropriate electrostatic repulsion between the particles and would prevent any case of agglomeration (Müller et al., 2000, Teeranachaideekul et al., 2007a). The preparation of NLCs for TEM analyses includes a dehydration step for solvent removal which may cause modifications on

particle size and explain the occurrence of agglomeration and then, the discrepancy found on particle sizes between TEM and DLS (de Carvalho et al., 2013, Liu et al., 2007a, Zheng et al., 2013a). The micrographs from the NLC particles formulated with Tween 80, which present a more hydrophilic character, are presented on **Figures 4.4, B 1-2**. It reveals a well-defined spherical polymorphic crystal structure of the lipid matrix. This crystallization form of the nanoparticle matrix offers a proper incorporation of active substances encapsulated and exclude its expulsion after a longer period of storage (Lacatusu et al., 2014).

4.3.2. Characterization of TOC-NLCs

4.3.2.1. α-Tocopherol encapsulation efficiency and drug loading capacity

The vegetable oil NLCs were enriched with TOC to evaluate the incorporation capacity of this lipophilic vitamin into the lipid matrix of the nanoparticles. Three concentrations of TOC (**Table 4.1**) were tested to assess the EE and DL in the lipid nanoparticles formulated with each tested vegetable oil, myristic acid (C14:0) as solid lipid (40:60, solid lipid, wt%: vegetable oil, wt% ratio) and Span 80 as surfactant. The results of the physicochemical characterization of TOC-NLCs prepared with three different concentrations of vitamin is presented in Table 3, including the values of EE and DL. The particle size increased significantly between the concentrations of 2 and 4 wt% of TOC with each vegetable oil, in a range of 27% for TOC-NLCs prepared with SF oil, 37% with SA oil, 14% with OV oil and 17% with CO oil. The incorporation of higher amounts of TOC could induce a morphologic alteration in the lipid matrix since this vitamin is a viscous oil and according to Hu et al. 2005 (Hu et al., 2005), the nanoparticles size is smaller by using less viscous oils in formulation (Badea et al., 2015, Hu et al., 2005). Moreover, as it may be observed there is a greater influence on particle size when TOC is introduced in formulations prepared with less viscous liquid oils as SA and SF oils. Likewise, comparing the particle size of TOC-NLCs with free NLCs prepared with each vegetable oil it was also noted a slight increase on their size. In the same way, the zeta potential values obtained for TOC-NLCs formulated with the selected vegetable oils have slightly changed when increasing TOC concentration but still assured a good physical stability with values between -45.7 ± 0.6 mV and -55.1 ± 2.1 mV (**Table 4.3**).

The EE and DL of TOC-NLCs were analyzed in order to understand which vegetable oil offers the best incorporation of the vitamin into the lipid matrix. All the lipid nanoparticle formulations prepared with each oil demonstrated a high ability to incorporate TOC in each three tested concentrations (from 2 to 4 wt%), showing high EE values above 79.4 ± 3.5 % (**Table 4.3**). Similarly, it was also obtained good DL values for all TOC-NLCs formulations. In more detail, lipid nanoparticles prepared with SA and SF oils and 2 wt% of TOC showed the highest DL values, 48.9 ± 0.3 % and 48.4 ± 0.5 %

respectively, from the maximum theoretical DL of 50.0 % which could be reached for this vitamin concentration.

Table 4.3 - Encapsulation efficiency (EE), drug loading capacity (DL) of TOC in the lipid matrix of NLCs, average particle size and zeta potential values of the optimized formulations (composed by Span 80 as surfactant, myristic acid with each vegetable oil enriched with 2, 3 and 4 wt% of TOC).

	TOC, wt%	*Particle size , nm*	*Zeta potential, mV*	*EE, %*	*DL, %*
SF	2.0	247 ± 2.9	-47,0 ± 2.0	96.9 ± 1.0	48.4 ± 0.5
	3.0	256 ± 2.3	-47,9 ± 1.3	95.8 ± 3.5	71.9 ± 2.5
	4.0	314 ± 4.7	-54,6 ± 0.7	81.1 ± 5.4	80.5 ± 5.4
SA	2.0	241 ± 3.0	-46.5 ± 0.9	97.9 ± 0.6	48.9 ± 0.3
	3.0	294 ± 2.9	-53.6 ± 2,4	92.9 ± 2.2	69.7 ± 1.2
	4.0	331 ± 7.7	-53.7 ± 0.9	83.5 ± 3.9	83.2 ± 3.9
OV	2.0	271 ± 3.9	-48.0 ± 0.8	80.9 ± 10.6	40.4 ± 6.0
	3.0	281 ± 5.4	-47.4 ± 0.8	80.1 ± 8.2	60.1 ± 6.5
	4.0	308 ± 4.9	-55.1 ± 2.1	80.7 ± 1.8	80.2 ± 1.8
CO	2.0	246.2 ± 5.3	-45.7 ± 0.6	89.3 ± 1.3	44.6 ± 0.7
	3.0	282.4 ± 14.6	-48.5 ± 0.6	87.6 ± 10.1	65.7 ± 7.3
	4.0	287.2 ± 4.4	-54.2 ± 1.5	79.4 ± 3.5	78.6± 3.4

The obtained results for DL demonstrate that the lipid matrixes of TOC-NLCs prepared with each vegetable oil can effectively load this lipophilic vitamin, and present similar loading capacities for each tested TOC concentration. The increase in the concentration of TOC resulted in a decrease of the DL capacity considering that the difference between the maximum theoretical values of DL that can be reached for each percentage of TOC (50 % for a concentration of 2 wt%, 75 % for 3 wt% and 100 for 4 wt%) and the effective DL value have also increased (**Figure 4.5**).

Furthermore, out of the four lipid matrices in study, the TOC-NLCs formulated with SA and SF oils and 2 wt% of TOC presented better EE values (97.9 ± 0.6 % and 96.9 ± 1.0% respectively) than the other two lipid nanoparticles formulations prepared with CO and OV oils (89.3 ± 1.3 and 80.9 ± 10.6 respectively). The amount of TOC encapsulated into each vegetable oil NLCs has influenced the EE. In this case, the same tendency demonstrated with the DL capacity was observed and like so a better entrapment in the lipid matrix was obtained with lower amounts of incorporated vitamin (**Table 4.3**). The drug entrapment in NLCs is mainly affected by the solubilization of the active compounds into the solid and liquid lipids and their partitioning between the oil and aqueous phases (Aslam et al., 2016). Having this in consideration, these values demonstrated an efficient solubility capacity of TOC on the lipid core in all formulations prepared with the selected vegetable oils.
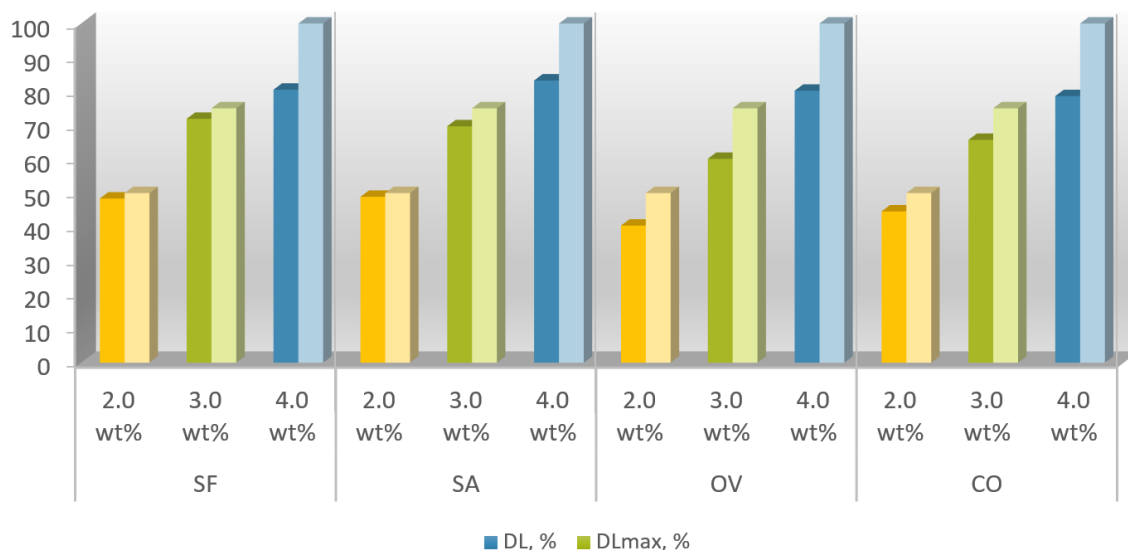
Figure 4.5 - DL capacity of the lipid matrix of TOC-NLCs prepared with each vegetable oil.

4.3.2.2. In vitro release studies

An equilibrium dialysis method was used to study the release behaviour of TOC-NLCs prepared with each vegetable oil (**Table 4.1**) and of a pure solution of TOC in water: ethanol (1:1 v/v) that was used as reference. The release profiles are displayed in **Figure 4.6.** The pure TOC solution was quickly released during the first 10h and the cumulative released amount was 91.0% after 48h.

Comparatively, there was no initial burst release for encapsulated TOC as it released slowly from the lipid matrices of TOC-NLCs prepared with each vegetable oil and 2 wt% of TOC. These lipid nanoparticles demonstrated to have similar release profiles (**Figure 4.6, A**). There was a slower release in the first 10h hours comparing with the control and the highest cumulative released value reached at that time was 32.3% and it was obtained with TOC-NLCs prepared using SA oil. However, after 48h the highest cumulative released was obtained with OV oil which was 43.7%, and followed by TOC-NLCs formulated with SA oil, 39.2%; CO oil, 36.3% and SF oil, 26.6%. When comparing this results with those obtained from the lipid nanocarriers loaded with 4 wt% of TOC (**Figure 4.6, B**) it was noted a slower release pattern at the initial stage, except for TOC encapsulated on lipid nanoparticles formulated with OV oil which release profile was improved and has reached a cumulative released of 35.7% after 10h. In fact, the release of TOC from the lipid matrix of the nanoparticles with this concentration has only started after 4h in formulations prepared with SA and CO oils.

TOC-NLCs formulated with SF oil demonstrated an even slower release profile reaching the lowest cumulative released of 27.0% after 48h. However, this value was slightly higher when comparing to what was reached with nanoparticles prepared with SF oil and a TOC concentration of 2wt%. The highest nanoparticles size that was obtained for formulations with 4 wt% of TOC (**Table 4.3**), could condition the dissolution and liberation of the encapsulated active compound which is

located in the matrix core and away from the surface of the nanoparticles. NLCs with smaller particle sizes provide enhanced specific surface area, improved wettability and consequently the release of encapsulated TOC (Mandpe and Pokharkar, 2015). The cumulative released amounts of TOC obtained at 48h for the formulations containing 4 wt% of TOC (51.0% for TOC-NLCs formulated with SA oil, 48.6% with CO oil, 39.6% with OV oil and 27.0% with SF oil) were higher than those with 2 wt%, this can be attributed to a higher availability of TOC provided with a higher internal concentration. Nevertheless, the final cumulative released values were much above the obtained with the pure TOC solution and this can be explained by a good accommodation and stronger interaction of TOC inside the lipid matrix, preventing diffusion and burst release from the TOC-NLCs. Moreover, the slow diffusion profiles coupled with the high EE results (**Table 4.3**) can establish that a higher amount of TOC was encapsulated deeply inside of the lipid core.
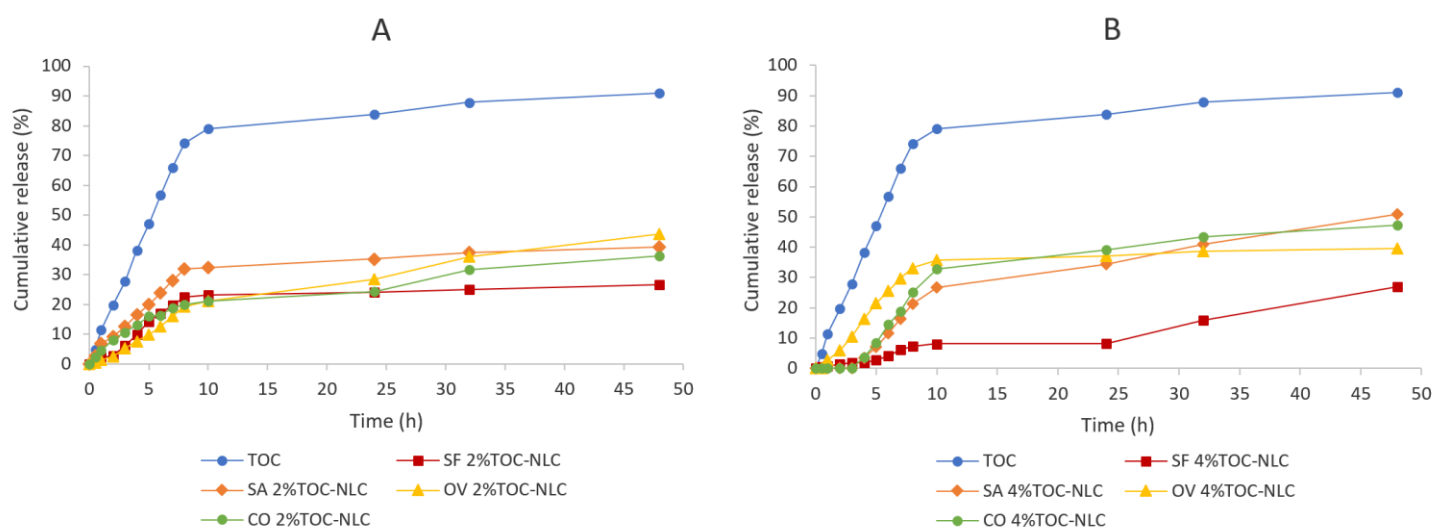
Figure 4.6 - Release profile of a pure TOC solution compared with different vegetable oil-NLCs dispersions in water: ethanol (1:1) as receptor medium.
A: 2 wt% loaded TOC loaded NLC dispersions;
B: 4 wt% loaded TOC loaded NLC dispersions.

These results demonstrate that the increase in TOC concentration significantly influenced the release pattern from the lipid nanoparticles. Moreover, further characterization through *in vitro* assays on reconstructed human epidermis should be performed to attend the purpose of topical administration of the developed TOC-NLC formulation.

4.3.2.3. Crystallinity studies

Differential scanning calorimetry (DSC) analysis was performed to evaluate the changes on the crystalline state of free NLCs and TOC-NLCs formulated using the selected vegetable oils with 2, 3 and 4 wt% of the lipophilic vitamin. DSC analysis of NLCs are useful to comprehend the interactions between the lipids and the loaded active compound and the mixing behaviour of solid lipids with liquid lipids (Nekkanti et al., 2009, Thakkar et al., 2014). DSC parameters such as melting temperatures, melting enthalpies and the crystallinity index (CI, %) were determined and studied for the bulk solid lipid used in formulations and for the free NLCs and TOC-NLCs (**Table 4.4**).

Table 4.4 - DSC parameters. Melting peak (°C), enthalpy (ΔH, Jg-1) and crystallinity index (CI, %) of the developed vegetable oil-NLC formulations enriched with 2, 3 and 4% of α-tocopherol in composition.

	TOC, wt%	*Melting point, °C*	*Entalphy, -J/g*	*CI, %*
SF	0.0	57.7	38.27	23.8
	2.0	41.5	35.9	22.3
	3.0	38.5	20.7	12.9
	4.0	38.3	16.8	10.4
SA	0.0	58.1	41.06	25.5
	2.0	41.5	24.4	15.2
	3.0	36.5	13.5	8.4
	4.0	35.2	9.6	6.0
OV	0.0	57.8	38.01	23.6
	2.0	40.6	22.7	14.1
	3.0	36.0	11.6	7.2
	4.0	35.9	11.6	7.2
CO	0.0	57.3	40.46	25.1
	2.0	41.1	28.9	18.0
	3.0	36.2	16.6	10.3
	4.0	36.7	13.6	8.5
Myristic acid	-	56.8	161.0	100

The DSC results showed that there are no significant differences in the degree of crystallinity obtained with the free lipid nanocarriers prepared with each vegetable oil, which varied between 25.5 and 23.6% for NLCs prepared with SA and OV oils respectively. These lower percentages of crystallinity and the apparent decrease on the energy for lipid modification (enthalpies ranging between 41.06 and 38.01 J/g for NLCs prepared with SA and CO oils respectively) when compared with the bulk crystalline solid lipid may indicate an amorphous phase as physical state of NLCs. Although, the obtained melting temperatures of the NLCs (between 58.1 and 57.3 °C for NLCs prepared with SA

and CO oils respectively) were in the same range of the pure myristic acid (56.8 °C). These results suggest that the chemical composition of the liquid lipid does not interfere in the physical state (crystallinity) of the lipid matrix.

Comparing the DSC results for TOC-NLCs prepared with different vitamin concentrations with those obtained for free NLCs it was observed a significant decrease on the melting temperatures along with a decrease on the energy of lipid modification (**Table 4.4**). This behaviour evidenced also a decrease on the degree of crystallinity. In order to illustrate this event, the DSC thermograms of the free NLCs and TOC-NLCs prepared SF oil were compared, as an example, in **Figure 4.7**. The endothermic peaks of the lipid matrix from the free NLCs to the TOC-NLCs prepared with 4wt% of lipid vitamin shifted to lower melting temperatures with the increase in TOC percentages. In fact, there was an evident decrease on melting point and onset temperature with an increase of TOC content in the lipids blend. This is in agreement with results previously reported by de Carvalho et al. 2013 (de Carvalho et al., 2013) which demonstrated that the incorporation of TOC led to a melting point depression and suggests that the TOC was completely dispersed in the solid lipid matrix of NLCs producing significant modifications on the physical state of the nanocarriers.
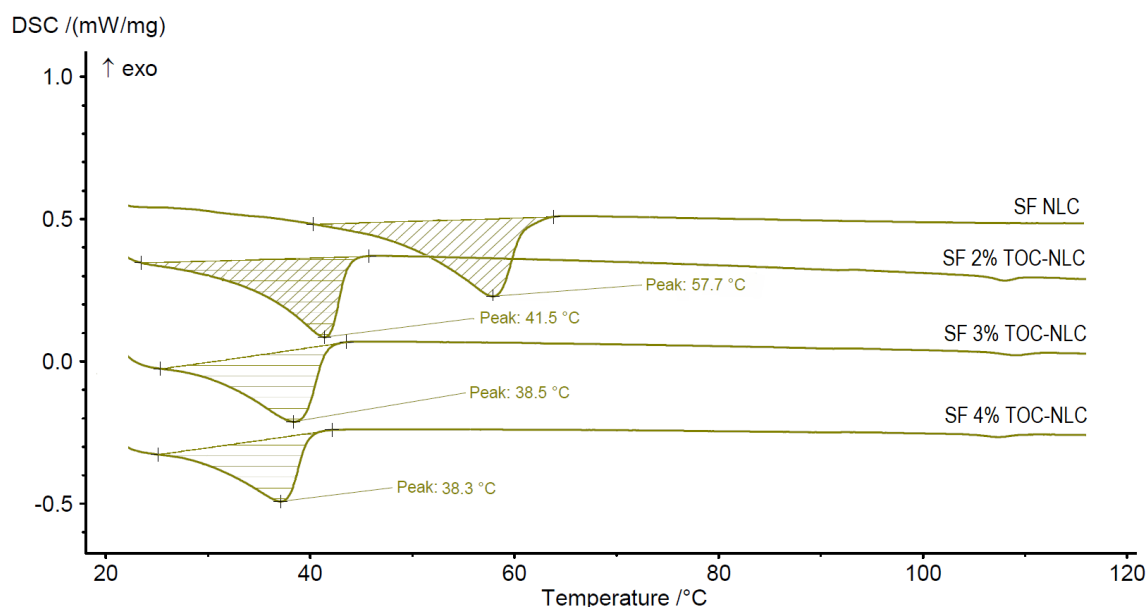
Figure 4.7 - DSC thermograms of NLC formulations prepared with SF as liquid lipid and enriched with 2, 3 and 4 wt% of TOC.

The width of each melting peak refers to the temperature span, mostly from the onset point to the ending point of the melting process which increases with oil percentage in the lipid blends, indicating an amorphous phase (Zheng et al., 2013a). Similar thermograms were obtained for the other TOC-NLCs formulations prepared with each vegetable oil. Another important aspect to be noted is the decrease on onset temperature which was higher than 40°C for free NLC formulations and much under this value for TOC-NLCs and this is referred by Gonzalez-Mira et al. 2011 (Gonzalez-Mira et al.,

2011) to be a prerequisite to develop lipid nanocarriers for topical applications. Having this in consideration and in order to revise this parameter is probably necessary to slightly increase the percentage of solid lipid in the formulation for higher TOC concentrations.

4.3.2.4. Effect of storage time on stability

The average particle size and PdI were selected as reference parameters to evaluate changes in the physical stability of the free NLCs and TOC-NLCs prepared with each vegetable oils and 2 wt% of TOC. The variation of particle size is a useful indicator of instability as the particle size increases before macroscopic changes are detected (Gonzalez-Mira et al., 2011). The effect of storage time was evaluated at room temperature over 4 and 8 months after the initial formulation preparation. In general, after 4 months the particle sizes of the lipid nanoparticles seemed to slightly increase in comparison to their initial values (**Figure 4.8**). After 8 months of storage, the average size increased specially in NLC formulations prepared with CO oil without TOC (29.5 % after 4 months and 45.3 % after 8 months). In this specific case was also observed an increase on PdI values which indicates a more heterogeneous population most likely due to the formation of some aggregates.
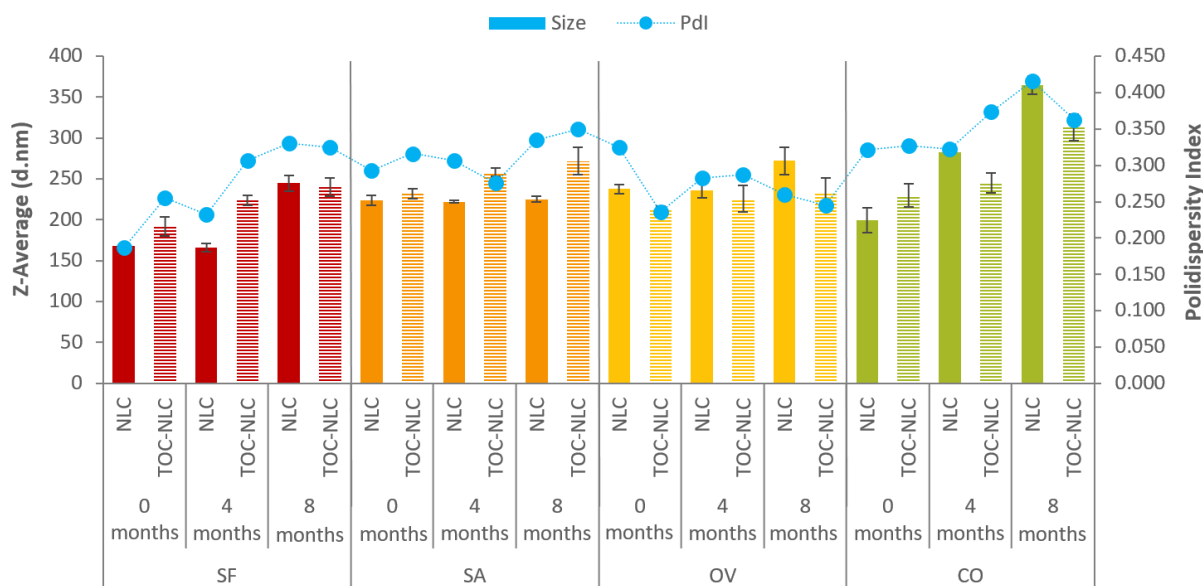
Figure 4.8 – Effect of storage on the particle size and PdI of free NLCs and TOC-NLCs prepared with each vegetable oil and 2 wt% of TOC during 4 and 8 months.

Despite the noticed increase on particle size, the vegetable oil NLC formulated with each oil still possessed the characteristic dimensions of lipid nanoparticles, remaining in the submicron range, with diameters ranging from 225 ± 3.5 nm (*p*-value= 0.438, α=0.05) and 365 ± 11.4 nm (*p*-value= 0.081, α=0.05) after 8 months. This could be related to the high negative electrical charge of zeta potential

values (above -48mV, **Table 4.3**) which indicates an appropriate electrostatic repulsion between the particles and predicts a good physical stability under time of storage (de Carvalho et al., 2013, Müller et al., 2000, Teeranachaideekul et al., 2007a). The more stable nanoparticles were obtained in the formulations prepared with SA and OV oils presenting both very small size variations after 8 months of storage (**Figure 4.8**). Moreover, the NLC formulations prepared with each vegetable oil and enriched with TOC were found to be in general, more stable than the free NLCs presenting very slight variations on particle size after storage.

4.3.2.5. Evaluation of antioxidant activity of TOC-NLCs

The antioxidant properties of the pure vegetable oils is related to their protective function in human skin against oxidative stress (Badea et al., 2015) and they are known to possess a vast source of antioxidants such as tocopherols, tocotrienols, carotenoids and also others more polar phenolic compounds (Prevc et al., 2013). The DPPH scavenging capacity assay was used to evaluate the *in vitro* antioxidant activity in a pure TOC solution and in each vegetable oil used in the preparation of the lipid nanoparticles, used as reference, and in free NLCs and TOC-NLCs. This test is based on the ability of DPPH radical to scavenge oxygenated free radicals (Lacatusu et al., 2014). The results are illustrated in **Figure 4.9** and showed that the produced free NLCs and TOC-NLCs with all vegetable oils presented high antioxidant activities with percentages above 56.7% ± 8.8 and 64.3% ± 8.2 respectively. These values were obtained with the lipid nanoparticles formulated with CO oil which displayed the lowest scavenging capacity.
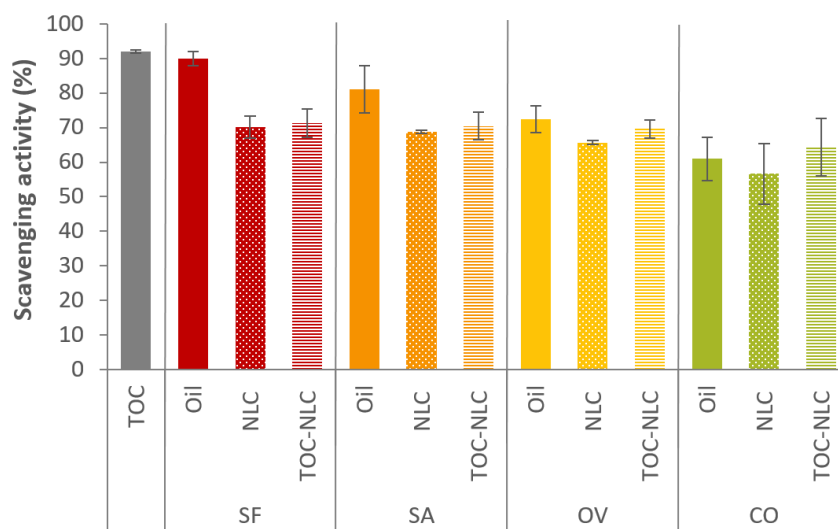
Figure 4.9 - Antioxidant activity measured from a pure TOC solution, from each used vegetable oil in the preparation of the lipid nanoparticles and from the free NLCs and TOC-NLCs formulations prepared with 2 wt% of TOC.

Comparatively, the pure TOC solution and the vegetable oils used as reference presented higher scavenging activities than the lipid nanoparticles (**Figure 4.9**). Despite that, the formulation of free NLCs with each vegetable oil resulted in free nanocarriers that manifest inherent good antioxidant activities (70.2% ± 3.2 with SF oil, 68.8% ± 0.4 with SA oil, 65.7% ± 0.5 with OV oil and 56.7% ± 8.8 with CO oil). Moreover, the enrichment of the lipid nanoparticles with TOC resulted in a slight improvement on the scavenging activity compared to those of free NLCs (**Figure 4.9**). In this case, the TOC-NLCs prepared with SF and SA oils presented exhibited higher values of antioxidant activity (71.2% ± 4.1 and 70.5% ± 4.0 respectively). This behaviour can be mainly attributed to the reactivity of antioxidants in dispersed systems being dependent on the location of both radical and antioxidant. For instance, the surfactant layer represents a physical barrier if the solubilization properties of antioxidants and radicals differ markedly (Heins et al., 2007) and the location represents a chemical environment that can be more or less favourable for the reaction (Oehlke et al., 2017). Based on these results, it is important to emphasize that using natural ingredients as vegetable oils in the formulation of NLCs provides effective lipid nanocarriers showing a high incorporation of lipid actives and a high antioxidant potential.

4.4. Conclusions

Four vegetable oils, presenting inherent beneficial bioactive properties were selected and successfully applied in new formulations of multifunctional free NLCs and TOC-NLCs. From the present study, it was demonstrated that the particle size, the size distribution and the surface charge of the lipid nanoparticles are significantly influenced by the composition of the lipids core and by the type of used surfactant. NLC formulations with different lipid matrices were obtained by the miniemulsion methodology, presenting a suitable nanoscale size between approximately 120 to 350 nm for free NLCs and approximately 240 to 315nm for TOC-NLCs.

All lipid nanocarriers prepared with the selected vegetable oils and enriched with TOC showed high EE values ($\leq$ 97,9%) and high DL capacities which proved to be dependent on the percentage of incorporated active vitamin. Also, the increase in the concentration of TOC resulted in a decrease of the DL capacity, considering the difference between the maximum values of DL that can be reached for each percentage of TOC. Out of the four lipid matrices and the three TOC concentrations in study, the TOC-NLCs prepared using SA and SF oils and 2 wt% of TOC presented the highest EE, 97.9 ± 0.6 % and 96.9 ± 1.0% respectively and DL capacities, 48.9 ± 0.3 % and 48.4 ± 0.5 %.

The release profiles of TOC-NLCs containing 2 and 4wt% of TOC was not influenced by the composition of lipids on the nanoparticles core from each vegetable oil, but it was noted a slower release pattern at the initial stage from TOC-NLCs prepared with the higher concentration of TOC. The highest reached cumulative released value after 48h was 51.0% and it was obtained using SA oil

in the formulation. This controlled release assures a high integration of the lipophilic TOC into the lipids core conferring its amplified protective effect and the minimization of its side-effects.

DSC analysis revealed that there are no significant differences in the degree of crystallinity obtained with the free NLCs prepared with each vegetable oil, thus, meaning that the chemical composition of the liquid lipid does not interfere in the physical state of the lipid matrix which pointed as an amorphous phase. The incorporation and increase of TOC concentration into the lipids core led to a decrease on the obtained onset and melting temperatures producing significant modifications on the physical state of the nanocarriers.

The evaluation of the antioxidant activity shown that all free NLCs prepared with each vegetable oil possess a good inherent scavenging activity. The highest values were obtained with the formulations using SF and SA, 70.2% ± 3.2 and 68.8% ± 0.4 respectively which were slightly improved by the encapsulation of TOC (71.2% ± 4.1 and 70.5% ± 4.0).

All the NLC formulations demonstrated to be stable for a period of eight months showing small variations on particle size.

In summary, this study strengthen the significant role of lipid nanocarriers in the development of efficient biocosmetic prototypes with multifunctional skin beneficial properties derived from the vegetable oils and with several advantages as they can be placed in long-term stable cosmetics, ensuring an appropriate release of actives and conceding an effective beneficial potential. Furthermore, this research delivered an important contribution for the development of advanced cosmetic products based on the use of natural ingredients originated from vegetable source

◢ CHAPTER V

OPTIMIZATION OF FORMULATION PARAMETERS OF NANOSTRUCTURED LIPID CARRIERS LOADED WITH RETINOIDS FOR TOPICAL ADMINISTRATION

Fátima Pinto, Dragana P.C. de Barros, Luis P. Fonseca

5.1. Introduction

5.2. Materials and Methods

5.3. Results and Discussion

5.4. Conclusions

5. Optimization of formulation parameters of nanostructured lipid carriers loaded with retinoids for topical administration

The purpose of this work was to develop and optimize a new bioactive delivery system based on lipid nanoparticles for the topical administration of retinyl palmitate (RP), tretinoin (TRT) and adapalene (ADP). A 5-factor, 3-level central composite design was applied to optimize selected formulation parameters of nanostructured lipid carriers (NLCs) synthesized using sunflower oil by the miniemulsions methodology. An optimized NLCs composition of 2.5% of total lipids, 2.0% of myristic acid and 0.5% of sunflower oil and 1.5% of surfactant was reached using RP as model retinoid. The type of surfactant was adjusted to improve the electrostatic stability of the lipid nanoparticles and the resultant optimized NLCs formulation was evaluated to incorporate TRT and ADP. Particle sizes of 134.5 ± 5.4 nm and zeta potential values of –57.0 ± 2.8 mV were obtained for optimized ADP-NLCs. High entrapment efficiency values were obtained as 84.4 ± 3.0%, 84.1 ± 7.8% and 73.7 ± 3.3% for RP-NLC, TRT-NLC and ADP-NLC, respectively. The melting temperatures of optimized delivery systems were all above 40 ºC, proving suitability for their use in topical administration. In vitro drug release studies demonstrated a well-controlled release of RP and TRT after 48h, considerably reducing their side effects.

5.1. Introduction

Recently, intense investigation has been dedicated to the topical administration of retinoids which was driven by its high potential in the treatment of many skin disorders (Fu et al., 2007). Retinoids are metabolically involved in such events as cellular division, differentiation, and keratinization of skin, which promotes numerous and well-established advantages in their topical delivery and consequently, in their use on the development of dermatological and cosmetic products (Morales et al., 2015). The improvement of wound healing, the increase on skin elasticity and moisture, and the prevention of photo-aging and fine wrinkles are some of the advantages attributed to retinoids (Lin et al., 2013, Thomas et al., 2013). Moreover, these active compounds present antimicrobial activity against the bacteria that typically causes acne (Raza et al., 2013c, Suggs et al., 2014). Chemically, they are lipophilic drugs structurally resultant from vitamin A (**Figure 5.1**) (Clares et al., 2014, Sekula-Gibbs et al.). As examples of vitamin A derivatives are retinyl palmitate (RP), tretinoin (TRT) and adapalene (ADP).

RP is the ester of vitamin A, it presents an important role in cellular differentiation and carcinogenesis prevention and is vastly used in cosmetics, namely in anti-aging formulations (Fu et al., 2007, Teixeira et al., 2010). TRT or all-trans retinoic acid, is a first generation retinoid and is widely used in the treatment of acne, photo-aged skin, psoriasis, skin cancer, cutaneous lupus erythematous

and other skin disorders (Rahman et al., 2015, Lin et al., 2013). ADP or 6-[3-(1-adamantyl)-4-methoxy-phenyl] naphthalene-2-carboxylic acid, is a third generation synthetic retinoid exhibiting keratolytic, anti-inflammatory, and antiseborrhoic actions (Bhalekar et al., 2015, Guo et al., 2014). However, the side effects of these retinoids are not acceptable and its topical administration has low patient compliance (Rahman et al., 2015). Once applied on skin, retinoids induce irritation resulting in redness, peeling, burning and stinging, aggravates eczema, particularly atopic dermatitis and blistering in treated areas (Clares et al., 2014, Lin et al., 2013, Rahman et al., 2015, Tirado-Sanchez et al., 2013, Guo et al., 2014). Furthermore, their high chemical instability by oxidation in the presence of air oxygen, light and acids, their poor water solubility and percutaneous absorption limits their use in topical formulations (Clares et al., 2014, Eskandar et al., 2009, Morales et al., 2015).
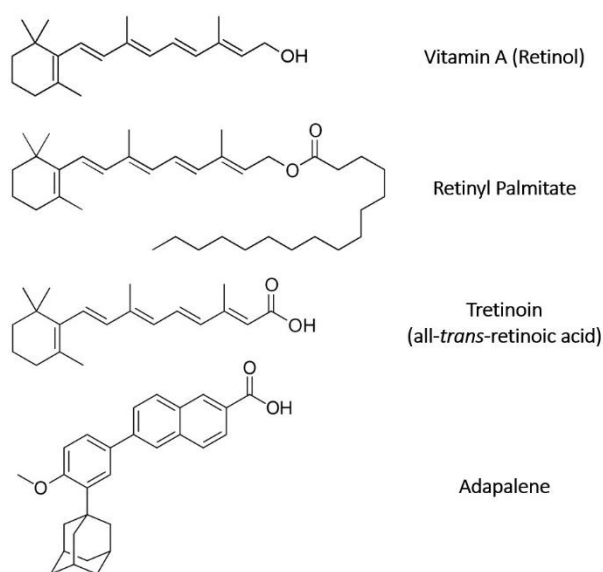
Figure 5.1 - Chemical structure of vitamin A and three examples of its derivatives retinoids that are under scope of this work (the structures were created using an online version of ChemDraw® JS).

Formulation design can play an important role in the optimization of novel carrier systems and overcome such drawbacks of retinoids in topical administration. Currently, research is still being done to develop suitable nanocarriers for the controlled delivery of retinoids, in order to enhance their efficiency and to reduce or even eliminate their secondary effects and physicochemical instability (Kandekar et al., 2018, Wang et al., 2018). Encapsulation of retinoids into lipid nanocarriers, as liposomes, nanoemulsions, ethosomes, proniosomes and nanoparticulate systems as solid lipid nanoparticles (SLNs) and nanostructured lipid carriers (NLCs) has been the aim of several studies in the past few decades (Fu et al., 2007, Morales et al., 2015, Raza et al., 2013c) and have demonstrated several benefits as enhanced photostability, bioavailability, controlled release, drug targeting and reduction of irritant effects (Bhalekar et al., 2015, Clares et al., 2014, Raza et al., 2013a).

The achievement of new bioactive lipid nanocarriers with wide spectrum health benefits and enhanced delivery properties relies in the use of appropriate renewable vegetable (as e.g. sunflower oil), based on their safety and sustainability (Lacatusu et al., 2014). Thus, it is important to apply such lipid raw materials sources with inherent bioactive properties on the design of lipid nanocarriers. NLCs are composed by a mixture of solid and liquid lipids that form solid nanoparticles at room temperature with several imperfections on its lipid matrix. This results in an improved drug loading capacity, and controlled drug release as advantages over SLNs (Müller et al., 2002b, Zheng et al., 2013b).

The present study intends to optimize a new formulation of NLCs using sunflower (SF) oil, which presents multiple skin bioactive properties, with the perspective of its application on the topical administration of RP, TRT and ADP. A central composite design (CCD) statistic approach was used in order obtain an optimized NLCs formulation with desirable attributes using RP as model retinoid. The optimized formulation was adjusted by changing the type of surfactant in order to improve the electrostatic stability of the lipid nanoparticles and was evaluated to incorporate another two retinoids as TRT and ADP. The developed RP-NLC, TRT-NLC and ADP-NLC dispersions were characterized in terms of particle size, morphology, surface charge, entrapment efficiency and drug loading capacity, crystallinity of the lipid matrix and in vitro release profile.

5.2. Material and Methods

5.2.1. Materials

Solid lipids: decanoic acid, C10:0 (≥98%); myristic acid, C14:0 (Sigma Grade, ≥99%) and stearic acid, C18:0 (≥95%) were purchased from Sigma-Aldrich (St. Louis, MO, USA). **Liquid lipid:** Sunflower oil (SF) was food grade product (Fula, Portugal). **Surfactants:** Tween 80, (polyoxyethylene sorbitan monooleate, HLB 15.0) was obtained from PanReacAppliChem (Darmstadt, Germany) and Span 80 (Sorbitan monooleate, HLB 4.7) from Alfa Aesar, ThermoFisher (Karlsruhe, Germany). The aqueous phase of miniemulsions was prepared with Milli-Q water. **Retinoids:** Tretinoin (TRT), retinoic acid (≥98%, HPLC powder) and Adapalene (ADP) Retinyl pamitate (RP) was cosmetic grade product purchased from MakingCosmetics® (Snoqualmie, Washington, USA); Acetonitrile RS, diclorometane RS and methanol RS were purchased from CARLO ERBA Reagents S.A.S. (Z.I. de Valdonne, France) special for HPLC/NMR 1 and 2,2-diphenyl-1-picrylhydrazyl (DPPH) was obtained from Sigma-Aldrich (St. Louis, MO, USA). All other reagents were of analytical grade.

5.2.2. Production of NLCs loaded with retinoids

All formulations of NLCs loaded with retinoids were prepared by the miniemulsions methodology (Landfester, 2003) using ultrasounds to generate an intensive shearing force. NLC formulations of the

experimental design were produced by mixing the lipid phase consisting in SF oil as the liquid lipid and one of three selected saturated fatty acids (decanoic acid, C10:0, melting point 31.6ºC; myristic acid, C14:0, melting point 54.4ºC and stearic acid, C18:0, melting point 69.3ºC) as solid lipids with RP (which was used as a model lipophilic drug to be encapsulated) and heated to 10ºC above the solid lipid melting point to prevent lipid memory effect (How et al., 2013, Jores et al., 2004) until forming a uniform and clear oil phase.

Thus, the lipid phase of the optimized NLCs was prepared in the same way using SF oil as liquid lipid, myristic acid, C14:0 as solid lipid and one of each selected retinoid (RP, TRT and ADP).

In all experiments, the uniform and clear lipid phase was added to the aqueous phase which consisted in one surfactant (Tween 80 was used to prepare the formulations of the factorial design and Span 80 was used in the optimized formulations) dissolved in Milli-Q water previously heated at the same temperature. Both phases were mixed using magnetic stirring at 300 rpm during 45 min and the pre-miniemulsion was fully homogenized with a probe-type sonicator (Sonopuls - Ultrasonic homogenizer, Bandelin, Germany) for 10 min (pulses of 10s on and 5s off, amplitude 48%). The resultant miniemulsions were left to be slowly cooled and stored at room temperature. Three replicates of each formulation from the 31 experiments generated by the design were prepared. The results were expressed as mean ± SD.

5.2.3. *Experimental design optimization*

A response surface methodology using a 5-factor, 3-level CCD was applied to optimize the formulation parameters of RP-NLCs, requiring a minimum of experiments (Gonzalez-Mira et al., 2011). The major factors affecting the physicochemical properties of the formulation, namely the total lipids concentration (X_1), the solid lipid concentration (X_2), the surfactant concentration (X_2), the RP concentration (X_4) and the number of carbons in the saturated fatty acid chain of the solid lipid (X_5) were selected and studied at three different levels coded as -1, 0 and 1. Particle size (Y_1), zeta potential (ZP) (Y_2) and EE, % (Y_3) were selected as dependent responses variables to be optimized. The dependent and independent variables with the actual values of their high, medium and low levels are given in **Table 5.1**. According to the CCD matrix generated by the software STATISTICA 10 (StatSoft, Inc., 2010, EUA), a total of 31 experiments, including 16 factorial points, 10 axial points and 5 replicated center points for estimation of the pure error sum of squares, were required **(Table 5.2)**. Each experiment was performed in triplicate and randomly to minimize the effects of variability from systematic errors. The nonlinear quadratic model equation generated by the design is as follows, **Equation 5.1**:

$$Y_n = \beta_0 + \sum_{i=1}^{5} \beta_i X_i + \sum_{i=1}^{5} \beta_{ii} X_i^2 + \sum_{i=1}^{4} \sum_{j>1}^{5} \beta_{ij} X_i X_j \qquad (5.1)$$

where Y_n characterizes the measured responses, β_0 is the intercept representing the arithmetic average of all 31 runs; β_i, β_{ii} and β_{ij} represents the linear, quadratic and interaction coefficients estimated from the observed experimental values of each response Y_n; X_i represents the coded levels of the independent variables; X_iX_j and X_i^2 the linear and quadratic interaction terms for one variable, β_{ij} (Mandpe and Pokharkar, 2015).

Table 5.1 - Factors and their coded and actual values on CCD.

Factors	Coded level, actual value		
Independent variables	Low (-1)	Center (0)	High (+1)
X_1 = *Total lipids concentration (% w/v)*	2.5	3.5	4.5
X_2 = *Solid lipid concentration (% w/v)*	40	60	80
X_3 = *Surfactant concentration (% w/v)*	1.5	2.5	3.5
X_4 = *RP concentration (% w/v)*	0.5	1.0	1.5
X_5 = *Number of carbons in the fatty acid chain length of the solid lipid*	10	14	18
Dependent variables	**Goals**		
Y_1 = *Particle size (nm)*	Minimize		
Y_2 = *Zeta potential (mV)*	Minimize		
Y_3 = *EE (%)*	Maximize		

*Mid-range value of PdI. It is the range over which the distribution algorithms best operate over (Shaw, 2013).

5.2.4. Physicochemical characterization of NLCs loaded with retinoids

5.2.4.1. Particle size, PdI and surface charge analysis

The hydrodynamic mean particle size (z-Average) and particle size distribution expressed as the PdI were determined by dynamic light scattering (DLS), using a Malvern Zetasizer Nano ZS (Malvern Instruments, UK). PdI is calculated from a cumulants analysis of the DLS-measured intensity autocorrelation function (Luykx et al., 2008). All measurements were performed at 25°C and using a 170º scattering angle. The processing was run by the software of the equipment and the particle size data were evaluated using intensity distribution. Each measurement was performed in triplicate and the data was given as average of three individual measurements. The reported values are the mean ± standard deviation (SD) of at least three different batches of each NLC formulation. The ZP reflects the electric charge on the particle surface and indicates the physical stability of colloidal systems. ZP was determined by measuring the electrophoretic mobility of the nanoparticles in an electric field, using the Helmholtz–Smoluchowsky equation in a Malvern Zetasizer Nano ZS equipment. Before

measurements the samples were diluted with Milli-Q water (1:10, v/v) and placed at a folded capillary cell (DTS1060) where an alternating voltage of ±150 mV was applied. Likewise, all measurements were performed at 25ºC, in triplicate and the mean ± SD value was reported.

5.2.4.2. Determination of entrapment efficiency (EE) and drug-loading capacity (DL)

The EE, % and DL, % of NLCs loaded with RP, TRT and ADP were calculated by measuring the concentration of each retinoid in the dispersion medium of the nanoparticles using a reverse-phase high-performance liquid chromatography (RP-HPLC) method. The non-encapsulated active substances were separated by an extraction procedure adapted from (Yakushina and Taranova, 1995) as it follows: 2.0 mL of each NLC dispersions was transferred into a 10 mL centrifuge tube and 2.0 ml of n-hexane (1:1, v/v) was added for the separation of RP and TRT, or 2.0 ml of chloroform (1:1, v/v) for the separation of ADP. Then, the tube was sealed with a rubber lid and the mixture was uniformly mixed with gentle magnetic stirring for 15 min 150 rpm. The mixture was then centrifuged at 3000 rpm for 10 min and the supernatant consisting on hexane or chloroform extracts were collected and evaporated under nitrogen to remove the solvent. The residue of each active substance was dissolved on the mobile phase for analysis. The HPLC analytic system was composed by a Lachrom, Merk-Hitachi L-7400 apparatus equipped with a quaternary pump, an auto-sampler unit and UV detector and by a Purospher® RP-18 endcapped column (Merk Millipore, EUA). The operating conditions for the RP-HPLC analysis of RP and TRT were set based on the methodology described by Yakushina and Taranova, (1995) (Yakushina and Taranova, 1995), as follows. An isocratic elution was performed using a mixture of acetonitrile, methanol and dichloromethane (60:20:20) as mobile phase, at a constant flow rate of 1.0 mL/min. The UV detector was set at 325 nm for the detection of RP and at 350 nm for the detection of TRT. The method was linear for RP and TRT standard solutions in concentrations varying from 0.2 to 100 µg/mL. For the analysis of ADP, the operating conditions were set as described by Chen et al. (2015) (Chen et al., 2015). A mixture of acetonitrile, tetrahydrofuran (THF) and water containing 0.1% acetic acid (25:50:25) was used as mobile phase in an isocratic elution with a constant flow rate of 0.8 mL/min, with the UV detector set at 270 nm. The method was linear for ADP standard solutions in concentrations ranging from 0.2 to 48 µg/mL. All standards and samples were filtered using a PTFE membrane 0.22µm (Merk Millipore, EUA) prior to injection and an injection volume of 10 µL was used in both methods. The EE, % and DL, % were calculated using **Equation 3.1** (presented in chapter 3, section 3.2.3.2.) and **Equation 4.1** (presented in chapter 4, section 4.2.3.2.), respectively. The reported results are the mean ± SD of at least three different batches of each NLC formulation.

5.2.4.3. Morphologic and structural analysis

The morphology and matrix structure of optimized formulations of NLCs loaded with RP, TRT and ADP were observed by transmission electron microscopy (TEM). Imaging was performed on a TEM equipment (Hitachi H-8100 II, Tokyo, Japan) with thermionic emission (LaB6) and 200kV acceleration voltage, resolution of 2.7 Å point to point, equipped with an energy dispersive spectroscopy (EDS) light elements detector. The sample was prepared by placing a drop of the dispersion into a copper grid with 200-mesh coated with carbon membranes and dried at air for 5 min. The grids were then observed with a high resolution MegaView II (Olympus Soft Imaging Solutions, Japan) and high side-mounted TEM CCD bottom-mounted camera system.

5.2.4.4. Assessment of the lipid matrix crystallinity

Differential scanning calorimetry (DSC) analysis was performed to investigate the degree of crystallinity of the optimized lipid nanoparticles loaded with RP, TRT and ADP. The thermograms were recorded using a DSC 200 F3 Maia (Netzsch, Germany). Approximately 5-6 mg of pure excipients and drugs or equivalent dried NLCs were weighted into standard aluminum pans and hermetically sealed. An empty pan was used as a reference. Each sample was submitted to a heating cycle from 20 to 110ºC, at the rate of 5ºC/min. A nitrogen purge was used to provide an inert gas atmosphere within the DCS cell at a flow rate of 60 ml/min. The melting points (Mp), and enthalpies (ΔH) were evaluated using the software Proteus Analysis (Netzsch, Germany).The determination of the crystallinity index (*CI*,%) was calculated from the enthalpy of fusion using **Equation 4.2** (presented in chapter 4, section 4.2.3.3.).

5.2.4.5. In vitro drug release

In vitro release studies were performed to evaluate the efficacy of optimized NLCs loaded with RP, TRT and ADP as delivery systems. The studies were conducted for 48 h, using a dialysis regenerated cellulose membrane (OrDial D14-MWCO 12,000-14,000flat width 25 mm, Orange Scientific, Belgium). Each membrane bag containing 5 mL of NLC suspension were immersed on 50 mL of receptor medium which was a mixture of citrate buffer (pH 4.0) and THF (4:1 v/v) containing 2 wt% SDS (Guo et al., 2014), and was maintained at 37 Cº with magnetic stirring at 300 rpm in a closed container to prevent evaporation (Zheng et al., 2013a). The receptor medium was collected in 1mL aliquots at pre-determined time points and replaced with the same volume of fresh medium. Samples were stored at 4 Cº prior to be analyzed. The released RP, TRT and ADP were quantified by HPLC using the conditions described in section 2.4.2. Also, the diffusion profile of control solutions of each tested active substance (0.5 mg/mL in receptor fluid) was observed, using the same dialysis process as for NLC dispersions. The reported values are the mean ± SD of two different batches of each NLC formulations and control solutions.

5.3. Results and Discussion

5.3.1. Design and optimization of RP-NLCs by CCD

From previous studies (Pinto et al., 2018), the independent variables that most affected the preparation and stabilization of NLCs were determined and the three upper, middle and lower concentration levels of the formulation components were selected. The critical independent variables were the total concentration of lipids (solid and liquid lipids), concentration of solid lipid, surfactant, drug loaded, and the number of carbons in the saturated fatty acid chain of the solid lipid.
The formulation variables were studied as function of particle size, ZP and the percent drug entrapment. The 5-factor, 3-level CCD generated 31 different formulations, for which the observed responses are summarized in **Table 5.2**.

5.3.1.1. Effect of independent variables on particle size

The value of the dependent variable, particle size (Y_1) was found to be between 112.3 ± 1.2nm and 2107.5 ± 19.0nm **(Table 5.2)**. Quadratic polynomial equations representing the linear and quadratic interactions for each response were generated, based on the obtained experimental data, and the significance of each regression coefficient was statistically evaluated by analysis of variance (ANOVA). The quantitative effects of the independent variables and their linear and quadratic interactions on particles size are represented on **Equation 5.2**:

$$
\begin{aligned}
Particle\ size, \boldsymbol{Y_1} = {} & 278{,}9 - 70.2X_1 + 112.8X_2 + 136.0X_3 - 81.61X_4 + 184.2X_5 - 99.3X_1X_2 \\
& - 101.1X_1X_3 - 127.3X_1X_4 - 103.4X_1X_5 + 129.6X_2X_3 - 98.1X_2X_4 \\
& + 122.9X_2X_5 - 116.0X_3X_4 + 127.4X_3X_5 - 94.8X_4
\end{aligned}
\tag{5.2}
$$

This equation is an adjusted model for which only the coefficients related to the independent variables with significant *p*-values ($p ≤ 0.05$) were used. A independent variable showing a lower *p*-value has a higher significant effect on the response. For this response (Y_1) the obtained regression equation is statistically significant ($R^2 = 0.97686$) and revealed that all five selected independent variables significantly influence the particle size. The first argument of the equation (278.9) refers to the mean of particle size that was obtained from the 31 experiments that were produced by the design and each respective replicates. The positive values before a factor in the above equation have a synergistic effect on the response, which indicates that these factors favors the final response, and on contrary, the negative values acts in an antagonistic way which infers an inverse relation of the independent variable to the final response (Aslam et al., 2016, Mandpe and Pokharkar, 2015).

Table 5.2 - CCD generated by STATISTICA 10 software with measured responses for the critical independent variables.

Formulation	Coded independent variables					Actual independent variables					Measured responses		
	X1	X2	X3	X4	X5	Lt	Ls	S	RP	Cn	Y1	Y3	Y4
F1	-1	-1	-1	-1	1	2.5	40	1.5	0.5	18	284.2 ± 2.5	-21.4 ± 0.7	97.4 ± 0.3
F2	-1	-1	-1	1	-1	2.5	40	1.5	1.5	10	192.6 ± 3.0	-22.2 ± 0.6	92.6 ± 1.2
F3	-1	-1	1	-1	-1	2.5	40	3.5	0.5	10	204.3 ± 3.6	-16.1 ± 0.5	96.3 ± 0.4
F4	-1	-1	1	1	1	2.5	40	3.5	1.5	18	334.4 ± 2.9	-15.1 ± 1.1	93.7 ± 1.0
F5	-1	1	-1	-1	-1	2.5	80	1.5	0.5	10	112.3 ± 1.2	-24.2 ± 1.8	93.1 ± 0.3
F6	-1	1	-1	1	1	2.5	80	1.5	1.5	18	296.3 ± 2.9	-18.1 ± 0.3	95.7 ± 0.9
F7	-1	1	1	-1	1	2.5	80	3.5	0.5	18	2107.5 ± 19.0	-15.1 ± 0.7	94.7 ± 0.5
F8	-1	1	1	1	-1	2.5	80	3.5	1.5	10	158.1 ± 3.8	-18.1 ± 0.4	97.5 ± 0.6
F9	1	-1	-1	-1	-1	4.5	40	1.5	0.5	10	188.9 ± 5.1	-23.2 ± 1.2	95.7 ± 1.3
F10	1	-1	-1	1	1	4.5	40	1.5	1.5	18	369.4 ± 5.5	-12.1 ± 1.6	98.1 ± 0.3
F11	1	-1	1	-1	1	4.5	40	3.5	0.5	18	356.1 ± 2.6	-14.1 ± 0.2	76.7 ± 3.1
F12	1	-1	1	1	-1	4.5	40	3.5	1.5	10	213.7 ± 2.7	-16.1 ± 0.3	81.9 ± 3.2
F13	1	1	-1	-1	1	4.5	80	1.5	0.5	18	253.2 ± 3.5	-20.2 ± 0.9	64.5 ± 1.1
F14	1	1	-1	1	-1	4.5	80	1.5	1.5	10	200.3 ± 3.4	-21.2 ± 0.4	94.2 ± 0.3
F15	1	1	1	-1	-1	4.5	80	3.5	0.5	10	209.2 ± 1.4	-17.1 ± 0.7	79.5 ± 1.5
F16	1	1	1	1	1	4.5	80	3.5	1.5	18	534.4 ± 8.7	-14.1 ± 0.6	20.7 ± 3.7
F17	-1	0	0	0	0	2.5	60	2.5	1,0	14	170.8 ± 5.4	-20.2 ± 0.8	98.5 ± 0.3
F18	1	0	0	0	0	4.5	60	2.5	1,0	14	272.0 ± 9.4	-16.1 ± 1.3	78.7 ± 0.3
F19	0	-1	0	0	0	3.5	40	2.5	1,0	14	160.1 ± 1.4	-17.1 ± 0.7	96.6 ± 0.6
F20	0	1	0	0	0	3.5	80	2.5	1,0	14	463.5 ± 5.0	-18.1 ± 0.7	95.2 ± 1.3
F21	0	0	-1	0	0	3.5	60	1.5	1,0	14	180.0 ± 6.8	-21.2 ± 0.6	89.0 ± 2.8
F22	0	0	1	0	0	3.5	60	3.5	1,0	14	408.0 ± 1.7	-15.1 ± 1.1	89.6 ± 2.3
F23	0	0	0	-1	0	3.5	60	2.5	0.5	14	271.0 ± 3.8	-20.2 ± 0.4	96.0 ± 0.9
F24	0	0	0	1	0	3.5	60	2.5	1.5	14	217.5 ± 2.3	-18.1 ± 0.5	99.3 ± 0.3
F25	0	0	0	0	-1	3.5	60	2.5	1,0	10	166.9 ± 9.2	-18.1 ± 0.6	94.4 ± 0.1
F26	0	0	0	0	1	3.5	60	2.5	1,0	18	427.4 ± 7.6	-11.1 ± 0.5	98.2 ± 0.1
F27 (C)	0	0	0	0	0	3.5	60	2.5	1,0	14	292.2 ± 6.7	-19.1 ± 0.8	98.5 ± 0.2
F28 (C)	0	0	0	0	0	3.5	60	2.5	1,0	14	209.1 ± 8.6	-15.1 ± 0.6	88.8 ± 1.2
F29 (C)	0	0	0	0	0	3.5	60	2.5	1,0	14	266.8 ± 8.0	-16.1 ± 0.3	86.0 ± 1.1
F30 (C)	0	0	0	0	0	3.5	60	2.5	1,0	14	251.1 ± 8.5	-15.1 ± 0.2	97.8 ± 1.5
F31 (C)	0	0	0	0	0	3.5	60	2.5	1,0	14	268.1 ± 8.7	-18.1 ± 0.5	91.2 ± 5.6

The statistical significance of the factors and their interactions was also explored using a Pareto chart **(Figure 5.2)**, as a complement to this analysis, with which is possible to measure quantitatively and qualitatively the contributions of each factor on the studied responses.

Figure 5.2 - Pareto chart showing the estimate standardized effect of independent variables and their interactions on particle size (Y_1).

The length of each bar in the chart corresponds to the standardized effect of the independent variables and their interactions on the response. The last bars remaining inside the reference line, which correspond to $p \leq 0.05$, represent the least contributing factors that are not significant to the final response. The analysis of particle size demonstrate that the number of carbons on the fatty acid chain of the solid lipid (X_5) and the surfactant concentration (X_3) are the factors that most affects this result **(Figure 5.2)**. Also, the particle size appears to be positively influenced by the solid lipid and surfactant concentrations as by the type of solid lipid (β_2 = +112.8, p = 0.00036; β_3 = +136.0, p = 0.00008 and β_5 = +184.2, p = 0.000006 respectively), which means that an increase in the surfactant and total lipids concentrations leads to an increase on the particle size. There is an optimum level of surfactant concentration which results in a reduction of the surface tension between the lipid and aqueous phases, leading to particles separation with lower sizes and consequently, to an increase on the surface area (Mandpe and Pokharkar, 2015, Thakkar et al., 2014). However, when this optimum level of surfactant concentration is overcome there is saturation, which could be attributed to the accumulation of excess surfactant molecules on the NLCs surface, preventing the particle size to decrease further (Bellissent-Funel, 1999, Dora et al., 2010). On the contrary, the particle size is negatively influenced by the concentrations of total lipids and RP (β_1 = -70.2, p = 0.0083 and β_4 = -81.61, p = 0.0034).

The mathematical relation between the factors and their interaction on particle size is further elucidated by response surface plots **(Figure 5.3)** which present the effects of factor interactions with major influence on particle size. The effect of X_2 (solid lipid concentration) and X_3 (surfactant

concentration) and their interaction, X_2X_3 when X_1, X_4 and X_5 are kept constant is shown on **Figure 5.3, A**.

Figure 5.3 - 3D-Response surface plots showing the effects of the independent variables with major influence on particle size (Y_1) of RP-NLCs.

A – Solid lipid concentration (X_2) and surfactant concentration (X_3),

B – Surfactant concentration (X_3) and number of carbons in the fatty acid chain length of the solid lipid (X_5),

C – Total lipids concentration (X_1) and RP concentration (X_4).

By simultaneously increasing the concentrations of solid lipid and surfactant an increase on particle size was observed which is justified by the positive values of β_{23} = +129.6, p = 0.0002. Increasing the solid lipid content will increase the viscosity on the NLCs matrix and increase the surface tension, thus forming larger particles. Besides the steric stabilization resulting from the surfactant is less effective (Gonzalez-Mira et al., 2011, Han et al., 2008, Jia et al., 2010). **Figures 5.3, B and C** show the effect of X_3 (surfactant concentration) and X_5 (number of carbons in the fatty acid chain length) and their interaction X_3X_5, and the effect of X_1 (Total lipids concentration) and X_4 (RP concentration) and their interaction X_1X_4, respectively. There is a positive effect of X_3X_5 on the particles size (β_{35} = +127.4, p = 0.0002) (**Figure 5.3, B**). This means that increasing the hydrophobicity

of the solid lipid and the surfactant concentration leads to an increase on particle size. In this case, the effect of higher viscosity in the lipid nanoparticles matrix is also evident as was presented above which will potentiate the increase on particle size. On the contrary, the concentrations of total lipids (X_1) and RP (X_4) on the NLCs formulation and their interaction demonstrated to have a negative effect on the particle size ($\beta_1 = -70.2$, $p = 0.0083$; $\beta_4 = -81.6$, $p = 0.0034$; $\beta_{14} = -127.3$, $p = 0.0002$) (**Figure 5.3, C**). The increase of total lipids and RP concentrations lead to smaller particles formation.

5.3.1.2. Effect of independent variables on zeta potential

The values of response Y_2 (ZP) ranged between -11.1 ± 0.5 mV and -24.3 ± 1.8 mV **(Table 5.2)**. The lowest value was obtained in formulation F5 with lowest levels (-1) of the independent variables except for the solid lipid concentration which was in the highest level ($+1$) **(Table 5.1)**. **Equation 5.3** represents the linear and quadratic interactions of response Y_2.

$$ZP, \boldsymbol{Y_2} = -17.5 + 2.2X_3 + 1.9X_5 - 1.0X_3X_4 + 2.8X_5^2 \tag{5.3}$$

The regression coefficient from the equation ($R^2 = 0.90836$) indicated a good fit and the average ZP value obtained from the 31 experiments was -17.5. The significant terms of this model were X_3 and X_5 and both present a positive relation with the response ($\beta_3 = +2.2$, $p = 0.00014$ and $\beta_5 = +1.9$, $p = 0.00042$, respectively). This can be illustrated in the Pareto chart obtained for ZP (**Figure 5.4, A**). The surfactant concentration (X_3) and number of carbons of fatty acids (X_5) were again, as for particle size, the independent variables that demonstrated to have most influence on ZP. As the surfactant concentration increases, the ZP also increase for less negative values once this factor has a positive effect on the response. The number of carbons in the fatty acid chain length of the solid lipid demonstrate a positive effect on ZP, meaning that when increasing the hydrophobicity of the solid lipid molecules, the ZP increases for less negative values. Both effects could be attributed to the accumulation of surfactant molecules on the NLCs surface probably due to hydrophobic interactions in which nonpolar groups of the molecules of surfactant and solid lipid could interact with each other (Bellissent-Funel, 1999, Thakkar et al., 2014). Despite RP concentration (X_4) present no significant effect on ZP, its interaction with the surfactant concentration (X_3X_4) demonstrated a negative effect on this response (**Figure 5.4, B**).
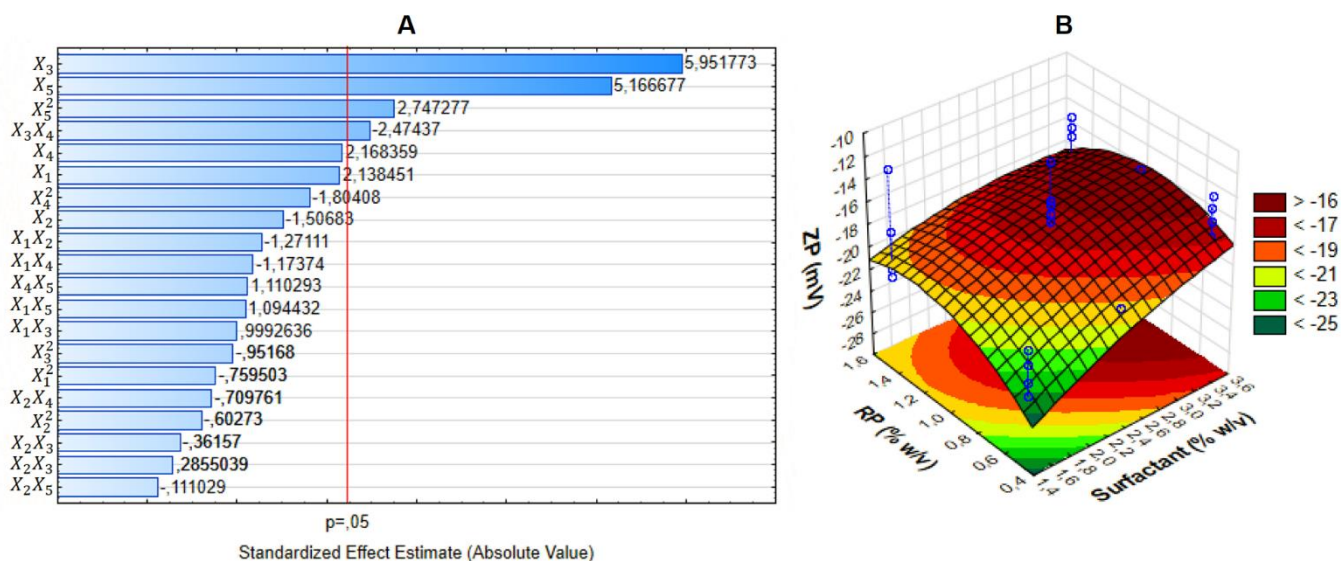
Figure 5.4 - On the left: (A) Pareto chart showing the estimate standardized effect of independent variables and their interactions on zeta potential (Y$_2$). On the right: (B) 3D-Response surface plot showing the effects of surfactant concentration (X$_3$) and RP concentration (X$_4$) on zeta potential (Y$_2$) of RP-NLCs.

ZP is an important variable that permits to predict the physical stability of dispersions. Theoretically, higher values of ZP ($\geq$|30|) tend to stabilize the NLCs dispersion and aggregation phenomena are less probable to occur due to electrostatic repulsions between particles with the same electrical charge (Gonzalez-Mira et al., 2010, Pinto et al., 2014). In this study, all formulations presented ZP values above –24.3 mV which indicates that this parameter needs to be further improved, for instance, by changing the type of used surfactant.

5.3.1.3. Effect of independent variables on entrapment efficiency

For response, Y_3 (%EE) the obtained values in the 31 generated experiments ranged between 20.7 ± 3.7% and 99.3 ± 0.3% (**Table 5.2**). Linear and quadratic interactions of Y_3 (%EE) are represented by **Equation 5.4**, which demonstrates that the influence of selected independent variables is statistically relevant with a regression coefficient of $R^2 = 0.94494$ indicating a good fit and the mean value equal to 94.2%.

$$\%EE, \boldsymbol{Y_3} = 94.2 - 9.4X_1 - 5.2X_2 - 5.0X_3 - 4.8X_5 - 5.9X_1X_2 - 6.0X_1X_3 - 5.8X_1X_5$$
$$- 5.5X_2X_5 - 5.2X_3X_4 \tag{5.4}$$

The regression equation of response, Y_3 shows a negative relation with four independent variables (X_1, X_2 X_3 and X_5), that are significant for the response. In this case, the total lipids concentration (X_1), and the solid lipid concentration (X_2), were the factors that most influenced the response ($\beta_1 = -9.4$, $p = 0.00007$ and $\beta_2 = -5.2$, $p = 0.0046$, respectively). This can also be evaluated by the analysis of Pareto chart (**Figure 5.5**) corresponding to Y_3. Moreover, it was demonstrated that X_1X_3, X_1X_2 and X_1X_5 are the interactions that present an evident effect on the response ($\beta_{13} = -6.0$, $p = 0.0027$, $\beta_{12} = -5.9$, $p = 0.0031$ and, $\beta_{15} = -5.8$, $p = 0.0034$, respectively), in the negative sense and that still, the concentration of total lipids (X_1) is the key factor on %EE results.
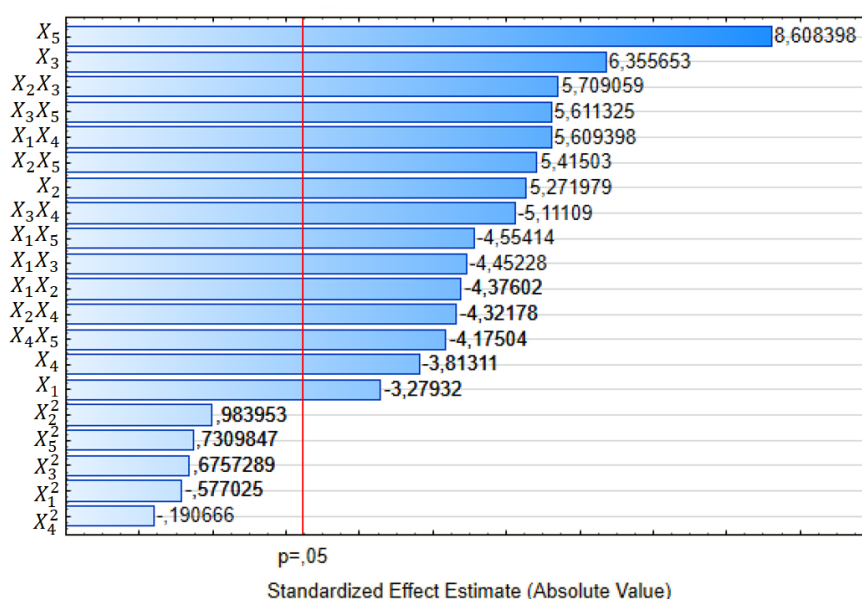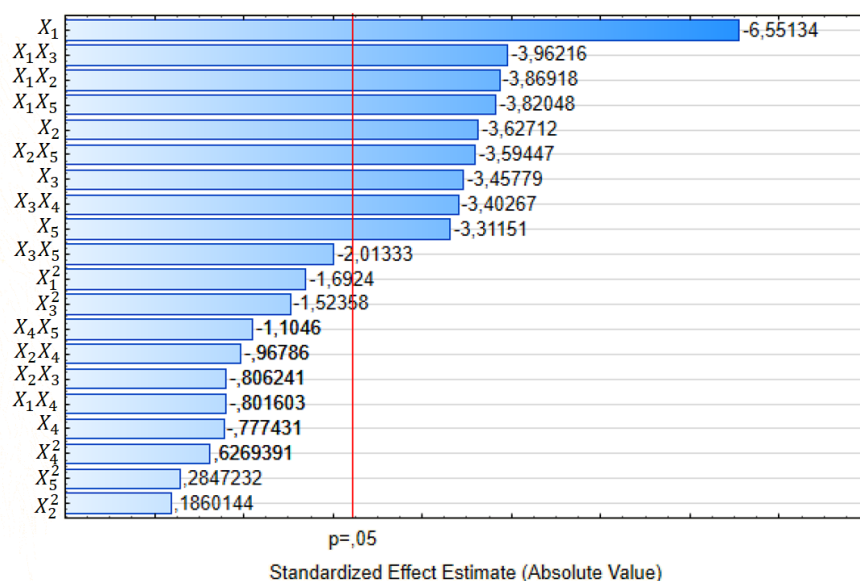

Figure 5.5 - Pareto chart showing the estimate standardized effect of independent variables and their interactions on entrapment efficiency (Y3).

The mathematical relation between these three factors is illustrated by the correspondent response surface plots as shown in **Figure 5.6 – A, B and C**, respectively. Increasing simultaneously the concentrations of total lipids and surfactant have a negative impact on %EE, meaning that consequently there is a decrease on %EE values (**Figure 5.6, A**). Although, there are good results (above 78.7 ± 0.3 %) in the medium level (0) for surfactant concentration (2.5%). This can be attributed, as mentioned above in the case of particle size, to an optimum ratio of lipids and surfactant required to stabilize the lipid nanoparticles. Moreover, increasing the surfactant concentration will consequently increase the aqueous phase viscosity and thereby decreasing the diffusion speed of the lipophilic active compounds entrapped in the lipid matrix (Liu et al., 2007a, Mandpe and Pokharkar, 2015).
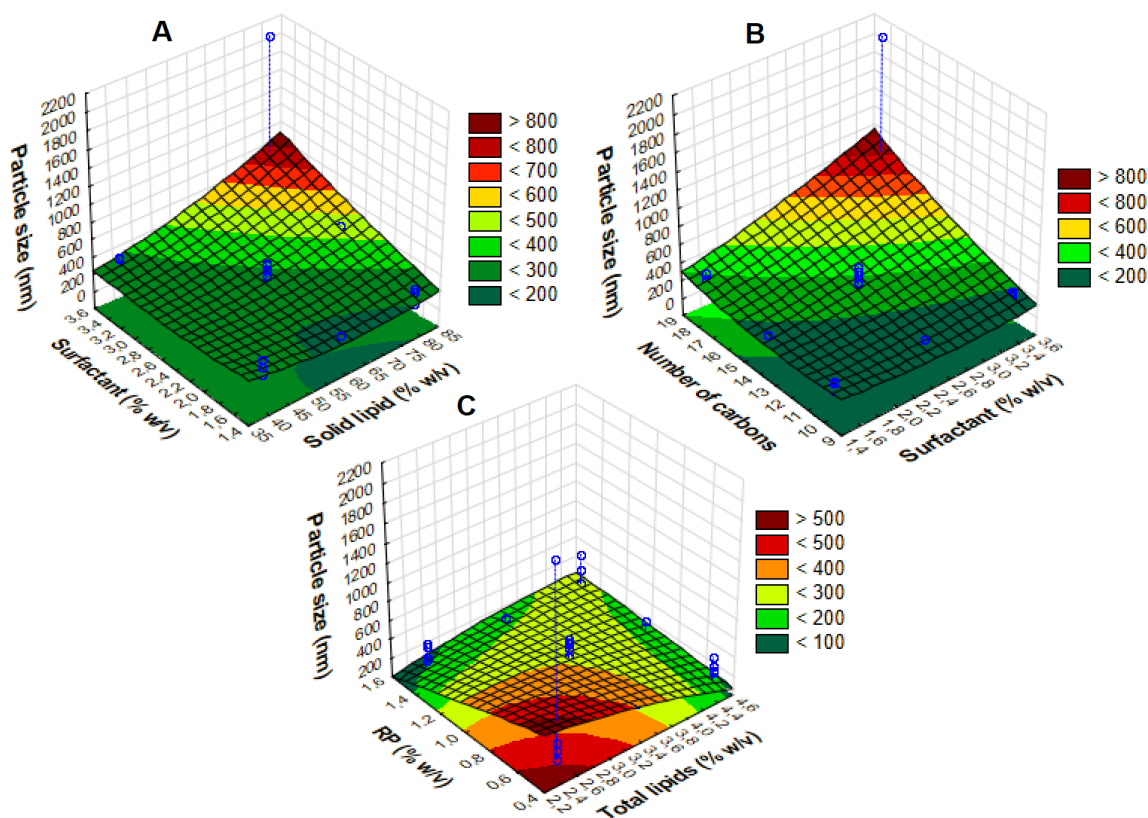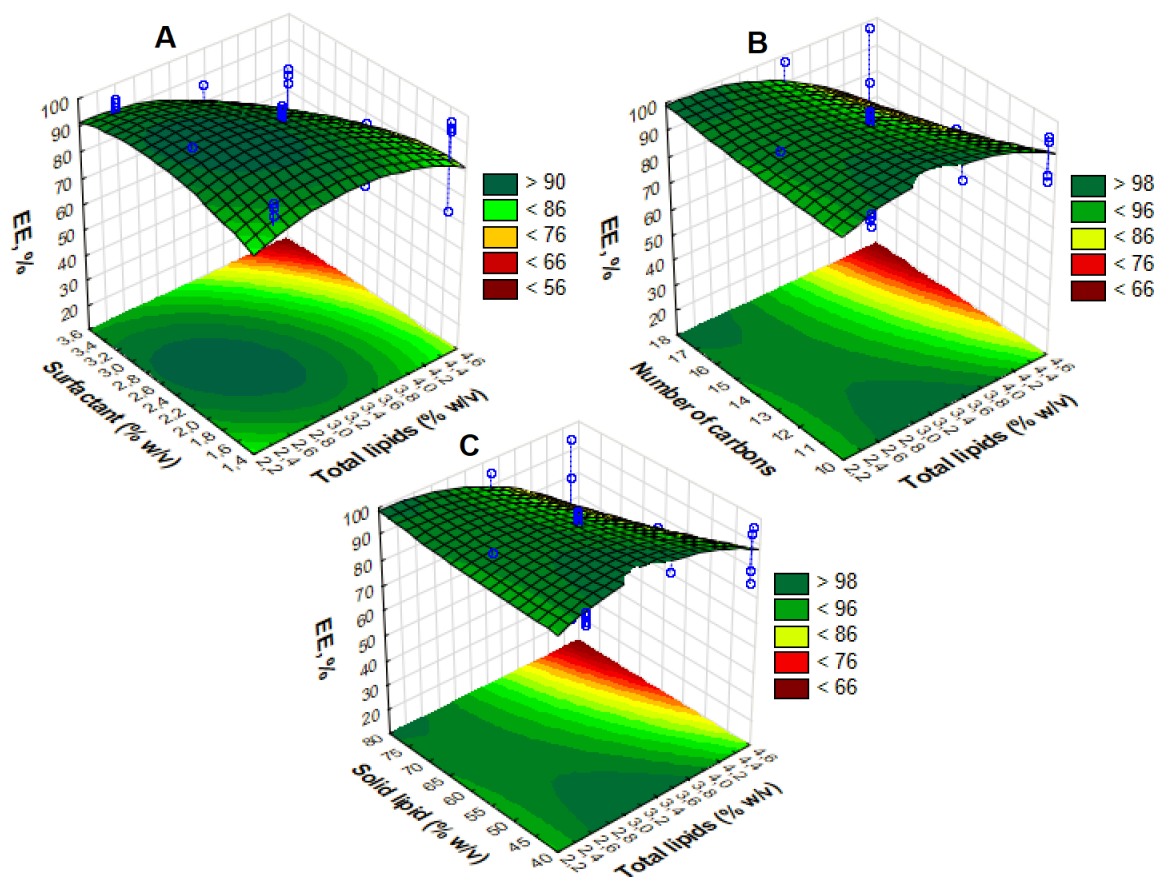
Figure 5.6 - 3D-Response surface plots showing the effects of the independent variables with major influence on encapsulation efficiency (Y3) of RP-NLCs.

A – Total lipids concentration (X_1) and surfactant concentration (X_3),

B – Total lipids concentration (X_1) and number of carbons in the fatty acid chain length of the solid lipid (X_5),

C – Total lipids concentration (X_1) and solid lipid concentration (X_2).

The increase of the total lipids concentration (X_1) simultaneously with the increase of the number of carbons on the fatty acid chain length of the solid lipid (X_5) and with the increase on the solid lipid concentration (X_2) also demonstrated to have a negative effect on the EE, % (**Figure 5.6, B and C**). Meaning that the formulations with higher levels (+1) (**Table 5.2**) of these factors revealed lower EE, % values. This can be related with two important aspects. The first aspect concerns the number of imperfections that can be formed in the lipid matrix. Decreasing the solid lipid concentration results in great imperfections on the crystal lattice of the lipid matrix, leaving enough space to accommodate a larger amount of drug resulting in an increase of %EE (Jenning and Gohla, 2001, Morales et al., 2015). The second aspect is associated with the solubility of the drug on the lipid matrix. Increasing the lipids concentration leads to the availability of a greater volume for solubilize the encapsulated drug (Reddy

131

et al., 2006) and increasing the amount of liquid lipids also improve the solubility of the drug and consequently the %EE (Mandpe and Pokharkar, 2015).

5.3.1.4. Optimized RP-NLCs formulation

An optimized RP-NLC formulation was obtained based on the results of CCD. Selected criteria were to minimize the particle size, adjust the surface electric charge of the particles to more negative values and maximize the entrapment efficiency. These criteria were applied to determine the profiles for predicted values and desirability using the response desirability profile tool of software STATISTICA 10® (**Figure 5.7**).
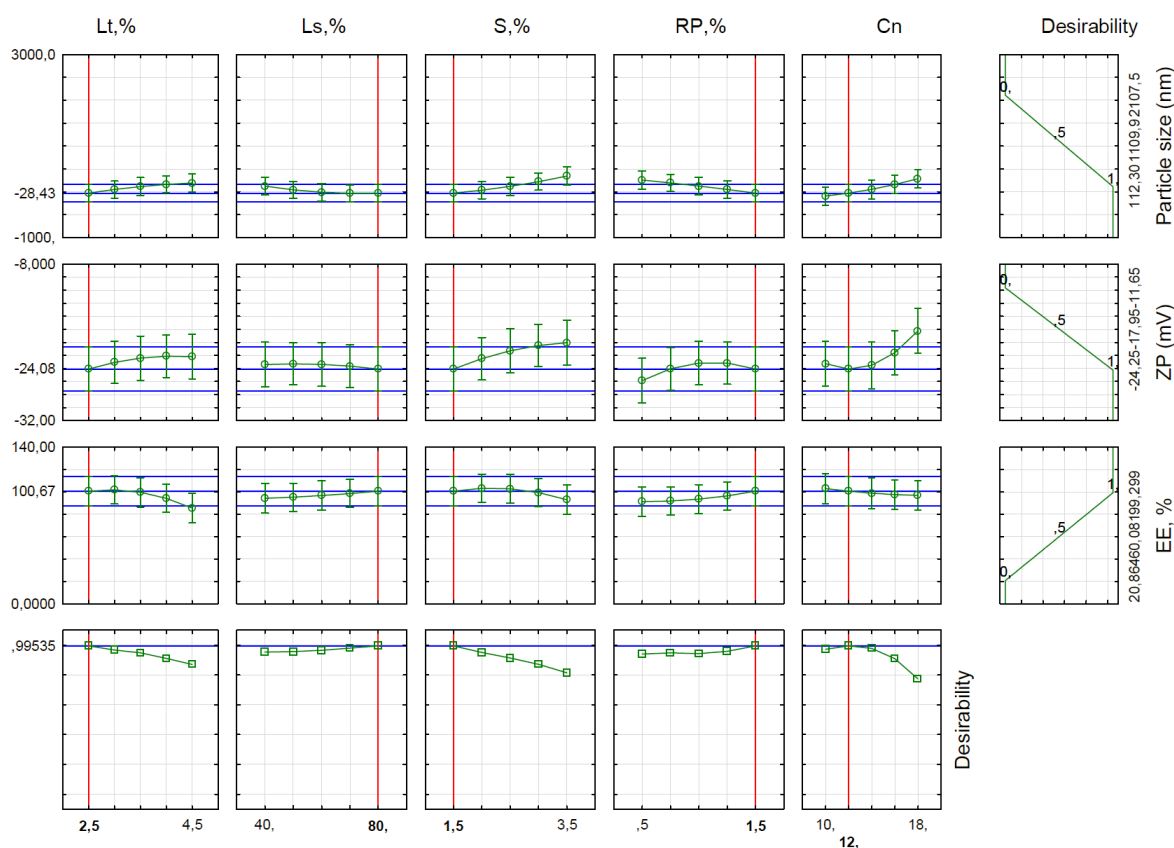
Figure 5.7 - Profiles of predicted values of independent variables for correspondent desirability of responses (particle size (Y_1), ZP (Y_2) and EE, % (Y_1)).

The optimum values of the independent variables in study were predicted according to the established desirability selected to each response (Y_1, Y_2 and Y_3). Maximum, minimum and medium values of each dependent variable in study were determined (**Table 5.1**) and desirability levels were attributed to each one ranging from 0.0 for undesirable results to 1.0 for very desirable results (**Figure 5.7**). **Table 5.3** summarizes the composition of the optimized RP-NLC formulation with the values reached for each independent variable in study.

Table 5.3 - Composition of the optimized RP-NLC formulation.

	Composition (%)					
Formulation	Total lipids	Lauric acid (C12:0)	Sunflower oil	Tween 80	RP	Water
Optimized RP-NLC	2.5	2.0	0.5	1.5	1.5	94.5

5.3.2. Characterization of optimized NLCs formulation loaded with retinoids

The CCD approach was applied in determining an optimized formulation of NLCs loaded with RP which served as a model retinoid. Although, two adjustments in the optimized NLCs composition were performed. According to response desirability profile (**Figure 5.7**) the optimum number of carbons in the fatty acid chain of the solid lipid is 12, which corresponds to lauric acid (C12:0). However, DSC analysis of RP-NLC formulations with this solid lipid revealed a melting point below the body temperature (37°C), which is not suitable for topical administrations (Morales et al., 2015). The melting point of lipid nanoparticles increases with the length of the fatty acid chain, and decreases with the degree of unsaturation (Souto and Muller, 2010). For this reason, myristic acid (C14:0) was chosen as solid lipid.

According to the experimental design results, the surface electrical charge of the particles (ZP) ranged between –11.1 ± 0.5 mV and –24.3 ± 1.8 mV which predicts a relatively low stability of the RP-NLC dispersions (Pinto et al., 2014). Thus, a different type of non-ionic surfactant, namely Span 80, was used instead of Tween 80 in order to potentiate more negative values of ZP by stabilizing effectively the lipid matrix by steric hinderance due to its more lipophilic character (HLB = 4.3) (Teeranachaideekul et al., 2007a).

Therefore, the formulation composition with Span 80 (1.5 wt%), total lipids (2.5 wt%) with myristic acid (2.0 wt%) and sunflower oil (0.5 wt%), was selected as the optimized NLC formulation to be further characterized.

In order to evaluate the potential of the optimized formulation to incorporate other retinoids, TRT and ADP were incorporated separately in a lower concentration (0.1 wt%), as RP and the resultant lipid nanoparticles (RP-NLC, TRT-NLC and ADP-NLC) were characterized. The incorporation of 0.1 wt% of TRT and ADP was tested based on the reported concentration of commercially available topical gels and creams containing these retinoids used in the treatment of moderate acne (Guo et al., 2014, PDR, 2000).

5.3.2.1. Particle size analysis and physical stability

The average particle size of the optimized RP-NLC, ADP-NLC and TRT-NLC dispersions were 162.0 ± 1.0 nm, 148.7 ± 6.6 nm, and 134.5 ± 5.4 nm respectively (**Figure 5.8**) with correspondent PdI values of 0.187 ± 0.016, 0.207 ± 0.006 and 0.244 ± 0.019, indicating a uniform particle size distribution. The polydispersity parameter measures the homogeneity of particles and as PdI values were below 0.250 they reflect relatively homogeneous particles, with low tendency of aggregation (Aslam et al., 2016, Mitri et al., 2011).
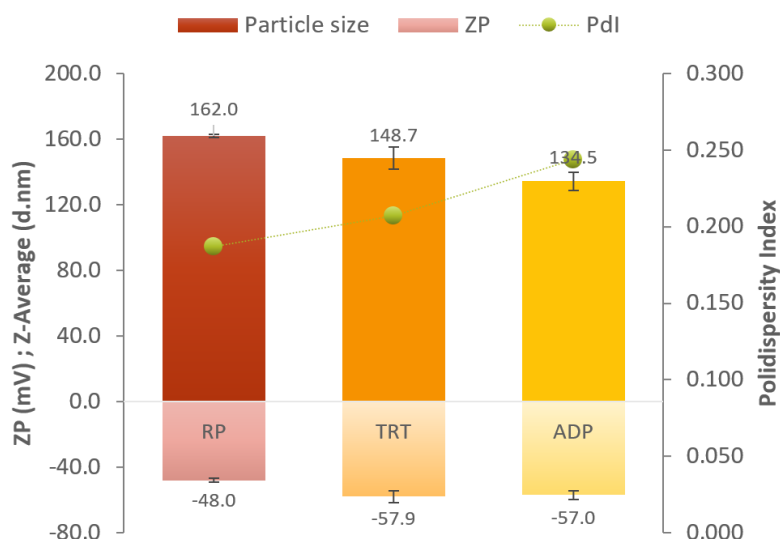
Figure 5.8 - Zeta potential values, Z-average particle sizes and polydispersity index
(PdI) of the optimized NLC loaded with RP, TRT and ADP.

The three NLC formulations showed an appropriate particle size in the nanometer range below 200 nm. According to Kohli and Alpar, 2004 (Kohli and Alpar, 2004) this is an appropriate size for NLCs aiming topical administration, since they demonstrated that particles with sizes between 50 and 500nm and negatively charged were able to permeate the skin. ADP-NLCs showed the lowest particle size (134.5 ± 5.4 nm) from the optimized dispersions formulated with the three tested topical active compounds. Comparing the three NLC dispersions formulated with RP, TRT and ADP it was observed that there is slight differences in particle size (RP-NLC>TRT-NLC>ADP-NLC). This may be attributed to the chemical structure of each retinoid (**Figure 5.1**) which might determine a specific conformational rearrangement in lipid matrix for each encapsulated compound. The formulation of RP-NLCs presented the highest particle size (162.0 ± 1.0 nm) most probably due to the hydrophobic tail of palmitic acid (C16:0) that defines the RP chemical structure.

ZP values of NLCs formulated with each retinoid ranged between –48.0 ± 1.4 mV and –57.9 ± 3.5 mV (**Figure 5.8**).The less negative value corresponds to RP-NLCs and the more negative value corresponds to TRT-NLCs. This indicates a very good colloidal stability for the three systems, as ZP

values ≥ |30| assures particle stability and avoid the formation of aggregates by electrostatic stabilization (Pinto et al., 2014). This results show that an alteration in the type of surfactant, in this case, replacing Tween 80 which is a more hydrophilic surfactant (HLB = 15.0) by Span 80 which has a more lipophilic character (HLB = 4.3) led to significant improvements on the electrostatic and steric stabilization of the lipid nanoparticles.

5.3.2.2. Morphology studies

The morphology of the optimized NLC nanoparticles loaded with RP, ADP and TRT was evaluated by TEM analysis. Micrographs presenting views collected from different regions of dried suspensions of RP-NLCs, ADP-NLCs and TRT-NLCs, with different amplification factors are shown in **Figure 5.9**. All formulations display discrete particles with a well-defined spherical or near-spherical morphology and the preservation of a solid particulate structure in the lipid matrix.

Analyzing in detail the morphology of the lipid matrix of each nanocarrier in study it is possible to observe some imperfections in the crystal lattice of the lipid matrix produced by the blend of liquid lipids with solid lipids, resulting in a considerable disturbance in the crystal order (Morales et al., 2015). These imperfections leads to an enhancement of the drug loading capacity by increasing the space to accommodate drug molecules and helps to improve its leaking which offers some flexibility in the modulation of drug release (Morales et al., 2015). Moreover, these images show that there are some differences in the structure of each lipid matrix indicating that this may be a consequence as mentioned above of a specific conformational rearrangement induced by the chemical structure of each incorporated retinoid. Another important aspect to notice is that the particle size are correspondent to those obtained by DLS analysis which validates both results.
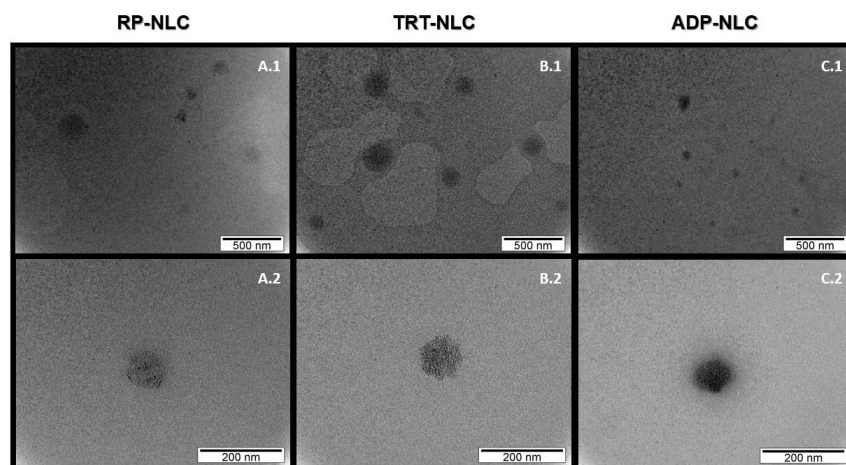
Figure 5.9 – TEM micrographs of optimized NLCs formulated with Span 80 as surfactant, SF oil and myristic acid (C14:0) as liquid and solid lipids and loaded with each retinoid in study, presented in views from different positions and amplification factors. A1-2: Optimized NLCs loaded with RP; B1-2: Optimized NLCs loaded with TRT; C1-2: Optimized NLCs loaded with ADP.

5.3.2.3. Crystallinity studies

DSC analysis was used to evaluate the interactions between lipids and incorporated drug, and the mixing behavior of solid and liquid lipids of the optimized NLC formulations with RP, TRT and ADP. The incorporation of a liquid lipid and drug to the solid lipid leads to modifications in the physical state or crystallinity of the solid lipid, in this case, myristic acid (C14:0). These lipid modifications in the nanocarriers matrix corresponds to determined gains or losses of energy that are measured by DSC as function of temperature (Aslam et al., 2016, Thakkar et al., 2014). DSC thermograms and determined parameters of optimized formulations of RP-NLC, TRT-NLC and ADP-NLC are presented in **Figure 5.10** and **Table 5.4**.

Endothermic peaks at 41.8 ºC, 42.0 ºC and 45.5 ºC were obtained, corresponding to the melting temperatures of TRT-NLC, RP-NLC and ADP-NLC, respectively. The concentration of added liquid lipid was equal in all formulations which indicates that the observed melting point depression in comparison with the pure solid lipid (56.8 ºC) was due to the incorporation of each lipophilic active compound, namely RP, TRT and ADP. However, the obtained blends are solid at body temperature and the melting temperature was higher than 40 ºC which is a prerequisite to develop NLC formulations for topical administration (Gonzalez-Mira et al., 2011). A decrease on the onset, endset and melting temperatures is associated to an increase on the crystal order disturbance, correspondent to the development of more imperfections in the lipid matrix (de Carvalho et al., 2013).
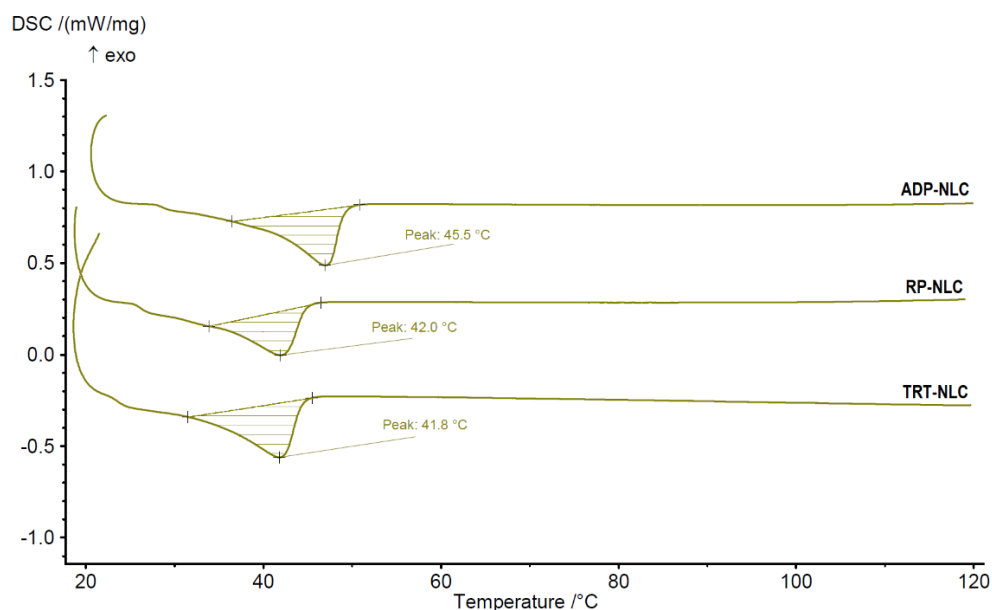
Figure 5.10 – DSC thermograms of optimized NLC formulations prepared with SF as liquid lipid and loaded with RP, TRT and ADP.

In this case, the endothermic peak from TRT-NLC formulation presented the highest decrease meaning that occurred an increase on the crystal order disturbance (**Figure 5.10**). However, when

comparing the obtained melting enthalpies and CI, % (**Table 5.4**), RP-NLC presented the lowest values for both parameters *(ΔH = −18.04 J/g, CI = 11.2 %)* which possibly indicates the fusion of RP with the crystalline lipid matrix, converting it into an amorphous form. RP displays the lowest melting point (Mp (RP) = 28 ºC) when compared with the other two retinoids in study (Mp (TRT) = 181.7 ºC and Mp (ADP) = 324.8 ºC) which justifies these results and indicates the solubilization, or molecular conversion, of these active substances into a less ordered crystalline structure of the lipid matrix during the NLC production process.

Table 5.4 - DSC parameters. Melting point (°C), enthalpy (ΔH, Jg-1) and crystallinity index (CI, %) of the optimized NLC formulations loaded with RP, TRT and ADP.

	Melting point, °C	Entalphy, -J/g	CI, %
RP-NLC	42.0	18.04	11.20
TRT-NLC	41.8	21.45	13.32
ADP-NLC	45.5	32.96	20.47
Myristic acid	56.8	161.0	100.0

5.3.2.4. Evaluation of entrapment efficiency and drug loading capacity

To evaluate the solubilization capacity of the three selected retinoids into the solid and liquid lipids of optimized NLCs prepared with SF oil, the EE, % and the DL, % were determined (**Figure 5.11**). The highest value of EE, % was obtained with RP (84.4 ± 3.0%). Also, high values of EE, % were obtained for TRT and ADP, corresponding to 84.1 ± 7.8% and 73.7 ± 3.3% respectively (**Figure 5.11**). Although, it was noticed that using an optimized total lipids concentration, the capacity of the lipid matrix to accommodate each retinoid is different, based on their lipophilicity (Lacatusu et al., 2014), which explains the small differences in the obtained values of EE,% for RP and TRT. Moreover, these results are in agreement with those obtained with the crystallinity study, which indicated that the lipid matrices of RP-NLC and TRT-NLC presented more imperfections in the lipid core due to their low values of enthalpy and CI, %, thus providing a higher EE, %.
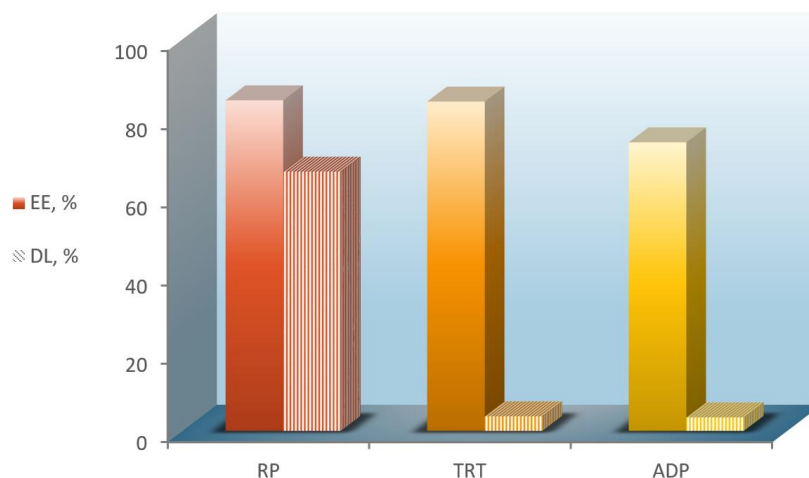
Figure 5.11 – Encapsulation efficiency of RP, TRT and ADP into the optimized NLCs and their correspondent drug loading capacity of the lipid matrix.

The DL, % of the optimized RP-NLC, TRT-NLC and ADP-NLC formulations were 66.2 ± 0.9%, 3.7 ± 1.4% and 3.4 ± 0.4% respectively (**Figure 5.11**). Although, the DL values that can be directly compared are those of TRT-NLCs and ADP-NLCs. For these formulations it was used the same bioactive substance concentration (0.1%) in the same total lipids concentration, corresponding to a theoretical maximum value of 5% DL capacity that could be reached. On the other hand, RP-NLC formulation contained a superior drug concentration (1.5%) for the same total lipid concentration used in the other two formulations (TRT-NLC and ADP-NLC), corresponding to a theoretical maximum value of 75% DL capacity that could be reached. Analyzing the differences between the DL, % and the correspondent theoretical maximum values, it was demonstrated the efficient capacity of the lipid matrices of the optimized formulation to load each type of these three retinoids, since the obtained values are very close of each maximum DL capacity.

5.3.2.5. In vitro release studies

Optimized NLC formulations with 1.5% RP, 0.1 % TRT and 0.1% ADP were subjected to *in vitro* release experiments through an equilibrium dialysis method. The release profiles of each retinoid encapsulated in the optimized NLC formulations were assessed against a control, with the same concentration of drug, correspondent to solutions of each pure retinoid as reference. The release profiles of all 6 batches are shown in **Figure 5.12**.
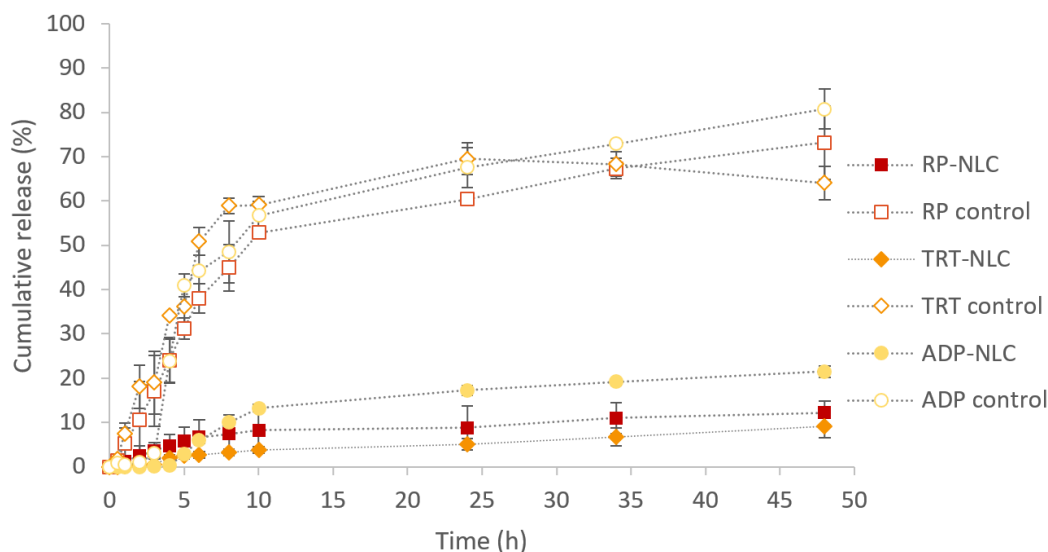
Figure 5.12 – Release profiles of RP, TRT and ADP from the optimized lipid nanocarriers and their correspondent control solutions.

The three retinoids in study, encapsulated in the lipid nanoparticles demonstrated a very slow release pattern in the first hours (up to 5h) of the experiment followed by well-controlled release until 48h. At the initial stage, ADP showed no release after 4h, but after 10h ADP released more quickly than the other two retinoids having reached a final cumulative release of 21.5 ± 1.3% at 48h. RP and TRT showed similar release patterns with a very well-controlled release along the 48h of the experiment reaching a cumulative release of 12.2 ± 2.7% and 9.1 ± 2.5%, respectively. These results may be related with the encapsulation efficiency study, meaning that the highest cumulative release of ADP is associated with its lowest encapsulation value. Moreover, the slow diffusion rates of RP and TRT from the lipid nanocarriers and their EE, % results demonstrate that these two retinoids were practically completely encapsulated inside the lipids core, presenting a better accommodation and preventing the diffusion from the nanocarriers (Lacatusu et al., 2014).

As estimated, the diffusion of the three control solutions of retinoids was much faster and above 60% after 48h (Figure 12). In this case was observed a more rapidly initial release until 10h with cumulative releases of 52.9 ± 1.2%, 59.1 ± 1.9% and 56.7 ± 3.1% for RP, TRT and ADP, respectively. The highest release value was also reached by the ADP control solution (80.7 ± 4.5%) which is about two times superior to the one for ADP encapsulated in the NLC particles. Similar results were obtained with the control solutions of RP and TRT which reached final cumulative release values of 73.1 ± 8.3% and 64.1 ± 3.8%, respectively.

This *in vitro* release study demonstrated that the optimized NLCs present an appropriate lipid matrix structure capable to incorporate RP, TRT and ADP and to assure their slow release, thus minimizing their side effects and conferring chemical stability.

5.4. Conclusions

A new NLC formulation containing sunflower oil and produced by the miniemulsions methodology for the topical administration of retinoids was successfully developed and optimized through the use of a CCD approach.

The polynomial equations and Pareto charts obtained from the CCD reasonably predicted the effects of the factors, or independent variables, and of their interactions that most affected each response, or dependent variables, in study. Therefore, it was found that the particle size and the surface charge of the lipid nanoparticles were mainly affected by the number of carbons on the fatty acid chain of the solid lipid and by the surfactant concentration. Also, the total lipids concentration mainly affected the encapsulation efficiency of RP, which was primarily used as a model drug for encapsulating on NLCs.

The optimal reached composition of 2.5% of total lipids, comprising 2.0% of myristic acid and 0.5% of sunflower oil and 1.5% of surfactant was effectively formulated and characterized with 1.5% of RP and 0.1% of TRT and ADP. The optimized RP-NLC, TRT-NLC and ADP-NLC formulations showed good particle sizes in the nanometer range below 134.5 ± 5.4 nm and high physical stability with zeta potential values above –57.9 ± 3.5mV which were improved by using Span 80 as surfactant. DSC thermograms showed that the melting temperatures of the three optimized NLC formulations loaded with retinoids were above 40 ºC which is a prerequisite for nanocarriers used in topical delivery. Moreover, the low enthalpy and crystallinity index values indicated the existence of imperfections in the lipid matrix of the nanoparticles which enables a higher encapsulation efficiency for drugs. Thus, as predicted the optimized lipid nanoparticles showed a high encapsulation efficiency for RP (84.4 ± 3.0%), TRT (84.1 ± 7.8%) and ADP (73.7 ± 3.3%).

The *in vitro* release profiles of these selected retinoids indicated a very well-controlled release for the three delivery systems, which contributes to reducing their secondary effects and physicochemical instability. Moreover, it was observed that ADP was released faster after 48h (21.5 ± 1.3%) and that RP and TRT displayed a slower release profile, reaching a cumulative released of 12.2 ± 2.7% and 9.1 ± 2.5 %, respectively after 48h. These results can be sustained by those presented in the encapsulation efficiency study which determines that highest obtained cumulative release of ADP from the lipid nanoparticles is associated with its lower obtained encapsulation efficiency.

This study provided a new optimized NLC formulation that was effectively applied for the encapsulation of RP, TRT and ADP and which was designated for further characterization through *in vitro* assays on reconstructed human epidermis, to serve the purpose of their topical administration.

◢ CHAPTER VI

IN VITRO ADMINISTRATION OF NANOSTRUCTURED LIPID CARRIERS ON A RECONSTRUCTED HUMAN EPIDERMIS MODEL

Fátima Pinto, Dragana P.C. de Barros, Sofia Souza, Vânia Diogo, Abel Oliva, Luis P. Fonseca
Journal of Controlled Release- Prepared for submission

6. *In vitro* administration of nanostructured lipid carriers on a reconstructed human epidermis model

This study aimed to evaluate the efficacy for the topical administration of nanostructured lipid carriers (NLCs). NLCs were produced by the miniemulsions methodology using sunflower oil and myristic acid through an *in vitro* reconstructed human epidermis (RHE) model. Retinyl palmitate (RP) and α-Tocopherol (TOC), two very important antioxidant active substances commonly used in dermal formulations were selected as model drugs and were encapsulated into the lipid nanoparticles. The fluorescent dye DiO was incorporated along with TOC in the NLCs formulation to enable a qualitative characterization of the *in vitro* absorption studies. Physicochemical characteristics as particle size, zeta potential, entrapment efficiency, drug loading capacity and crystallinity of the lipid matrix of empty NLCs, RP-NLCs and TOC-DiO-NLCs were characterized. Additionally, it was also important to define their surface morphology, by atomic force microscopy and their internal structure, by transmission electron microscopy. Appropriate lipid nanoparticles for topical administration were obtained with sizes of ≈ 200 nm, good electrostatic stability (between -48 and -80mV) and melting temperatures above 40°C. *In vitro* absorption studies using the RHE model for RP-NLCs and TOC-DiO-NLCs were performed into customized Franz diffusion cells and quantitatively characterized by HPLC analysis and qualitatively characterized by fluorescence microscopy and confocal laser scanning microscopy (CLSM). RP and TOC permeation profiles showed a controlled release with cumulative amounts of 270.5 ± 102.7 µg and 103.7 ± 50.6 µg, respectively after 24h. The CLSM analysis confirmed the results obtained by fluorescence microscopy, suggesting that TOC-DiO-NLCs remained primarily in the *stratum corneum* (SC) layers and enabled the permeation of the active compound across the cultured skin membrane. *In vitro* skin irritation testing on the RHE was also performed and demonstrated that the produced NLCs formulations were non-irritants. Thus, the produced NLCs proven to be a feasible strategy to enhance the topical administration of lipophilic actives.

6.1. Introduction

Skin is the most extensive organ of human body and a major barrier, protecting it from oxidative stress and photo-aging originated by exogenous sources as UV radiation, air pollutants, toxins and other precursor agents of reactive oxygen species and free radicals (Abla and Banga, 2013). Natural antioxidants, as vitamins, present effective anti-ageing, anti-inflammatory, anti-carcinogenic, and anti-microbial properties and therefore, the topical supplementation of skin with these substances helps to

maintain its protective effect and fight the oxidative stress (Costa and Santos, 2017). Vitamins are frequently used in cosmetic formulations based on the concept that these bioactive compounds can efficiently permeate across epidermis into derma and subcutaneous tissues (Gabbanini et al., 2010). Still, there are few reports assessing the skin absorption of vitamins from cosmetic formulations (Gabbanini et al., 2010) but it is well established that these active substances have low skin bioavailability due to their reduced solubility, ineffective skin permeability and chemical instability during storage (Gasperlin and Gosenca, 2011). α-Tocopherol (TOC) and retinyl palmitate (RP) are examples of vitamins with strong antioxidant properties that have been widely used in cosmetic products (Abla and Banga, 2014, Oliveira et al., 2014, Sorg et al., 2005).

TOC or vitamin E, is considered the most active, lipophilic, membrane-bound antioxidant in human skin where it acts in the slowdown of the collagen breakdown process (Abla and Banga, 2014, Mahamongkol et al., 2005). In addition, the topical delivery of TOC promotes skin protection against UV-induced lipid peroxidation, carcinogenic and mutagenic activity and chemical agents (Gasperlin and Gosenca, 2011, Thiele and Ekanayake-Mudiyanselage, 2007).

RP belongs to the group of retinoids, is an ester of retinol (vitamin A) combined with palmitic acid (C16:0) and is the predominant form of vitamin A on epidermis. RP is enzymatically converted to retinol once it is absorbed by the skin and then to retinoic acid which is the biologically active retinoid (Oliveira et al., 2014). The topical application of RP is less irritating for the skin in comparison with the pure retinoic acid as consequence of the lengthier process that must take place for it to be converted into retinoic acid, but is equally effective (Fu et al., 2007). Although TOC and RP are being extensively used in cosmetic industry, there is limited information about their qualitative and quantitative absorption and distribution within the different skin stratums (Abla and Banga, 2013, Abla and Banga, 2014, Melot et al., 2009). Moreover, some antioxidants as the case of TOC and RP present poor water solubility, light sensitivity and mostly the second skin irritability (Abla and Banga, 2013, Abla and Banga, 2014). In order to overcome these drawbacks, TOC and RP can be incorporated into lipid nanocarriers, protecting them from degradation, decreasing their side effects and guaranteeing their controlled targeted release (Montenegro, 2014). There are several types of lipid nanocarriers that have been used to incorporate antioxidants as solid lipid nanoparticles (SLNs), nanostructured lipid carriers (NLCs), nanoemulsions and nanocapsules, among others for improving skin therapy (Morales et al., 2015, Santos et al., 2008).

Lipid nanoparticles are composed of solid lipids (SLN) dispersed in an aqueous medium and stabilized by surfactants forming O/W colloidal nanoemulsions or by a blend of solid and liquid lipids, in the case of NLCs (Costa and Santos, 2017). SLNs are the first generation of lipid nanoparticles presenting although, inferior drug loading capacity and stability in comparison with NLCs (Müller et al., 2007). These later nanoparticle carriers are the second generation of lipid nanoparticles which due to the combination of an oil with the solid lipid creates imperfections in the crystal lattice of their lipid matrix forming more space to accommodate active substances (Morales et al., 2015). NLCs may enhance the penetration of active substances on skin due to their adhesiveness to the surface and

144

binding tightly to the skin they produce an occlusive effect that improves skin hydration and the diffusion of the formulation (Abla and Banga, 2014, Chen-yu et al., 2012).

The development, manufacturing and quality control of cosmetics and dermatological products requires toxicological testing and hazard analysis to protect human health and the environment (Costa and Santos, 2017, Schafer-Korting et al., 2006). Animal welfare is of ethical concern of EU regulations thus, there is an urgent requirement to create and validate new alternatives to animal experiments (Gabbanini et al., 2010, Mittal et al., 2008, Schafer-Korting et al., 2006). Human skin models have become generally accepted for hazard analysis of derma-cosmetic products (De Wever et al., 2015). The Organization for Economic Cooperation and Development (OECD) approved test guidelines to study the skin absorption and irritation in vitro using reconstructed human epidermis (RHE) models (OECD, 2004, OECD, 2015). RHE is fairly similar to native human epidermis both in terms of morphology and lipid composition consisting on human keratinocytes and/or fibroblasts (De Wever et al., 2015, Lombardi Borgia et al., 2008). Despite being indicated as less selective than native epidermis, RHE can be used as a valid alternative for *in vitro* testing of topical formulations (Gabbanini et al., 2009, Gabbanini et al., 2010).

Until date, there are still few reports describing the *in vitro* absorption and irritation of active substances incorporated in lipid nanoparticles on RHE models (Schlupp et al., 2011, Santos Maia et al., 2002) and even on native human epidermis (Abla and Banga, 2014, Oh et al., 2006). Moreover, the mechanism of the improved transport mediated by these nanocarriers is not yet fully disclosed (Schlupp et al., 2011).

The design of dermal delivery systems requires the knowledge of principles to promote the incorporation of active substances into the carrier and also to mediate its consequent permeation through the skin (Lombardi Borgia et al., 2005). Therefore, it is essential and necessary to quantify the amount of incorporated active compound inside the lipid matrix and its localization at the target site. Marker agents (dyes or spin probes) can be incorporated along with active compounds into the lipid matrix of nanoparticles or be attached to their surface (Schlupp et al., 2011, Stecova et al., 2007). This allows to identify the location of the delivery system in a defined skin strata and to qualitatively characterize the permeation profile using fluorescence microscopy and image analysis (Lieb et al., 1992). Additionally, confocal laser scanning microscopy allows the determination of the permeation profile of the nanoparticles or active compound to which is added the fluorescent probe across the skin layers (Schlupp et al., 2011).

The present work proposes the characterization of NLCs formulations without and with the incorporation of two antioxidant vitamins as TOC and RP regarding their particle size and distribution, surface charge and electrostatic stability, lipid matrix crystallinity, and entrapment efficiency and drug loading capacity. Moreover, it aims to study the permeation and distribution of the formulated lipid nanoparticles across the RHE model strata, following the OECD Test Guideline 428. This procedure involved the incorporation of one fluorescent probe, DiO into NLCs containing TOC (TOC-DiO-NLCs) which method has not been yet reported in literature. Also, the skin irritability was also tested on RHE

models according the OECD Test Guideline 439, to validate the safety of all NLC formulations for topical administration.

6.2. Materials and Methods

6.2.1. Materials

Solid lipid: myristic acid, C14:0 (Sigma Grade, ≥99%) was purchased from Sigma-Aldrich (St. Louis, MO, USA). **Liquid lipid:** Sunflower oil (SF) was food grade product (Fula, Portugal). **Surfactant:** Span 80 (Sorbitan monooleate, HLB 4.7) from Alfa Aesar (Haverhill, Massachusetts, EUA). The aqueous phase of miniemulsions was prepared with Milli-Q water. **Active compounds:** α-Tocopherol (TOC) was obtained from Glicerinas e Parafinas de Portugal (Lisboa, Portugal) and Retinyl pamitate (RP) was cosmetic grade product purchased from MakingCosmetics® (Snoqualmie, Washington, USA); Acetonitrile RS, diclorometane RS and methanol RS were purchased from CARLO ERBA Reagents S.A.S. (Z.I. de Valdonne, France) special for HPLC/1NMR. The fluorophores DiOC18(3) (3,3'-Dioctadecyloxacarbocyanine Perchlorate (DiO) and eBioscience™ DRAQ5™, Phosphate-Buffered Saline (PBS) pH 7.4, 1X and MTT (3-(4,5-Dimethylthiazol-2-yl)-2,5-Diphenyltetrazolium Bromide) were purchased from TermoFisher Scientific (Waltham, Massachusetts, EUA); Formalin solution, neutral buffered, 10%, sacarose (Sigma Grade, ≥99.8%), the fluorophore 4′,6-Diamidine-2′-phenylindole dihydrochloride (DAPI) and 2-Propanol BioReagent, for molecular biology, ≥99.5% were purchased from Sigma-Aldrich (St. Louis, MO, USA); All other reagents were of analytical grade.

6.2.2. Production of NLCs

The miniemulsions methodology (Landfester, 2003) which is based on ultrasounds dispersion was used in the preparation of NLCs formulations. The lipid phase consisted in SF oil as the liquid lipid, and myristic acid (C14:0, melting point 54.4ºC) as solid lipid. Both lipids were mixed without or with each active compound (RP and TOC) and were heated to 10ºC above the solid lipid melting point to prevent lipid memory effect (How et al., 2013, Jores et al., 2004) until forming a uniform and clear oil phase. In formulations with TOC, the lipophilic tracer DiO was directly incorporated without any previous dilution in the lipid phase. The aqueous phase consisted in Span 80 as the surfactant, dissolved in Milli-Q water which was heated at the same temperature of the lipid phase. This phase was added to the aqueous phase and in a first step, both phases were mixed by magnetic stirring at 300 rpm during 45 min. The resultant pre-miniemulsion was then fully homogenized with a probe-type sonicator (Sonopuls - Ultrasonic homogenizer, Bandelin, Germany) during 10 min. The final

nanoemulsion was subsequently cooled to room temperature and stored. **Table 6.1** provides the detailed composition of each NLCs formulations which were prepared in duplicate.

Table 6.1 – Composition of NLCs formulations.

Formulations	Total Lipids, wt%	Myristic acid, wt%	Sunflower oil, wt%	Span 80, wt%	Bioactive substance, wt%	DiO, wt%
Empty NLC	2.5	2.0	0.5	1.5	-	-
RP-NLC	2.5	2.0	0.5	1.5	1.5	-
TOC-DiO-NLC	2.5	2.0	0.5	1.5	1.5	0.05

6.2.3. Characterization of NLCs

6.2.3.1. Analysis of particle size, PdI and surface charge of NLCs

The particle size (z-Average) and its distribution expressed as the polydispersity index (PdI) were measured by dynamic light scattering (DLS), using a Malvern Zetasizer Nano ZS (Malvern Instruments, UK). All measurements were performed at 25°C and using a 170º scattering angle. The processing was run by the software of the equipment and the particle size data was evaluated using intensity distribution. Each sample without dilution was measured in triplicate and the data was given as average of three individual records. The reported values are the mean ± standard deviation (SD) of at least three different batches of each NLC formulation. Using the same equipment, ZP was determined by measuring the electrophoretic mobility of the nanoparticles in an electric field, using the Helmholtz–Smoluchowsky equation. Before measurements the samples were diluted with Milli-Q water (1:10, v/v). All measurements were performed at 25ºC, in triplicate and the mean ± SD value was reported.

6.2.3.2. Evaluation of the lipid matrix crystalline state

Differential scanning calorimetry (DSC) analysis was performed to analyse the crystalline state of NLCs without and with the incorporation of RP and TOC-DiO. The thermograms were recorded using a DSC 200 F3 Maia (Netzsch, Germany). A nitrogen purge was used to provide an inert gas atmosphere within the DCS cell at a flow rate of 60 ml/min. Approximately 5-6 mg of pure dried NLCs were weighted into standard aluminum pans and hermetically sealed. An empty pan was used as a reference. Each sample was submitted to a heating cycle from 20 to 110ºC, at the rate of 5ºC/min. The melting points (Mp, °C), and enthalpies ($\Delta H, J g^{-1}$) were evaluated using the software Proteus Analysis (Netzsch, Germany). The determination of the crystallinity index (*CI*, %) was calculated from

the enthalpy of fusion using **Equation 4.2** (presented in chapter 4, section 4.2.3.3.). The solid lipid used in this study was myristic acid (ΔH = 161 Jg-1, Mp = 56.8 °C).

6.2.3.3. *Determination of entrapment efficiency (EE) and drug-loading capacity (DL)*

The EE, % and DL, % were calculated by measuring the concentration of each bioactive compound in the dispersion medium of the nanoparticles using a reverse-phase high-performance liquid chromatography (RP-HPLC) method. The non-encapsulated bioactive substances were separated by an extraction procedure adapted from (Yakushina and Taranova, 1995) as it follows, 2.0 mL of NLCs dispersions were transferred into a centrifuge tube with 2.0 ml of n-hexane (1:1, v/v). Then, the tube was sealed and the mixture was uniformly mixed with gentle magnetic stirring for 15 min at 150 rpm. The mixture was then centrifuged at 3000 rpm for 10 min and the supernatant consisting on hexane extract was collected and evaporated under nitrogen to remove the organic solvent. The residue of each active substance was dissolved on the mobile phase for analysis. The HPLC analytic system was composed by a Lachrom, Merk-Hitachi L-7400 apparatus equipped with a quaternary pump, an auto-sampler unit and UV detector and by a Purospher® RP-18 endcapped column (Merk Millipore, EUA). The operating conditions for the RP-HPLC analysis were set based on the methodology described by Yakushina and Taranova, (1995) (Yakushina and Taranova, 1995), as follows. An isocratic elution was performed using a mixture of acetonitrile, methanol and dichloromethane (60:20:20) as mobile phase, at a constant flow rate of 1.0 mL/min. The UV detector was set at 325 nm for the detection of RP and at 290 nm for the detection of TOC. The method was linear for RP and TOC standard solutions in concentrations varying from 0.2 to 100 µg/mL. All standards and samples were filtered using a PTFE membrane 0.22µm (Merk Millipore, EUA) prior to injection and an injection volume of 10 µL was used in both methods. The EE, % and DL, % were calculated using **Equation 3.1** (presented in chapter 3, section 3.2.3.2.) and **Equation 4.1** (presented in chapter 4, section 4.2.3.2.), respectively.The reported results are the mean ± SD of at least three different batches of each NLC formulation.

6.2.3.4. *Morphologic and structural analysis*

The NLCs topography was analysed by atomic force microscopy (AFM) and the internal matrix structure of the lipid nanoparticles was observed by transmission electron microscopy (TEM).

TEM Imaging was performed on a TEM equipment Hitachi H-8100 II (Tokyo, Japan) with thermionic emission (LaB6) and 200kV acceleration voltage, resolution of 2.7 Å point to point, equipped with an energy dispersive spectroscopy (EDS) light elements detector. The sample was prepared by placing a drop of the dispersion into a copper grid with 200-mesh coated with carbon membranes and dried at air for 5 min. The grids were then observed with a CCD MegaView II bottom-mounted camera.

AFM procedure for NLCs surface analysis was performed according to (Paradiso et al., 2014). An AFM microscope NanoSurf Easyscan 2 (tip-scanning type) was used to get topographic images at a lower scale. A drop of NLCs dispersion previously diluted (1:10) was placed on a glass slide and left to dry. The scan was done at room temperature in AFM contact mode on areas of 20 × 20 µm2, at a scan rate of 1 Hz. Imaging data were analysed with the using the WSxM 5.0 develop 6.4 software.

6.2.3.5. *In vitro skin absorption studies*

6.2.3.5.1. *Reconstruction of human epidermis on polycarbonate filters*

The reconstruction of stratified human epidermis on polycarbonate filters (inserts) was performed following the procedure described by De Vuyst et al. 2013 (De Vuyst et al., 2014) with a few adaptations (**Appendix A**) which briefly is as follows. Human epidermal keratinocytes were purchased from Life Technologies (Thermo Fisher Scientific, Massachusetts, EUA) instead of being obtained by biopsy. Once received, keratinocytes were placed at -80°C for two days and after they were moved into liquid nitrogen in order to reduce viability losses. The procedure of thawing the keratinocytes for culture growth in serum-free conditions was followed as recommended by Life Technologies for these type of cells. All further steps of the procedure, including the preparation of culture medium and trypsinization were proceeded according to De Vuyst et al. 2013 (De Vuyst et al., 2014).

6.2.3.5.2. *Permeation study using Franz diffusion cells*

In vitro release studies of TOC-DiO-NLC dispersions were performed using engineered static Franz diffusion cells designed in the Biomolecular Diagnostic research group at Instituto de Tecnologia Química e Biológica da Universidade Nova de Lisboa (ITQB NOVA, Oeiras, Portugal) with an effective diffusional area of 1.45 cm^2 and a chamber capacity of 13.9 mL to properly accommodate the inserts used to support the RHE **(Figure 6.1, A)**.

The study was conducted according to the conditions established in the OECD Guideline 428 (2004) (OECD, 2004). The inserts supporting the formed RHE were mounted on the receptor compartment of Franz diffusion cells which were filled with the receptor medium and were left to hydrate during 1h in a thermostatic water bath at 37°C ± 0.5°C with constant stirring at 250 rpm. The receptor fluid consisted in a solution of ethanol: water (1:1 v/v) used to test lipophilic substances and ensuring that sink conditions are maintained. After the hydration period, the filters position was verified to avoid bubbles formation and 500 µL of the nanoparticles dispersion were applied to the donor compartment, sealing all orifices with parafilm to prevent evaporation. Aliquots of 1 mL were withdrawn at established time intervals (up to 24 h) and replaced with the same volume of fresh receptor medium.

The experiment was performed using five Franz diffusion cells running in parallel with the same conditions, having into account the variability of the cultured tissues and the results were expressed as mean ± SD (**Figure 6.1, B and C**).
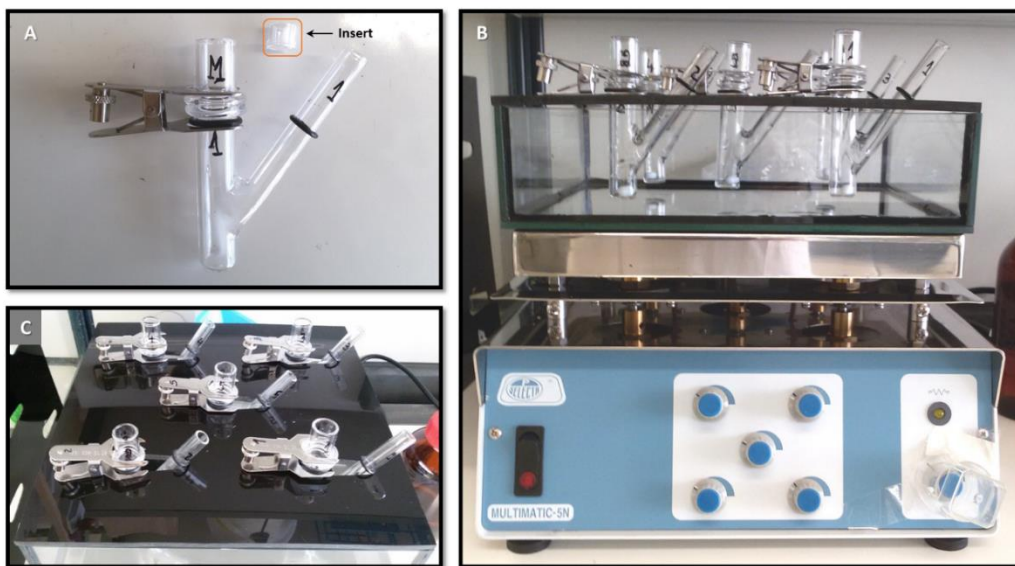
Figure 6.1 – Franz diffusion cell apparatus. (A) Customized Franz cell and polycarbonate filter (insert); (B) Thermostatized water bath; (C) Five Franz cells running in parallel with the same conditions.

All samples were collected for vials and kept at -20°C until analyzed by HPLC as described in section 2.3.2. The cumulative amount (Q_t) of TOC permeated through RHE supported by a polycarbonate filter was calculated by the **Equation 6.1**:

$$Q_t = \left(C_n \times V_s + \sum_{i-1}^{n-1} C_i \times V_r \right)/S \tag{6.1}$$

where C_n is the bioactive substance concentration (µg/mL) in the receptor medium at each sampling time "n", C_i is the bioactive substance concentration (µg/mL) at time "i", V_r (mL) is the volume of the receiver solution, V_s (mL) is the volume of the sample and S characterizes the sectional area of tissue (cm^2). The cumulative amount (µg/cm^2) of TOC was plotted as a function of time which enabled to determine the permeation rate at steady state (J, µg/cm^{2}h) from the slope of the linear regression. The lag time (h) was determined by extrapolating the linear portion of the curve to the X-axis (when y=0). The permeability coefficient (P, x10^{-4} cm/h) was calculated by the **Equation 6.2**:

$$P = J/C_0 \tag{6.2}$$

where J is the steady state flux (µg/cm^2 h) and C_0 is the initial drug concentration in donor side (µg mL^{-1}) (Ren et al., 2014).

6.2.3.5.3. Histological analysis and fluorescence microscopy

For the histological analysis after the permeation studies, the inserts were removed from the Franz diffusion cells and their surface supporting the RHE was carefully washed with PBS, pH 7.4 (1X) with 1 mL to remove remained TOC-DiO-NLCs. After this step, the inserts were fixed in 10% acetic formalin for a minimum of 24h at room temperature. Right before being cryopreserved, the RHE on polycarbonate filters was detached from the inserts using a small scalpel and then they were immersed in sucrose 30% to cryoprotect the tissues. The cryofixation of the tissues was followed by cryostat sectioning, cutting 25 µm thick sections before preparing 6 µm for histological analysis. Some tissue sections were conventionally stained with hematoxylin-crythrosine to allow a regular morphological analysis of RHE while others were hydrated and stained with DAPI for fluorescent staining DNA of cells nuclei. The tissues were then examined by light microscopy and analytical fluorescence light microscopy using an inverted microscope Nikon Eclipse 2000-S (Tokyo, Japan) equipped with a 60x scanning objective (Plan Fluor, Nikon, Tokyo, Japan) and a 10x eyepiece. Images were recorded by a camera (Evolution MP colour Media Cybernetics, Rockville, USA) coupled to the microscope and using the software Image-Pro Plus 7 (Media Cybernetics, Rockville, USA). For fluorescence imaging the filters Nikon B-2E/C and Nikon UV-2E/C were used to detect DAPI and DiO fluorescent stains, respectively. ImageJ public-domain software was used to analyze and process the images.

6.2.3.5.4. Confocal laser scanning microscopy (CLSM)

For CLSM, the inserts were previously prepared as described for the histological analysis. After, the RHE on polycarbonate filters was detached from the inserts using a small scalpel and stained with DRAQ5, diluted 1:1000 in PBS to visualize cell´s nuclei. The tissue was then embedded in PBS and mounted with epidermis side faced down on glass coverslips. This sample was then microscopically examined without any additional tissue processing on a Leica SP5 confocal system mounted on a Leica DM6000 inverted laser scanning microscope (Wetzlar, Germany) equipped with an Argon-ion laser (458,476,488,514nm lines) + 561nm and 633nm lasers and with 3x spectral PMT detectors. Confocal Z-series stacks were acquired using a 20x 0.7NA objective and spectral detection adjusted for the emission of DiO and DRAQ5 fluorescent probes with 488nm and 568nm laser lines. 3D reconstructions and XZ stacks were obtained using Leica's LAS-AF software.

6.2.3.6. In vitro skin irritation test

RP-NLCs, TOC-DiO-NLCs formulations and the respective loaded active substances were tested for skin irritation. The procedure of the *in vitro* skin irritation test was followed as described by Kandárová et al. 2009 (Kandárová et al., 2009) and according to the conditions established on OECD Test Guideline 439 (OECD, 2015). This test is based on the production of reversible damage to the skin following the application of a test substance (OECD, 2015). Some adaptations to the procedure

were introduced as the use of the RHE model that was cultured in our lab (**Appendix A**) which was applied for discrimination between irritants of United Nations Globally Harmonized System (UN GHS) category 2 or 1 and non-irritants (Kandárová et al., 2009, Nations, 2007). This test occurred during a period of 3 days, consisting of a 60 minute exposure on day 1 and 42 hour post-incubation time and MTT viability assay on day 3 with medium exchange on day 2. A single testing run was composed by three replicate RHE tissues for each test substance (empty NLC, TOC, RP, TOC-NLCs and RP-NLCs), as well as for the positive control (SDS, 5% w/v aqueous solution) and for the negative control (PBS solution). The substance exposure lasted for 60 min of which 35 min the tissues were kept in an incubator at 37°C. The tissue surfaces were then extensively washed to remove the test substances and after being blotted was added fresh medium. After 24h this medium was exchanged and the tissues were incubated for an additional period of 18h. At the end of the 42 hour post-incubation time, the cell viability in RHE model was measured by an enzymatic conversion of the vital dye MTT. The tissues were transferred into a MTT solution and incubated for 3h and the resultant purple-blue formazan salt was extracted using isopropanol during 2 hours. The optical absorption of the extracted formazan was determined using a microplate reader spectrophotometer (SpectraMax 340, Molecular Devices, San Jose, USA). A test substance is classified as an irritant if the tissue viability is reduced 50% relatively to the treated tissues as negative control.

6.3. Results and Discussion

6.3.1. Physicochemical characterization of produced NLCs

6.3.1.1. Particle size and physical stability

NLCs formulations were characterized regarding their particle size, the respective polydispersity index (PdI) values and surface charge, prior the evaluation of their performance on a RHE model. **Table 6.2** summarizes the obtained values for empty NLCs, RP-NLCs and NLCs loaded with TOC and with the fluorophore DiO (TOC-DiO-NLCs, with its composition on **Table 6.1**). As expected based on previous results (Chapters 4 and 5), the encapsulation of RP and TOC-DiO promoted a slight increase on particle size (appx 7% for RP-NLC and appx 15% for TOC-DiO-NLCs) in comparison with the formulation of empty NLCs which presented the lowest value (173 ± 3.6 nm). This demonstrate the dependence of the particle size on the concentration of the loaded active (Kuchler et al., 2009). The conformational rearrangement between the lipid matrix and the encapsulated compounds may be dependent of the molecular architecture of the active substance, which may justify the differences in particle sizes with the same lipids formulation and different active compounds or without any incorporation.

It should also be noted that the PdI values for the studied formulations were all lower than 0.3, which is considered an optimal value for the dispersion and homogeneity of these nanoparticles (Iqbal et al., 2012). Empty NLCs were highly homogeneously distributed with a very low PdI value of 0.181 ± 0.013 and also NLCs loading each RP and TOC-DiO revealed a uniform size distribution, presenting very close PdI values (**Table 6.2**).

The particle size is a very important parameter that influences the effects of NLCs on skin, as for instance their occlusion effect and permeation (Sala et al., 2018). As referenced by Mardhiah Adib et al., 2016 (Mardhiah Adib et al., 2016) the particle size should be less than 260 nm for achieving skin absorption due to a higher occlusion and interaction with the skin surface. Moreover, by manipulating the particle size of lipid nanoparticles, different occlusion effects can be obtained (Souto and Müller, 2007).

The surface charge of the prepared lipid nanoparticle formulations was expressed by the obtained ZP values which were all below –30 mV (**Table 6.2**), assuring an electrostatic stability for the prepared NLCs formulations (Vitorino et al., 2014). It was observed an accentuated difference between the ZP values of TOC-DiO-NLCs formulation in comparison with the two others. This may be attributed with the location of the encapsulated active that could be entrapped on the inside of the lipid matrix or could be located on the surface of the nanoparticle, interacting with the surfactant layer. In this case, the ZP values obtained for empty NLCs (–50.2 ± 1.1 mV) are close to those obtained for RP-NLCs (–47.8 ± 1.1 mV), which may indicate that RP, being and lipophilic compound could be interacting with the lipids matrix inside the nanoparticles core, while the TOC-DiO, could be located more to the surface of the nanoparticles. On the other hand, the fluorescence of DiO probe may be interfering on this result since the ZP values obtained for TOC-NLCs without this fluorophore were -52.0 ± 0.9 mV, which is a more close value to those obtained for empty NLCs and RP-NLCs. The surface charge characterized by ZP values is another important parameter to be considered regarding the performance of NLCs on skin. Despite the information about the electrostatic stability of the nanoparticles, the ZP values also determine the absorption conditions on skin as the diffusion coefficient or the type of skin permeation pathway (Benson, 2012).

6.3.1.2. *Crystallinity of lipid matrix and loading efficiency*

The crystallinity state and the loading efficiency of the produced NLCs formulations were evaluated as these factors are described to mutually interplay on the release modulation of active compounds (Müller et al., 2016). DSC analysis was performed to evaluate the crystallinity state of empty NLCs, RP-NLCs and TOC-DiO-NLCs (**Table 6.2**). The resultant enthalpies and crystallinity indexes of RP-NLCs (-18.61 J/g, 11.6 %) and TOC-DiO-NLCs (-17.65 J/g, 11.0 %) were considerably lower in comparison with empty NLCs (-33.02 J/g, 20.5 %). This indicates that the incorporation of RP and TOC resulted in a disturbance of the lipid crystal lattice also verified by a slight decrease on the respective melting temperatures (**Table 6.2**). Depending on the solubility of the encapsulated active

compound, crystallization of the melt can result in a monolithic solid solution or a solid dispersion containing the active compound in a homogenous distribution or forming clusters (Schäfer-Korting et al., 2007). In this case, the obtained low crystalline indexes indicated that most probably the nanoparticles solidified after cooling but did not recrystallized, remaining in an amorphous state.

Table 6.2 – Physicochemical properties, DSC parameters and loading efficiency of produced formulations with empty NLCs, RP-NLCs and TOC-DiO-NLCs.

	Empty NLCs	*RP-NLCs*	*TOC-DiO-NLCs*
Particle size (nm)	173 ± 3.6	186 ± 5.4	200 ± 8.6
Polydispersity index	0.181 ± 0.013	0.297 ± 0.038	0.239 ± 0.028
Zeta potential (mV)	-50.2 ± 1.1	-47.8 ± 1.1	-80.7 ± 2.3
Onset temperature, °C	51.0	39.8	39.3
Melting point, °C	54.1	44.6	43.9
Endset temperature, °C	56.4	47.0	45.6
Enthalpy, -J/g	33.02	18.61	17.65
Crystallinity index, %	20.5	11.6	11.0
Entrapment efficiency, %	-	85.5 ± 3.8	80.8 ± 11.4
Drug loading capacity, %	-	69.6 ± 1.2	66.8 ± 9.4

The entrapment efficiency and loading capacity results are in agreement with the previous findings (Chapters 4 and 5), as the lipid matrix composition of produced NLCs demonstrated a high ability to incorporate RP and TOC with EE,% values of 85.5 ± 3.8% and 80.8 ± 11.4%, respectively and high DL, % of 69.6 ± 1.2% and 66.8 ± 9.4% from a theoretical maximum value of 75%. Different types of mixed lipids form less densely packed lattices favouring the incorporation of active compounds. Moreover, the number of defects increases in lipid mixtures of which are either solid or fluid at room temperature (Schäfer-Korting et al., 2007), which is the case for RP-NLCs and TOC-DiO-NLCs. In fact, the loading efficiency increases with reduced or lacking crystallinity (Jores et al., 2005).

The melting temperatures of the produced NLCs are higher than 40 ºC (**Table 6.2**) which confirms that the nanoparticles are solid at body temperature, being fulfilled the prerequisite for their topical administration (Gonzalez-Mira et al., 2011).

6.3.2. *Analysis of surface morphology and internal structure*

Primarily to *in vitro* absorption skin studies, TEM analysis was performed to analyze the morphology and internal structure of RP-NLCs and TOC-DiO-NLCs and AFM was complementary used to evaluate their shape and morphological surface. The diameter of the nanoparticles observed in the TEM (**Figure 6.2, A**) corroborates the DLS measurements (RP-NLCs presented an average particle size of 186 ± 5.4 nm and TOC-DiO-NLCs of 200 ± 8.6 nm). Also, TEM images showed particles with a compact internal structure which illustrates the results obtained from the DSC analysis.

On the other hand, the AFM images (**Figure 6.2, B**) obtained in contact mode showed flattened nanoparticles with a slight higher particle size of approximately 250 nm for RP-NLCs and 350 nm for TOC-DiO-NLCs and only 3–5 nm in height. This may be due to the occurrence of particle adhesion to the glass slide surface which supports the nanoparticles during the vacuum drying process for sample preparation (Hu et al., 2005), inducing a slight expansion over their diameter and consequently the deformation of their spherical shape into more flattened particles. This results are very close to those reported by Hu et al. 2005 (Hu et al., 2005), that used this technique in tapping mode to characterize NLCs prepared with stearic acid and oleic acid by the high pressure homogenization methodology. The three-dimensional AFM analysis showed some discrepancies regarding the surface morphology and texture of each NLCs formulations (**Figure 6.2, B**), indicating that the TOC-DiO-NLCs formulation is more dense presenting lower flattened particles.
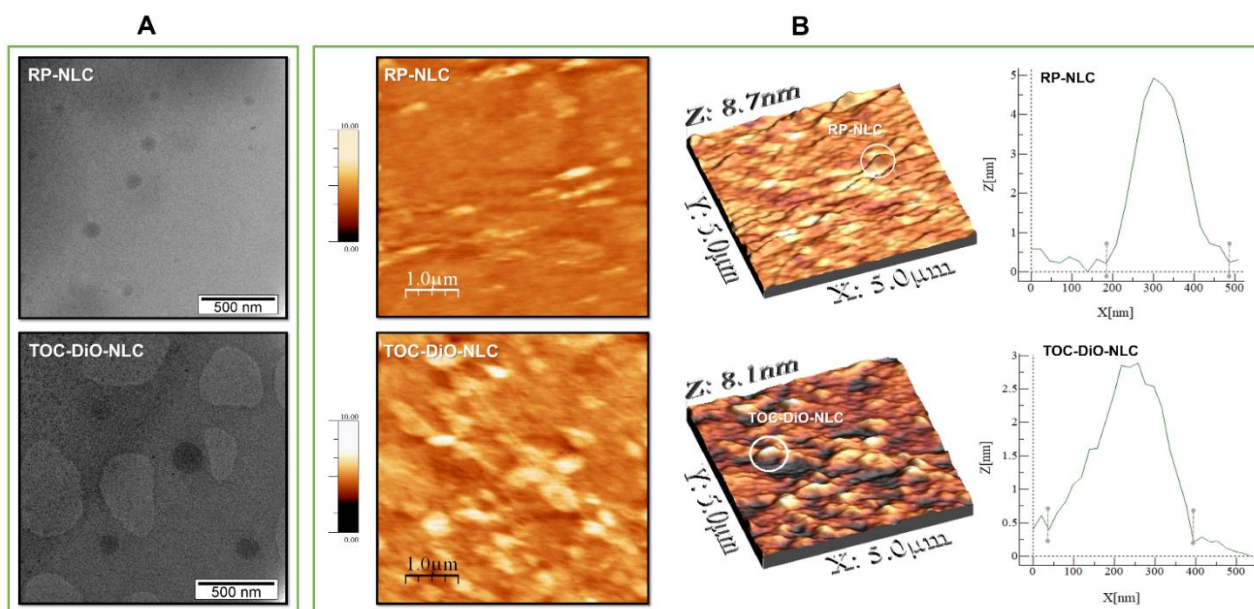
Figure 6.2 – (A) TEM images of both prepared formulations containing RP-NLCs and TOC-DiO-NLCs (B) AFM images of RP-NLCs and TOC-DiO-NLCs in contact mode: 2D captured cross-sections (left); three-dimensional (3D) image from the captured cross-sections (middle); respective cross-section height profiles (right).

6.3.3. *In vitro* skin absorption studies

6.3.3.1. *In vitro* permeation profiles on a RHE model

The permeation profiles of RP-NLCs and TOC-DiO-NLCs were studied to evaluate the release profile and skin absorption of these two antioxidant actives, using a RHE model which may replicate the topical absorption by native human epidermis. This study was performed in sink conditions, using a concentration of 1.5 % of each active substance in the same NLCs composition (**Table 6.1**). The release profiles of RP and TOC were drawn to compare the absorption of each RP-NLCs and TOC-DiO-NLCs formulation (**Figure 6.3**). Additionally, the permeation parameters, including the permeation rate at steady state (J, μg/cm^2 h) and the skin permeability coefficient (P, x 10^4 cm h), were determined and are listed in **Table 6.3**.
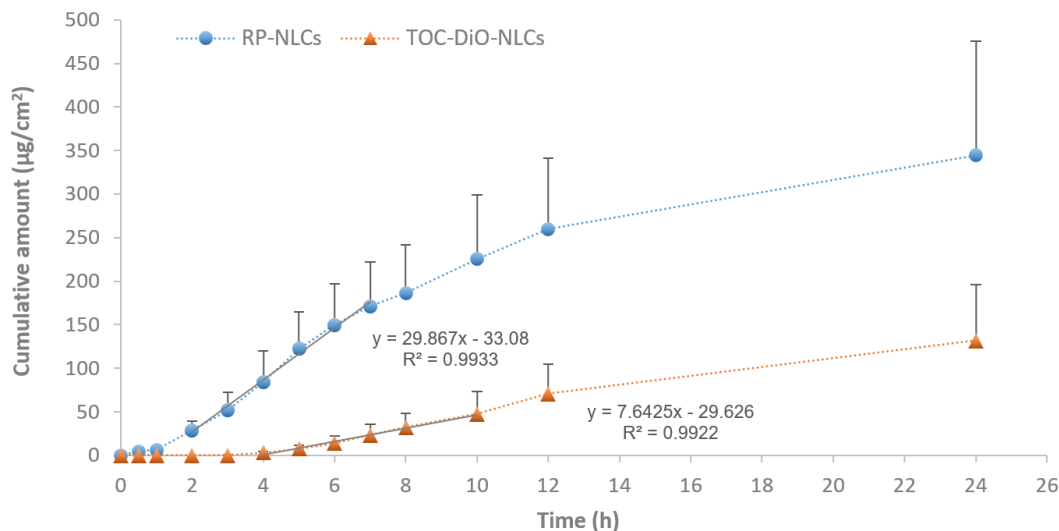
Figure 6.3 – *In vitro* permeation profiles of RP and TOC cumulative amounts released from NLCs through a RHE model. Plots were obtained from two experiments with each tested active compound running in the same experimental conditions with five replicates.

As shown in **Figure 6.3**, irrespectively of their lipophilicity, RP and TOC permeated through the RHE model presenting a controlled release over a period of 24h, although, RP was released much more rapidly than TOC. NLCs may enhance the permeation of these two actives in two ways, firstly the active substance is carried through SC and there it accumulates; and secondly, a concentration gradient favors the permeation to occur improving a rapid diffusion and inducing a higher flux (Ren et al., 2014). The diffusion process is dependent of the physicochemical properties and solubility of the analyses in the aqueous receptor fluid. As RP and TOC are two very apolar compounds (log P_{ow} (TOC) = 12.2 and log P_{ow} (RP) = 15.51, as respective partition coefficients), they present a very unfavorable partition (donor/ receptor) which is not balanced by the larger concentration gradient (Gabbanini et al.,

2010). Also, it was expected that TOC being less apolar then RP would present a higher solubility in the aqueous receptor and consequently a higher diffusion and skin permeability coefficient. However, RP presented a much higher permeation rate and permeability coefficient than TOC (**Table 6.3**). This may be justified by the enzymatic conversion of RP to retinol after being absorbed by the skin (Oliveira et al., 2014), losing its fatty acid chain that may be more deeply incorporated into the lipid matrix of the nanoparticles and delivering the less apolar retinol (log P_{ow} (Retinol) = 7.6). Generally, retinoids remain mainly on the surface of epidermis as they present low permeation into skin, mainly due to the SC being an effective barrier or because the molecules are broken before percutaneous absorption (Clares et al., 2014, Teixeira et al., 2010). Although, it is hypothesized that after the release of retinol from the NLCs in the SC, the aliphatic chain of retinol will insert itself within the aliphatic chains of the SC lipids and fluidized them which will allow a faster diffusion through it (Abla and Banga, 2013, Melot et al., 2009).

Table 6.3 – Cumulative percentage amount, lag-time and permeability parameters (permeation rate at steady state, J and skin permeability coefficient, P) for RP and TOC released from NLCs through an *in vitro* RHE model.

	RP-NLCs	*TOC-NLCs*
Cumulative % amount* (%/cm^2)	0.11 ± 0.04	0.04 ± 0.02
Total mass* (μg)	270.5 ± 102.7	103.7 ± 50.6
Lag-time (h)	1.2 ± 0.3	3.9 ± 0.2
P (x10^{-4}, cm/h)	19.9 ± 5.6	5.1 ± 2.8
J (μg/cm^{2}h)	29.9 ± 8.4	7.6 ± 4.1
R^2	0.9933	0.9922

* values obtained after 24h of the absorption study.

The lag-time for RP-NLCs was about 1h, reaching a cumulative released amount of 270.5 ± 102.7 μg after 24h, while the continuous permeation of TOC only started after about 4h until reach a cumulative released amount of 103.7 ± 50.6 μg after 24h (**Table 6.3**). Clares et al. 2014 (Clares et al., 2014), performed an *ex vivo* permeation study for RP loaded in SLNs through native human epidermis and also obtained a continuous permeation of RP, approximately 1h since the beginning of the experiment but however, a much lower cumulative amount of 3.64 ± 0.28 μg after 38h was obtained. Abla and Banga 2014 (Abla and Banga, 2014), reported that TOC loaded in NLCs did not permeated through native human skin over a period of 24h. These are contrary results to those obtained in the present study which can demonstrate that the used RHE may not be a reliable model for dermal penetration studies. *In vitro* RHE models have proven to be useful in toxicity, pharmacology and efficacy studies, clearly offering advantages compared to the use of human cadaver/ or animal skin in terms of reproducibility, availability in large numbers, metabolism, and typical ''tissue response'',

157

although these models are not exact copies of human skin *in vivo* and in fact their biggest limitation is still their relatively weak barrier function (De Wever et al., 2015). Thus, in order to validate this results it would be advantageous to perform an *ex vivo* permeation study using native human skin, since it was not found in literature another study describing the *in vitro* permeation of NLCs through a RHE model.

To estimate the influence of the formulated nanocarriers on the bioavailability of the active compounds, the obtained results were compared with those reported by Gabbanini et al. 2010 (Gabbanini et al., 2010), which performed an *in vitro* analysis of retinol acetate and TOC from different types of cosmetic formulations (O/W and W/O emulsions) through a RHE model. The reported results shown that formulations having water in the external phase (O/W emulsions or lotions), released the vitamins significantly more rapidly than W/O emulsions, although the actual contribution of the formulation depended on the physicochemical properties of the analyte. Retinol acetate in O/W emulsions showed a permeation rate of 0.063 ± 0.019 mg/cm^2 h and a permeation coefficient of $0.36 \pm 0.11 \times 10^5$ cm/h which were much lower values compared with those obtained in this study for RP (**Table 6.3**) with a much higher lag-time of 6.15 ± 1.38 h in comparison with 1.2 ± 0.3 h obtained in this study. In the case of TOC in O/W emulsions, the reported lag-time was > 21h and the permeation parameters were both approximately 0. This results indicates that the formulated NLCs were effective carriers for both RP and TOC demonstrating a controlled release over a period of 24h and enhancing the permeation of these two antioxidants though the skin.

6.3.3.2. *Histology and fluorescence microscopy analysis*

The cultured skin membranes were histologically examined to evaluate the effect of TOC-DiO-NLCs 24h upon their administration. The tissues exposed to this fluorescent-labeled lipid nanocarriers displayed barrier properties and other morphological features similar to the RHE model that was not subjected to the absorption assay, presenting a general epidermal architecture resembling native epidermis (**Figure 6.4, A** and **B**). After the absorption study the tissues presented a uniformly layered SC with larger Interlamellar gaps between SC and the topmost layer of the epidermis (**Figure 6.4, B**). This effect might probably be attributed to the hydration and occlusion capacity of NLCs. These findings are in agreement with the results obtained by Clares et al, 2014 (Clares et al., 2014), who also noted the same features on native human skin revealing a significant increase in skin hydration provided by the administration of lipid nanoparticles. The occlusion capacity is very a desirable property for topical formulations, since the hydration content is one of the most important factors that help in maintaining optimum skin conditions (Souto and Muller, 2008). This effect occurs after the dermal application of lipid nanoparticles that adhere to the skin forming a thin film layer which prevents water loss and dehydration. This effect is size dependent and thus, smaller the size of the particles is, the higher is the occlusion factor (Muller et al., 2011).
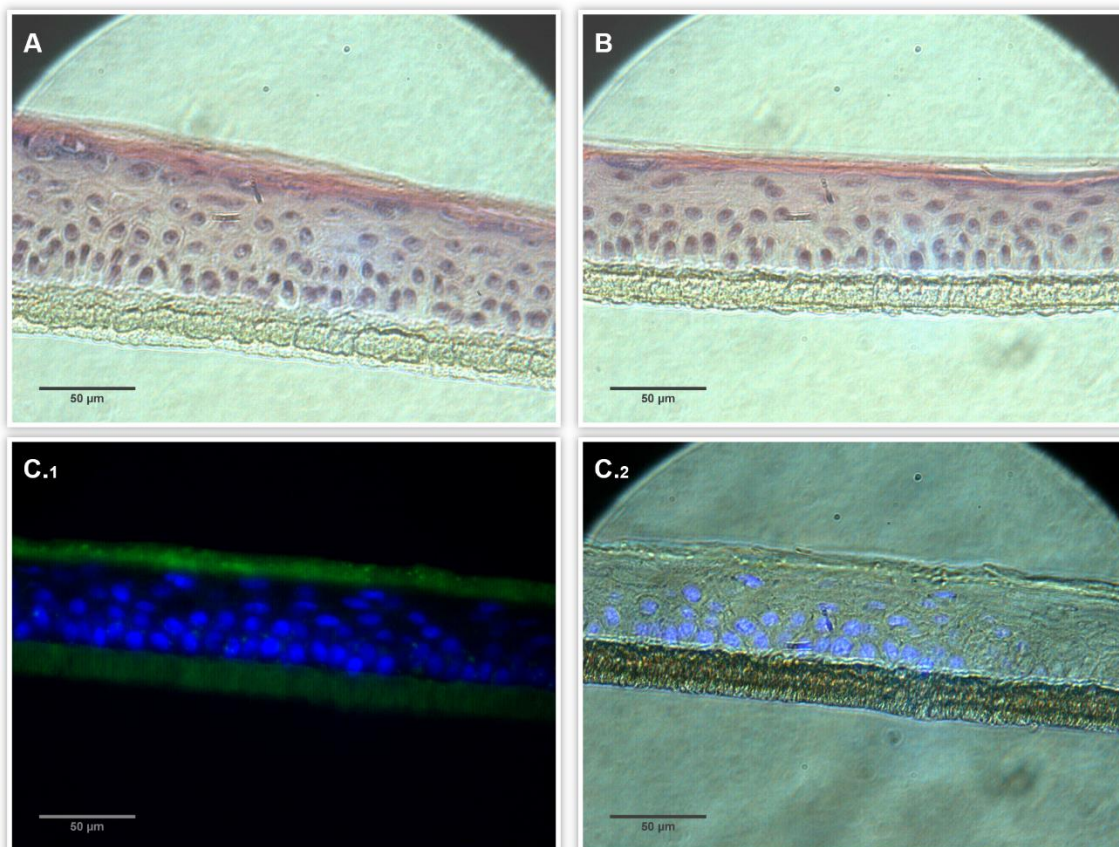
Figure 6.4 – Photomicrographs of skin cross-sections after the in vitro skin absorption study with TOC-DiO-NLCs. (A) Histological characterization of the used RHE model on a polycarbonate filter. Skin cross-section (6 μm) of RHE cryopreserved in 30% sucrose and stained with hematoxylin-crythrosine; (B) Histological characterization of the used RHE model after the in vitro skin absorption study in Franz diffusion cells; (C) Fluorescence microscopy image characterizing the in vitro skin absorption study of TOC-DiO-NLCs. The fluorescence image of one cryopreserved RHE cross-section was obtained using the software Image J by merging two fluorescence channels from the same micrograph. The blue colour corresponds to the fluorescent probe DAPI (Ex/Em of 358/ 461nm) that stains the cells nuclei and the green colour corresponds to DiO fluorescence (Ex/Em of 484/ 501nm) of labelled TOC-DiO-NLCs.

Fluorescence microscopy was used to visualize the location of TOC-DiO-NLCs and to qualitatively characterize the permeability profile of TOC. At the end of the *in vitro* absorption study, the permeation profile of TOC-DiO-NLCs was analyzed by fluorescence microscopy (**Figure 6.4, C**). The green fluorescent fluorophore DiO was incorporated into the lipid matrix in order to localize of the lipid nanoparticles and the blue fluorophore DAPI was used to characterize the cells nuclei. The DiO, a lipophilic tracer belonging to the carbocyanine family has been used as a marker of PLGA (poly (lactide-co-glycolide)) nanoparticles (Gaumet et al., 2009, Shah et al., 2012), of lipid nanocapsules and *Acinetobacter baumannii* bacterial membrane (Montagu et al., 2016). The visualization of obtained

fluorescence microscopy images qualitatively indicates the most pronounced trends of fluorescent staining located at the various skin strata. It was observed that the TOC-DiO-NLCs are primarily located at the upper layer in SC where the green colour is more intense. At the bottom, where the polycarbonate filter is located, is also observed green fluorescence which may possibly be justified by the passage of TOC-DiO through this membrane. As demonstrated, intact lipid particles do not penetrate into SC, although the permeation and absorption of their components (lipids and surfactant) through the skin is to be expected (Lombardi Borgia et al., 2005).

6.3.3.3. *Qualitative skin permeation profile by CLSM*

The localization of TOC-DiO-NLCs was also visualized by CSLM after the *in vitro* absorption study. The major advantage of CLSM is that the tissue to be analyzed is optically sectioned without tissue fixation and/or sectioning, thus enabling the visualization of the depth-dependent distribution of fluorescent probes to be visualized (Alvarez-Roman et al., 2004, Teixeira et al., 2010). This technique can provide information on the penetration pathway or permeation route of substances or particles across the skin (Contri et al., 2011).

Before the analysis, skin cross-sections were hydrated and stained with the fluorescent probe DRAQ5 that was used to label the cell nuclei, in red and contrast with the fluorescence-loaded nanoparticles represented in green. **Figure 6.5** shows a cross-section of skin layers from *xz* – image stacks (A) and the resultant 3D reconstructions of confocal *z*-stacks from the same skin section. The TOC-DiO-NLCs green color fluorescence indicates a uniform permeation into skin, being more accentuated in the SC and decreasing through the deeper layers of the epidermis model (**Figure 6.5, A**). It was thus confirmed what was observed by fluorescence microscopy analysis, that the lipid nanoparticles stayed mostly in the first skin layer, the SC. This uniform permeation may indicate that the penetration pathway of TOC-DiO-NLCs is intercellular through thin pores of the skin (Teixeira et al., 2010). Also, it was observed that the nanoparticles distribution along the skin surface was not homogeneous. At some specific spots it was detected targeted aggregates of TOC-DiO-NLCs characterized by an increase in green fluorescence forming large dots (**Figure 6.5, B**). This findings may confirm the accumulation of nanoparticles at thin pores of the skin, then following the intercellular permeation pathway.

Published data indicated that ibuprofen-loaded microemulsions accumulated primarily in SC and then permeated the skin through viable native human dermis and preferentially through the follicular route (Ren et al., 2014). In a different way, nanospheres of poly(l-lactide-co-glycolide) covalent-bounded with fluorescein and Texas Red as drug model did not permeated the skin, the fluorescein remained on the skin surface, while Texas Red was released and accumulated in the SC (Stracke et al., 2006). These conclusions demonstrate nanocarrier type is crucial for skin permeation of active compounds, being dependent upon the formulation nature and properties. Thus, it can be stated that

there is no rule to predict the permeation of nanoparticles, since it relies on unique characteristic of each system, such as surface properties, rigidity and particle sizes.

The results obtained in this study confirmed the permeation of NLCs through the SC, carrying the active compound (TOC) and enabling its permeation across the cultured skin membrane. This occurrence may be related with the affinity and interaction of the lipids matrix of the nanoparticles for the lipids of the SC, as well with their physicochemical characteristics.
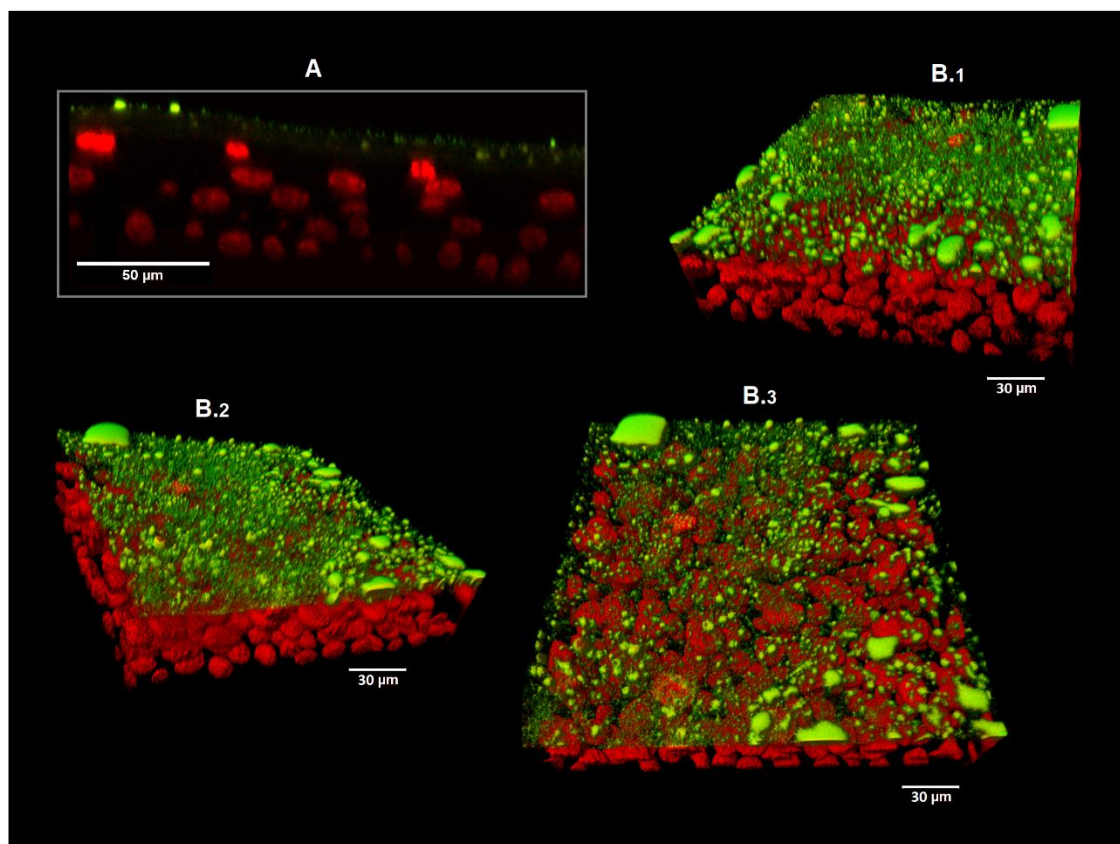
Figure 6.5 - Confocal images of skin cross-sections after the *in vitro* absorption study with TOC-DiO-NLCs. (A) Cross-sectional (xz-stacks mode) image of skin layers; (B) 3D reconstruction from confocal z-series stacks of skin layers. The red colour corresponds to the fluorescent probe DRAQ5 (Ex/Em of 647/ 681nm) that stains the cells nuclei and the green colour corresponds to DiO fluorescence (Ex/Em of 484/ 501nm) of labelled TOC-DiO-NLCs.

6.3.4. *In vitro skin irritation test*

An *in vitro* skin irritation testing was performed using the RHE model for evaluating the produced NLCs formulations and the two active substances that were encapsulated in each formulation (RP and TOC). This procedure was based on the OEDC Test Guideline 439 (OECD, 2015), following the

established conditions for the EpiDerm skin irritation test (Kandárová et al., 2009). The cell viability was measured by an enzymatic conversion of the vital dye MTT and the results are shown in **Figure 6.6**. The positive control (PC) consisted in an aqueous solution of SDS, 5% w/v and for the negative control (NC), defining 100% of cell viability was used a PBS solution.

The formulations of empty NLCs, TOC-DiO-NLCs and RP-NLCs presented tissue viabilities above 50% (**Figure 6.6**) and were thus classified as non-irritant. After exposure to TOC, the obtained cell viability was also a high value (96.5 ± 0.2%), suggesting that this active substance is non-irritant to the skin. However, it was observed a reduction in tissue viability below 50%, referenced to the NC after exposure to RP (38.5 ± 0.3%) which proved that this active substance is classified as a skin irritant of Category 1 or 2 according to UN GHS. Since this *in vitro* skin irritation testing method cannot resolve the classification between UN GHS Categories 1 and 2, further information on skin corrosion was required to decide on its final classification (OECD, 2015). On the contrary, after exposure to RP-NLCs the obtained cell viability value was the highest (102.5 ± 1.3%, referenced to the NC) being thus, this formulation classified as non-irritant and was demonstrated that the encapsulation of RP in NLCs covered its associated cytotoxicity.
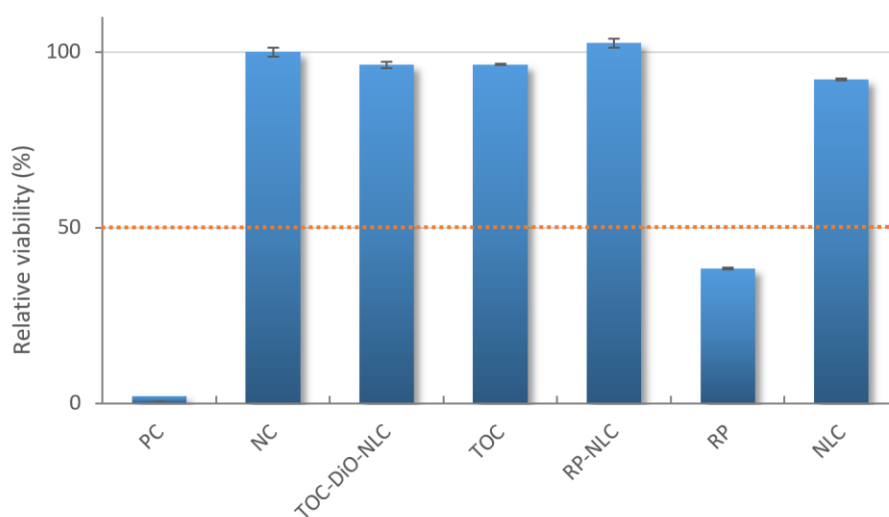
Figure 6.6 - Persistence of cell viability in RHE model. The cell viability was determined by measuring the reduction of a tetrazolium dye MTT solution by a spectrophotometer after an incubation period of 60 min with each substance (TOC and RP) or formulation (TOC-DiO-NLCs and RP-NLCs) to be tested. PC – Positive control (aqueous solution of SDS, 5% w/v); NC – PBS pH7.4 (1X).

6.3. Conclusions

NLCs formulations produced by the miniemulsions methodology, using sunflower oil and myristic acid as the constituent lipids of the nanoparticles matrix, and RP and TOC as lipophilic drug models, were effectively characterized and evaluated regarding their performance on an *in vitro* RHE model. The incorporation of a fluorescence dye along with TOC was reported for the first time in NLCs formulations and enabled a qualitative analysis of the location and permeation profile for the produced lipid nanoparticles after the *in vitro* absorption studies using the RHE model by fluorescence microscopy and CLSM.

Empty NLCs, RP-NLCs and TOC-DiO-NLCs demonstrated very good physicochemical properties for their application in dermal formulations, presenting particle sizes of approximately 200 nm, good electrostatic and melting temperatures above 40°C. The tested NLCs formulation showed a high entrapment efficiency and a high drug loading capacity for RP and TOC, which corroborated the obtained low crystallinity indices of these nanoparticles that indicated a disturbance in the lipid crystal lattice also verified by a slight decrease on their respective melting temperatures.

The permeability profiles of RP and TOC obtained in the *in vitro* absorption studies, indicated a controlled release presenting cumulative amounts of 270.5 ± 102.7 µg and 103.7 ± 50.6 µg, respectively after 24h. These values are much higher comparatively to other results reported in literature that were performed through native human skin, which may be related to the relatively weak barrier function of the *in vitro* RHE model used in this study. In order to validate this results it would be advantageous to perform an *ex vivo* absorption study using native human skin, since it was not found in literature another study describing the *in vitro* permeation of NLCs through a RHE model. The histology examination of the cultured skin membranes, 24h upon the administration of TOC-DiO-NLCs, revealed that the tissues presented a uniformly layered SC with larger interlamellar gaps between SC and the topmost layer of the epidermis, which might probably be attributed to the hydration and occlusion capacity of NLCs. The analysis by fluorescence microscopy and CLSM indicated a uniform permeation of TOC-DiO-NLCs into skin and that these lipid nanoparticles remained primarily located at the *SC* allowing the carrying and permeation of TOC across the tissue. It was also observed a heterogeneous distribution of the nanoparticles along the skin surface, which may indicate the accumulation of nanoparticles at thin pores of the skin, then following the intercellular permeation pathway.

Very high cell viabilities above 50% were obtained in the *in vitro* skin irritation testing, for all the produced NLCs formulations, classifying them as non-irritants. Moreover, it was demonstrated that the incorporation of RP that was classified as an irritant to the skin on NLCs successfully covered its associated cytotoxicity.

It was overall concluded that the produced NLCs are a feasible delivery system for the topical administration of lipophilic active compounds and that may be suitable to be incorporated into dermal formulations.

◢ CHAPTER VII

CONCLUSIONS

7. Conclusions

7.1.   Main Achievements

The production conditions of SLNs and NLCs, with appropriate properties for topical administration were established and optimized based on the miniemulsions methodology. It was demonstrated that the emulsification process have a significant influence on the physicochemical properties of these nanocarriers. SLNs produced using an ultrasounds probe presented more suitable characteristics, regarding their particle size and electrostatic stability, in comparison to magnetic stirring. The conditions set for the production of SLNs were successfully used for the production of NLCs presenting also appropriate properties for topical administration.

The optimization of NLCs composition was performed using four different vegetable oils as liquid lipids presenting inherent beneficial bioactive properties, thus conferring a multifunctional character to the nanoparticles. Moreover, the effect of an increase in the solid lipid fatty acid chain length was evaluated in the physicochemical properties of NLCs and also, the influence of four non-ionic surfactants with different HLB values was assessed. From this study, it was verified that the particle size, the size distribution and the electrostatic stability of the lipid nanoparticles are significantly influenced by the composition of the lipids core and by the type of used surfactant. Formulations of empty NLCs with different lipid matrices were obtained with an appropriate nanoscale size for topical administration and electrostatic stability. The lipid nanoparticles formulated with surfactants of hydrophilic character presented a polymorphic crystal structure of the lipid matrix, resembling NLCs of type I, which enables a proper incorporation of active substances encapsulated and exclude its expulsion after a longer period of storage.

Vegetable oil NLCs enriched with TOC which was used as a lipophilic drug model were successfully obtained presenting suitable physicochemical characteristics for topical administration, high EE values and high DL capacities. TOC-NLCs prepared with each vegetable oil demonstrated a well-controlled release profile in comparison with the standard TOC solution, thus indicating a high integration of TOC into the lipids core conferring to it an amplified protective effect and the minimization of its side-effects. Moreover, empty NLCs and TOC-NLCs prepared with each vegetable oil presented a good antioxidant capacity and remained stable for a period of 8 months.

Central composite design proved to be a powerful tool for studying the effects of NLCs formulation parameters and properties aiming to maximize their efficacy for topical administration. It was reached an optimal NLCs composition using RP, as a retinoid model to be encapsulated, which was then effectively used to incorporate TRT and ADP. Optimized RP-NLCs, TRT-NLCs and ADP-NLCs were obtained with appropriate particle sizes in the nanometre range, good electrostatic stability, high encapsulation efficiencies and very well-controlled release profiles for RP, TRT and ADP, reducing their secondary effects and physicochemical instability.

The optimized NLCs formulations prepared using sunflower oil and myristic acid as liquid and solid lipids, respectively and RP and TOC as lipophilic model drugs were tested *in vitro* using a 3D RHE model to assess their skin absorption and release profiles and their skin irritancy. The fluorescent dye DiO was effectively incorporated along with TOC, thus enabling a qualitative characterization of TOC-DiO-NLCs on *in vitro* absorption studies by fluorescence microscopy and CLSM. These studies revealed that TOC-DiO-NLCs permeated uniformly into skin and that these lipid nanoparticles remained primarily located at the *SC* allowing the carrying and permeation of TOC across the tissue. Moreover, it was shown a heterogeneous distribution of the lipid nanoparticles along the skin surface accumulating at thin pores of the skin, thus indicating that their permeation followed the intercellular pathway. The *in vitro* skin irritation testing of empty NLCs, RP-NLCs and TOC-DiO-NLCs formulations classified them and their ingredients as non-irritants. Also, it was proved that the incorporation of RP, which was labeled as an irritant substance to the skin in NLCs, successfully covered its associated cytotoxicity.

The designed NLCs formulations demonstrated to be a viable delivery system for the topical administration of lipophilic active compounds and may be considered as a promising proof-of-concept in the development of efficient biocosmetic prototypes with multifunctional skin beneficial properties derived from their natural ingredients.

7.2.   Future perspectives

The outlined future work includes:

(1) Investigate the potential of the NLCs formulation prepared by the miniemulsions methodology, using sunflower oil and myristic acid as liquid and solid lipids to incorporate hydrophilic active compounds by functionalizing their hydrophilic outer layer. The strategy is to test different mixtures of surfactants with high and low HLB values in order to simultaneously obtain a higher stabilization of the lipid core and of the outermost layer. Having reached a suitable composition in terms of surfactants mixtures and proportions, which would confer to the lipid nanoparticles appropriate physicochemical properties for topical administration, it would be advantageous to assess their functionalization with hydrophilic actives with dermal relevance as topical vitamins and enzymes. This study may additionally be coupled to the investigation of the encapsulation of lipophilic active compounds in the lipid matrix of the nanoparticles coupled with the functionalization of their hydrophilic outer layer, aiming to reach a higher dermal therapeutic level.

(2) Deliver a final formulation of NLCs testing the incorporation of the previously optimized lipid nanoparticles on commercial gelling agents, to improve its rheological behaviour and to ensure enhanced stability in effective topical applications. Although topical formulations can be produced consisting exclusively of lipid nanoparticles, their desired physicochemical properties can be adjusted by incorporating them in gels or creams. This study would address the use of different gelling agents, such as cellulose derivatives and to adjust the lipid nanoparticle content in view of achieving a sustainable cost effective formulation.

(3) A further interesting point to be outlined is to establish appropriate conditions for the scale up of the lipid nanoparticles production process. The miniemulsions methodology is a simple and effective method, allowing a fast screening of different formulations compositions at lab scale and is very useful to define a proof-of-concept. However, this methodology based in the use of ultrasounds cannot be used at industrial scale. Thus, it is important at this stage to evaluate the production of the optimized NLCs formulation through the miniemulsions methodology by another production methodology that would allow its scale up, as for instance high pressure homogenization.

(4) In view of an improvement in the stability of the physicochemical properties of the lipid nanoparticles during storage, it is crucial to develop a pre-treatment procedure for their lyophilisation. This pre-treatment may consist in concentrating the lipid nanoparticles or adjusting their composition by adding a cryoprotectant agent as for instance, glucose, fructose or sorbitol that have been used to decrease aggregations. Moreover, after the establishment of the pre-treatment procedure and set the conditions for the lyophilisation of the lipid nanoparticles it is necessary to evaluate its effect on their physicochemical properties in different storage conditions and periods.

(5) Concerning the *in vitro* absorption studies for the characterization of the lipid nanoparticles permeation and release profiles. It was found that the 3D *in vitro* RHE model that was used in this work demonstrated a relatively weak barrier function, which is assumed in literature to be an intrinsic characteristic of these *in vitro* cultured skin membranes. Thus, in order to validate the obtained results it would be advantageous to compare the absorption efficacy of the formulated lipid nanoparticles for topical administration through *ex vivo* native human or animal skin with the used RHE model.

APPENDIX A

PROCEDURE FOR RECONSTRUCTION OF HUMAN EPIDERMIS ON POLYCARBONATE FILTERS

APPENDIX A – Procedure for reconstruction of human epidermis on polycarbonate filters followed for the assays developed in Chapter 6

Keratinocytes were purchased from Life Technologies (Human Epidermal Keratinocytes, neonatal). This procedure was developed according to (De Vuyst et al., 2014) with a few adaptations as follows:

1. Thawing the keratinocytes, culture setting and culture growth

1.1. Preparation of supplemented medium KBM®-2 for culture setting

- A glass of water was heated to 37°C overnight, the day before the experience;
- In the day after, the SingleQuots® KGM-2® was thawed in the water bath at 37°C;
- The following list of material was taken into the laminar flow chamber:

    a. KBM®-2 Medium

    b. Antibiotics Pen/Strep stock

    c. SingleQuots® KGM-2®

    d. Schott flask x1

    e. Blue and yellow micropipette tips

    f. Sterile 25mL pipette x1

    g. Parafilm (x8, for both media flasks, antibiotics and SingleQuots® KGM-2®)

- KBM®-2 medium (100mL) was gently swirled and transferred to a Schott flask;
- Each supplement was added to the KBM®-2 medium to reach the final concentrations of 10ng/mL hEGF, 5µg/mL Insulin, 50µg/mL BPE, 5×10^{-7}M Hydrocortisone, 5µg/mL Transferrin, 50U/mL Penicillin G and 50µg/mL Streptomycin;
- The supplemented medium was stored at 4°C, which demonstrated to be stable at this temperature for one month.

1.2. Preparation of supplemented medium EpiLife® for culture growth

- A glass of water was heated to 37°C overnight, the day before the experience;
- In the day after, the Human Keratinocyte Growth Supplement (HKGS) was thawed in the water bath at 37°C;
- The following list of material was taken into the laminar flow chamber:

    a. EpiLife® Medium

    b. 0.06M Calcium Chloride

    c. Antibiotics Pen/Strep stock

    d. HKGS

    e. Blue and yellow micropipette tips

f. Schott flask x1

g. Sterile 5mL pipettes x3

h. Parafilm (x2, for the medium and antibiotics)

- EpiLife® medium (500mL) was gently swirled and transferred to a Schott flask;

- Each supplement was added to the EpiLife® medium to reach the final concentrations of 0.2% Bovine Pituitary Extract (BPE), 0.2ng/mL Human recombinant epidermal growth factor (hEGF), 0.18µg/mL Hydrocortisone, 5µg/mL Insulin and 5 µg/mL Transferrin, 2,5 mL Antibiotics – Penicillin G and Streptomycin stock, 5mL HKGS and 0,5 mL of 0.06M Calcium Chloride;

- The supplemented medium was stored at 4°C, which demonstrated to be stable at this temperature for one month.

1.3. Thawing the vial of cells and setting the keratinocytes culture

- A glass of water was heated to 37°C overnight, the day before the experience;

- The following list of material was taken into the laminar flow chamber:

a. KBM®-2 supplemented medium previously prepared

b. 20µL of trypan blue in small eppendorf

c. 50mL falcon and rack

d. Sterile 2mL, 5mL, 10mL pipettes x1

e. Blue and yellow micropipette tips

f. T_{75}-Flasks

- A vial (1mL) containing keratinocytes was removed from liquid nitrogen storage and its lower half was immediately submerged into the 37°C water bath for 1-2mins until the cells were thawed;

- KBM®-2 supplemented medium (4 mL) for culture setting was transferred to a 50mL falcon;

- The cell suspension (20µL) was transferred to a 2mL pipette and mixed with 20µL of trypan blue to perform the cell counting in a hemacytometer (the procedure will be described in the following section) to determine the number of viable cells per mL;

- After the cell counting, an appropriate volume of KBM®-2 supplemented medium was added to dilute the remaining cells in the vial to a concentration of 1.25×10^4 viable cells/mL and then the volume of culture medium and cells were distributed into T_{75}-flasks and were left in an humidified cell culture incubator at 37°C, 5% CO2/95% air;

- The culture medium was changed after 24-36 hours from KBM®-2 supplemented culture setting medium to EpiLife® culture growth medium (**Figure 1**);

- The EpiLife® culture growth medium was changed every two days until the cells reach a confluency of around 50% (**Figure 2**) and then was changed every day until the cells reach confluency of around 70-80% (**Figure 3**);

- The cells were then trypsinized (the procedure will be described in a posterior section) and posteriorly settled in new cultures, repeating twice the steps of section 1.3;

- The cells from the 3rd passage are ready to perform the reconstruction of epidermis on polycarbonate filters.
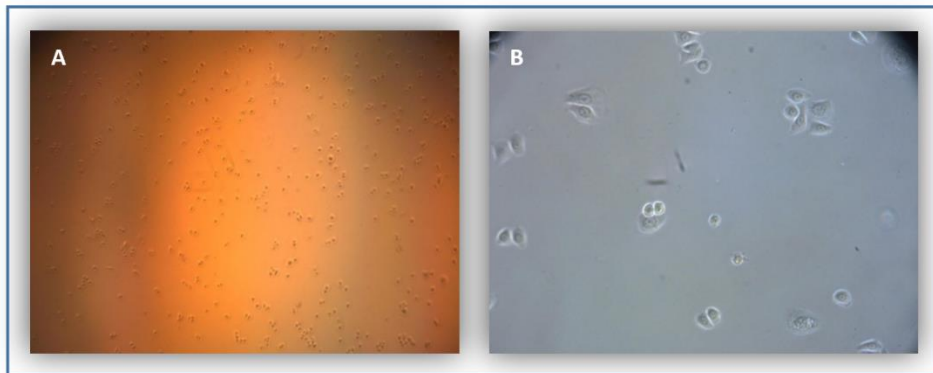
Figure 1 – Keratinocytes culture settle after day 1 with medium exchange. (A) Magnification of 40x; (B) Magnification of 600x.
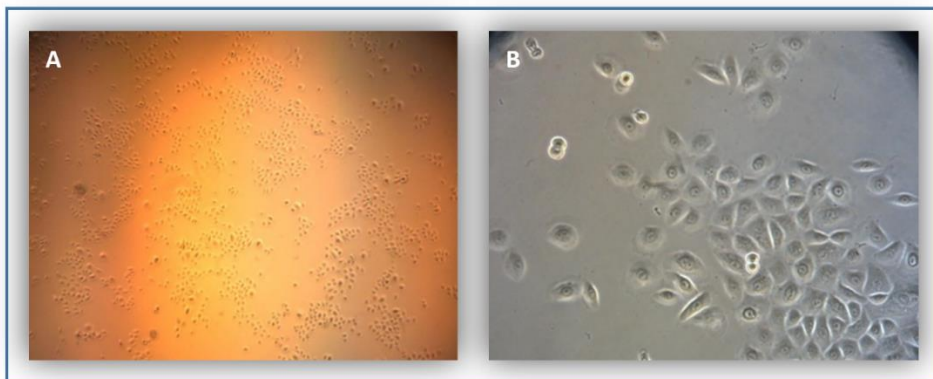
Figure 2 – Keratinocytes culture displaying a confluency of around 50%. (A) Magnification of 40x; (B) Magnification of 600x.
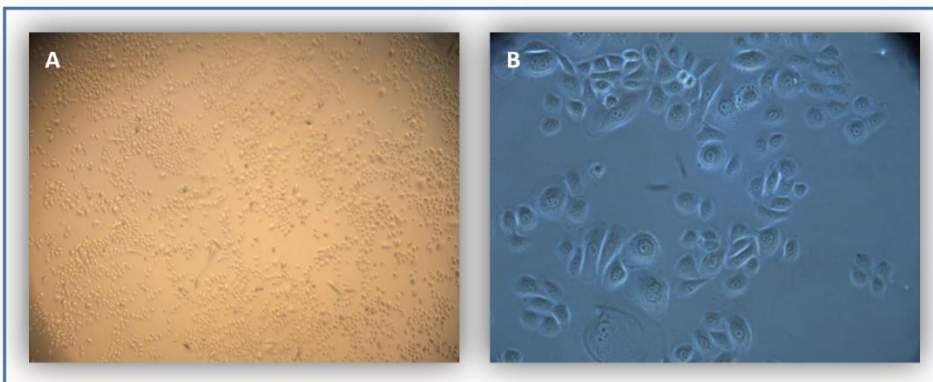
Figure 3 – Keratinocytes culture displaying a confluency of around 70-80%. (A) Magnification of 40x; (B) Magnification of 600x.

2. Counting cells in a Hemacytometer or Neubauer Chamber

The trypan blue exclusion assay allows for a direct identification and enumeration of live (unstained) and dead (blue) cells in a given population. It is based on the action of trypan blue azo dye which is impermeable to viable cell membranes and therefore can only enter on cells with compromised membranes (**Figure 4**). Upon entry into non-viable cells, trypan blue binds to intracellular proteins thereby rendering the cells a bluish colour.
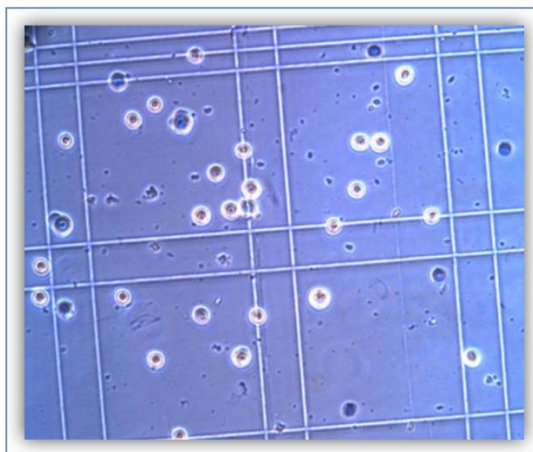
Figure 4 – Viable (bright white colored) and non-viable (blue colored) keratinocytes at the hemacytometer chamber after the mixture with the trypan blue dye.

- The hemacytometer was carefully cleaned with 70% EtOH and a coverslip was placed above one of the chambers;
- The cells mixed with the trypan blue solution (10 µL) were carefully placed (attention to not overfill) into one chamber compartment of the hemacytometer with a micropipete under the coverslip (**Figure 5**);
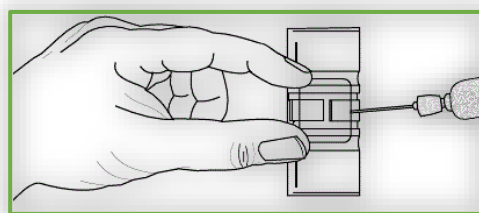
Figure 5 – Placing the sample into the hemacytometer chamber (LaboratoryInfo.com, 2016).

- The hemacytometer´s chamber was observed under the microscope to count the cells. The counting started in the the first counting grid square, following the rule (Bastidas, 2016): Cells touching the upper and left limits are counted, unlike cells touching the lower and right limits which are not included in the counting (**Figure 6**). Then, the process was repeated at other three grid squares and the results from the four readings were writhed for the further calculations;

 - After the counting, the coverslip was discarded and the hemacytometer was cleaned with 70% EtOH.
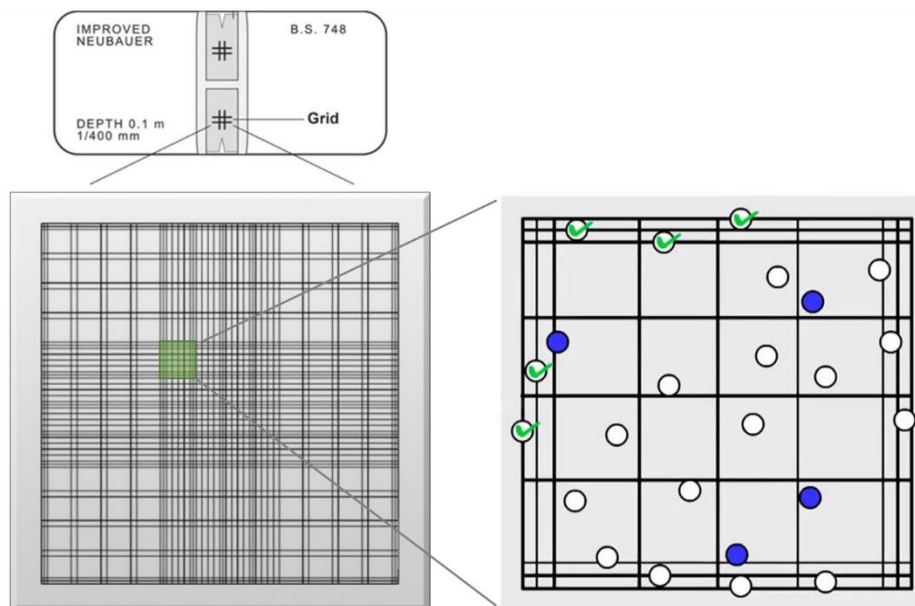
Figure 6 – Representation of a hemacytometer, with 2 chambers and gridded squares in each one with a detail of one grid square in one of the chambers where the rule of counting cells is exemplified. Adapted from (http://www.lo-laboroptik.com/, 2018).

- Calculations:

i. Dilution factor (D_f)

$$D_f = \frac{V_f}{V_i} = \frac{40\mu L}{20\mu L} = 2$$

V_i – Initial volume of cells

V_f – Volume of cells and trypan blue

ii. Average number of viable cells in each square (C_v)

$$C_v(cells/mL) = \frac{number\ of\ live\ cells\ in\ \#\ squares}{\#\ of\ squares}$$

iii. Count cell density/concentration (C_D)

$$C_D = C_v \times D_f \times 10^4$$

iv. Count total cells in your sample (C_T)

$$C_T = C_D \times V$$

V – Volume in which the cells are suspended

v. Viability (%)

$$Viability\ (\%) = \frac{Live\ cell\ count}{Live + Dead\ cell\ count} \times 100$$

3. Trypsinization of keratinocytes

3.1. Preparation of Solution A (250 mL) for washing the cells

- HEPES buffer was dissolved in approximately 200mL of Milli-Q water and the pH was adjusted at 7.4 with 10 M NaOH;
- All other components were added to this solution as follows and the pH was measured again before adjusting the final volume;

    a. 10.0 mM Glucose,

    b. 3.0 mM KCl,

    c. 130.0 mM NaCl,

    d. 1.0 mM Na$_2$HPO$_4$·7H$_2$O (or anhydrous),

    e. 0.0033 mM Phenol Red

    f. 30.0 mM HEPES

- The solution A was sterilized with a 0.22µm cellulose filter under the laminar flow chamber and stored refrigerated at 4°C.

3.2. Preparation of trypsin solution (100 mL) to dissociate the keratinocytes from the T-flasks and blocking solution (40 mL) to stop the action of trypsin

- The trypsin solution was prepared by transferring 200 mL of solution A to a glass to which was added 20 mg of EDTA (to reach the concentration of 0,01% EDTA), the pH was measured and set at 7.4 with NaOH;

- Then, 25mg of trypsin were added to 100mL of the solution A with 0,01% EDTA to obtain a 0.025% trypsin solution;

- This solution was sterilized with a 0.22µm cellulose filter and was left on ice.

- The blocking solution was prepared by transferring 40 mL of solution A to a glass and adding 800 µL of dialysed fetal calf serum (solution A containing 2% dialysed fetal calf serum).

- This solution was left on ice.

3.3. Trypsinization of 2nd and 3rd passage keratinocytes

Attention! – During trypsinization can occur some damage to cultured keratinocytes which may result from: (1) excessive exposure time to the trypsin/EDTA solution; (2) High room temperatures during trypsinization and (3) excessive mechanical agitation.

- Before starting the following material was prepared and taken into the laminar flow chamber:

   a. Trypsin and blocking solutions on ice;
   b. Sterile 5mL pipettes x1;
   c. Sterile 25mL pipettes x4;
   d. 50mL centrifugation tube x3 and rack;

- The exhausted culture medium was removed from the T-flask and 3mL of trypsin solution were gently added to the cells. The T-flask was then carefully agitated to guarantee that the trypsin solution was uniformly spread;

- The trypsinization process was analyzed under the microscope to verify the occurrence of cells detachment from the T-flasks;

- Under the microscope, the keratinocytes culture was incubated at room temperature until the cells become completely round, generally after 8-10 mins (**Figure 7, A**). After approximately 8 minutes some dry blows are given very gently to the lateral part of the T-flask to guarantee that the cells detach from it and that are loose on movement (**Figure 7, B**);

- Immediately after the ice-cold blocking solution (12 mL) was added to stop the trypsin effect.

- The keratinocytes suspension was then transferred to 10 mL tubes and was centrifuged at 1270 rpm and 4°C for 7 mins;

- The supernatant was aseptically discarded with a special attention to not aspirate also the cell pellet;

- The cell suspension was kept on ice until one of the following possible procedures were followed: (1) culture setting for a next passage, (2) reconstruction of epidermis with 3rd passage keratinocytes or (3) cryopreservation.
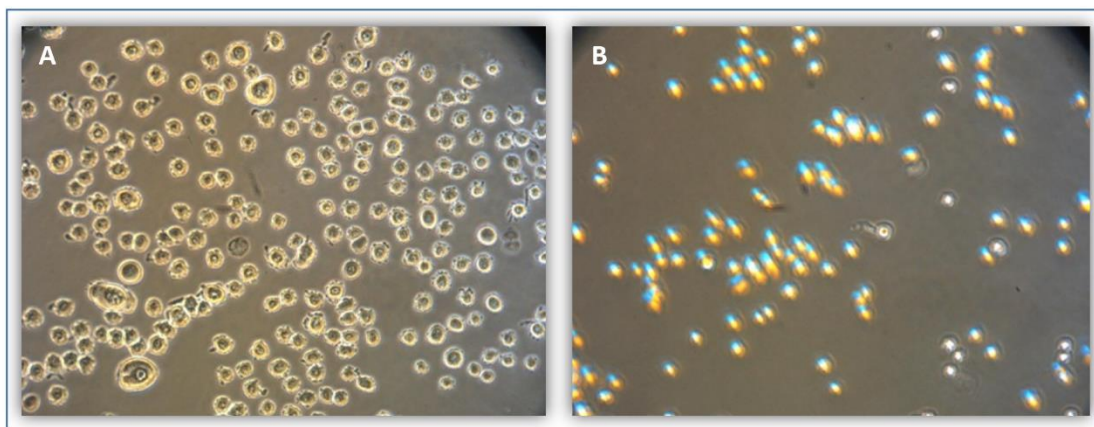
Figure 7 – Keratinocytes during the trypsinization process. (A) Keratinocytes displaying a round morphology being detached from the T-flask after 8 min with trypsin; (B) Keratinocytes completely detached from the T-flask and on movement after a gently blows on the lateral part of the flask.

4. Reconstruction of human epidermis on polycarbonate filters using 3rd passage keratinocytes

4.1. Preparation of solutions and culture mediums:

- Supplemented EpiLife® medium for culture growth (section 1.2)
- Sterilized solution of 0,5M $CaCl_2$:
    a.   0,14701g of $CaCl2 \cdot 2H2O$ was dissolved in 2mL of Milli-Q water;
    b.   This solution was filtered, covered with aluminium foil to avoid exposure to light and was kept on ice (this solution can be stored at -20°C).
- Reconstitution of Keratinocyte 100µg/mL Growth Factor:
    a.   1X Phospate Buffered Saline (PBS) solution (pH 7.4)
    b.   One pellet of KGF (10µg) was dissolved in 100µL of sterile PBS under the laminar flow hood (if KGF is in liquid phase (10µL), it is diluted in 90µL of sterile PBS);
    c.   The solution was kept on ice.
- Solution of 25mg/mL vitamin C:
    a.   25mg of L-ascorbic acid was dissolved in 1mL of Milli-Q water;
    b.   This solution was filtered, covered with aluminium foil to avoid exposure to light and was kept on ice (this solution can only be used at the day of preparation).
- Preparation of 50mL of medium for culture growth containing 1.5mM Ca^{2+} (work under the hood):
    a.   EpiLife medium for culture growth (50 mL) was transferred to one falcon and was supplemented with 144µL of 0,5M $CaCl_2$ solution;

b. The bottle of supplemented medium was sealed with parafilm and swirled to ensure a homogeneous solution;

c. The medium was kept on ice.

- Preparation of medium for epidermis reconstruction at an air-liquid interface (100mL)

(EpiLife® medium for culture growth with 1.5mM Ca^{2+}, 50µg/mL vitamin C and 10ng/mL KGF) EpiLife® for culture growth (100 mL) was transferred to one Schott flask and was supplemented with:

a. 288µL of 0,5M CaCl2 solution;

b. 10µL of 100µg/mL KGF solution;

c. 200µL of 25mg/mL vitamin C solution;

d. The bottle of supplemented medium was sealed with parafilm and swirled to ensure a homogeneous solution;

e. The medium was kept on ice.

- Preparation of freezing solution (the final concentration of freezing conditions are: 80% medium, 10% DMSO, 10% dialysed fetal calf serum);

4.2. Reconstruction of epidermis:

- The following list of material was taken into the laminar flow chamber:

a. Supplemented EpiLife medium for culture growth;

b. Solutions of Ca2+, KGF and vitamin C;

c. Dialysed fetal calf serum;

d. Centrifugation tube with 3rd passage keratinocytes (section 3.3)

e. 6-well culture microplate;

f. Polycarbonate culture inserts with 12mm diameter and 0.4µm diameter pore size x6;

g. 50mL falcon x2 and rack;

h. Schott flask x1;

i. Sterile 1mL, 2mL and 10mL pipettes;

j. Sterile tweezers x1;

k. Parafilm;

- The keratinocytes pellet (section 3.3) was re-suspended on 2-3mL of ice-cold medium for culture growth supplemented with 1.5mM calcium;

- After cells counting, the suspension was diluted with medium for culture growth containing 1.5mM calcium to a minimal cell density of 3×10^5 cells/mL;

- 6 polycarbonate culture inserts were placed into a 6-well culture microplate before adding the culture medium (This will avoid the formation of air bubbles between the filters and the bottom of the microplate);

- 2.5mL of EpiLife® medium for culture growth containing 1.5mM calcium and vitamin C was transferred into the each well of the microplate;

- 500μL of keratinocyte suspension was transferred to the upper chamber of each insert

- The cells were incubated at 37°C in a humidified atmosphere containing 5% CO_2;

- After 24h, the culture was exposed to the air-liquid interface by carefully removing the culture medium in the upper compartment of the insert;

- The medium in the microplate compartment was replaced with 1.5 mL of EpiLife® medium for culture growth containing 1.5mM calcium and vitamin C;

- This culture medium was replaced every 48h and after 11 days of culture at the air–liquid interface, the RHE was morphologically fully differentiated (**Figure 8**).
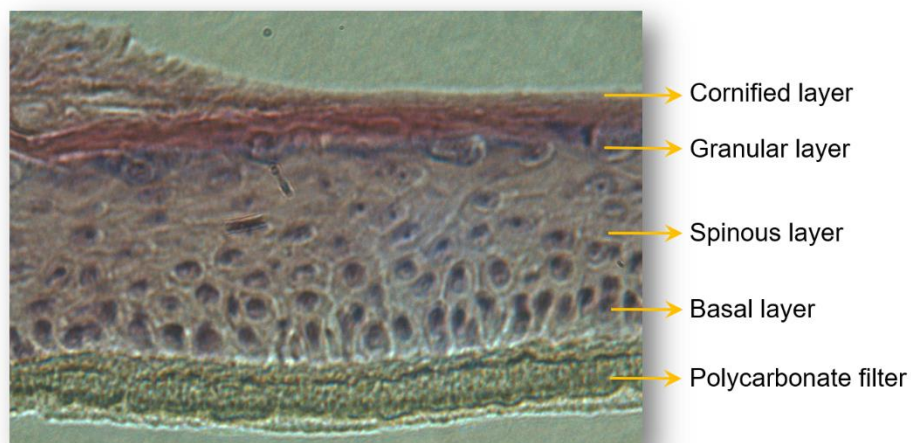
Figure 8 – Reconstructed human epidermis (RHE) at day 11. The cultured RHE was fixed in 10 % formalin and embedded in paraffin, then histological sections perpendicular to the surface of RHE were prepared and stained with hematoxylin-erythrosine to allow the morphological analysis.

5. Cryopreservation of keratinocytes

- The following list of material was taken into the laminar flow chamber:

   a. EpiLife medium for culture growth;

   b. DMSO;

   c. Dialysed fetal calf serum;

   d. Centrifugation tubes with cell pellet (section)

   e. Cryopreservation tubes;

   f. Sterile 2mL pipettes x2;

   g. Sterile 5mL pipettes x2;

   h. Sterile 10mL pipettes x2;

1. Parafilm

- The pellet of keratinocytes from trypsinization (section 3.3) was re-suspend in 2mL of ice-cold EpiLife® medium for culture growth and was kept on ice;

- After counting the cells, were diluted with ice-cold EpiLife medium to achieve a concentration of 2 x 10^6 cells/mL and the same volume of freezing solution was added same volume (e.g. 1mL of EpiLife® + 1 mL of freezing solution);

- One aliquot (1 mL) of cells in freezing solution was transferred into each ice-cold cryopreservation tubes, which were then placed into a polystyrene isolating box and stored at -80°C for 24h and after into liquid nitrogen.

REFERENCES

ABDEL-SALAM, F. S., AMMAR, H. O., ELKHESHEN, S. A. & MAHMOUD, A. A. 2017. Anti-inflammatory sunscreen nanostructured lipid carrier formulations. *Journal of Drug Delivery Science and Technology,* 37**,** 13-19.

ABDOLAHPOUR, S., MAHDIEH, N., JAMALI, Z., AKBARZADEH, A. & TOLIYAT, T. 2017. Development of Doxorubicin-Loaded Nanostructured Lipid Carriers: Preparation, Characterization, and In Vitro Evaluation on MCF-7 Cell Line. *BioNanoScience*, 7**,** 32-37

ABLA, M. J. & BANGA, A. K. 2013. Quantification of skin penetration of antioxidants of varying lipophilicity. *International Journal of Cosmetics Science,* 35**,** 19-26.

ABLA, M. J. & BANGA, A. K. 2014. Formulation of tocopherol nanocarriers and in vitro delivery into human skin. *Int J Cosmet Sci,* 36**,** 239-46.

ABLA, M. J., SINGH, N. D. & BANGA, A. K. 2016. Role of nanotechnology in skin delivery of drugs. Percutaneous Penetration Enhancers Chemical Methods in Penetration Enhancement. *Springer. Berlin, Heidelberg.* 1-33

ADITYA, N., MACEDO, A. S., DOKTOROVOVA, S., SOUTO, E. B., KIM, S., CHANG, P.-S. & KO, S. 2014. Development and evaluation of lipid nanocarriers for quercetin delivery: a comparative study of solid lipid nanoparticles (SLN), nanostructured lipid carriers (NLC), and lipid nanoemulsions (LNE). *LWT-Food Science and Technology,* 59**,** 115-121.

ADITYA P. NAYAK, E. S. F. S., RAYASA S.R. MURTHY AND ELIANA B. SOUTO 2011. Lipid Nanoparticles in Cancer Therapy: Past, Present and Future. Lipid Nanocarriers in Cancer Diagnosis and Therapy. Eliana B. Souto ed. Shawbury, Shrewsbury, Shropshire, SY4 4NR, United Kingdom Smithers Rapra.

AGRAWAL, Y., PETKAR, K. C. & SAWANT, K. K. 2010. Development, evaluation and clinical studies of Acitretin loaded nanostructured lipid carriers for topical treatment of psoriasis. *International Journal of Pharmaceutics,* 401**,** 93-102.

AKHOOND ZARDINI, A., MOHEBBI, M., FARHOOSH, R. & BOLURIAN, S. 2018. Production and characterization of nanostructured lipid carriers and solid lipid nanoparticles containing lycopene for food fortification. *Journal of Food Science and Technology,* 55**,** 287-298.

ALEXANDER, A., DWIVEDI, S., AJAZUDDIN, GIRI, T. K., SARAF, S., SARAF, S. & TRIPATHI, D. K. 2012. Approaches for breaking the barriers of drug permeation through transdermal drug delivery. *Journal of Controlled Release,* 164**,** 26-40.

ALI, H., EL-SAYED, K., SYLVESTER, P. W. & NAZZAL, S. 2010. Molecular interaction and localization of tocotrienol-rich fraction (TRF) within the matrices of lipid nanoparticles: evidence studies by Differential Scanning Calorimetry (DSC) and

Proton Nuclear Magnetic Resonance spectroscopy ((1)H NMR). *Colloids and Surfaces B Biointerfaces,* 77**,** 286-97.

ALVAREZ-ROMAN, R., NAIK, A., KALIA, Y. N., FESSI, H. & GUY, R. H. 2004. Visualization of skin penetration using confocal laser scanning microscopy. *Eur J Pharm Biopharm,* 58**,** 301-16.

ALVAREZ-TRABADO, J., DIEBOLD, Y. & SANCHEZ, A. 2017. Designing Lipid Nanoparticles for Topical Ocular Drug Delivery. *International journal of pharmaceutics*.

ARAÚJO, J., NIKOLIC, S., EGEA, M. A., SOUTO, E. B. & GARCIA, M. L. 2011. Nanostructured lipid carriers for triamcinolone acetonide delivery to the posterior segment of the eye. *Colloids and Surfaces B: Biointerfaces,* 88**,** 150-157.

ARGENTA, D. F., BIDONE, J., KOESTER, L. S., BASSANI, V. L., SIMOES, C. M. O. & TEIXEIRA, H. F. 2018. Topical Delivery of Coumestrol from Lipid Nanoemulsions Thickened with Hydroxyethylcellulose for Antiherpes Treatment. *AAPS PharmSciTech,* 19**,** 192-200.

ARYA, J., HENRY, S., KALLURI, H., MCALLISTER, D. V., PEWIN, W. P. & PRAUSNITZ, M. R. 2017. Tolerability, usability and acceptability of dissolving microneedle patch administration in human subjects. *Biomaterials,* 128**,** 1-7.

ASLAM, M., AQIL, M., AHAD, A., NAJMI, A. K., SULTANA, Y. & ALI, A. 2016. Application of Box–Behnken design for preparation of glibenclamide loaded lipid based nanoparticles: Optimization, in vitro skin permeation, drug release and in vivo pharmacokinetic study. *Journal of Molecular Liquids,* 219**,** 897-908.

ATTAMA, A. A., MOMOH, M. A. & BUILDERS, P. F. 2012. Lipid Nanoparticulate Drug Delivery Systems: A Revolution in Dosage Form Design and Development. *In:* SEZER, A. D. (ed.) *Recent Advances in Novel Drug Carrier Systems.* 107-140

AUXENFANS, C., FRADETTE, J., LEQUEUX, C., GERMAIN, L., KINIKOGLU, B., BECHETOILLE, N., BRAYE, F., AUGER, F. A. & DAMOUR, O. 2009. Evolution of three dimensional skin equivalent models reconstructed in vitro by tissue engineering. *Eur J Dermatol,* 19**,** 107-13.

AZEEM, A., KHAN, Z. I., AQIL, M., AHMAD, F. J., KHAR, R. K. & TALEGAONKAR, S. 2009. Microemulsions as a Surrogate Carrier for Dermal Drug Delivery. *Drug Development and Industrial Pharmacy,* 35**,** 525-547.

BADEA, G., LĂCĂTUŞU, I., BADEA, N., OTT, C. & MEGHEA, A. 2015. Use of various vegetable oils in designing photoprotective nanostructured formulations for UV protection and antioxidant activity. *Industrial Crops and Products,* 67**,** 18-24.

BAKONYI, M., BERKÓ, S., KOVÁCS, A., BUDAI-SZŰCS, M., KIS, N., ERŐS, G., CSÓKA, I. & CSÁNYI, E. 2018. Application of quality by design principles in the development and evaluation of semisolid drug carrier systems for the transdermal delivery of lidocaine. *Journal of Drug Delivery Science and Technology,* 44**,** 136-145.

BALAKRISHNAN, A., REGE, B. D., AMIDON, G. L. & POLLI, J. E. 2004. Surfactant-mediated dissolution: Contributions of solubility enhancement and relatively low micelle diffusivity. *Journal of pharmaceutical sciences,* 93**,** 2064-2075.

BALBOA, E. M., SOTO, M. L., NOGUEIRA, D. R., GONZÁLEZ-LÓPEZ, N., CONDE, E., MOURE, A., VINARDELL, M. P., MITJANS, M. & DOMÍNGUEZ, H. 2014. Potential of antioxidant extracts produced by aqueous processing of renewable resources for the formulation of cosmetics. *Industrial Crops and Products,* 58**,** 104-110.

BANGA, A. K. 2011. Transdermal and intradermal delivery of therapeutic agents: application of physical technologies, *CRC Press* Book.

BANGHAM, A. D. & HORNE, R. W. 1964. Negative staining of phospholipids and their structural modification by surface-active agents as observed in the electron microscope. *Journal of Molecular Biology,* 8**,** 660-IN10.

BASTIDAS, O. 2016. Cell Counting with Neubauer Chamber - Basic Hemocytometer Usage. *http://www.celeromics.com/en/resources/docs/Articles/Cell-counting-Neubauer-chamber.pdf*

BELLAS, E., SEIBERG, M., GARLICK, J. & KAPLAN, D. L. 2012. In vitro 3D full-thickness skin-equivalent tissue model using silk and collagen biomaterials. *Macromol Biosci,* 12**,** 1627-36.

BELLISSENT-FUNEL, M. C. 1999. Hydration Processes in Biology: Theoretical and Experimental Approaches, *NATO Science Series: Life Sciences*, 305**,** IOS Press.

BELOQUI, A., SOLINIS, M. A., RODRIGUEZ-GASCON, A., ALMEIDA, A. J. & PREAT, V. 2016. Nanostructured lipid carriers: Promising drug delivery systems for future clinics. *Nanomedicine,* 12**,** 143-61.

BENSON, H. A. 2012. Skin structure, function, and permeation. *Topical and Transdermal Drug Delivery: Principles and Practice***,** 1-22.

BHALEKAR, M., UPADHAYA, P. & MADGULKAR, A. 2015. Formulation and evaluation of Adapalene-loaded nanoparticulates for epidermal localization. *Drug Deliv Transl Res,* 5**,** 585-95.

BHISE, K., KASHAW, S. K., SAU, S. & IYER, A. K. 2017. Nanostructured lipid carriers employing polyphenols as promising anticancer agents: quality by design (QbD) approach. *International journal of pharmaceutics,* 526**,** 506-515.

BHOYAR, N., GIRI, T. K., TRIPATHI, D. K., ALEXANDER, A. & AJAZ, A. 2012. Recent advances in novel drug delivery system through gels: Review. *Journal of Pharmacy and Allied Health Sciences* 2**,** 21-29

BISSETT, D. L., OBLONG, J. E. & BERGE, C. A. 2005. Niacinamide: A B vitamin that improves aging facial skin appearance. *Dermatologic Surgery,* 31**,** 860-5; discussion 865.

BJORKEGREN, S., KARIMI, R. F., MARTINELLI, A., JAYAKUMAR, N. S. & HASHIM, M. A. 2015. A new emulsion liquid membrane based on a palm oil for the extraction of heavy metals. *Membranes (Basel),* 5**,** 168-79.

BLASI, P., SCHOUBBEN, A., ROMANO, G. V., GIOVAGNOLI, S., DI MICHELE, A. & RICCI, M. 2013. Lipid nanoparticles for brain targeting II. Technological characterization. *Colloids and Surfaces B: Biointerfaces,* 110**,** 130-137.

BOCCA, C., CAPUTO, O., CAVALLI, R., GABRIEL, L., MIGLIETTA, A. & GASCO, M. R. 1998. Phagocytic uptake of fluorescent stealth and non-stealth solid lipid nanoparticles. *International Journal of Pharmaceutics,* 175**,** 185-193.

BRISAERT, M. & PLAIZIER-VERCAMMEN, J. 2000. Investigation on the photostability of a tretinoin lotion and stabilization with additives. *International Journal of Pharmaceutics,* 199**,** 49-57.

BUNJES, H., KOCH, M. H. & WESTESEN, K. 2003. Influence of emulsifiers on the crystallization of solid lipid nanoparticles. *Journal of Pharmaceutical Sciences,* 92**,** 1509-20.

BUNJES, H., STEINIGER, F. & RICHTER, W. 2007. Visualizing the Structure of Triglyceride Nanoparticles in Different Crystal Modifications. *American Chemical Society*, 23 (7)**,** pp 4005–4011

BYUN, Y., HWANG, J. B., BANG, S. H., DARBY, D., COOKSEY, K., DAWSON, P. L., PARK, H. J. & WHITESIDE, S. 2011. Formulation and characterization of α-tocopherol loaded poly ε-caprolactone (PCL) nanoparticles. *LWT - Food Science and Technology,* 44**,** 24-28.

CALIXTO, G. M. F., BERNEGOSSI, J., DE FREITAS, L. M., FONTANA, C. R. & CHORILLI, M. 2016. Nanotechnology-based drug delivery systems for photodynamic therapy of cancer: a review. *Molecules,* 21**,** 342.

CARBONE, C., MARTINS-GOMES, C., PEPE, V., SILVA, A., MUSUMECI, T., PUGLISI, G., FURNERI, P. & SOUTO, E. 2018. Repurposing itraconazole to the benefit of skin cancer treatment: a combined azole-DDAB nanoencapsulation strategy. *Colloids and Surfaces B: Biointerfaces,* 167**,** 337-344

CASANOVA, F. & SANTOS, L. 2016. Encapsulation of cosmetic active ingredients for topical application--a review. *Journal of Microencapsulation,* 33**,** 1-17.

CASTRO, G., ORÉFICE, R., VILELA, J., ANDRADE, M. & FERREIRA, L. 2007. Development of a new solid lipid nanoparticle formulation containing retinoic acid for topical treatment of acne. *Journal of Microencapsulation*, 24(5):395-407

CAVALLI, R., BARGONI, A., PODIO, V., MUNTONI, E., ZARA, G. P. & GASCO, M. R. 2003. Duodenal administration of solid lipid nanoparticles loaded with different percentages of tobramycin. *Journal of Pharmaceutical Sciences,* 92**,** 1085-94.

CEVC, G. & VIERL, U. 2010. Nanotechnology and the transdermal route: A state of the art review and critical appraisal. *Journal of Controlled Release,* 141**,** 277-299.

CHARCOSSET, C., EL-HARATI, A. & FESSI, H. 2005. Preparation of solid lipid nanoparticles using a membrane contactor. *Journal of Control Release,* 108**,** 112-20.

CHARCOSSET, C. & FESSI, H. 2005. Preparation of nanoparticles with a membrane contactor. *Journal of Membrane Science,* 266**,** 115-120.

CHATTOPADHYAY, P., SHEKUNOV, B. Y., YIM, D., CIPOLLA, D., BOYD, B. & FARR, S. 2007. Production of solid lipid nanoparticle suspensions using supercritical fluid extraction of emulsions (SFEE) for pulmonary delivery using the AERx system. *Advances in Drug Delivery Reviews,* 59**,** 444-53.

CHE MAN, Y. B. & TAN, C.-P. 2012. CHAPTER 2 - Carotenoids A2 - GUNSTONE, FRANK D. *Lipids for Functional Foods and Nutraceuticals.* Woodhead Publishing.

CHEN-YU, G., CHUN-FEN, Y., QI-LU, L., QI, T., YAN-WEI, X., WEI-NA, L. & GUANG-XI, Z. 2012. Development of a Quercetin-loaded nanostructured lipid carrier formulation for topical delivery. *International Journal of Pharmaceutics,* 430**,** 292-298.

CHEN, C. C., TSAI, T. H., HUANG, Z. R. & FANG, J. Y. 2010. Effects of lipophilic emulsifiers on the oral administration of lovastatin from nanostructured lipid carriers: physicochemical characterization and pharmacokinetics. *European Journal of Pharmaceutics and Biopharmaceutics,* 74**,** 474-82.

CHEN, G., HOU, S.-X., HU, P., HU, Q.-H., GUO, D.-D. & XIAO, Y. 2008. In vitro dexamethasone release from nanoparticles and its pharmacokinetics in the inner ear after administration of the drug-loaded nanoparticles via the round window. *Southern medical journal*, 28(6):1022-4.

CHEN, J., WEI, N., LOPEZ-GARCIA, M., AMBROSE, D., LEE, J., ANNELIN, C. & PETERSON, T. 2017. Development and evaluation of resveratrol, Vitamin E, and epigallocatechin gallate loaded lipid nanoparticles for skin care applications. *European Journal of Pharmaceutics and Biopharmaceutics,* 117**,** 286-291.

CHEN, Y.-C., TSAI, P.-J., HUANG, Y.-B. & WU, P.-C. 2015. Optimization and Validation of High-Performance Chromatographic Condition for Simultaneous Determination of Adapalene and Benzoyl Peroxide by Response Surface Methodology. *PLoS ONE,* 10**,** e0120171.

CHITTENDEN, J. T., BROOKS, J. D. & RIVIERE, J. E. 2014. Development of a mixed-effect pharmacokinetic model for vehicle modulated in vitro transdermal flux of topically applied penetrants. *Journal of Pharmaceutial Sciences,* 103**,** 1002-12.

CHOI, S. W., PANGENI, R. & PARK, J. W. 2017. Nanoemulsion-Based Hydrogel for Topical Delivery of Highly Skin-Permeable Growth Factor Combinations: Preparation and In Vitro Evaluation. *Journal of Nanoscience and Nanotechnology,* 17**,** 2363-369.

CICERALE, S., LUCAS, L. & KEAST, R. 2012. Antimicrobial, antioxidant and anti-inflammatory phenolic activities in extra virgin olive oil. *Current opinion in biotechnology,* 23**,** 129-135.

CIRRI, M., BRAGAGNI, M., MENNINI, N. & MURA, P. 2012. Development of a new delivery system consisting in "drug – in cyclodextrin – in nanostructured lipid carriers" for ketoprofen topical delivery. *European Journal of Pharmaceutics and Biopharmaceutics,* 80**,** 46-53.

CLARES, B., CALPENA, A. C., PARRA, A., ABREGO, G., ALVARADO, H., FANGUEIRO, J. F. & SOUTO, E. B. 2014. Nanoemulsions (NEs), liposomes (LPs)

and solid lipid nanoparticles (SLNs) for retinyl palmitate: effect on skin permeation. *International journal of pharmaceutics,* 473**,** 591-598.

CONSTANTINIDES, P. P., LAMBERT, K. J., TUSTIAN, A. K., SCHNEIDER, B., LALJI, S., MA, W., WENTZEL, B., KESSLER, D., WORAH, D. & QUAY, S. C. 2000. Formulation development and antitumor activity of a filter-sterilizable emulsion of paclitaxel. *Pharmaceutical Research,* 17**,** 175-82.

CONTRI, R. V., FIEL, L. A., POHLMANN, A. R., GUTERRES, S. S. & BECK, R. C. 2011. Transport of substances and nanoparticles across the skin and in vitro models to evaluate skin permeation and/or penetration. *Nanocosmetics and Nanomedicines.* Springer.

CORTESI, R., ESPOSITO, E., LUCA, G. & NASTRUZZI, C. 2002. Production of lipospheres as carriers for bioactive compounds. *Biomaterials,* 23**,** 2283-2294.

CORTESI, R., VALACCHI, G., MURESAN, X. M., DRECHSLER, M., CONTADO, C., ESPOSITO, E., GRANDINI, A., GUERRINI, A., FORLANI, G. & SACCHETTI, G. 2017. Nanostructured lipid carriers (NLC) for the delivery of natural molecules with antimicrobial activity: production, characterisation and in vitro studies. *J Microencapsul,* 34**,** 63-72.

COSTA, R. & SANTOS, L. 2017. Delivery systems for cosmetics - From manufacturing to the skin of natural antioxidants. *Powder Technology,* 322**,** 402-416.

DA SILVA, G. H. R., RIBEIRO, L. N., MITSUTAKE, H., GUILHERME, V. A., CASTRO, S. R., POPPI, R. J., BREITKREITZ, M. C. & DE PAULA, E. 2017. Optimised NLC: a nanotechnological approach to improve the anaesthetic effect of bupivacaine. *International Journal of Pharmaceutics,* 529**,** 253-263.

DANESHMAND, S., JAAFARI, M. R., MOVAFFAGH, J., MALAEKEH-NIKOUEI, B., IRANSHAHI, M., SEYEDIAN MOGHADDAM, A., TAYARANI NAJARAN, Z. & GOLMOHAMMADZADEH, S. 2018. Preparation, characterization, and optimization of auraptene-loaded solid lipid nanoparticles as a natural anti-inflammatory agent: In vivo and in vitro evaluations. *Colloids and Surfaces B: Biointerfaces,* 164**,** 332-339.

DARIO, M. F., OLIVEIRA, F. F., MARINS, D. S. S., BABY, A. R., VELASCO, M. V. R., LÖBENBERG, R. & BOU-CHACRA, N. A. 2018. Synergistic photoprotective activity of nanocarrier containing oil of Acrocomia aculeata (Jacq.) Lodd. Ex. Martius—Arecaceae. *Industrial Crops and Products,* 112**,** 305-312.

DAS, S. & CHAUDHURY, A. 2011. Recent advances in lipid nanoparticle formulations with solid matrix for oral drug delivery. *Aaps Pharmscitech,* 12**,** 62-76.

DE CARVALHO, S. M., NORONHA, C. M., FLORIANI, C. L., LINO, R. C., ROCHA, G., BELLETTINI, I. C., OGLIARI, P. J. & BARRETO, P. L. M. 2013. Optimization of α-tocopherol loaded solid lipid nanoparticles by central composite design. *Industrial Crops and Products,* 49**,** 278-285.

DE NÓVOA, E. G., FÁVARO, R., SILVINO, T. S., RIBEIRO, F. C., SANTOS, R. M. & COSTA, A. 2015. Menopause and Cosmeceuticals. *Skin, Mucosa and Menopause.* Springer.

DE VRINGER, T. 1997. Topical preparation containing a suspension of solid lipid particles. *Google Patents.*

DE VUYST, E., CHARLIER, C., GILTAIRE, S., DE GLAS, V., DE ROUVROIT, C. L. & POUMAY, Y. 2014. Reconstruction of normal and pathological human epidermis on polycarbonate filter. *Methods in Molecular Biology,* 1195**,** 191-201.

DE WEVER, B., KURDYKOWSKI, S. & DESCARGUES, P. 2015. Human skin models for research applications in pharmacology and toxicology: Introducing NativeSkin®, the "missing link" bridging cell culture and/or reconstructed skin models and human clinical testing. *Applied In Vitro Toxicology,* 1**,** 26-32.

DHAVAMANI, S., POORNA CHANDRA RAO, Y. & LOKESH, B. R. 2014. Total antioxidant activity of selected vegetable oils and their influence on total antioxidant values in vivo: a photochemiluminescence based analysis. *Food Chemistry,* 164**,** 551-5.

DOKTOROVOVA, S., SHEGOKAR, R., FERNANDES, L., MARTINS-LOPES, P., SILVA, A. M., MULLER, R. H. & SOUTO, E. B. 2014a. Trehalose is not a universal solution for solid lipid nanoparticles freeze-drying. *Pharmaceutical Development and Technology,* 19**,** 922-9.

DOKTOROVOVA, S., SOUTO, E. B. & SILVA, A. M. 2014b. Nanotoxicology applied to solid lipid nanoparticles and nanostructured lipid carriers - a systematic review of in vitro data. *European Journal of Pharmaceutics and Biopharmaceutics,* 87**,** 1-18.

DORA, C. P., SINGH, S. K., KUMAR, S., DATUSALIA, A. K. & DEEP, A. 2010. Development and characterization of nanoparticles of glibenclamide by solvent displacement method. *Acta Poloniae Pharmaceutica,* 67**,** 283-90.

DORRANI, M., GARBUZENKO, O. B., MINKO, T. & MICHNIAK-KOHN, B. 2016. Development of edge-activated liposomes for siRNA delivery to human basal epidermis for melanoma therapy. *Journal of Controlled Release,* 228**,** 150-158.

DRAELOS, Z. D. 2012. Cosmetics, categories, and the future. *Dermatologic Therapy,* 25**,** 223-8.

DURÁN-LOBATO, M., ENGUIX-GONZÁLEZ, A., FERNÁNDEZ-ARÉVALO, M. & MARTÍN-BANDERAS, L. 2013. Statistical analysis of solid lipid nanoparticles produced by high-pressure homogenization: a practical prediction approach. *Journal of Nanoparticle Research,* 15**,** 1443.

EKAMBARAM, P., SATHALI, A. A. H. & PRIYANKA, K. 2012. Solid lipid nanoparticles: a review. *Scientific Reviews and Chemical Communications,* 2.

EL MAGHRABY, G. M., BARRY, B. W. & WILLIAMS, A. C. 2008. Liposomes and skin: From drug delivery to model membranes. *European Journal of Pharmaceutical Sciences,* 34**,** 203-222.

ESCOBAR-CHÁVEZ, J. J., RODRÍGUEZ-CRUZ, I. M., DOMÍNGUEZ-DELGADO, C. L., DÍAZ-TORRES, R., REVILLA-VÁZQUEZ, A. L. & ALÉNCASTER, N. C. 2012. Nanocarrier systems for transdermal drug delivery. *Recent Advances in Novel Drug Carrier Systems. 8,* 201-240 Intech.

ESKANDAR, N. G., SIMOVIC, S. & PRESTIDGE, C. A. 2009. Chemical stability and phase distribution of all-trans-retinol in nanoparticle-coated emulsions. *International Journal of Pharmaceutics,* 376**,** 186-94.

ESTANQUEIRO, M., AMARAL, M. H. & LOBO, J. M. S. 2017. Lipid-Based Nanocarriers in Cancer Therapy. *Multifunctional Systems for Combined Delivery, Biosensing and Diagnostics,* 51-66

ESTANQUEIRO, M., CONCEICAO, J., AMARAL, M. H. & SOUSA LOBO, J. M. 2014. Characterization, sensorial evaluation and moisturizing efficacy of nanolipidgel formulations. *International Journal of Cosmetic Science,* 36**,** 159-66.

ESTELLA-HERMOSO DE MENDOZA, A., RAYO, M., MOLLINEDO, F. & BLANCO-PRIETO, M. J. 2008. Lipid nanoparticles for alkyl lysophospholipid edelfosine encapsulation: Development and in vitro characterization. *European Journal of Pharmaceutics and Biopharmaceutics,* 68**,** 207-213.

FADDA, P., MONDUZZI, M., CABOI, F., PIRAS, S. & LAZZARI, P. 2013. Solid lipid nanoparticle preparation by a warm microemulsion based process: influence of microemulsion microstructure. *International Journal of Pharmaceutics,* 446**,** 166-75.

FANG, C.-L., A AL-SUWAYEH, S. & FANG, J.-Y. 2013. Nanostructured lipid carriers (NLCs) for drug delivery and targeting. *Recent patents on nanotechnology,* 7**,** 41-55.

FANG, J.-Y., FANG, C.-L., LIU, C.-H. & SU, Y.-H. 2008. Lipid nanoparticles as vehicles for topical psoralen delivery: Solid lipid nanoparticles (SLN) versus nanostructured lipid carriers (NLC). *European Journal of Pharmaceutics and Biopharmaceutics,* 70**,** 633-640.

FENG, L. & MUMPER, R. J. 2013. A Critical Review of Lipid-based Nanoparticles for Taxane Delivery. *Cancer letters,* 334**,** 157-175.

FLATEN, G. E., PALAC, Z., ENGESLAND, A., FILIPOVIC-GRCIC, J., VANIC, Z. & SKALKO-BASNET, N. 2015. In vitro skin models as a tool in optimization of drug formulation. *European Journal of Pharmaceutical Sciences,* 75**,** 10-24.

FRIEDLAND, J. A. & BUCHEL, E. W. 2000. Skin care and the topical treatment of aging skin. *Clinics in Plastic Surgery,* 27**,** 501-6.

FRIEDRICH, H., FREDERIK, P. M., DE WITH, G. & SOMMERDIJK, N. A. 2010. Imaging of self-assembled structures: interpretation of TEM and cryo-TEM images. *Angewandte Chemie International Edition,* 49**,** 7850-8.

FU, P. P., XIA, Q., BOUDREAU, M. D., HOWARD, P. C., TOLLESON, W. H. & WAMER, W. G. 2007. Physiological role of retinyl palmitate in the skin. *Vitam Horm,* 75**,** 223-56.

GABBANINI, S., LUCCHI, E., CARLI, M., BERLINI, E., MINGHETTI, A. & VALGIMIGLI, L. 2009. In vitro evaluation of the permeation through reconstructed human epidermis of essentials oils from cosmetic formulations. *Journal of Pharmaceutical and Biomedical Analysis,* 50**,** 370-376.

GABBANINI, S., MATERA, R., BELTRAMINI, C., MINGHETTI, A. & VALGIMIGLI, L. 2010. Analysis of in vitro release through reconstructed human epidermis and

synthetic membranes of multi-vitamins from cosmetic formulations. *Journal of Pharmaceutical and Biomedical Analysis,* 52**,** 461-7.

GANESAN, P. & NARAYANASAMY, D. 2017. Lipid nanoparticles: Different preparation techniques, characterization, hurdles, and strategies for the production of solid lipid nanoparticles and nanostructured lipid carriers for oral drug delivery. *Sustainable Chemistry and Pharmacy,* 6**,** 37-56.

GARCÊS, A., AMARAL, M., LOBO, J. S. & SILVA, A. 2017. Formulations based on solid lipid nanoparticles (SLN) and nanostructured lipid carriers (NLC) for cutaneous use: A review. *European Journal of Pharmaceutical Sciences, 112, 159-167*

GASCO, M. R. 1993. Method for producing solid lipid microspheres having a narrow size distribution. *Google Patents.*

GASCO, M. R. 2002. Microparticles for drug delivery across mucosa and the blood-brain barrier. *Google Patents*.

GASPERLIN, M. & GOSENCA, M. 2011. Main approaches for delivering antioxidant vitamins through the skin to prevent skin ageing. *Expert Opinion on Drug Delivery,* 8**,** 905-19.

GATTU, S. & MAIBACH, H. I. 2011. Modest but increased penetration through damaged skin: an overview of the in vivo human model. *Skin Pharmacology and Physiology,* 24**,** 2-9.

GAUMET, M., GURNY, R. & DELIE, F. 2009. Localization and quantification of biodegradable particles in an intestinal cell model: the influence of particle size. *European Journal of Pharmaceutical Sciences,* 36**,** 465-73.

GAUMET, M., VARGAS, A., GURNY, R. & DELIE, F. 2008. Nanoparticles for drug delivery: The need for precision in reporting particle size parameters. *European Journal of Pharmaceutics and Biopharmaceutics,* 69**,** 1-9.

GODIN, B. & TOUITOU, E. 2007. Transdermal skin delivery: predictions for humans from in vivo, ex vivo and animal models. *Advanced Drug Delivery Reviews,* 59**,** 1152-61.

GOKCE, E. H., KORKMAZ, E., DELLERA, E., SANDRI, G., BONFERONI, M. C. & OZER, O. 2012. Resveratrol-loaded solid lipid nanoparticles versus nanostructured lipid carriers: evaluation of antioxidant potential for dermal applications. *International Journal of Nanomedicine,* 7**,** 1841-50.

GOMES, G. V. D. L., BORRIN, T. R., CARDOSO, L. P., SOUTO, E. & PINHO, S. C. D. 2013. Characterization and shelf life of β-carotene loaded solid lipid microparticles produced with stearic acid and sunflower oil. *Brazilian Archives of Biology and Technology,* 56**,** 663-671.

GONZALEZ-MIRA, E., EGEA, M. A., GARCIA, M. L. & SOUTO, E. B. 2010. Design and ocular tolerance of flurbiprofen loaded ultrasound-engineered NLC. *Colloids and Surfaces B Biointerfaces,* 81**,** 412-21.

GONZALEZ-MIRA, E., EGEA, M. A., SOUTO, E. B., CALPENA, A. C. & GARCIA, M. L. 2011. Optimizing flurbiprofen-loaded NLC by central composite factorial design for ocular delivery. *Nanotechnology,* 22**,** 045101.

GUIMARÃES, K. L. & RÉ, M. I. 2011. Lipid nanoparticles as carriers for cosmetic ingredients: The first (SLN) and the second generation (NLC). *Nanocosmetics and nanomedicines,* 101-122

GUO, C., KHENGAR, R. H., SUN, M., WANG, Z., FAN, A. & ZHAO, Y. 2014. Acid-responsive polymeric nanocarriers for topical adapalene delivery. *Pharmaceutical Research,* 31**,** 3051-9.

GUTIÉRREZ, F. J., ALBILLOS, S. M., CASAS-SANZ, E., CRUZ, Z., GARCÍA-ESTRADA, C., GARCÍA-GUERRA, A., GARCÍA-REVERTER, J., GARCÍA-SUÁREZ, M., GATÓN, P. & GONZÁLEZ-FERRERO, C. 2013. Methods for the nanoencapsulation of β-carotene in the food sector. *Trends in food science & technology,* 32**,** 73-83.

HAN, F., LI, S., YIN, R., LIU, H. & XU, L. 2008. Effect of surfactants on the formation and characterization of a new type of colloidal drug delivery system: Nanostructured lipid carriers. *Colloids and Surfaces A: Physicochemical and Engineering Aspects,* 315**,** 210-216.

HARRIS, J. R. 2007. Negative staining of thinly spread biological samples. *Electron Microscopy,* 369**,** 107-42

HEINS, A., MCPHAIL, D. B., SOKOLOWSKI, T., STÖCKMANN, H. & SCHWARZ, K. 2007. The Location of Phenolic Antioxidants and Radicals at Interfaces Determines Their Activity. *Lipids,* 42**,** 573-582.

HEJRI, A., KHOSRAVI, A., GHARANJIG, K. & HEJAZI, M. 2013. Optimisation of the formulation of beta-carotene loaded nanostructured lipid carriers prepared by solvent diffusion method. *Food Chemistry,* 141**,** 117-23.

HEURTAULT, B., SAULNIER, P., PECH, B., PROUST, J.-E. & BENOIT, J.-P. 2003. Physico-chemical stability of colloidal lipid particles. *Biomaterials,* 24**,** 4283-4300.

HOSSEINKHANI, B., CALLEWAERT, C., VANBEVEREN, N. & BOON, N. 2015. Novel biocompatible nanocapsules for slow release of fragrances on the human skin. *New Biotechnolology,* 32**,** 40-6.

HOW, C. W., RASEDEE, A. & ABBASALIPOURKABIR, R. 2013. Characterization and cytotoxicity of nanostructured lipid carriers formulated with olive oil, hydrogenated palm oil, and polysorbate 80. *IEEE Trans Nanobioscience,* 12**,** 72-8.

LO-LABOROPTIK. 2018. *Neubauer - Improved* [Online]. http://www.lo-laboroptik.com/. [Accessed 11-06-2018].

HU, F.-Q., JIANG, S.-P., DU, Y.-Z., YUAN, H., YE, Y.-Q. & ZENG, S. 2005. Preparation and characterization of stearic acid nanostructured lipid carriers by solvent diffusion method in an aqueous system. *Colloids and Surfaces B: Biointerfaces,* 45**,** 167-173.

HU, X., GUO, Y., WANG, L., HUA, D., HONG, Y. & LI, J. 2011. Coenzyme Q10 nanoparticles prepared by a supercritical fluid-based method. *The Journal of Supercritical Fluids,* 57**,** 66-72.

IQBAL, M. A., MD, S., SAHNI, J. K., BABOOTA, S., DANG, S. & ALI, J. 2012. Nanostructured lipid carriers system: recent advances in drug delivery. *Journal of Drug Targeting,* 20**,** 813-30.

JACOBI, U., GAUTIER, J., STERRY, W. & LADEMANN, J. 2005. Gender-related differences in the physiology of the stratum corneum. *Dermatology,* 211**,** 312-7.

JAIN, A., JAIN, P., KURMI, J., JAIN, D., JAIN, R., CHANDEL, S., SAHU, A., MODY, N., UPADHAYA, S. & JAIN, A. 2014. Novel strategies for effective transdermal drug delivery: a review. *Critical Reviews™ in Therapeutic Drug Carrier Systems,* 31**,** 219-72.

JAIN, K. K. 2008. Nanomedicine: application of nanobiotechnology in medical practice. *Medical Principles and Practice,* 17**,** 89-101.

JAISWAL, P., GIDWANI, B. & VYAS, A. 2016. Nanostructured lipid carriers and their current application in targeted drug delivery. *Artificial Cells, Nanomedicine, and Biotechnology,* 44**,** 27-40.

JEE, J.-P., LIM, S.-J., PARK, J.-S. & KIM, C.-K. 2006. Stabilization of all-trans retinol by loading lipophilic antioxidants in solid lipid nanoparticles. European Journal of Pharmaceutics and Biopharmaceutics. 63*,* 134-9

JENNING, V. & GOHLA, S. H. 2001. Encapsulation of retinoids in solid lipid nanoparticles (SLN). *Journal of Microencapsulation,* 18**,** 149-58.

JENNING, V., GYSLER, A., SCHAFER-KORTING, M. & GOHLA, S. H. 2000a. Vitamin A loaded solid lipid nanoparticles for topical use: occlusive properties and drug targeting to the upper skin. *European Journal of Pharmaceutics and Biopharmaceutics,* 49**,** 211-8.

JENNING, V., THUNEMANN, A. F. & GOHLA, S. H. 2000b. Characterisation of a novel solid lipid nanoparticle carrier system based on binary mixtures of liquid and solid lipids. *Interntional Journal of Pharmaceutics,* 199**,** 167-77.

JENSEN, L. B., PETERSSON, K. & NIELSEN, H. M. 2011. In vitro penetration properties of solid lipid nanoparticles in intact and barrier-impaired skin. *European Journal of Pharmaceutics and Biopharmaceutics,* 79**,** 68-75.

JIA, L. J., ZHANG, D. R., LI, Z. Y., FENG, F. F., WANG, Y. C., DAI, W. T., DUAN, C. X. & ZHANG, Q. 2010. Preparation and characterization of silybin-loaded nanostructured lipid carriers. *Drug Delivery,* 17**,** 11-8.

JØRAHOLMEN, M. W., ŠKALKO-BASNET, N., ACHARYA, G. & BASNET, P. 2015. Resveratrol-loaded liposomes for topical treatment of the vaginal inflammation and infections. *European Journal of Pharmaceutical Sciences,* 79**,** 112-121.

JORES, K., HABERLAND, A., WARTEWIG, S., MADER, K. & MEHNERT, W. 2005. Solid lipid nanoparticles (SLN) and oil-loaded SLN studied by spectrofluorometry and Raman spectroscopy. *Pharmaceutical Research,* 22**,** 1887-97.

JORES, K., MEHNERT, W., DRECHSLER, M., BUNJES, H., JOHANN, C. & MADER, K. 2004. Investigations on the structure of solid lipid nanoparticles (SLN) and oil-loaded

solid lipid nanoparticles by photon correlation spectroscopy, field-flow fractionation and transmission electron microscopy. *Journal of Control Release,* 95**,** 217-27.

JOSE, A., LABALA, S., NINAVE, K. M., GADE, S. K. & VENUGANTI, V. V. K. 2018. Effective Skin Cancer Treatment by Topical Co-delivery of Curcumin and STAT3 siRNA Using Cationic Liposomes. *AAPS PharmSciTech,* 19**,** 166-175.

KACI, M., BELHAFFEF, A., MEZIANE, S., DOSTERT, G., MENU, P., VELOT, É., DESOBRY, S. & ARAB-TEHRANY, E. 2018. Nanoemulsions and topical creams for the safe and effective delivery of lipophilic antioxidant coenzyme Q10. *Colloids and Surfaces B: Biointerfaces,* 167**,** 165-175.

KANDÁROVÁ, H., HAYDEN, P., KLAUSNER, M., KUBILUS, J. & SHEASGREEN, J. 2009. An In Vitro Skin Irritation Test (SIT) using the EpiDerm Reconstructed Human Epidermal (RHE) Model. *Journal of Visualized Experiments : JoVE,* 1366.

KANDEKAR, S. G., DEL RIO-SANCHO, S., LAPTEVA, M. & KALIA, Y. N. 2018. Selective delivery of adapalene to the human hair follicle under finite dose conditions using polymeric micelle nanocarriers. *Nanoscale,* 10**,** 1099-1110.

KARAK, N. 2012. Vegetable oils and their derivatives. Vegetable Oil-Based Polymers. *Woodhead Publishing*.

KARN-ORACHAI, K., SMITH, S. M., PHUNPEE, S., TREETHONG, A., PUTTIPIPATKHACHORN, S., PRATONTEP, S. & RUKTANONCHAI, U. R. 2014. The effect of surfactant composition on the chemical and structural properties of nanostructured lipid carriers. *Journal of Microencapsulatio,* 31**,** 609-18.

KAUR, G., BEDI, P. & NARANG, J. K. 2017. Targeting alopecia with topical nanocarriers. *World Journal of Pharmacy and Pharmaceutical sciences,* 6**,** 326-333

KAUR, I. P., BHANDARI, R., BHANDARI, S. & KAKKAR, V. 2008. Potential of solid lipid nanoparticles in brain targeting. *Journal of Controlled Release,* 127**,** 97-109.

KECK, C. M., KOVACEVIC, A., MULLER, R. H., SAVIC, S., VULETA, G. & MILIC, J. 2014. Formulation of solid lipid nanoparticles (SLN): the value of different alkyl polyglucoside surfactants. *International Journal of Pharmaceutics,* 474**,** 33-41.

KERSCHER, M. & BUNTROCK, H. 2016. Cosmetics and cosmeceuticals. *Cosmetic Medicine and Surgery,* 9**,** 77-88

KHAN, S., SHAHARYAR, M., FAZIL, M., BABOOTA, S. & ALI, J. 2016. Tacrolimus-loaded nanostructured lipid carriers for oral delivery – Optimization of production and characterization. *European Journal of Pharmaceutics and Biopharmaceutics,* 108**,** 277-288.

KHERADMANDNIA, S., VASHEGHANI-FARAHANI, E., NOSRATI, M. & ATYABI, F. 2010. Preparation and characterization of ketoprofen-loaded solid lipid nanoparticles made from beeswax and carnauba wax. *Nanomedicine: Nanotechnology, Biology and Medicine,* 6**,** 753-759.

KLIGMAN, A. M., GROVE, G. L., HIROSE, R. & LEYDEN, J. J. 1986. Topical tretinoin for photoaged skin. *Journal of the American Academy of Dermatology,* 15**,** 836-59.

KNORR, F., LADEMANN, J., PATZELT, A., STERRY, W., BLUME-PEYTAVI, U. & VOGT, A. 2009. Follicular transport route--research progress and future perspectives. *European Journal of Pharmaceutics and Biopharmaceutics,* 71**,** 173-80.

KOHLI, A. K. & ALPAR, H. O. 2004. Potential use of nanoparticles for transcutaneous vaccine delivery: effect of particle size and charge. *International Journal of Pharmaceutics,* 275**,** 13-17.

KORTING, H. C. & SCHAFER-KORTING, M. 2010. Carriers in the topical treatment of skin disease. *Handbook of Experimental Pharmacology***,** 435-68.

KORTING, H. C. & SCHÄFER-KORTING, M. 2010. Carriers in the topical treatment of skin disease. *Drug delivery,* 197**,** 435-68

KUCHLER, S., ABDEL-MOTTALEB, M., LAMPRECHT, A., RADOWSKI, M. R., HAAG, R. & SCHAFER-KORTING, M. 2009. Influence of nanocarrier type and size on skin delivery of hydrophilic agents. *International Journal of Pharmaceutics,* 377**,** 169-72.

KUCHLER, S., STRUVER, K. & FRIESS, W. 2013. Reconstructed skin models as emerging tools for drug absorption studies. *Expert Opinion on Drug Metabolism & Toxicology,* 9**,** 1255-63.

KULLAVANIJAYA, P. & LIM, H. W. 2005. Photoprotection. *Journal of the American Academy of Dermatology,* 52**,** 937-58; quiz 959-62.

KUMARI, A., YADAV, S. K., PAKADE, Y. B., SINGH, B. & YADAV, S. C. 2010. Development of biodegradable nanoparticles for delivery of quercetin. *Colloids and Surfaces B: Biointerfaces,* 80**,** 184-92.

KUSHWAHA, A. K., VUDDANDA, P. R., KARUNANIDHI, P., SINGH, S. K. & SINGH, S. 2013. Development and evaluation of solid lipid nanoparticles of raloxifene hydrochloride for enhanced bioavailability. *BioMed Research International,* 2013**,** 584549.

LABORATORYINFO.COM. 2016. *Manual Cell Counting With Neubauer Chamber* [Online]. https://laboratoryinfo.com/manual-cell-counting-neubauer-chamber/. [Accessed 11-06-2018].

LABOUTA, H. I., THUDE, S. & SCHNEIDER, M. 2013. Setup for investigating gold nanoparticle penetration through reconstructed skin and comparison to published human skin data. *Journal of Biomedical Optics,* 18**,** 061218.

LACATUSU, I., BADEA, N., OVIDIU, O., BOJIN, D. & MEGHEA, A. 2012. Highly antioxidant carotene-lipid nanocarriers: synthesis and antibacterial activity. *Journal of Nanoparticle Research,* 14**,** 902.

LACATUSU, I., NICULAE, G., BADEA, N., STAN, R., POPA, O., OPREA, O. & MEGHEA, A. 2014. Design of soft lipid nanocarriers based on bioactive vegetable oils with multiple health benefits. *Chemical Engineering Journal,* 246**,** 311-321.

LACERDA, S. P., CERIZE, N. N. & RE, M. I. 2011. Preparation and characterization of carnauba wax nanostructured lipid carriers containing benzophenone-3. *International Journal of Cosmetic Science,* 33**,** 312-21.

LADEMANN, J., KNORR, F., RICHTER, H., JUNG, S., MEINKE, M., RÜHL, E., ALEXIEV, U., CALDERÓN, M. & PATZELT, A. 2015. Hair follicles as a target structure for nanoparticles. *Journal of Innovative Optical Health Sciences,* 8**,** 1530004.

LAM, P. L. & GAMBARI, R. 2014. Advanced progress of microencapsulation technologies: In vivo and in vitro models for studying oral and transdermal drug deliveries. *Journal of Controlled Release,* 178**,** 25-45.

LANDFESTER, K. 2001. The generation of nanoparticles in miniemulsions. *Advanced Materials,* 13**,** 765-768.

LANDFESTER, K. 2003. Miniemulsions for Nanoparticle Synthesis. *Colloid Chemistry II,* 75-123

LANDFESTER, K. 2006. Synthesis of colloidal particles in miniemulsions. *Annual Review of Materials Research,* 36**,** 231-279.

LANDFESTER, K. & MUSYANOVYCH, A. 2010. Targeted Polymeric Nanoparticles. *Antibody Engineering,* 417-428

LANE, M. E. 2013. Skin penetration enhancers. *International Journal of Pharmaceutics,* 447**,** 12-21.

LAOUINI, A., FESSI, H. & CHARCOSSET, C. 2012a. Membrane emulsification: A promising alternative for vitamin E encapsulation within nano-emulsion. *Journal of Membrane Science,* 423-424**,** 85-96.

LAOUINI, A., JAAFAR-MAALEJ, C., LIMAYEM-BLOUZA, I., SFAR, S., CHARCOSSET, C. & FESSI, H. 2012b. Preparation, characterization and applications of liposomes: state of the art. *Journal of colloid Science and Biotechnology,* 1**,** 147-168.

LASOŃ, E., SIKORA, E., MIASTKOWSKA, M., SOCHA, P. & OGONOWSKI, J. 2017. NLC delivery systems for alpha lipoic acid: Physicochemical characteristics and release study. *Colloids and Surfaces A: Physicochemical and Engineering Aspects,* 532**,** 57-62.

LASON, E., SIKORA, E. & OGONOWSKI, J. 2013. Influence of process parameters on properties of Nanostructured Lipid Carriers (NLC) formulation. *Acta Biochimica Polonica,* 60**,** 773-7.

LEE, J. B., LEE, D. R., CHOI, N. C., JANG, J., PARK, C. H., YOON, M. S., LEE, M., WON, K., HWANG, J. S. & KIM, B. M. 2015. Efficient dermal delivery of retinyl palmitate: progressive polarimetry and Raman spectroscopy to evaluate the structure and efficacy. *European Journal of Pharmaceutical Sciences,* 78**,** 111-120.

LERCH, S., DASS, M., MUSYANOVYCH, A., LANDFESTER, K. & MAILANDER, V. 2013. Polymeric nanoparticles of different sizes overcome the cell membrane barrier. *European Journal of Pharmaceutics and Biopharmaceutics,* 84**,** 265-74.

LI, D., WU, Z., MARTINI, N. & WEN, J. 2011a. Advanced carrier systems in cosmetics and cosmeceuticals: a review. *Journal of Cosmetic Science,* 62**,** 549-563.

LI, H., ZHAO, X., MA, Y., ZHAI, G., LI, L. & LOU, H. 2009. Enhancement of gastrointestinal absorption of quercetin by solid lipid nanoparticles. *Journal of Controlled Release,* 133**,** 238-244.

LI, Y., FESSI, H. & CHARCOSSET, C. 2011b. Preparation of indomethacin-loaded lipid particles by membrane emulsification. *Advanced Science Letters,* 4**,** 591-595.

LI, Z., LI, X.-W., ZHENG, L.-Q., LIN, X.-H., GENG, F. & YU, L. 2010. Bovine serum albumin loaded solid lipid nanoparticles prepared by double emulsion method. *Chemical Research in Chinese Universities,* 26**,** 136-141.

LIEB, L. M., RAMACHANDRAN, C., EGBARIA, K. & WEINER, N. 1992. Topical delivery enhancement with multilamellar liposomes into pilosebaceous units: I. In vitro evaluation using fluorescent techniques with the hamster ear model. *Journal of Investigative Dermatology,* 99**,** 108-13.

LIN, C. H., FANG, Y. P., AL-SUWAYEH, S. A., YANG, S. Y. & FANG, J. Y. 2013. Percutaneous absorption and antibacterial activities of lipid nanocarriers loaded with dual drugs for acne treatment. *Biological and Pharmaceutical Bulletin,* 36**,** 276-86.

LIN, Y. K., HUANG, Z. R., ZHUO, R. Z. & FANG, J. Y. 2010. Combination of calcipotriol and methotrexate in nanostructured lipid carriers for topical delivery. *International Journal of Nanomedicine,* 5**,** 117-28.

LIU, C.-H. & WU, C.-T. 2010. Optimization of nanostructured lipid carriers for lutein delivery. *Colloids and Surfaces A: Physicochemical and Engineering Aspects,* 353**,** 149-156.

LIU, J., GONG, T., WANG, C., ZHONG, Z. & ZHANG, Z. 2007a. Solid lipid nanoparticles loaded with insulin by sodium cholate-phosphatidylcholine-based mixed micelles: Preparation and characterization. *International Journal of Pharmaceutics,* 340**,** 153-162.

LIU, J., HU, W., CHEN, H., NI, Q., XU, H. & YANG, X. 2007b. Isotretinoin-loaded solid lipid nanoparticles with skin targeting for topical delivery. *International Journal of Pharmaceutics*, 328**,** 191-5

LODÉN, M. 2005. The clinical benefit of moisturizers. *Journal of the European Academy of Dermatology and Venereology,* 19**,** 672-688.

LOHANI, A., VERMA, A., JOSHI, H., YADAV, N. & KARKI, N. 2014. Nanotechnology-based cosmeceuticals. *ISRN Dermatology,* 2014**,** 843687.

LOMBARDI BORGIA, S., REGEHLY, M., SIVARAMAKRISHNAN, R., MEHNERT, W., KORTING, H. C., DANKER, K., RÖDER, B., KRAMER, K. D. & SCHÄFER-KORTING, M. 2005. Lipid nanoparticles for skin penetration enhancement—correlation to drug localization within the particle matrix as determined by fluorescence and parelectric spectroscopy. *Journal of Controlled Release,* 110**,** 151-163.

LOMBARDI BORGIA, S., SCHLUPP, P., MEHNERT, W. & SCHÄFER-KORTING, M. 2008. In vitro skin absorption and drug release – A comparison of six commercial

prednicarbate preparations for topical use. *European Journal of Pharmaceutics and Biopharmaceutics,* 68**,** 380-389.

LOVELYN, C. & ATTAMA, A. A. 2011. Current state of nanoemulsions in drug delivery. *Journal of Biomaterials and Nanobiotechnology,* 2**,** 626.

LUCKS, S. & MULLER, R. 1993. Medication Vehicles Made of Solid Lipid Particles (Solid Lipid Nanospheres-SLN). *Google Patents*.

LUYKX, D. M., PETERS, R. J., VAN RUTH, S. M. & BOUWMEESTER, H. 2008. A review of analytical methods for the identification and characterization of nano delivery systems in food. *Journal of Agricultural and Food Chemistry,* 56**,** 8231-47.

MAHAMONGKOL, H., BELLANTONE, R. A., STAGNI, G. & PLAKOGIANNIS, F. M. 2005. Permeation study of five formulations of alpha-tocopherol acetate through human cadaver skin. *International Journal of Cosmetic Science,* 56**,** 91-103.

MANDPE, L. & POKHARKAR, V. 2015. Quality by design approach to understand the process of optimization of iloperidone nanostructured lipid carriers for oral bioavailability enhancement. *Pharmaceutical development and technology,* 20**,** 320-329.

MANSOUR, H. M., PARK, C. W. & BAWA, R. 2016. Design and development of approved nanopharmaceutical products. *Handbook of Clinical Nanomedicine: Nanoparticles, Imaging, Therapy and Clinical Applications, Pan Stanford Publishing Pte. Ltd.,* 233-272

MARCATO, P. D., CAVERZAN, J., ROSSI-BERGMANN, B., PINTO, E. F., MACHADO, D., SILVA, R. A., JUSTO, G. Z., FERREIRA, C. V. & DURAN, N. 2011. Nanostructured polymer and lipid carriers for sunscreen. Biological effects and skin permeation. *Journal of Nanoscience and Nanotechnology,* 11**,** 1880-6.

MARDHIAH ADIB, Z., GHANBARZADEH, S., KOUHSOLTANI, M., YARI KHOSROSHAHI, A. & HAMISHEHKAR, H. 2016. The Effect of Particle Size on the Deposition of Solid Lipid Nanoparticles in Different Skin Layers: A Histological Study. *Advanced Pharmaceutical Bulletin,* 6**,** 31-6.

MARTO, J., SANGALLI, C., CAPRA, P., PERUGINI, P., ASCENSO, A., GONÇALVES, L. & RIBEIRO, H. 2017. Development and characterization of new and scalable topical formulations containing N-acetyl-d-glucosamine-loaded solid lipid nanoparticles. *Drug Development and Industrial Pharmacy,* 43**,** 1792-1800.

MD, S., HAQUE, S., MADHESWARAN, T., ZEESHAN, F., MEKA, V. S., RADHAKRISHNAN, A. K. & KESHARWANI, P. 2017. Lipid based nanocarriers system for topical delivery of photosensitizers. *Drug Discovery Today,* 22**,** 1274-1283.

MEHNERT, W. & MÄDER, K. 2001. Solid lipid nanoparticles: Production, characterization and applications. *Advanced Drug Delivery Reviews,* 47**,** 165-196.

MELOT, M., PUDNEY, P. D., WILLIAMSON, A. M., CASPERS, P. J., VAN DER POL, A. & PUPPELS, G. J. 2009. Studying the effectiveness of penetration enhancers to deliver retinol through the stratum cornum by in vivo confocal Raman spectroscopy. *Journal of Control Release,* 138**,** 32-9.

MEZEI, M. 2017. Liposomes and the skin. *Liposomes in drug delivery.* London: Routledge.

MIHRANYAN, A., FERRAZ, N. & STRØMME, M. 2012. Current status and future prospects of nanotechnology in cosmetics. *Progress in Materials Science,* 57**,** 875-910.

MISHRA, B., PATEL, B. B. & TIWARI, S. 2010. Colloidal nanocarriers: a review on formulation technology, types and applications toward targeted drug delivery. *Nanomedicine,* 6**,** 9-24.

MISHRA, P. R., AL SHAAL, L., MÜLLER, R. H. & KECK, C. M. 2009. Production and characterization of Hesperetin nanosuspensions for dermal delivery. *International Journal of Pharmaceutics,* 371**,** 182-189.

MITREA, E., OTT, C. & MEGHEA, A. 2014. New Approaches on the Synthesis of Effective Nanostructured Lipid Carriers. *Revista de Chimie*, 65**,** 50-55

MITRI, K., SHEGOKAR, R., GOHLA, S., ANSELMI, C. & MULLER, R. H. 2011. Lipid nanocarriers for dermal delivery of lutein: preparation, characterization, stability and performance. *International Journal of Pharmaceutics,* 414**,** 267-75.

MITTAL, A., SARA, U. V., ALI, A. & AQIL, M. 2008. The effect of penetration enhancers on permeation kinetics of nitrendipine in two different skin models. *Biological and Pharmaceutical Bulletin,* 31**,** 1766-72.

MOGHDDAM, S. M. M., AHAD, A., AQIL, M., IMAM, S. S. & SULTANA, Y. 2017. Optimization of nanostructured lipid carriers for topical delivery of nimesulide using Box–Behnken design approach. *Artificial cells, Nanomedicine, and Biotechnology,* 45**,** 617-624.

MOJAHEDIAN, M. M., DANESHAMOUZ, S., SAMANI, S. M. & ZARGARAN, A. 2013. A novel method to produce solid lipid nanoparticles using n-butanol as an additional co-surfactant according to the o/w microemulsion quenching technique. *Chemistry and Physics of Lipids,* 174**,** 32-8.

MONTAGU, A., JOLY-GUILLOU, M. L., GUILLET, C., BEJAUD, J., ROSSINES, E. & SAULNIER, P. 2016. Demonstration of the interactions between aromatic compound-loaded lipid nanocapsules and Acinetobacter baumannii bacterial membrane. *International Journal of Pharmaceutics,* 506**,** 280-288.

MONTENEGRO, L. 2014. Nanocarriers for skin delivery of cosmetic antioxidants. *Journal of Chemical and Pharmaceutical Research,* 2**,** 73-92.

MONTENEGRO, L., CAMPISI, A., SARPIETRO, M. G., CARBONE, C., ACQUAVIVA, R., RACITI, G. & PUGLISI, G. 2011. In vitro evaluation of idebenone-loaded solid lipid nanoparticles for drug delivery to the brain. *Drug Development and Industrial Pharmacy,* 37**,** 737-46.

MONTENEGRO, L., LAI, F., OFFERTA, A., SARPIETRO, M. G., MICICCHÈ, L., MACCIONI, A. M., VALENTI, D. & FADDA, A. M. 2016. From nanoemulsions to nanostructured lipid carriers: A relevant development in dermal delivery of drugs and cosmetics. *Journal of Drug Delivery Science and Technology,* 32**,** 100-112.

MONTENEGRO, L., PASQUINUCCI, L., ZAPPALÀ, A., CHIECHIO, S., TURNATURI, R. & PARENTI, C. 2017. Rosemary essential oil-loaded lipid nanoparticles: In vivo topical activity from gel vehicles. *Pharmaceutics,* 9**,** 48.

MORADI, A., SADAT FARBOUD, E., AHMAD NASROLLAHI, S., NASSIRI KASHANI, M. & DINARVAND, R. 2017. Tretinoin Loaded Nanostructured Lipid Carrier (NLC): Safe and Effective Drug Delivery System. *Nanoscience & Nanotechnology-Asia,* 7**,** 221-229.

MORALES, J. O., VALDES, K., MORALES, J. & OYARZUN-AMPUERO, F. 2015. Lipid nanoparticles for the topical delivery of retinoids and derivatives. *Nanomedicine,* 10**,** 253-69.

MU, L. & SPRANDO, R. L. 2010. Application of nanotechnology in cosmetics. *Pharmaceutical Research,* 27**,** 1746-1749.

MUKHERJEE, S., DATE, A., PATRAVALE, V., KORTING, H. C., ROEDER, A. & WEINDL, G. 2006. Retinoids in the treatment of skin aging: an overview of clinical efficacy and safety. *Clinical interventions in aging,* 1**,** 327.

MULLER R. H., M. W., AND SOUTO E. B. 2005. Solid Lipid Nanoparticles (SLN) and Nanostructured Lipid Carriers (NLC) for Dermal Delivery. *In:* ROBERT L. BRONAUGH, H. I. M. (ed.) Percutaneous Absorption: Drugs - Cosmetics - Mechanisms - Methodology. *Taylor & Francis Group.*

MÜLLER, R. H., ALEXIEV, U., SINAMBELA, P. & KECK, C. M. 2016. Nanostructured lipid carriers (NLC): the second generation of solid lipid nanoparticles. *Percutaneous Penetration Enhancers Chemical Methods in Penetration Enhancement.* Springer.

MULLER, R. H., BECKER, R., KRUSS, B. & PETERS, K. 1999. Pharmaceutical nanosuspensions for medicament administration as systems with increased saturation solubility and rate of solution. *Google Patents.*

MULLER, R. H., MADER, K. & GOHLA, S. 2000. Solid lipid nanoparticles (SLN) for controlled drug delivery - a review of the state of the art. *European Journal of Pharmaceutics and Biopharmaceutics,* 50**,** 161-77.

MÜLLER, R. H., PETERSEN, R. D., HOMMOSS, A. & PARDEIKE, J. 2007. Nanostructured lipid carriers (NLC) in cosmetic dermal products. *Advanced Drug Delivery Reviews,* 59**,** 522-530.

MÜLLER, R. H., RADTKE, M. & WISSING, S. A. 2002a. Nanostructured lipid matrices for improved microencapsulation of drugs. *International Journal of Pharmaceutics,* 242**,** 121-128.

MÜLLER, R. H., RADTKE, M. & WISSING, S. A. 2002b. Solid Lipid Nanoparticles (SLN) and Nanostructured Lipid Carriers (NLC) in Cosmetic and Dermatological Preparations. *Advanced Drug Delivery Reviews,* 54**,** S131-S155

MÜLLER, R. H., RUNGE, S. A., RAVELLI, V., THÜNEMANN, A. F., MEHNERT, W. & SOUTO, E. B. 2008. Cyclosporine-loaded solid lipid nanoparticles (SLN®): Drug–lipid physicochemical interactions and characterization of drug incorporation. *European Journal of Pharmaceutics and Biopharmaceutics,* 68**,** 535-544.

MULLER, R. H., SHEGOKAR, R. & KECK, C. M. 2011. 20 years of lipid nanoparticles (SLN and NLC): present state of development and industrial applications. *Curr Drug Drug Discovery Today: Technologies,* 8**,** 207-27.

MÜLLER, R. M., SINAMBELA, P. & KECK, C. 2013. NLC - The invisible dermal patch for moisturizing & skin protection.

MÜLLER, S. L. A. R. 1991. Medication vehicles made of solid lipid particles (solid lipid nanospheres - SLN). *Germany patent application*.

NADA, A. H., ZAGHLOUL, A. A., HEDAYA, M. M. & KHATTAB, I. S. 2014. Development of novel formulations to enhance in vivo transdermal permeation of tocopherol. *Acta Pharmaceutica,* 64**,** 299-309.

NATIONS, U. 2007. Globally Harmonized System of Classification and Labeling of Chemicals (GHS) Second revised edition. New York and Geneva: UN.

NEKKANTI, V., PILLAI, R., VENKATESHWARLU, V. & HARISUDHAN, T. 2009. Development and characterization of solid oral dosage form incorporating candesartan nanoparticles. *Pharmaceutical development and technology,* 14**,** 290-298.

NETTO MPHARM, G. & JOSE, J. 2017. Development, characterization, and evaluation of sunscreen cream containing solid lipid nanoparticles of silymarin. *Journal of Cosmetic Dermatology*.

NETZLAFF, F., KOSTKA, K.-H., LEHR, C.-M. & SCHAEFER, U. F. 2006. TEWL measurements as a routine method for evaluating the integrity of epidermis sheets in static Franz type diffusion cells in vitro. Limitations shown by transport data testing. *European Journal of Pharmaceutics and Biopharmaceutics,* 63**,** 44-50.

NETZLAFF, F., LEHR, C. M., WERTZ, P. W. & SCHAEFER, U. F. 2005. The human epidermis models EpiSkin, SkinEthic and EpiDerm: an evaluation of morphology and their suitability for testing phototoxicity, irritancy, corrosivity, and substance transport. *European Journal of Pharmaceutics and Biopharmaceutics,* 60**,** 167-78.

NICULAE, G., LACATUSU, I., BADEA, N., MEGHEA, A. & STAN, R. 2014. Influence of vegetable oil on the synthesis of bioactive nanocarriers with broad spectrum photoprotection. *Open Chemistry,* 12**,** 837-850.

NOOR, N. M., SHEIKH, K., SOMAVARAPU, S. & TAYLOR, K. M. G. 2017. Preparation and characterization of dutasteride-loaded nanostructured lipid carriers coated with stearic acid-chitosan oligomer for topical delivery. *European Journal of Pharmaceutics and Biopharmaceutics,* 117**,** 372-384.

NORIEGA-PELAEZ, E. K., MENDOZA-MUNOZ, N., GANEM-QUINTANAR, A. & QUINTANAR-GUERRERO, D. 2011. Optimization of the emulsification and solvent displacement method for the preparation of solid lipid nanoparticles. *Drug Development and Industrial Pharmacy,* 37**,** 160-6.

OBEIDAT, W. M., SCHWABE, K., MÜLLER, R. H. & KECK, C. M. 2010. Preservation of nanostructured lipid carriers (NLC). *European Journal of Pharmaceutics and Biopharmaceutics,* 76**,** 56-67.

OECD 2004. Guideline for the testing of chemicals - Skin Absorption: in vitro method. Member countries.

OECD 2015. Guidelines for the testing of chemicals - In vitro skin irritation: Reconstructed human epidermis test method.

OEHLKE, K., BEHSNILIAN, D., MAYER-MIEBACH, E., WEIDLER, P. G. & GREINER, R. 2017. Edible solid lipid nanoparticles (SLN) as carrier system for antioxidants of different lipophilicity. *PLoS One,* 12**,** e0171662.

OH, Y. K., KIM, M. Y., SHIN, J. Y., KIM, T. W., YUN, M. O., YANG, S. J., CHOI, S. S., JUNG, W. W., KIM, J. A. & CHOI, H. G. 2006. Skin permeation of retinol in Tween 20-based deformable liposomes: in-vitro evaluation in human skin and keratinocyte models. *Journal of Pharmacy and Pharmacology,* 58**,** 161-6.

OLIVEIRA, D. R. B., MICHELON, M., DE FIGUEIREDO FURTADO, G., SINIGAGLIA-COIMBRA, R. & CUNHA, R. L. 2016. β-Carotene-loaded nanostructured lipid carriers produced by solvent displacement method. *Food Research International,* 90**,** 139-146.

OLIVEIRA, M. B., PRADO, A. H. D., BERNEGOSSI, J., SATO, C. S., LOURENÇO BRUNETTI, I., SCARPA, M. V., LEONARDI, G. R., FRIBERG, S. E. & CHORILLI, M. 2014b. Topical application of retinyl palmitate-loaded nanotechnology-based drug delivery systems for the treatment of skin aging. *BioMed research international,* 2014**,** 7

OSTERTAG, F., WEISS, J. & MCCLEMENTS, D. J. 2012. Low-energy formation of edible nanoemulsions: factors influencing droplet size produced by emulsion phase inversion. *Journal of Colloid and Interface Science,* 388**,** 95-102.

PADAMWAR, M. N. & POKHARKAR, V. B. 2006. Development of vitamin loaded topical liposomal formulation using factorial design approach: drug deposition and stability. *International Journal of Pharmaceutics,* 320**,** 37-44.

PANG, J., LIU, X., SHEN, B., SHEN, C., LIAN, W., LIU, J., HU, C., ZHONG, R., XU, R. & YUAN, H. 2017. Preparation of isopsoralen loaded nanostructured carrier and its in vitro transdermal permeation characteristics. *Journal of Chinese Materia Medica,* 42**,** 2473-2478.

PAOLICELLI, P., VARANI, G., PACELLI, S., OGLIANI, E., NARDONI, M., PETRALITO, S., ADROVER, A. & CASADEI, M. A. 2017. Design and characterization of a biocompatible physical hydrogel based on scleroglucan for topical drug delivery. *Carbohydrate polymers,* 174**,** 960-969.

PARADISO, P., GALANTE, R., SANTOS, L., ALVES DE MATOS, A. P., COLACO, R., SERRO, A. P. & SARAMAGO, B. 2014. Comparison of two hydrogel formulations for drug release in ophthalmic lenses. *Journal of Biomedical Materials Research Part B: Applied Biomaterials,* 102**,** 1170-80.

PARDEIKE, J., HOMMOSS, A. & MÜLLER, R. H. 2009b. Lipid nanoparticles (SLN, NLC) in cosmetic and pharmaceutical dermal products. *International Journal of Pharmaceutics,* 366**,** 170-184.

PATHAK, P. & NAGARSENKER, M. 2009. Formulation and evaluation of lidocaine lipid nanosystems for dermal delivery. *AAPS PharmSciTech,* 10**,** 985-92.

PATHAN, I. B., JAWARE, B. P., SHELKE, S. & AMBEKAR, W. 2018. Curcumin loaded ethosomes for transdermal application: Formulation, optimization, in-vitro and in-vivo study. *Journal of Drug Delivery Science and Technology,* 44**,** 49-57.

PATRAVALE, V., DANDEKAR, P. & JAIN, R. 2012. *Nanoparticulate systems as drug carriers: the need. Woodhead Publishing*, eBook ISBN: 9781908818195

PDR, T. 2000. Physicians' Desk Reference 2000 *Medical Economics Company, Inc.*

PENG, L.-H., WEI, W., SHAN, Y.-H., CHONG, Y.-S., YU, L. & GAO, J.-Q. 2017. Sustained release of piroxicam from solid lipid nanoparticle as an effective anti-inflammatory therapeutics in vivo. *Drug Development and Industrial Pharmacy,* 43**,** 55-66.

PEREZ, A. P., ALTUBE, M. J., SCHILRREFF, P., APEZTEGUIA, G., CELES, F. S., ZACCHINO, S., DE OLIVEIRA, C. I., ROMERO, E. L. & MORILLA, M. J. 2016. Topical amphotericin B in ultradeformable liposomes: Formulation, skin penetration study, antifungal and antileishmanial activity in vitro. *Colloids and Surfaces B: Biointerfaces,* 139**,** 190-198.

PINTO, F., DE BARROS, D. P. C. & FONSECA, L. P. 2018. Design of multifunctional nanostructured lipid carriers enriched with α-tocopherol using vegetable oils. *Industrial Crops and Products,* 118**,** 149-159.

PINTO, M. F., MOURA, C. C., NUNES, C., SEGUNDO, M. A., COSTA LIMA, S. A. & REIS, S. 2014. A new topical formulation for psoriasis: Development of methotrexate-loaded nanostructured lipid carriers. *International Journal of Pharmaceutics,* 477**,** 519-526.

PIVETTA, T. P., SIMÕES, S., ARAÚJO, M. M., CARVALHO, T., ARRUDA, C. & MARCATO, P. D. 2018. Development of nanoparticles from natural lipids for topical delivery of thymol: Investigation of its anti-inflammatory properties. *Colloids and Surfaces B: Biointerfaces,* 164**,** 281-290.

POLAND, C. A., LARSEN, P.B., READ, S.A.K., VARET, J., HANKIN, S.M., LAM, H.R. 2016. *Assessment if Nano-enabled Technologies in Cosmetics*, The Danish Environmental Protection Agency.

POPLE, P. V. & SINGH, K. K. 2006. Development and evaluation of topical formulation containing solid lipid nanoparticles of vitamin A. *AAPS PharmSciTech,* 7**,** 91.

PRASAD, S., MUKHOPADHYAY, A., KUBAVAT, A., KELKAR, A., MODI, A., SWARNKAR, B., BAJAJ, B., VEDAMURTHY, M., SHEIKH, S. & MITTAL, R. 2012. Efficacy and safety of a nano-emulsion gel formulation of adapalene 0.1% and clindamycin 1% combination in acne vulgaris: a randomized, open label, active-controlled, multicentric, phase IV clinical trial. *Indian Journal of Dermatology Venereology and Leprology,* 78**,** 459-67.

PRATIWI, L., FUDHOLI, A., MARTIEN, R. & PRAMONO, S. 2017. Self-nanoemulsifying Drug Delivery System (Snedds) for Topical Delivery of Mangosteen Peels (Garcinia

Mangostana L.,): Formulation Design and In vitro Studies. *Journal of Young Pharmacists,* 9**,** 341.

PREVC, T., SEGATIN, N., ULRIH, N. P. & CIGIC, B. 2013. DPPH assay of vegetable oils and model antioxidants in protic and aprotic solvents. *Talanta,* 109**,** 13-9.

PRIANO, L., ESPOSTI, D., ESPOSTI, R., CASTAGNA, G., DE MEDICI, C., FRASCHINI, F., GASCO, M. R. & MAURO, A. 2007. Solid lipid nanoparticles incorporating melatonin as new model for sustained oral and transdermal delivery systems. *Journal of Nanoscience and Nanotechnology,* 7**,** 3596-601.

PUGLIA, C. & BONINA, F. 2012. Lipid nanoparticles as novel delivery systems for cosmetics and dermal pharmaceuticals. *Expert Opinion in Drug Delivery,* 9**,** 429-41.

PUGLIA, C., LAURO, M. R., OFFERTA, A., CRASCÌ, L., MICICCHÈ, L., PANICO, A. M., BONINA, F. & PUGLISI, G. 2017. Nanostructured lipid carriers (NLC) as vehicles for topical administration of sesamol: in vitro percutaneous absorption study and evaluation of antioxidant activity. *Planta medica,* 83**,** 398-404.

PUGLIA, C., SARPIETRO, M. G., BONINA, F., CASTELLI, F., ZAMMATARO, M. & CHIECHIO, S. 2011. Development, Characterization, and In Vitro and In Vivo Evaluation of Benzocaine- and Lidocaine-Loaded Nanostructrured Lipid Carriers. *Journal of Pharmaceutical Sciences,* 100**,** 1892-1899.

PURI, D. 2010. Lipid nanoparticles (SLN, NLC): A novel approach for cosmetic and dermal pharmaceutical. *Journal of Global Pharma Technology,* 2**,** 1-15.

PUTHLI, S. P., PUTHLI, M. S., MACEDO, A. S. & SOUTO, E. B. 2012. Intellectual Property and Nanopharmaceuticals. *Patenting Nanomedicines.* Springer.

QIAN, C. & MCCLEMENTS, D. J. 2011. Formation of nanoemulsions stabilized by model food-grade emulsifiers using high-pressure homogenization: factors affecting particle size. *Food Hydrocolloids,* 25**,** 1000-1008.

QIDWAI, A., KHAN, S., MD, S., FAZIL, M., BABOOTA, S., NARANG, J. K. & ALI, J. 2016. Nanostructured lipid carrier in photodynamic therapy for the treatment of basal-cell carcinoma. *Drug Deliv,* 23**,** 1476-85.

RADOMSKA, A., DOBRUCKI, R. & MÜLLER, R. 1999. Chemical stability of the lipid matrices of solid lipid nanoparticles (SLN) development of an analytical method and determination of long-term stability. *Pharmazie,* 54**,** 903-909.

RAHMAN, S. A., ABDELMALAK, N. S., BADAWI, A., ELBAYOUMY, T., SABRY, N. & EL RAMLY, A. 2015. Formulation of tretinoin-loaded topical proniosomes for treatment of acne: in-vitro characterization, skin irritation test and comparative clinical study. *Drug Delivery,* 22**,** 731-9.

RAZA, K., SINGH, B., LOHAN, S., SHARMA, G., NEGI, P., YACHHA, Y. & KATARE, O. P. 2013a. Nano-lipoidal carriers of tretinoin with enhanced percutaneous absorption, photostability, biocompatibility and anti-psoriatic activity. *International Journal of Pharmaceutics,* 456**,** 65-72.

RAZA, K., SINGH, B., SINGAL, P., WADHWA, S. & KATARE, O. P. 2013b. Systematically optimized biocompatible isotretinoin-loaded solid lipid nanoparticles

(SLNs) for topical treatment of acne. *Colloids and Surfaces B: Biointerfaces,* 105**,** 67-74.

RAZA, K., SINGH, B., SINGLA, S., WADHWA, S., GARG, B., CHHIBBER, S. & KATARE, O. P. 2013c. Nanocolloidal carriers of isotretinoin: antimicrobial activity against Propionibacterium acnes and dermatokinetic modeling. *Molecular Pharmaceutics,* 10**,** 1958-63.

REDDY, L. H., VIVEK, K., BAKSHI, N. & MURTHY, R. S. 2006. Tamoxifen citrate loaded solid lipid nanoparticles (SLN): preparation, characterization, in vitro drug release, and pharmacokinetic evaluation. *Pharmaceutical Development and Technology,* 11**,** 167-77.

REN, Q., DENG, C., MENG, L., CHEN, Y., CHEN, L., SHA, X. & FANG, X. 2014. In vitro, ex vivo, and in vivo evaluation of the effect of saturated fat acid chain length on the transdermal behavior of ibuprofen-loaded microemulsions. *Journal of Pharmaceutical Sciences,* 103**,** 1680-91.

RESZKO, A. E., BERSON, D. & LUPO, M. P. 2009. Cosmeceuticals: practical applications. *Dermatologic Clinics,* 27**,** 401-16, v.

RIDOLFI, D. M., MARCATO, P. D., JUSTO, G. Z., CORDI, L., MACHADO, D. & DURAN, N. 2012. Chitosan-solid lipid nanoparticles as carriers for topical delivery of tretinoin. *Colloids and Surfaces B: Biointerfaces,* 93**,** 36-40.

RIGANO I., G. G., RASTRELLI F. 2006. Vegetable Oils – The Base of New Active Principles. *SÖFW-Journal,* 132**,** 8.

RIVIERE, J. E. & PAPICH, M. G. 2001. Potential and problems of developing transdermal patches for veterinary applications. *Advanced Drug Delivery Reviews*, 50, 175-203.

ROCHA, V., MARQUES, C., FIGUEIREDO, J. L., GAIO, A. R., COSTA, P. C., SOUSA LOBO, J. M. & ALMEIDA, I. F. 2017. In vitro cytotoxicity evaluation of resveratrol-loaded nanoparticles: Focus on the challenges of in vitro methodologies. *Food and Chemical Toxicology*, 103, 214-222.

ROSLI, N., HASHAM, R., AZIZ, A. A. & AZIZ, R. 2015. Formulation and characterization of nanostructured lipid carrier encapsulated Zingiber zerumbet oil using ultrasonication technique. *Journal of Advanced Research,* 11**,** 16-23.

SABERI, A. H., FANG, Y. & MCCLEMENTS, D. 2012. Fabrication of vitamin E-enriched nanoemulsions: Factors affecting particle size using spontaneous emulsification. *Journal of Colloid and Interface Science,* 391**,** 95-102

SAHLE, F. F., GERECKE, C., KLEUSER, B. & BODMEIER, R. 2017. Formulation and comparative in vitro evaluation of various dexamethasone-loaded pH-sensitive polymeric nanoparticles intended for dermal applications. *International Journal of Pharmaceutics,* 516**,** 21-31.

SALA, M., DIAB, R., ELAISSARI, A. & FESSI, H. 2018. Lipid nanocarriers as skin drug delivery systems: Properties, mechanisms of skin interactions and medical applications. *International Journal of Pharmaceutics,* 535**,** 1-17.

SALAVKAR, S., TAMANEKAR, R. & ATHAWALE, R. 2011. Antioxidants in skin ageing-Future of dermatology. *International Journal of Green Pharmacy,* 5**,** 161.

SANAD, R. A., ABDELMALAK, N. S., ELBAYOOMY, T. S. & BADAWI, A. A. 2010. Formulation of a novel oxybenzone-loaded nanostructured lipid carriers (NLCs). *AAPS PharmSciTech,* 11**,** 1684-94.

SANTO, I. E., PEDRO, A. S., FIALHO, R. & CABRAL-ALBUQUERQUE, E. 2013a. Characteristics of lipid micro- and nanoparticles based on supercritical formation for potential pharmaceutical application. *Nanoscale Research Letters,* 8**,** 386-386.

SANTOS MAIA, C., MEHNERT, W., SCHALLER, M., KORTING, H. C., GYSLER, A., HABERLAND, A. & SCHAFER-KORTING, M. 2002. Drug targeting by solid lipid nanoparticles for dermal use. *Journal of Drug Targeting,* 10**,** 489-95.

SANTOS, P., WATKINSON, A. C., HADGRAFT, J. & LANE, M. E. 2008. Application of microemulsions in dermal and transdermal drug delivery. *Skin Pharmacology and Physiology,* 21**,** 246-59.

SARAF, S., SAHU, S., KAUR, C. D. & SARAF, S. 2010. Comparative measurement of hydration effects of herbal moisturizers. *Pharmacognosy Research,* 2**,** 146-51.

SCHAFER-KORTING, M., BOCK, U., GAMER, A., HABERLAND, A., HALTNER-UKOMADU, E., KACA, M., KAMP, H., KIETZMANN, M., KORTING, H. C., KRACHTER, H. U., LEHR, C. M., LIEBSCH, M., MEHLING, A., NETZLAFF, F., NIEDORF, F., RUBBELKE, M. K., SCHAFER, U., SCHMIDT, E., SCHREIBER, S., SCHRODER, K. R., SPIELMANN, H. & VUIA, A. 2006. Reconstructed human epidermis for skin absorption testing: results of the German prevalidation study. *ATLA: Alternatives to Lab Animals,* 34**,** 283-94.

SCHÄFER-KORTING, M., MEHNERT, W. & KORTING, H.-C. 2007. Lipid nanoparticles for improved topical application of drugs for skin diseases. *Advanced Drug Delivery Reviews,* 59**,** 427-443.

SCHLUPP, P., BLASCHKE, T., KRAMER, K. D., HOLTJE, H. D., MEHNERT, W. & SCHAFER-KORTING, M. 2011. Drug release and skin penetration from solid lipid nanoparticles and a base cream: a systematic approach from a comparison of three glucocorticoids. *Skin Pharmacol Physiol,* 24**,** 199-209.

SCHOLER, N., OLBRICH, C., TABATT, K., MULLER, R. H., HAHN, H. & LIESENFELD, O. 2001. Surfactant, but not the size of solid lipid nanoparticles (SLN) influences viability and cytokine production of macrophages. *International Journal of Pharmaceutics,* 221**,** 57-67.

SCHUBERT, M. & MÜLLER-GOYMANN, C. 2003. Solvent injection as a new approach for manufacturing lipid nanoparticles–evaluation of the method and process parameters. *European Journal of Pharmaceutics and Biopharmaceutics,* 55**,** 125-131.

SCHUBERT, M. A. & MULLER-GOYMANN, C. C. 2005. Characterisation of surface-modified solid lipid nanoparticles (SLN): influence of lecithin and nonionic emulsifier. *European Journal of Pharmaceutics and Biopharmaceutics,* 61**,** 77-86.

SCHULMAN, J. H., STOECKENIUS, W. & PRINCE, L. M. 1959. Mechanism of Formation and Structure of Micro Emulsions by Electron Microscopy. *The Journal of Physical Chemistry,* 63**,** 1677-1680.

SCHWARZ, J. C., WEIXELBAUM, A., PAGITSCH, E., LOW, M., RESCH, G. P. & VALENTA, C. 2012. Nanocarriers for dermal drug delivery: influence of preparation method, carrier type and rheological properties. *International Journal of Pharmaceutics,* 437**,** 83-8.

SCIENCES, P. 2009. Emulsions and Emulsification. *Particle Sciences - Drug Development Services.*

SEKULA-GIBBS, S., UPTMORE, D. & OTILLAR, L. Retinoids. *Journal of the American Academy of Dermatology,* 50**,** 405-415.

SEVERINO, P., ANDREANI, T., MACEDO, A. S., FANGUEIRO, J. F., SANTANA, M. H., SILVA, A. M. & SOUTO, E. B. 2012. Current State-of-Art and New Trends on Lipid Nanoparticles (SLN and NLC) for Oral Drug Delivery. *Journal of Drug Delivery,* 2012**,** 750891.

SEVERINO, P., FANGUEIRO, J. F., CHAUD, M. V., CORDEIRO, J., SILVA, A. M. & SOUTO, E. B. 2016. Advances in nanobiomaterials for topical administrations: new galenic and cosmetic formulations. *Nanobiomaterials in Galenic Formulations and Cosmetics. Applications of Nanobiomaterials,*10**,** 1-23.

SEVERINO, P., SILVEIRA, E. F., LOUREIRO, K., CHAUD, M. V., ANTONINI, D., LANCELLOTTI, M., SARMENTO, V. H., DA SILVA, C. F., SANTANA, M. H. A. & SOUTO, E. B. 2017. Antimicrobial activity of polymyxin-loaded solid lipid nanoparticles (PLX-SLN): Characterization of physicochemical properties and in vitro efficacy. *European Journal of Pharmaceutical Sciences,* 106**,** 177-184.

SHAH, P. P., DESAI, P. R. & SINGH, M. 2012. Effect of oleic acid modified polymeric bilayered nanoparticles on percutaneous delivery of spantide II and ketoprofen. *Journal of Control Release,* 158**,** 336-45.

SHAH, R., ELDRIDGE, D., PALOMBO, E. & HARDING, I. 2015. Lipid Nanoparticles: Production, Characterization and Stability. *SpringerBriefs in Pharmaceutical Science & Drug Development, e*Book

SHARMA, S. & SARANGDEVOT, K. 2012. Nanoemulsions for cosmetics. *IJARPB,* 1**,** 408-415.

SHAW, R. 2013. Dynamic Light Scattering Training - Achieving reliable nano particle sizing. *Ata Scientific Pty. Ltd.*

SHI, F., ZHAO, J. H., LIU, Y., WANG, Z., ZHANG, Y. T. & FENG, N. P. 2012. Preparation and characterization of solid lipid nanoparticles loaded with frankincense and myrrh oil. *International Journal of Nanomedicine,* 7**,** 2033-43.

SIDDIQUI, A., ALAYOUBI, A., EL-MALAH, Y. & NAZZAL, S. 2014. Modeling the effect of sonication parameters on size and dispersion temperature of solid lipid nanoparticles (SLNs) by response surface methodology (RSM). *Pharmaceutical Development and Technology,* 19**,** 342-6.

SITTERBERG, J., OZCETIN, A., EHRHARDT, C. & BAKOWSKY, U. 2010. Utilising atomic force microscopy for the characterisation of nanoscale drug delivery systems. *European Journal of Pharmaceutics and Biopharmaceutics,* 74**,** 2-13.

SIVARAMAKRISHNAN, R., NAKAMURA, C., MEHNERT, W., KORTING, H. C., KRAMER, K. D. & SCHAFER-KORTING, M. 2004. Glucocorticoid entrapment into lipid carriers--characterisation by parelectric spectroscopy and influence on dermal uptake. *Journal of Control Release,* 97**,** 493-502.

SORG, O., ANTILLE, C., KAYA, G. & SAURAT, J. H. 2006. Retinoids in cosmeceuticals. *Dermatologic Therapy,* 19**,** 289-96.

SORG, O., KUENZLI, S., KAYA, G. & SAURAT, J. H. 2005. Proposed mechanisms of action for retinoid derivatives in the treatment of skin aging. *Journal of Cosmetic Dermatology,* 4**,** 237-44.

SOUTO, E., ALMEIDA, A. & MÜLLER, R. 2007. Lipid nanoparticles (SLN®, NLC®) for cutaneous drug delivery: structure, protection and skin effects. *Journal of Biomedical Nanotechnology,* 3**,** 317-331.

SOUTO, E. B., FANGUEIRO, J. F. & MÜLLER, R. H. 2013. Solid lipid nanoparticles (SLN™). *Fundamentals of Pharmaceutical Nanoscience.* Springer.

SOUTO, E. B. & MULLER, R. H. 2008. Cosmetic features and applications of lipid nanoparticles (SLN, NLC). *International Journal of Cosmetics Science,* 30**,** 157-65.

SOUTO, E. B. & MULLER, R. H. 2010. Lipid nanoparticles: effect on bioavailability and pharmacokinetic changes. *Handbook of Experimental Pharmacology***,** 115-41.

SOUTO, E. B. & MÜLLER, R. H. 2007. Lipid nanoparticles (SLN and NLC) for drug delivery. *Journal of Biomedical Nanotechnology*, 3**,** 317-331

SOUTO, E. B., WISSING, S. A., BARBOSA, C. M. & MULLER, R. H. 2004. Development of a controlled release formulation based on SLN and NLC for topical clotrimazole delivery. *International Journal of Pharmaceutics,* 278**,** 71-7.

SOUZA, C. & CAMPOS, P. M. M. 2017. Development and photoprotective effect of a sunscreen containing the antioxidants Spirulina and dimethylmethoxy chromanol on sun-induced skin damage. *European Journal of Pharmaceutical Sciences,* 104**,** 52-64.

SOUZA, M. P., VAZ, A. F. M., CORREIA, M. T. S., CERQUEIRA, M. A., VICENTE, A. A. & CARNEIRO-DA-CUNHA, M. G. 2014. Quercetin-Loaded Lecithin/Chitosan Nanoparticles for Functional Food Applications. *Food and Bioprocess Technology,* 7**,** 1149-1159.

SPIELMANN, H., HOFFMANN, S., LIEBSCH, M., BOTHAM, P., FENTEM, J. H., ESKES, C., ROGUET, R., COTOVIO, J., COLE, T., WORTH, A., HEYLINGS, J., JONES, P., ROBLES, C., KANDAROVA, H., GAMER, A., REMMELE, M., CURREN, R., RAABE, H., COCKSHOTT, A., GERNER, I. & ZUANG, V. 2007. The ECVAM international validation study on in vitro tests for acute skin irritation: report on the validity of the EPISKIN and EpiDerm assays and on the Skin Integrity Function Test. *ATLA: Alternatives to Lab Animals,* 35**,** 559-601.

STECOVA, J., MEHNERT, W., BLASCHKE, T., KLEUSER, B., SIVARAMAKRISHNAN, R., ZOUBOULIS, C. C., SELTMANN, H., KORTING, H. C., KRAMER, K. D. & SCHAFER-KORTING, M. 2007. Cyproterone acetate loading to lipid nanoparticles for topical acne treatment: particle characterisation and skin uptake. *Pharmaceutical Research,* 24**,** 991-1000.

STRACKE, F., WEISS, B., LEHR, C. M., KONIG, K., SCHAEFER, U. F. & SCHNEIDER, M. 2006. Multiphoton microscopy for the investigation of dermal penetration of nanoparticle-borne drugs. *Journal of Investigative Dermatology,* 126**,** 2224-33.

SUGGS, A., OYETAKIN-WHITE, P. & BARON, E. D. 2014. Effect of botanicals on inflammation and skin aging: analyzing the evidence. *Inflammation & Allergy - Drug Targets,* 13**,** 168-76.

SURASSMO, S., SUKTHAM, K., YOSTAWONKUL, J., SAENGKRIT, N. & RUKTANONCHAI, U. 2017. Potential and bioaccessibility of Pueraria mirifica-loaded nanostructure lipid carriers for its impact on the biopharmaceutical application. *Planta Medica International Open,* 4**,** Tu-PO-42.

TAMAYO, I., GAMAZO, C., DE SOUZA REBOUÇAS, J. & IRACHE, J. M. 2017. Topical immunization using a nanoemulsion containing bacterial membrane antigens. *Journal of Drug Delivery Science and Technology,* 42**,** 207-214.

TAN, S. W., BILLA, N., ROBERTS, C. R. & BURLEY, J. C. 2010. Surfactant effects on the physical characteristics of Amphotericin B-containing nanostructured lipid carriers. *Colloids and Surfaces A: Physicochemical and Engineering Aspects,* 372**,** 73-79.

TEERANACHAIDEEKUL, V., BOONME, P., SOUTO, E. B., MULLER, R. H. & JUNYAPRASERT, V. B. 2008a. Influence of oil content on physicochemical properties and skin distribution of Nile red-loaded NLC. *Journal of Control Release,* 128**,** 134-41.

TEERANACHAIDEEKUL, V., CHANTABURANAN, T. & JUNYAPRASERT, V. B. 2017. Influence of state and crystallinity of lipid matrix on physicochemical properties and permeation of capsaicin-loaded lipid nanoparticles for topical delivery. *Journal of Drug Delivery Science and Technology,* 39**,** 300-307.

TEERANACHAIDEEKUL, V., MULLER, R. H. & JUNYAPRASERT, B. 2007a. Encapsulation of ascorbyl palmitate in nanostructured lipid carriers (NLC) - Effects of formulation parameters on physicochemical stability. *International Journal of Pharmaceutics,* 340**,** 198-206.

TEERANACHAIDEEKUL, V., SOUTO, E. B., B JUNYAPRASERT, V. & H MÜLLER, R. 2007b. Cetyl palmitate-based NLC for topical delivery of Coenzyme Q(10) - Development, physicochemical characterization and in vitro release studies. *European Journal of Pharmaceutics and Biopharmaceutics*, 67**,** 141-8.

TEERANACHAIDEEKUL, V., SOUTO, E. B., MÜLLER, R. H. & JUNYAPRASERT, V. B. 2008b. Physicochemical characterization and in vitro release studies of ascorbyl palmitate-loaded semi-solid nanostructured lipid carriers (NLC gels). *Journal of Microencapsulation,* 25**,** 111-120.

TEHRANIFAR, A., SELAHVARZI, Y., KHARRAZI, M. & BAKHSH, V. J. 2011. High potential of agro-industrial by-products of pomegranate (Punica granatum L.) as the powerful antifungal and antioxidant substances. *Industrial Crops and Products,* 34**,** 1523-1527.

TEIXEIRA, Z., ZANCHETTA, B., MELO, B. A., OLIVEIRA, L. L., SANTANA, M. H., PAREDES-GAMERO, E. J., JUSTO, G. Z., NADER, H. B., GUTERRES, S. S. & DURAN, N. 2010. Retinyl palmitate flexible polymeric nanocapsules: characterization and permeation studies. *Colloids and Surfaces B Biointerfaces,* 81**,** 374-80.

TEWES, F., CORRIGAN, O. & HEALY, A. 2013. Surfactants in Pharmaceutical Products and Systems. *Encyclopedia of Pharmaceutical Science and Technology,*

THAKKAR, H. P., DESAI, J. L. & PARMAR, M. P. 2014b. Application of Box-Behnken design for optimization of formulation parameters for nanostructured lipid carriers of candesartan cilexetil. *Asian Journal of Pharmaceutics (AJP): Free full text articles from Asian J Pharm,* 8, 81-89.

THIELE, J. J. & EKANAYAKE-MUDIYANSELAGE, S. 2007. Vitamin E in human skin: organ-specific physiology and considerations for its use in dermatology. *Molecular Aspects of Medicine,* 28**,** 646-67.

THOMAS, J. R., DIXON, T. K. & BHATTACHARYYA, T. K. 2013a. Effects of topicals on the aging skin process. *Facial Plastic Surgery Clinics of North America,* 21**,** 55-60.

TIAN, H., LU, Z., LI, D. & HU, J. 2018. Preparation and characterization of citral-loaded solid lipid nanoparticles. *Food Chemistry,* 248**,** 78-85.

TIRADO-SANCHEZ, A., ESPINDOLA, Y. S., PONCE-OLIVERA, R. M. & BONIFAZ, A. 2013. Efficacy and safety of adapalene gel 0.1% and 0.3% and tretinoin gel 0.05% for acne vulgaris: results of a single-center, randomized, double-blinded, placebo-controlled clinical trial on Mexican patients (skin type III-IV). *Journal of Cosmetic Dermatology,* 12**,** 103-7.

TRIPLETT, M. D. & RATHMAN, J. F. 2009. Optimization of β-carotene loaded solid lipid nanoparticles preparation using a high shear homogenization technique. *Journal of Nanoparticle Research,* 11**,** 601-614.

TROMBINO, S., CASSANO, R., MUZZALUPO, R., PINGITORE, A., CIONE, E. & PICCI, N. 2009. Stearyl ferulate-based solid lipid nanoparticles for the encapsulation and stabilization of beta-carotene and alpha-tocopherol. *Colloids Surfaces B Biointerfaces,* 72**,** 181-7.

TSAI, M.-J., HUANG, Y.-B., FANG, J.-W., FU, Y.-S. & WU, P.-C. 2015. Preparation and Characterization of Naringenin-Loaded Elastic Liposomes for Topical Application. *PLOS ONE,* 10**,** e0131026.

ÜNER, M., WISSING, S. A., YENER, G. & H MÜLLER, R. 2005. Skin moisturizing effect and skin penetration of ascorbyl palmitate entrapped in Solid Lipid Nanoparticles (SLN) and Nanostructured Lipid Carriers (NLC) incorporated into hydrogel. *Pharmazie*, 60**,** 751-5

VALDES, C., BUSTOS, G., MARTINEZ, J. L. & LAURIDO, C. 2018. Antinociceptive antibiotics-loaded into solid lipid nanoparticles of prolonged release: Measuring pharmacological efficiency and time span on chronic monoarthritis rats. *PLOS ONE,* 13**,** e0187473.

VAN GELE, M., GEUSENS, B., BROCHEZ, L., SPEECKAERT, R. & LAMBERT, J. 2011. Three-dimensional skin models as tools for transdermal drug delivery: challenges and limitations. *Expert Opinion on Drug Delivery,* 8**,** 705-20.

VÁZQUEZ-GONZÁLEZ, M. L., CALPENA, A. C., DOMÈNECH, Ò., MONTERO, M. T. & BORRELL, J. H. 2015. Enhanced topical delivery of hyaluronic acid encapsulated in liposomes: A surface-dependent phenomenon. *Colloids and Surfaces B: Biointerfaces,* 134**,** 31-39.

VINARDELL, M. P. & MITJANS, M. 2015. Nanocarriers for delivery of antioxidants on the skin. *Cosmetics,* 2**,** 342-354.

VITORINO, C., ALMEIDA, A., SOUSA, J., LAMARCHE, I., GOBIN, P., MARCHAND, S., COUET, W., OLIVIER, J. C. & PAIS, A. 2014. Passive and active strategies for transdermal delivery using co-encapsulating nanostructured lipid carriers: in vitro vs. in vivo studies. *European Journal of Pharmaceutics and Biopharmaceutics,* 86**,** 133-44.

WANG, F., HE, S. & CHEN, B. 2018. Retinoic acid-loaded alginate microspheres as a slow release drug delivery carrier for intravitreal treatment. *Biomedicine & Pharmacotherapy,* 97**,** 722-728.

WANG, S. & SCHORK, F. J. 1994. Miniemulsion polymerization of vinyl acetate with nonionic surfactant. *Journal of Applied Polymer Science,* 54**,** 2157-2164.

WEBER, S., ZIMMER, A. & PARDEIKE, J. 2014. Solid Lipid Nanoparticles (SLN) and Nanostructured Lipid Carriers (NLC) for pulmonary application: A review of the state of the art. *European Journal of Pharmaceutics and Biopharmaceutics,* 86**,** 7-22.

WEISSIG, V., PETTINGER, T. K. & MURDOCK, N. 2014. Nanopharmaceuticals (part 1): products on the market. *International Journal of Nanomedicine,* 9**,** 4357-73.

WISSING, S. & MÜLLER, R. 2003. The influence of solid lipid nanoparticles on skin hydration and viscoelasticity - In vivo study. *European Journal of Pharmaceutics and Biopharmaceutics*, 56**,** 67-72.

WISSING, S., MÜLLER, R., MANTHEI, L. & MAYER, C. 2004. Structural Characterization of Q10-Loaded Solid Lipid Nanoparticles by NMR Spectroscopy. *Pharmaceutical Research*, 21**,** 400–405

WISSING, S. A., LIPPACHER, A. & MÜLLER, R. H. 2001. Investigations on the occlusive properties of solid lipid nanoparticles (SLN). *Journal of Cosmetic Science*, 52**,** 313-324.

YADAV, N., KHATAK, S. & SARA, U. S. 2013. Solid lipid nanoparticles-a review. *International Journal of Applied Pharmaceutics,* 5**,** 8-18.

YAKUSHINA, L. & TARANOVA, A. 1995. Rapid HPLC simultaneous determination of fat-soluble vitamins, including carotenoids, in human serum. *Journal of Pharmaceutical and Biomedical Analysis,* 13**,** 715-8.

YAN, L., YANG, Y., ZHANG, W. & CHEN, X. 2014. Advanced materials and nanotechnology for drug delivery. *Advanced Materials,* 26**,** 5533-5540.

YAZDANI-ARAZI, S. N., GHANBARZADEH, S., ADIBKIA, K., KOUHSOLTANI, M. & HAMISHEHKAR, H. 2017. Histological evaluation of follicular delivery of arginine via nanostructured lipid carriers: a novel potential approach for the treatment of alopecia. *Artificial cells, Nanomedicine, and Biotechnology,* 45**,** 1379-1387.

YENILMEZ, E. & YAZAN, Y. 2010. Release of vitamin E from different topical colloidal delivery systems and their in vitro-in vivo evaluation. *Turkish Journal Of Pharmaceutical Sciences,* 7**,** 167-187.

YOU, P., YUAN, R. & CHEN, C. 2017. Design and evaluation of lidocaine-and prilocaine-coloaded nanoparticulate drug delivery systems for topical anesthetic analgesic therapy: a comparison between solid lipid nanoparticles and nanostructured lipid carriers. *Drug design, Development and Therapy,* 11**,** 2743.

ZADEH, B. S. M., BARATI, N., HASSANI, M. & RAHIM, F. 2010. Development of solid lipid nanoparticles as Eschar delivery system for Nitrofurazone using Taguchi design approach. *International Journal of Research in Pharmaceutical Sciences,* 1**,** 466-72.

ZHAI, Y. & ZHAI, G. 2014. Advances in lipid-based colloid systems as drug carrier for topic delivery. *Journal of Control Release,* 193**,** 90-9.

ZHENG, M., FALKEBORG, M., ZHENG, Y., YANG, T. & XU, X. 2013. Formulation and characterization of nanostructured lipid carriers containing a mixed lipids core. *Colloids and Surfaces A: Physicochemical and Engineering Aspects,* 430**,** 76-84.

ZHUANG, C. Y., LI, N., WANG, M., ZHANG, X. N., PAN, W. S., PENG, J. J., PAN, Y. S. & TANG, X. 2010. Preparation and characterization of vinpocetine loaded nanostructured lipid carriers (NLC) for improved oral bioavailability. *International Journal of Pharmaceutics,* 394**,** 179-85.

ZIELIŃSKA, A. & NOWAK, I. 2014. Fatty acids in vegetable oils and their importance in cosmetic industry. *CHEMIK nauka-technika-rynek,* 1**,** 103-110.

ZIELIŃSKA, A. & NOWAK, I. 2016. Solid lipid nanoparticles and nanostructured lipid carriers as novel carriers for cosmetic ingredients. *Nanobiomaterials in Galenic Formulations and Cosmetics.* Elsevier. eBook ISBN: 9780323428910